

Discovering new pathways in thrombus formation

Citation for published version (APA):

Nagy, M. (2019). *Discovering new pathways in thrombus formation*. [Doctoral Thesis, Maastricht University]. Gildeprint Drukkerijen. <https://doi.org/10.26481/dis.20191107mn>

Document status and date:

Published: 07/11/2019

DOI:

[10.26481/dis.20191107mn](https://doi.org/10.26481/dis.20191107mn)

Document Version:

Publisher's PDF, also known as Version of record

Please check the document version of this publication:

- A submitted manuscript is the version of the article upon submission and before peer-review. There can be important differences between the submitted version and the official published version of record. People interested in the research are advised to contact the author for the final version of the publication, or visit the DOI to the publisher's website.
- The final author version and the galley proof are versions of the publication after peer review.
- The final published version features the final layout of the paper including the volume, issue and page numbers.

[Link to publication](#)

General rights

Copyright and moral rights for the publications made accessible in the public portal are retained by the authors and/or other copyright owners and it is a condition of accessing publications that users recognise and abide by the legal requirements associated with these rights.

- Users may download and print one copy of any publication from the public portal for the purpose of private study or research.
- You may not further distribute the material or use it for any profit-making activity or commercial gain
- You may freely distribute the URL identifying the publication in the public portal.

If the publication is distributed under the terms of Article 25fa of the Dutch Copyright Act, indicated by the "Taverne" license above, please follow below link for the End User Agreement:

www.umlib.nl/taverne-license

Take down policy

If you believe that this document breaches copyright please contact us at:

repository@maastrichtuniversity.nl

providing details and we will investigate your claim.

*Discovering new pathways in thrombus
formation*

Magdolna Nagy

Discovering new pathways in thrombus formation

Thesis Maastricht University

ISBN 978-94-6323-864-9

Production: Gildeprint Drukkerijen

© Magdolna Nagy, Maastricht 2019

Cover design by Evelien Jagtman (www.evelienjagtman.com)

Discovering new pathways in thrombus formation

PROEFSCHRIFT

ter verkrijging van de graad van doctor aan de Universiteit Maastricht,
op gezag van de Rector Magnificus, Prof. Dr. Rianne M. Letschert,
volgens het besluit van het College van Decanen,
in het openbaar te verdedigen op

donderdag 7 november 2019 om 10.00 uur

door

Magdolna Nagy

Geboren op 3 december 1988 te Cegléd, Hongarije

Promotores

Prof. Dr. J.W.M. Heemskerk

Prof. Dr. S.P. Watson (University of Birmingham, United Kingdom)

Copromotor

Dr. J.M.E.M. Cosemans

Beoordelingscommissie

Prof. Dr. C.P.M. Reutelingsperger (voorzitter)

Dr. E.A.M. Beckers

Dr. M. Jandrot-Perrus (INSERM, Paris Diderot University, France)

Prof. Dr. I. Hers (University of Bristol, United Kingdom)

Prof. Dr. M.A.M.J. van Zandvoort

This project was supported by the Interreg V Euregio Meuse-Rhine program (Poly-Valve) and the Maastricht Heart+Vascular Centre (HVC).

Financial support by Stichting Hart Onderzoek Nederland (www.hartonderzoek.nl) is gratefully acknowledged.

Financial support for publication of this thesis by the Dutch Heart Foundation is gratefully acknowledged.

Contents

Chapter 1	General introduction	7
Chapter 2	Use of microfluidics to assess the platelet-based coagulation	23
Chapter 3	Multiple roles of store-operated calcium entry in thrombo-inflammation	43
Chapter 4	Variable impairment of platelet functions in patients with severe, genetically linked immune deficiencies	73
Chapter 5	Thrombus-induced micro-localisation and activation of neutrophils: roles of platelet-derived chemokines	100
Chapter 6	Comparative analysis of microfluidics thrombus formation in multiple genetically modified mice: link to thrombosis and hemostasis	131
Chapter 7	Comparison of the GPVI inhibitors losartan and honokiol in platelet activation	163
Chapter 8	Tight junction-like structures in platelet-platelet interactions	185
Chapter 9	Bioactive glucagon-like peptide 1 suppresses thrombus growth under flow: beneficial antithrombotic effect of dipeptidyl peptidase 4 inhibition	199
Chapter 10	General discussion	231
Chapter 11	Summary	243
	Samenvatting	251
	Valorization	259
	Curriculum Vitae	265
	Publications	273
	Acknowledgement	281

Chapter 1

General introduction

Collagen-dependent thrombus formation

Platelets are crucial blood cell fragments in hemostasis and arterial thrombosis.^{1,2} Upon vascular injury, the platelets in the circulation rapidly respond to form a hemostatic plug and initiate the coagulation process to stop bleeding and ensure proper hemostasis. On the other hand, upon a rupture or denudation of an inflammatory atherosclerotic plaque, platelets may trigger occlusive thrombus formation, with as a consequence of arterial thrombosis.^{2,3} According to classical concepts, improper platelet activation is more associated with arterial thrombosis, while undesired coagulation and fibrin clotting is more associated with venous thrombosis and thromboembolism.^{4,5} By implication, to ensure hemostasis but prevent thrombosis, the processes of platelet activation and coagulation must be tightly regulated.

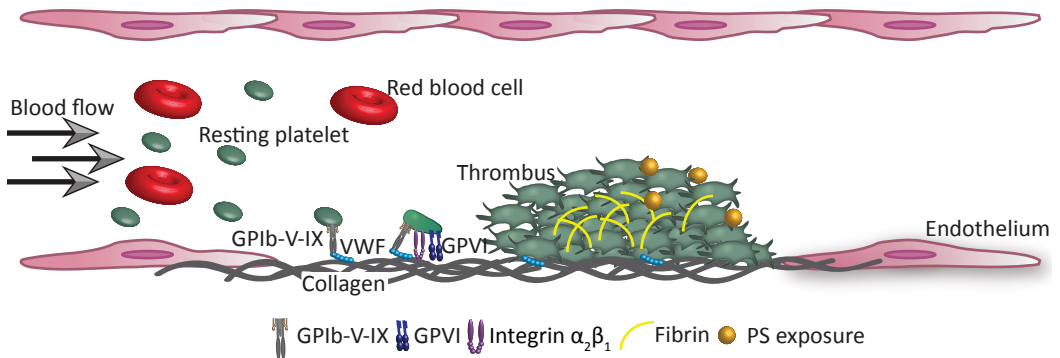


Figure 1. Overview of collagen-dependent thrombus formation. Upon vascular injury, resting circulating platelets are captured by von Willebrand factor (vWF) via GPIb-V-IX receptor. Subsequently, platelets bind to collagen via glycoprotein VI (GPVI) and integrin $\alpha_2\beta_1$. This initial activation traps other platelets to form thrombus.

Injury of the vessel wall provides a strong trigger for circulating platelets to interact with subendothelial layers in a shear-dependent way. Under high arterial shear condition, the primary adhesion of platelets is to von Willebrand factor (VWF) that is bound to exposed collagen fibers (Figure 1). VWF allows platelet capturing via the glycoprotein (GP) Ib-V-IX complex, with as a result platelet tethering. Subsequent firm adhesion of the platelets to collagen is mediated via the receptors glycoprotein VI and integrin $\alpha_2\beta_1$.^{2,6} Ligation of glycoprotein VI initiates clustering,⁷ followed by tyrosine phosphorylation of the immunoreceptor tyrosine-based activation motif (ITAM) in the adjacent Fc receptor γ -chain, which then leads to a cascade of protein tyrosine phosphorylation reactions via Src-family kinases and Syk.⁸ Signaling downstream

of Syk accomplishes phosphorylation and activation of phospholipase-C (PLC) $\gamma 2$, resulting in cytosolic calcium (Ca^{2+}) immobilization and downstream platelet activation responses. The latter include granule secretion and integrin $\alpha_{\text{IIb}}\beta_3$ activation, both of which processes are essential for the formation of a platelet thrombus.^{2,8} The platelet α - and δ -granules are rich source of paracrine and autocrine substances, for instance adenosine diphosphate (ADP), adenosine triphosphate (ATP) and fibrinogen, which provide positive feedback loops to potentiate and to sustain the initial activation steps.¹ In addition, activated platelets release thromboxane A_2 in a cyclooxygenase-dependent way. Also at later stages, thrombus growth relies on activation of integrin $\alpha_{\text{IIb}}\beta_3$ which binds fibrinogen, acting as a bridge between neighboring platelets.⁹ Recently, glycoprotein VI has also been shown to interact with fibrinogen and fibrin, thus suggesting a new role for this receptor in thrombus growth.^{10,11}

Platelet Ca^{2+} homeostasis as a key modulator of platelet function

Elevated cytosolic Ca^{2+} is an important second messenger in platelet activation. In resting platelets, the cytosolic Ca^{2+} concentration is low (<100 nM),¹² whereas the intracellular stores in the dense tubular system concentrate Ca^{2+} at a high concentration (100-400 μM).¹³ Upon platelet activation, rapid release of Ca^{2+} from the stores triggers Ca^{2+} entry from the extracellular medium through various Ca^{2+} channels. The pattern and extent of Ca^{2+} release and accompanying entry depend on the type of platelet stimuli (Figure 2). For instance, thrombin activation via the protease-activated receptors (PAR) 1 and 4 induces repetitive spiking Ca^{2+} rises in human platelets, while collagen acting via glycoprotein VI evokes a prolonged high Ca^{2+} elevation.¹⁴ These various Ca^{2+} responses depend on the isoform of PLC that is activated: PLC $\beta 2/3$ in case of thrombin and PLC $\gamma 2$ in case of collagen, and thereby on the extent of diacylglycerol and inositol-1,4,5-triphosphate production.¹⁵ Furthermore, it is known that thrombin stimulation triggers the pathway of receptor-operated Ca^{2+} entry, whereas collagen stimulation causes store-operated Ca^{2+} entry (SOCE).^{15,16} As the result of a continued high cytosolic Ca^{2+} , the negatively charged phospholipid phosphatidylserine becomes exposed at the platelet outer surface, which provides a surface for local thrombin generation thus stimulation of the coagulation process.^{17,18}

Considering that a sustained high Ca^{2+} level is required for phosphatidylserine exposure and that SOCE activity contributes to the prolonged Ca^{2+} rise, there is a continued interest in the importance of platelet SOCE in the context of hemostasis and thrombosis.¹⁴ The key molecular regulators of SOCE are stromal interaction molecule-1

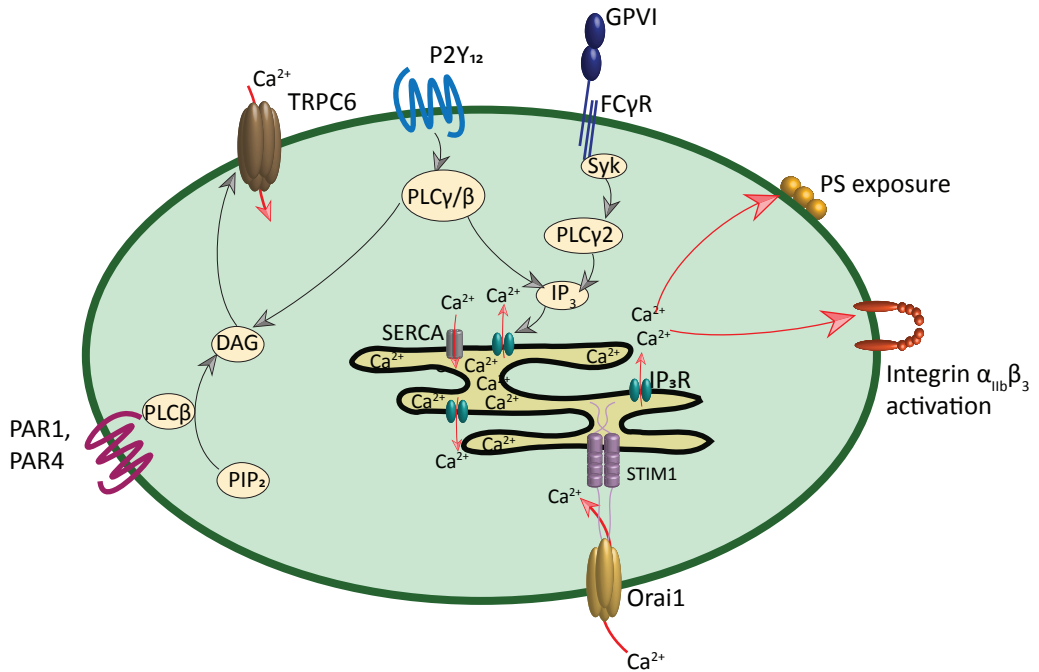


Figure 2. Summary of calcium homeostasis in platelets. Upon stimulation with platelet agonists such as thrombin, collagen or ADP, phospholipase C (PLC) isoforms-mediated production of inositol-1,4,5 trisphosphate (IP_3) and diacylglycerol (DAG) regulate Ca^{2+} entry in platelets. IP_3 activates the IP_3 receptor (IP_3R) in the endoplasmic reticulum membrane enabling Ca^{2+} mobilization through its Ca^{2+} channel pore. The Ca^{2+} depletion of the endoplasmic reticulum triggers the Ca^{2+} sensor STIM1 to open Orai1 Ca^{2+} channels in the plasma membrane, allowing extracellular Ca^{2+} influx into the platelet. Intracellular Ca^{2+} level elevation results in platelet procoagulant activity (PS exposure) and integrin $\alpha_{IIb}\beta_3$ activation.

(STIM1) and the Ca^{2+} channel, Orai1. STIM1 is located at the endoplasmic reticulum membrane, where it senses the Ca^{2+} store content.¹⁹ Upon platelet activation, Ca^{2+} store depletion triggers the redistribution and dimerization of STIM1, causing it to interact with the plasma membrane. At this stage, STIM1 activates and opens the plasma membrane Ca^{2+} channel Orai1, resulting in entry of extracellular Ca^{2+} .²⁰ Both *in vivo* and *in vitro* studies using human or mouse blood with pharmacological inhibitors have demonstrated that absence or blockage of these proteins markedly impairs platelet Ca^{2+} signaling and clearly affects thrombus formation.²¹⁻²³ While the roles of STIM1 and Orai1 for mouse platelet properties are well-studied today, only incidental reports describe the consequences of defects of STIM1 or Orai1 in human platelets. In addition, also for clinical reasons, there is a need for systematically comparing the importance of SOCE in platelets and other blood cells.

Platelet-leukocyte interactions

Platelets as well as leukocytes have for long been recognized to contribute to atherosclerotic plaque development, microvascular thrombosis and venous thromboinflammation.^{18,24,25} These observations have led to few investigations on the interactions between these cell types. *In vivo* and *in vitro* studies demonstrated that platelets and leukocytes interact with each other in inflammatory and thrombotic processes.²⁶⁻²⁸

Studies focusing on the crosstalk between leukocytes (in particular neutrophils) and platelets have revealed several cross-cellular receptor pairs (Figure 3). These are the P-selectin-PSGL1 (P-selectin glycoprotein ligand-1), CD40L-CD40 and glycoprotein Ib-neutrophil integrin β_2 (CD18) axes, which are considered to be the primarily regulators of platelet adhesion to leukocytes.²⁹⁻³¹ Furthermore, a number of platelet-derived substances were found to have a leukocyte-attracting potential; these include the chemokines platelet factor 4 (CXCL4), neutrophil-activating peptide-2 (NAP-2, CXCL7) and RANTES (CCL5); and further platelet-activating factors.^{29,32-35} A similar spectrum of chemokines plays a role in leukocyte attachment to the endothelium. Platelet-leukocyte interaction also stimulates the leukocytes to migrate by chemotactic gradients.³⁶

In the contexts of sepsis and sterile inflammation, it has been postulated that the communication of neutrophils with platelets triggers the formation of neutrophil extracellular traps (NETs).³⁷⁻³⁹ These NETS are defined as a network of externalized deoxyribonucleic acid (DNA) containing histones and granular proteases and function

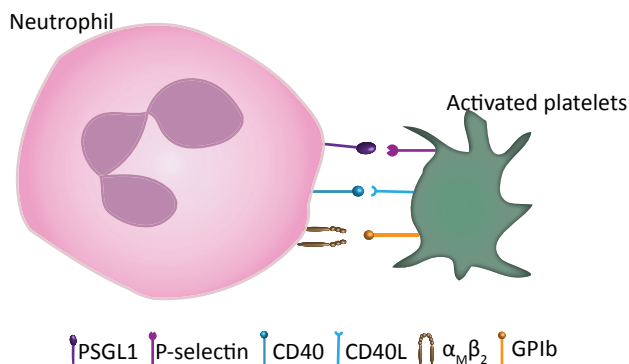


Figure 3. Established neutrophil-platelet interactions with relevant receptors. Neutrophils are recruited to activated platelets via multiple receptor-ligand interaction. The neutrophil tethering to activated platelets is initiated by P-selectin and PSGL1 on platelet and neutrophils and followed by interaction between CD40 and CD40L; $\alpha_M\beta_2$ and GPIb.

to kill bacteria.⁴⁰ The platelet-dependent NET formation may involve both direct contact via adhesion molecules and indirect stimulation via soluble substances.^{41,42} However, the literature is not unambiguous. For instance, P-selectin has been proposed to enhance NET formation in mouse.⁴¹ On the other hand, in human platelets, blockage of P-selectin did not appear to affect NET formation, nor did recombinant P-selectin.⁴³

Irrespective of the formation of NETs, only limited data are available on signaling mechanisms that lead to platelet-induced neutrophil activation. Earlier studies demonstrated that PAF stimulates neutrophils, as deduced from an intracellular Ca^{2+} elevation.⁴⁴ Recent work showed that such Ca^{2+} rises can regulate neutrophil degranulation, migration, phagocytosis and integrin activation.^{45,46} However, in the context of thrombus formation, activation responses of neutrophils have hardly been investigated.

Junctional contacts in platelet-platelet interactions

In a growing thrombus, platelet aggregates are held together via fibrinogen bridges, and these aggregates are separated from patches of phosphatidylserine exposing ballooned platelets with.^{47,48} The aggregated platelets undergo contraction to form a solid thrombus.⁴⁹ In a thrombus there is considerable heterogeneity of platelet types. The thrombus core region has been shown consisting of activated, tightly packed platelets, and the outer shell region of loosely adhered platelets with a low activation stage.⁵⁰⁻⁵¹ Platelets in the core region undergo contraction, which process contributes to thrombus stability.⁴⁹ The observation that a thrombus is partly contracted can raise the question by which other mechanisms than only fibrinogen bridges the aggregating platelets are held together.

In tissue-forming cells, such as epithelial and endothelial cells, different types of tight connections exist between the adjacent cells. So-called *gap junctions* are present that serve for cross-cellular communication, while *adherens junctions* anchor the cells to each other, and *tight junctions* provide a paracellular transport between the cells.^{52,53} Both the adherens and tight junctions are associated with the actin cytoskeleton, and their formation relies on cytoskeleton re-organization.⁵² Given the extensive junctional formation in tissue-forming, interacting cells, it can be postulated that aggregating and contracting platelets are also held together by such connections.

A number of proteins are highly expressed in platelets that are implicated in gap junctions in other cell types, in particular the isoforms connexin-37 and connexin-40.⁵⁴ Recent work demonstrated that these connexins can instigate gap junctional formation between neighboring platelets, and that genetic deletion or pharmacological blockage

of the connexin-40 resulted in impaired platelet aggregation, while blockage of connexin 37 increased aggregation of platelet-rich plasma. Together, these data provided the first evidence for a regulatory role of gap junctions in platelet-platelet interaction.⁵⁵⁻⁵⁷

In addition to connexins, platelets appear to express several tight junction proteins, which can regulate distinct platelet activation processes. For instance, the junctional adhesion molecule-A (JAM-A), as a component of tight junctions in other cell types,⁵⁸ was found to be a negative regulator of platelet integrin $\alpha_{IIb}\beta_3$ outside-in signaling.^{59,60} In mice, the deletion of JAM-A resulted in platelet hyperreactivity and enhanced clot retraction. Another tight junction protein expressed in platelets, *i.e.* endothelial cell specific adhesion molecule (ESAM), was shown to localize at sites of platelet-platelet interactions. The deletion of this protein resulted in an increased thrombus formation.⁶¹ So far, the precise roles of JAM-A and ESAM in platelet tight junction formation are still unresolved. Interestingly, proteomic analyses indicated that platelets also express additional sets of tight junction proteins, such as zona occludens-2 (ZO-2) and claudin-5.⁶² These proteins have been investigated in epithelial cells,⁶³ but so far not in platelets.

Based on this information, the hypothesis can be raised that the formation of tight, adherens and/or gap junctions is instrumental to platelet aggregation and contraction in a thrombus and, hence, contributes to intra-thrombus heterogeneity.

Inherited and acquired changes in platelet functions

A wide range of inherited or acquired platelet function disorders are associated with impaired hemostasis and bleeding.⁶⁴⁻⁶⁶ In many cases, these are disorders are characterized by a reduction in platelet count accompanying reduced platelet functions.^{66,67} Herein, the genetic defect can manifest as altered megakaryopoiesis, reduced proplatelet formation and/or platelet dysfunction, thus leading to receptor or signaling protein defects.^{66,68} More limited are the cases where there is evidence for an increase in platelet function, associating with a higher risk of thrombosis.^{67,69}

In several instances, genetic platelet function defects are accompanied by immune cell deficiencies. For instance, platelet activation processes are known to be impaired in case of mutations that are linked to immune deficiencies such as the Wiskott-Aldrich syndrome, leukocyte adhesion deficiency-III (LAD-III), and the Stormorken syndrome.⁷⁰⁻⁷² Immune deficiency can furthermore be caused by mutations in the *STIM1* or *ORAI1* genes. Patients with such mutations usually suffer from thrombocytopenia and a mild bleeding diathesis.⁷¹ However, platelet activation in these patients has not been studied comprehensively. On the other hand, it is known that blockage of the Orai1 channel *in*

vitro resulted in impaired Ca^{2+} signaling and reduced whole-blood thrombus formation.⁷³ This pharmacological evidence is in line with the results of murine studies, reporting impaired arterial thrombus formation *in vivo* and increased bleeding times.^{22,23,74,75} Given this, it is hence of relevance to better determine the Ca^{2+} signaling and subsequent responses leading to thrombus formation of platelets from patients with genetic defects in STIM1 or Orai1 in detail.

Congenital platelet disorders can also result from a defect in adhesive receptors, *e.g.* Glanzmann's thrombasthenia (integrin $\alpha_{\text{IIb}}\beta_3$ deficiency), platelet-type von Willebrand disease (glycoprotein Ib-V-IX defects), or glycoprotein VI deficiency. These receptor deficiencies usually manifest as impairments in platelet adhesion and/or aggregation.⁶⁵ Given the focus of this thesis, I shall concentrate below on glycoprotein VI.

Glycoprotein VI is the major collagen receptor on platelets and a key player in platelet activation upon vascular injury.⁷⁶ Patients carrying a *GP6* mutation, leading to the absence of glycoprotein VI, manifest only a minor bleeding diathesis.^{77,78} This is in line with mouse studies confirming that the lack of glycoprotein VI does not cause severe bleeding, in spite of a strong protective effect against experimentally induced arterial thrombosis.⁷⁹⁻⁸¹ Based on these findings, and the fact that the receptor is exclusively expressed in the platelet lineage, glycoprotein VI has become an interesting target for new antiplatelet therapies.⁸² At present, several glycoprotein VI antagonists are in development and tested in clinical trials. For instance, Revacept, a soluble dimeric glycoprotein VI-Fc fusion protein is used in a phase II clinical trial.⁸³ Monoclonal antibody derived fragments (Fab) against GPVI, such as Fab9012.2 has been proven to block GPVI efficiently as well.^{84,85} However, the latter was not suitable for *in vivo* use in human due to its rodent origin. Therefore a humanized Fab variant, ACT07 has been developed based on the epitope of Fab9012.2.⁸⁵ ACT07 have been enrolled into phase II clinical trials with acute ischemic stroke.⁸⁶

Platelet functions can also be altered in an acquired way, *i.e.* without genetic predisposition.⁶⁷ Negative priming is, per definition, consequence of treatment with antiplatelet drugs such as aspirin or inhibitors of the platelet P2Y_{12} receptors for ADP. On the other hand, several disorders such as hyperlipidemia, type II diabetes mellitus and metabolic syndrome can lead to platelet hyperreactivity, *i.e.* positive platelet priming, and as a consequence to an increased cardiovascular risk.⁸⁷⁻⁸⁹ Increased platelet reactivity can be due by plasma lipid levels, oxidative stress, partial endothelial dysfunction or

hyperglycemia.^{90,91} This positive priming effect is an important issue in treatments as positively primed platelets has appeared to contribute to the resistance to antiplatelet therapy.⁹²

Regarding diabetes mellitus, patients are sometimes treated with new glucose lowering drugs, of which the dipeptidyl peptidase 4 (DPP4) antagonists and glucagon-like peptide 1 (GLP1) receptor agonists show promising results.^{87,93} These drugs act by blocking the proteolytic activity of DPP4 and thereby elevating the uncleaved GLP1 hormone level which results in higher insulin secretion.^{94,95} Given the fact that platelets also express dipeptidyl peptidases⁶², and are reported to contain the GLP1 receptor⁹⁶, it can be expected that patient treatment with DPP4 antagonists affects platelet activation processes, but this has not been examined in detail.

Microfluidic devices for studying thrombosis and hemostasis in whole blood

In current clinical practice, a panel of platelet function tests is used to explain bleeding tendencies and to determine the efficacy of antiplatelet therapies.⁹⁷⁻¹⁰⁰ The majority of these tests are carried out under stasis or in slowly stirred platelet suspensions, and hence do not take into account the role of high-shear blood flow. An exception is the Platelet Function Analyzer-100 (PFA-100), which detect platelet aggregation at high shear (5,000-6,000 s^{-1}). However, this device appears to be relatively insensitive to (mild) platelet dysfunctions.^{101,102} Microfluidics devices, in which whole blood is perfused through a small flow chamber, also act in a shear-based way. A recent overview paper indicate

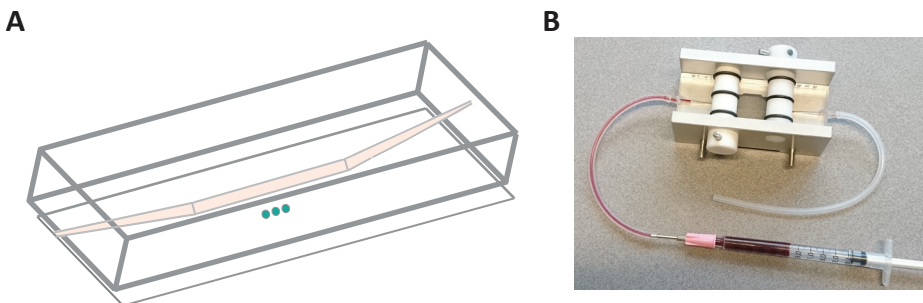


Figure 4. General setup of the Maastricht microfluidics parallel-plate flow chamber. (A) Schematic representation of the Maastricht flow chamber. Light pink indicates the channel through which blood is perfused (dimensions: 50 μ M depth, 3 mm width). Green dots represent the coating on a coverslip that is mounted into a holder together with the chamber. **(B)** Aluminium holder with bolts for the attachment of coverslip to the flow chamber.

that the aberrations in flow-dependent thrombus formation measured with such devices correlates with an altered bleeding time and altered arterial thrombosis in multiple genetically deficient mice.¹⁰³

Of the various types of microfluidic devices, in particular parallel-plate flow chambers (Figure 4) are of current interest for monitoring of the combined processes of platelet adhesion, aggregation and thrombus formation under defined flow conditions.¹⁰⁴⁻¹⁰⁶ In addition, these devices allow simultaneous detection of platelet and coagulation activity can be performed.¹⁰⁷ This makes it even possible to identify combination of platelet- and coagulation-based bleeding disorders.^{81,104,108-111}

Aims and outline of the thesis

In this thesis, so far non-characterized aspects of thrombus formation are studied to better understand in greater detail how blood platelets regulate this process in interaction with vessel wall components, the blood plasma and leukocytes. In **Chapter 1**, a brief introduction is given of relevant signaling pathways and roles of platelets in the context of thrombus formation. **Chapter 2** provides an overview of the currently available microfluidic devices for studying platelet and coagulation processes in flowed whole blood. This chapter also includes practical guidance on technical aspects on how to measure these processes. **Chapter 3** describes the regulation and importance of calcium homeostasis for the activation of platelets and other blood cells, in particular focusing on the role of SOCE. Discussed are in detail how an impairment in SOCE can influence thrombo-inflammatory reactions. The dysregulation of SOCE can be associated with genetically linked immune-deficiencies that affect platelet activation processes. **Chapter 4** studies the roles of platelets in thrombus formation for nine patients with rare immunodeficiencies, and it unravels when and how specific mutations in SOCE genes can alter platelet function in this process. **Chapter 5** aims to understand how the platelets in a thrombus trigger adhesion and activation processes in leukocytes, in particular neutrophils. This study focuses on how platelet-released substances, mostly playing a role in inflammation, induce intracellular Ca²⁺ rises in neutrophils and subsequent cellular responses. The next **Chapter 6** re-analyzes previous datasets, in which platelet activation and thrombus formation were studied in blood from multiple genetically modified mice. By a systematic comparison of the earlier collected data it is aimed to obtain better insight into the signaling pathways, by which the primarily collagen receptor glycoprotein VI, steers platelet activation in shear-dependent thrombus formation. A network is constructed revealing novel genes with a potential role in glycoprotein VI-dependent

thrombus formation. The corresponding proteins may be targets for novel antiplatelet therapy. **Chapter 7** examines how two small molecules, losartan and honokiol, alter platelet activation processes via interference with the glycoprotein VI receptor as well as underlying signaling pathways. **Chapter 8** describes a new concept of platelet-platelet communication via distinct inter-cellular junctions, which so far have not been investigated in this cell type. **Chapter 9** takes forward the concept of platelet priming, by studying the roles of dipeptidyl peptidase isoforms in plasma (or stored in platelets) in thrombus formation and related platelet activation processes. In **Chapter 10**, the most important findings of this thesis are critically discussed in relation to the literature.

References

1. Van der Meijden PEJ, Heemskerk JWM. Platelet biology and functions: new concepts and clinical perspectives. *Nat Rev Cardiol*. 2019; 16: 166-179.
2. Versteeg HH, Heemskerk JW, Levi M, Reitsma PH. New fundamentals in hemostasis. *Physiol Rev*. 2013; 93: 327-358.
3. Libby P, Pasterkamp G, Crea F, Jang IK. Reassessing the mechanisms of acute coronary syndromes. *Circ Res*. 2019; 124: 150-160.
4. Tan KT, Lip GY. Red vs white thrombi: treating the right clot is crucial. *Arch Intern Med*. 2003; 163: 2534-2535.
5. Koupenova M, Kehrel BE, Corkrey HA, Freedman JE. Thrombosis and platelets: an update. *Eur Heart J*. 2017; 38: 785-791.
6. Ruggeri ZM, Mendolicchio GL. Interaction of von Willebrand factor with platelets and the vessel wall. *Hamostaseologie*. 2015; 35: 211-224.
7. Poulter NS, Pollitt AY, Owen DM, et al. Clustering of glycoprotein VI (GPVI) dimers upon adhesion to collagen as a mechanism to regulate GPVI signaling in platelets. *J Thromb Haemost*. 2017; 15: 549-564.
8. Nieswandt B, Watson SP. Platelet-collagen interaction: is GPVI the central receptor? *Blood*. 2003; 102: 449-461.
9. Cosemans JM, Angelillo-Scherrer A, Mattheij NJ, Heemskerk JW. The effects of arterial flow on platelet activation, thrombus growth, and stabilization. *Cardiovasc Res*. 2013; 99: 342-352.
10. Mammadova-Bach E, Ollivier V, Loyau S, et al. Platelet glycoprotein VI binds to polymerized fibrin and promotes thrombin generation. *Blood*. 2015; 126: 683-691.
11. Mangin PH, Onselaer MB, Receveur N, et al. Immobilized fibrinogen activates human platelets through glycoprotein VI. *Haematologica*. 2018; 103: 898-907.
12. Rink TJ, Sage SO. Calcium signaling in human platelets. *Annu Rev Physiol*. 1990; 52: 431-449.
13. Dolan AT, Diamond SL. Systems modeling of Ca²⁺ homeostasis and mobilization in platelets mediated by IP3 and store-operated Ca²⁺ entry. *Biophys J*. 2014; 106: 2049-2060.
14. Heemskerk JW, Mattheij NJ, Cosemans JM. Platelet-based coagulation: different populations, different functions. *J Thromb Haemost*. 2013; 11: 2-16.
15. Varga-Szabo D, Braun A, Nieswandt B. Calcium signaling in platelets. *J Thromb Haemost*. 2009; 7: 1057-1066.
16. Harper MT, Poole AW. Store-operated calcium entry and non-capacitative calcium entry have distinct roles in thrombin-induced calcium signalling in human platelets. *Cell Calcium*. 2011; 50: 351-358.
17. Munnix IC, Harmsma M, Giddings JC, et al. Store-mediated calcium entry in the regulation of phosphatidylserine exposure in blood cells from Scott patients. *Thromb Haemost*. 2003; 89: 687-695.
18. Rademakers T, Douma K, Hackeng TM, et al. Plaque-associated vasa vasorum in aged apolipoprotein E-deficient mice exhibit proatherogenic functional features in vivo. *Arterioscler Thromb Vasc Biol*. 2013; 33: 249-256.
19. Shen WW, Frieden M, Demaurex N. Local cytosolic Ca²⁺ elevations are required for stromal interaction molecule 1 (STIM1) de-oligomerization and termination of store-operated Ca²⁺ entry. *J Biol*

- Chem.* 2011; 286: 36448-36459.
20. Stathopoulos PB, Zheng L, Li GY, Plevin MJ, Ikura M. Structural and mechanistic insights into STIM1-mediated initiation of store-operated calcium entry. *Cell.* 2008; 135: 110-122.
 21. Gilio K, van Kruchten R, Braun A, *et al.* Roles of platelet STIM1 and Orai1 in glycoprotein VI- and thrombin-dependent procoagulant activity and thrombus formation. *J Biol Chem.* 2010; 285: 23629-23638.
 22. Varga-Szabo D, Braun A, Kleinschnitz C, *et al.* The calcium sensor STIM1 is an essential mediator of arterial thrombosis and ischemic brain infarction. *J Exp Med.* 2008; 205: 1583-1591.
 23. Braun A, Varga-Szabo D, Kleinschnitz C, *et al.* Orai1 (CRACM1) is the platelet SOC channel and essential for pathological thrombus formation. *Blood.* 2009; 113: 2056-2063.
 24. Ionita MG, van den Borne P, Catanzariti LM, *et al.* High neutrophil numbers in human carotid atherosclerotic plaques are associated with characteristics of rupture-prone lesions. *Arterioscler Thromb Vasc Biol.* 2010; 30: 1842-1848.
 25. Weber C, Noels H. Atherosclerosis: current pathogenesis and therapeutic options. *Nat Med.* 2011; 17: 1410-1422.
 26. Soehnlein O. Decision shaping neutrophil-platelet interplay in inflammation: From physiology to intervention. *Eur J Clin Invest.* 2018; 48.
 27. Deppermann C. Platelets and vascular integrity. *Platelets.* 2018; 29: 549-555.
 28. Rossaint J, Zarbock A. Platelets in leucocyte recruitment and function. *Cardiovasc Res.* 2015; 107: 386-395.
 29. Ghasemzadeh M, Hosseini E. Platelet-leukocyte crosstalk: Linking proinflammatory responses to procoagulant state. *Thromb Res.* 2013; 131: 191-197.
 30. Lievens D, Zerneck A, Seijkens T, *et al.* Platelet CD40L mediates thrombotic and inflammatory processes in atherosclerosis. *Blood.* 2010; 116: 4317-4327.
 31. Wang Y, Sakuma M, Chen Z, *et al.* Leukocyte engagement of platelet glycoprotein Iba α via the integrin Mac-1 is critical for the biological response to vascular injury. *Circulation.* 2005; 112: 2993-3000.
 32. Hartwig H, Drechsler M, Lievens D, *et al.* Platelet-derived PF4 reduces neutrophil apoptosis following arterial occlusion. *Thromb Haemost.* 2014; 111: 562-564.
 33. Koenen RR, von Hundelshausen P, Nesmelova IV, *et al.* Disrupting functional interactions between platelet chemokines inhibits atherosclerosis in hyperlipidemic mice. *Nat Med.* 2009; 15: 97-103.
 34. von Hundelshausen P, Koenen RR, Weber C. Platelet-mediated enhancement of leukocyte adhesion. *Microcirculation.* 2009; 16: 84-96.
 35. Kulkarni S, Woollard KJ, Thomas S, Oxley D, Jackson SP. Conversion of platelets from a proaggregatory to a proinflammatory adhesive phenotype: role of PAF in spatially regulating neutrophil adhesion and spreading. *Blood.* 2007; 110: 1879-1886.
 36. Ghasemzadeh M, Kaplan ZS, Alwis I, *et al.* The CXCR1/2 ligand NAP-2 promotes directed intravascular leukocyte migration through platelet thrombi. *Blood.* 2013; 121: 4555-4566.
 37. Carestia A, Kaufman T, Rivadeneyra L, *et al.* Mediators and molecular pathways involved in the regulation of neutrophil extracellular trap formation mediated by activated platelets. *J Leukoc Biol.* 2016; 99: 153-162.
 38. Liu S, Su X, Pan P, *et al.* Neutrophil extracellular traps are indirectly triggered by lipopolysaccharide and contribute to acute lung injury. *Sci Rep.* 2016; 6: 37252.
 39. McDonald B, Davis RP, Kim SJ, *et al.* Platelets and neutrophil extracellular traps collaborate to promote intravascular coagulation during sepsis in mice. *Blood.* 2017; 129: 1357-1367.
 40. Brinkmann V, Reichard U, Goosmann C, *et al.* Neutrophil extracellular traps kill bacteria. *Science.* 2004; 303: 1532-1535.
 41. Etulain J, Martinod K, Wong SL, *et al.* P-selectin promotes neutrophil extracellular trap formation in mice. *Blood.* 2015; 126: 242-246.
 42. Rossaint J, Herter JM, Van Aken H, *et al.* Synchronized integrin engagement and chemokine activation is crucial in neutrophil extracellular trap-mediated sterile inflammation. *Blood.* 2014; 123: 2573-2584.
 43. Maugeri N, Campana L, Gavina M, *et al.* Activated platelets present high mobility group box 1 to neutrophils, inducing autophagy and promoting the extrusion of neutrophil extracellular traps. *J Thromb Haemost.* 2014; 12: 2074-2088.
 44. Sage SO, Pintado E, Mahaut-Smith MP, Merritt JE. Rapid kinetics of agonist-evoked changes in cytosolic free Ca²⁺ concentration in fura-2-loaded human neutrophils. *Biochem J.* 1990; 265: 915-918.
 45. Immler R, Simon SI, Sperandio M. Calcium signalling and related ion channels in neutrophil recruitment and function. *Eur J Clin Invest.* 2018; 48 Suppl 2: e12964.

46. Hubner K, Surovtsova I, Yserentant K, Hansch M, Kummer U. Ca²⁺ dynamics correlates with phenotype and function in primary human neutrophils. *Biophys Chem.* 2013; 184: 116-125.
47. Munnix IC, Kuijpers MJ, Auger J, *et al.* Segregation of platelet aggregatory and procoagulant microdomains in thrombus formation: regulation by transient integrin activation. *Arterioscler Thromb Vasc Biol.* 2007; 27: 2484-2490.
48. de Witt SM, Verdood R, Cosemans JM, Heemskerk JW. Insights into platelet-based control of coagulation. *Thromb Res.* 2014; 133 Suppl 2: S139-148.
49. Calaminus SD, Auger JM, McCarty OJ, *et al.* MyosinIIa contractility is required for maintenance of platelet structure during spreading on collagen and contributes to thrombus stability. *J Thromb Haemost.* 2007; 5: 2136-2145.
50. Welsh JD, Stalker TJ, Voronov R, *et al.* A systems approach to hemostasis: 1. The interdependence of thrombus architecture and agonist movements in the gaps between platelets. *Blood.* 2014; 124: 1808-1815.
51. Ivanciu L, Stalker TJ. Spatiotemporal regulation of coagulation and platelet activation during the hemostatic response in vivo. *J Thromb Haemost.* 2015; 13: 1949-1959.
52. Hartsock A, Nelson WJ. Adherens and tight junctions: structure, function and connections to the actin cytoskeleton. *Biochim Biophys Acta.* 2008; 1778: 660-669.
53. Figueroa XF, Duling BR. Gap junctions in the control of vascular function. *Antioxid Redox Signal.* 2009; 11: 251-266.
54. Molica F, Stierlin FB, Fontana P, Kwak BR. Pannexin- and connexin-mediated intercellular communication in platelet function. *Int J Mol Sci.* 2017; 18.
55. Angelillo-Scherrer A, Fontana P, Burnier L, *et al.* Connexin 37 limits thrombus propensity by down-regulating platelet reactivity. *Circulation.* 2011; 124: 930-939.
56. Vaiyapuri S, Jones CI, Sasikumar P, *et al.* Gap junctions and connexin hemichannels underpin hemostasis and thrombosis. *Circulation.* 2012; 125: 2479-2491.
57. Vaiyapuri S, Moraes LA, Sage T, *et al.* Connexin40 regulates platelet function. *Nat Commun.* 2013; 4: 2564.
58. Severson EA, Parkos CA. Mechanisms of outside-in signaling at the tight junction by junctional adhesion molecule A. *Ann N Y Acad Sci.* 2009; 1165: 10-18.
59. Karshovska E, Zhao Z, Blanchet X, *et al.* Hyperreactivity of junctional adhesion molecule A-deficient platelets accelerates atherosclerosis in hyperlipidemic mice. *Circ Res.* 2015; 116: 587-599.
60. Naik MU, Stalker TJ, Brass LF, Naik UP. JAM-A protects from thrombosis by suppressing integrin $\alpha_{IIb}\beta_3$ -dependent outside-in signaling in platelets. *Blood.* 2012; 119: 3352-3360.
61. Stalker TJ, Wu J, Morgans A, *et al.* Endothelial cell specific adhesion molecule (ESAM) localizes to platelet-platelet contacts and regulates thrombus formation in vivo. *J Thromb Haemost.* 2009; 7: 1886-1896.
62. Burkhart JM, Vaudel M, Gambaryan S, *et al.* The first comprehensive and quantitative analysis of human platelet protein composition allows the comparative analysis of structural and functional pathways. *Blood.* 2012; 120: e73-82.
63. Traweger A, Toepfer S, Wagner RN, *et al.* Beyond cell-cell adhesion: Emerging roles of the tight junction scaffold ZO-2. *Tissue Barriers.* 2013; 1: e25039.
64. Jurk K, Kehrel BE. Inherited and acquired disorders of platelet function. *Transfus Med Hemother.* 2007; 34: 6-19.
65. Nurden AT, Nurden P. Congenital platelet disorders and understanding of platelet function. *Br J Haematol.* 2014; 165: 165-178.
66. Lentaigne C, Freson K, Laffan MA, Turro E, Ouwehand WH. Inherited platelet disorders: toward DNA-based diagnosis. *Blood.* 2016; 127: 2814-2823.
67. Baaten C, ten Cate H, van der Meijden PEJ, Heemskerk JWM. Platelet populations and priming in hematological diseases. *Blood Rev.* 2017; 31: 389-399.
68. Nurden AT, Freson K, Seligsohn U. Inherited platelet disorders. *Haemophilia.* 2012; 18 Suppl 4: 154-160.
69. Cassar K, Bachoo P, Ford I, Greaves M, Brittenden J. Platelet activation is increased in peripheral arterial disease. *J Vasc Surg.* 2003; 38: 99-103.
70. Sereni L, Castiello MC, Marangoni F, *et al.* Autonomous role of Wiskott-Aldrich syndrome platelet deficiency in inducing autoimmunity and inflammation. *J Allergy Clin Immunol.* 2018; 142: 1272-1284.
71. Lacruz RS, Feske S. Diseases caused by mutations in ORAI1 and STIM1. *Ann N Y Acad Sci.* 2015; 1356: 45-79.
72. Jurk K, Schulz AS, Kehrel BE, *et al.* Novel integrin-dependent platelet malfunction in siblings with

- leukocyte adhesion deficiency-III (LAD-III) caused by a point mutation in FERMT3. *Thromb Haemost.* 2010; 103: 1053-1064.
73. van Kruchten R, Braun A, Feijge MA, *et al.* Antithrombotic potential of blockers of store-operated calcium channels in platelets. *Arterioscler Thromb Vasc Biol.* 2012; 32: 1717-1723.
74. Bergmeier W, Oh-Hora M, McCarl CA, *et al.* R93W mutation in *Orai1* causes impaired calcium influx in platelets. *Blood.* 2009; 113: 675-678.
75. Grosse J, Braun A, Varga-Szabo D, *et al.* An EF hand mutation in *Stim1* causes premature platelet activation and bleeding in mice. *J Clin Invest.* 2007; 117: 3540-3550.
76. Rayes J, Watson SP, Nieswandt B. Functional significance of the platelet immune receptors GPVI and CLEC-2. *J Clin Invest.* 2019; 129: 12-23.
77. Matus V, Valenzuela G, Saez CG, *et al.* An adenine insertion in exon 6 of human GP6 generates a truncated protein associated with a bleeding disorder in four Chilean families. *J Thromb Haemost.* 2013; 11: 1751-1759.
78. Dumont B, Lasne D, Rothschild C, *et al.* Absence of collagen-induced platelet activation caused by compound heterozygous GPVI mutations. *Blood.* 2009; 114: 1900-1903.
79. Pachel C, Mathes D, Arias-Loza AP, *et al.* Inhibition of platelet GPVI protects against myocardial ischemia-reperfusion injury. *Arterioscler Thromb Vasc Biol.* 2016; 36: 629-635.
80. Goebel S, Li Z, Vogelmann J, *et al.* The GPVI-Fc fusion protein Revacept improves cerebral infarct volume and functional outcome in stroke. *PLoS One.* 2013; 8: e66960.
81. Lehmann M, Ashworth K, Manco-Johnson M, *et al.* Evaluation of a microfluidic flow assay to screen for von Willebrand disease and low von Willebrand factor levels. *J Thromb Haemost.* 2018; 16: 104-115.
82. Andrews RK, Arthur JF, Gardiner EE. Targeting GPVI as a novel antithrombotic strategy. *J Blood Med.* 2014; 5: 59-68.
83. Ungerer M, Rosport K, Bultmann A, *et al.* Novel antiplatelet drug revacept (dimeric glycoprotein VI-Fc) specifically and efficiently inhibited collagen-induced platelet aggregation without affecting general hemostasis in humans. *Circulation.* 2011; 123: 1891-1899.
84. Lecut C, Feeney LA, Kingsbury G, *et al.* Human platelet glycoprotein VI function is antagonized by monoclonal antibody-derived Fab fragments. *J Thromb Haemost.* 2003; 1: 2653-2662.
85. Mangin PH, Tang C, Bourdon C, *et al.* A humanized glycoprotein VI (GPVI) mouse model to assess the antithrombotic efficacies of anti-GPVI agents. *J Pharmacol Exp Ther.* 2012; 341: 156-163.
86. Acticor. Acute ischemic stroke interventional study. (<https://ClinicalTrials.gov/show/NCT03803007>).
87. Patti G, Cavallari I, Andreotti F, *et al.* Prevention of atherothrombotic events in patients with diabetes mellitus: from antithrombotic therapies to new-generation glucose-lowering drugs. *Nat Rev Cardiol.* 2019; 16: 113-130.
88. Santilli F, Vazzana N, Liani R, Guagnano MT, Davi G. Platelet activation in obesity and metabolic syndrome. *Obes Rev.* 2012; 13: 27-42.
89. Wang N, Tall AR. Cholesterol in platelet biogenesis and activation. *Blood.* 2016; 127: 1949-1953.
90. Rollini F, Franchi F, Muniz-Lozano A, Angiolillo DJ. Platelet function profiles in patients with diabetes mellitus. *J Cardiovasc Transl Res.* 2013; 6: 329-345.
91. Kaur R, Kaur M, Singh J. Endothelial dysfunction and platelet hyperactivity in type 2 diabetes mellitus: molecular insights and therapeutic strategies. *Cardiovasc Diabetol.* 2018; 17: 121.
92. Blair TA, Moore SF, Hers I. Circulating primers enhance platelet function and induce resistance to antiplatelet therapy. *J Thromb Haemost.* 2015; 13: 1479-1493.
93. Scheen AJ. Cardiovascular effects of dipeptidyl peptidase-4 inhibitors: from risk factors to clinical outcomes. *Postgrad Med.* 2013; 125: 7-20.
94. Deacon CF. Physiology and Pharmacology of DPP-4 in Glucose Homeostasis and the Treatment of Type 2 Diabetes. *Front Endocrinol (Lausanne).* 2019; 10: 80.
95. Tomlinson B, Hu M, Zhang Y, Chan P, Liu ZM. An overview of new GLP-1 receptor agonists for type 2 diabetes. *Expert Opin Investig Drugs.* 2016; 25: 145-158.
96. Steven S, Jurk K, Kopp M, *et al.* Glucagon-like peptide-1 receptor signalling reduces microvascular thrombosis, nitro-oxidative stress and platelet activation in endotoxaemic mice. *Br J Pharmacol.* 2017; 174: 1620-1632.
97. Lordkipanidze M. Platelet Function Tests. *Semin Thromb Hemost.* 2016; 42: 258-267.
98. Lassila R. Platelet Function Tests in Bleeding Disorders. *Semin Thromb Hemost.* 2016; 42: 185-190.
99. Whiting D, DiNardo JA. TEG and ROTEM: technology and clinical applications. *Am J Hematol.* 2014; 89: 228-232.
100. Vries MJ, van der Meijden PE, Kuiper GJ, *et al.* Preoperative screening for bleeding disorders: A

- comprehensive laboratory assessment of clinical practice. *Res Pract Thromb Haemost.* 2018; 2: 767-777.
101. Harrison P. The role of PFA-100 testing in the investigation and management of haemostatic defects in children and adults. *Br J Haematol.* 2005; 130: 3-10.
 102. Hayward CP, Harrison P, Cattaneo M, Ortel TL, Rao AK. Platelet function analyzer (PFA)-100 closure time in the evaluation of platelet disorders and platelet function. *J Thromb Haemost.* 2006; 4: 312-319.
 103. Baaten C, Meacham S, de Witt SM, *et al.* A synthesis approach of mouse studies to identify genes and proteins in arterial thrombosis and bleeding. *Blood.* 2018; 132: e35-e46.
 104. Brouns SLN, van Geffen JP, Heemskerk JWM. High-throughput measurement of human platelet aggregation under flow: application in hemostasis and beyond. *Platelets.* 2018; 29: 662-669.
 105. Sakariassen KS, Aarts PA, de Groot PG, Houdijk WP, Sixma JJ. A perfusion chamber developed to investigate platelet interaction in flowing blood with human vessel wall cells, their extracellular matrix, and purified components. *J Lab Clin Med.* 1983; 102: 522-535.
 106. Neeves KB, Maloney SF, Fong KP, *et al.* Microfluidic focal thrombosis model for measuring murine platelet deposition and stability: PAR4 signaling enhances shear-resistance of platelet aggregates. *J Thromb Haemost.* 2008; 6: 2193-2201.
 107. Van Kruchten R, Cosemans JM, Heemskerk JW. Measurement of whole blood thrombus formation using parallel-plate flow chambers - a practical guide. *Platelets.* 2012; 23: 229-242.
 108. de Witt SM, Swieringa F, Cavill R, *et al.* Identification of platelet function defects by multi-parameter assessment of thrombus formation. *Nat Commun.* 2014; 5: 4257.
 109. Colace TV, Fogarty PF, Panckeri KA, Li R, Diamond SL. Microfluidic assay of hemophilic blood clotting: distinct deficits in platelet and fibrin deposition at low factor levels. *J Thromb Haemost.* 2014; 12: 147-158.
 110. Schoeman RM, Lehmann M, Neeves KB. Flow chamber and microfluidic approaches for measuring thrombus formation in genetic bleeding disorders. *Platelets.* 2017; 28: 463-471.
 111. Li R, Grosser T, Diamond SL. Microfluidic whole blood testing of platelet response to pharmacological agents. *Platelets.* 2017; 28: 457-462.

Chapter 2

Use of microfluidics to assess the platelet-based control of coagulation

Nagy M, Heemskerk JWM, Swieringa F

*Platelets 2017; 28(5):441-448
Reprinted with permission*

Abstract

This paper provides an overview of the various types of microfluidic devices that are employed to study the complex processes of platelet activation and blood coagulation in whole blood under flow conditions. We elaborate on how these devices are used to detect impaired platelet-dependent fibrin formation in blood from mice or patients with specific bleeding disorders. We provide a practical guide on how to assess formation of a platelet-fibrin thrombus under flow, using equipment that is present in most laboratories. In addition, we describe current insights on how blood flow and shear rate alter the location of platelet populations, von Willebrand factor, coagulation factors and fibrin in a growing thrombus. Finally, we discuss possibilities and limitations for the clinical use of microfluidic devices to evaluate a hemostatic or prothrombotic tendency in patient blood samples.

Introduction

Platelets play a crucial role in thrombosis and hemostasis by their ability to adhere at sites of vascular injury, then aggregate and provide a procoagulant surface for thrombin generation and fibrin formation. In a damaged vessel wall, several subendothelial matrix components form a potent surface for platelet adhesion, including exposed collagen, laminin and fibrinogen, while other subendothelial components, in particular tissue factor (TF), trigger the coagulation process¹ (Figure 1A). Together, exposed TF and the adhered and activated platelets propagate the formation of a platelet-fibrin thrombus, in a way influenced by the local hemodynamic environment. An important factor herein is the wall shear rate of flowing blood, which varies from low ($<500\text{ s}^{-1}$) in the veins and venules to higher values ($>1500\text{ s}^{-1}$) in the arteries and arterioles.² Typical for the adhesion of platelets at high wall shear rate is that it is greatly enhanced by the interaction with von Willebrand factor (VWF), which by itself is captured by collagen, laminin and other matrix proteins. The VWF is produced as a multimeric protein by endothelial cells and, after partial degradation, circulates in the blood plasma at high concentrations.

In the majority of *in vivo* models of hemostasis and thrombosis, platelet aggregation is accompanied by prominent fibrin formation and both processes are considered to be required for maximal, occlusive thrombus formation.³ The importance of coagulation is also apparent from the fact that the majority of dissected thrombi in human arteries as well as veins contain both platelet-rich and fibrin-rich regions.⁴ Another hemodynamic factor is provided by a flow-dependent control of the coagulation process.⁵ Current evidence indicates that the relative extent of fibrin deposition decreases with increased

blood flow rate, which is explained by an increased dilution of the formed thrombin at higher blood flow.⁵ This can explain why in the venous blood compartment a ‘red’ thrombus is formed, consisting of red blood cells and small platelet clumps encapsulated in an extensive fibrin network. In contrast, in the arterial system with high blood flow mostly a ‘white’ thrombus is generated that is highly enriched in platelet aggregates, but also contains fibrin fibers

Based on flow studies and autopsies of such arterial and venous thrombi, there is no doubt that feed-forward interactions between platelets and coagulation are

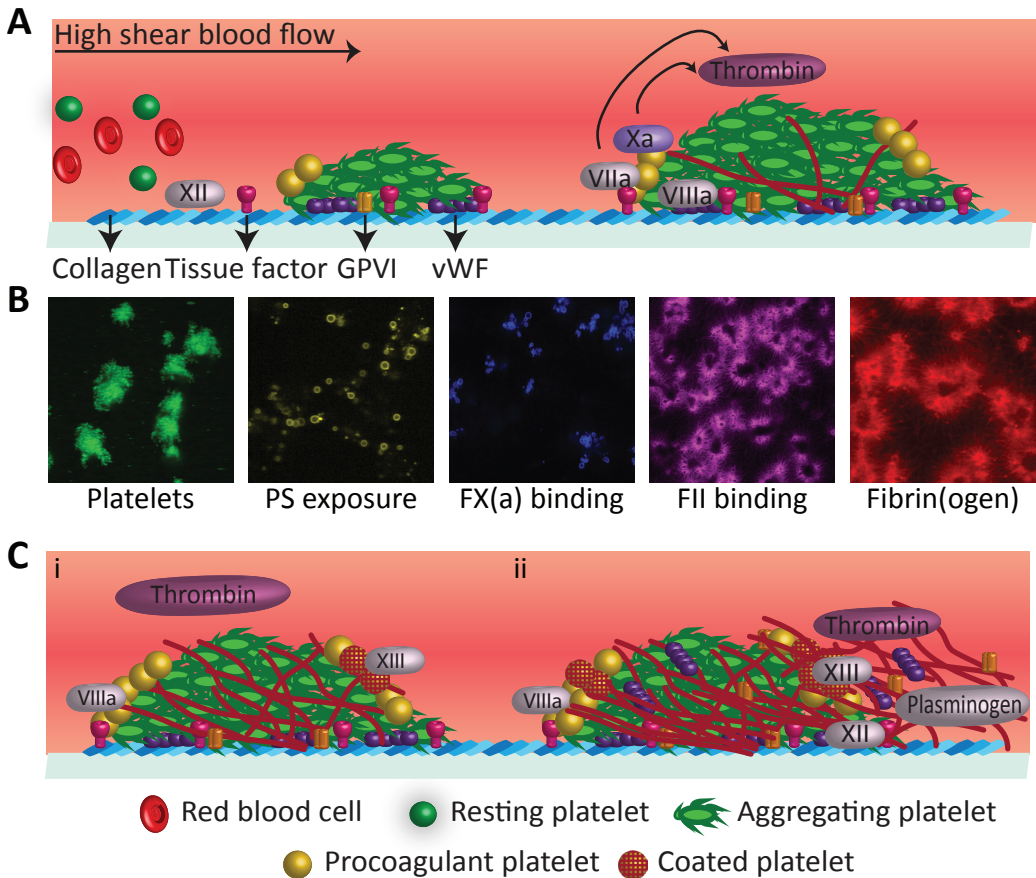


Figure 1. Platelet-based coagulation processes in a thrombus. (A) Key adhesive platelet ligands and coagulation proteins during the buildup of a platelet-fibrin thrombus. Indicated are platelet adhesion to and activation on collagen/VWF and triggering of the extrinsic (via TF) and intrinsic (via collagen) coagulation pathways. (B) Microscopic images (scale bar represents 20 μm) showing distinct location of platelets and coagulation factors in a thrombus generated at lower shear rate (200 s^{-1}). Note the difference between the aggregated and single, PS-exposing platelets, and the highly similar label pattern of fibrin and thrombin. (C) Later stages of platelet-fibrin thrombus formation with: (i) extension of an intra-thrombus fibrin network around contracted platelets with a likely role of FXII and fibrin-bound VWF/FVIII; and (ii) fibrin extension outside of the platelet thrombus with roles of fibrin-bound thrombin and plasmin. For further description, see text.

important in physiology. This has led to the concept of platelet-based coagulation.^{1,3,6} A key intermediary process herein is that platelets under specific conditions (*e.g.* prolonged intercellular Ca^{2+} rises) are capable to form a procoagulant surface by exposing the negatively charged phospholipid phosphatidylserine (PS). The PS exposure greatly promotes coagulation factor binding and thereby enforces the processes of thrombin generation and fibrin formation.⁷⁻⁹ Detailed studies indicate that the blood flow rate is an important controlling factor, as it determines the transport rates of coagulation factors to and from the procoagulant surface and thereby the extent of fibrin polymerization.^{5,10} Studies also indicate that higher blood flow stimulates fibrin degradation, by enhancing activity of the fibrinolysis activator plasmin.^{11,12}

These and other studies have led to the development of assays in which both platelet function and coagulation activity can be examined. Static tube or well plate assays have been employed, such as whole blood thromboelastography and thrombin generation, but these have as a disadvantage that massive amounts of thrombin are generated. The high thrombin, being a strong platelet agonist, makes it difficult to detect subtle changes in the functional activities of platelets. To overcome this limitation, tests using small-scale microfluidic devices have been developed, in general with a higher sensitivity towards alterations in both platelet and coagulation activation. Such microfluidic devices provide a well-controlled three-dimensional environment, operating with whole blood flowed at defined, physiological (venous or arterial) or pathological (stenotic) wall shear rates. Their small size allows use of only small amounts of blood. In combination with standard fluorescence microscopy, most microfluidic devices can operate in real-time at high-resolution, observing the adhesion of single platelets and formation of individual fibrin fibres.^{13,14}

Microfluidic flow devices and technical aspects to study platelet-based coagulation

Applications of microfluidic devices for studying platelet activation in combination with coagulation are relatively new. At present, only a limited set of studies is published, in which provisions are made for a precise control of the coagulation system. Table 1 provides an overview of typical devices and methodologies that are being used to assess platelet-dependent coagulation under flow by measurement of thrombin or fibrin formation.

The devices employed usually have flow channel dimensions of 50-100 μm depth (although some papers describe even smaller channels), in this case requiring less than

500 μl of whole blood, depending on the experimental endpoint¹⁵ (Table I). The flow channels can be fabricated from different blood-compatible materials, ranging from (albumin-blocked or siliconized) glass and hard plastics to soft polymers such as polydimethylsiloxane (PDMS). The latter PDMS channels can be custom-made in a cost-effective way with easily adaptable dimensions.¹³ However, when using homemade polymerizing and contracting PDMS material, the channels should be checked for microscopic surface irregularities, which can cause local changes in flow dynamics affecting platelet deposition and/or roof-top fibrin formation (unpublished data). Extensive polishing of the PDMS channel overcomes these shortcomings.

Commonly used microfluidic devices contain rectangular or square channels (opposed to the round glass capillaries formerly used), in order to provide a laminar blood flow pattern through the channel,¹⁶ although the flow profile near the channel's corners is disturbed.¹⁴ In order to minimize wall effects, the advice is that rectangular chambers have a minimal width to depth ratio of ≥ 10 .¹³ The Maastricht parallel-plate flow chamber commonly used in our lab (depth 50 μm , width 3 mm) fulfills this requirement.¹⁵ Specific multichannel designs have been used, in which several flow channels run in parallel or are connected to the same inlet or the same outlet, such as reviewed elsewhere.¹³

Various strategies can be employed in microfluidic studies to control the coagulation process, for example the use of specific blood anticoagulants, a selected thrombogenic surface, and adaptation of the blood flow rate (Table I). Most commonly, (human or mouse) blood is anticoagulated with trisodium citrate or corn trypsin inhibitor (CTI). While trisodium citrate blood requires re-calcification to allow the clotting, the addition of CaCl_2 is not needed with CTI-treated blood. Critical in either case is to prevent residual thrombin activity by drawing the blood without constraints, mixing it well with the anticoagulant medium, and limit the time for experimentation. The most widely used thrombogenic surface for flow perfusion studies is collagen type I,¹⁷ due to its prominent platelet activation and ability to trigger the intrinsic coagulation system via factor (F)XII.¹⁸ In recent years, several studies have used surfaces consisting of both collagen and TF, specifically to trigger the 'fast' extrinsic coagulation system of FVII, which enhances the dynamic formation of a platelet-fibrin thrombus.¹⁹ As summarized in Table II, each of the various anticoagulants has specific advantages and disadvantages, when targeting the intrinsic or extrinsic coagulation pathways.

As a key modulator of thrombus formation, the blood flow rate is usually varied to monitor platelet-dependent coagulation either at venous, arterial or pathological (e.g. stenotic) shear conditions (Table I). The blood flow rate affects platelet-fibrin clot in different ways. First, there is the well known effect of higher wall shear rate on

Table I. Microfluidic devices and methodologies used to study platelet-based control of coagulation

Method	Chamber type	Chamber material	Anticoagulant	Re-calcification	Surface	Shear rate (s^{-1})	Measured process	Subjects	Ref.
I	A		Trisodium citrate	Mixing during assay \pm added TF	Collagen I	1,000	Platelet deposition and fibrin formation	Hemophilia patients	26
	B		Trisodium citrate	Mixing during assay; Y-shaped mixing tube	Collagen I \pm TF	150 - 1,000	Platelet deposition and fibrin formation	Patients with hemostatic insufficiency	20
	C	Maastricht parallel-plate flow chamber	Trisodium citrate	Mixing during assay + added extra TF	Collagen I, plaque material	500 - 5,000	Platelet deposition and fibrin formation	Healthy volunteers	25
	D		Trisodium citrate	Mixing during assay	Plaque material	500	Platelet deposition and disaggregation	Healthy volunteers and patients with FXII deficiency	27
II	Parallel plate flow chamber	PDMS	Trisodium citrate	Prior to assay	Plaque material or collagen I + TF	1,500	Platelet deposition	Healthy volunteers	51
III	Microfluidic flow chamber	PDMS	Trisodium citrate	Prior to assay	Collagen I \pm TF	100 - 1,000	Platelet deposition and fibrin formation	Hemophilia A patients	52
IV	A			Not required	Collagen I \pm TF, VWF	100 - 1,000		Healthy volunteers	53
	B	8-channel flow device	PDMS	Not required	Collagen I	100 - 1,000	Platelet deposition and fibrin formation	Hemophilia patients	29, 54
	C		CTI	Not required	Collagen I \pm kaolin or TF	100 - 1,000		Healthy volunteers	55
	D			Not required	Collagen I \pm TF	100		Healthy volunteers	47, 56

Table I. (continued)

Method	Chamber type	Chamber material	Anticoagulant	Re-calcification	Surface	Shear rate (s ⁻¹)	Measured process	Subjects	Ref.
A	T-TAS flow device	Hard plastic	Trisodium citrate	Prior to assay	Collagen I + thromboplastin	240	Fibrin -rich thrombus	VWD type 1 patients	57
B			Trisodium citrate + CTI	Prior to assay	Collagen I + TF	330 - 1,100	Thrombus formation and embolization	Patients undergoing cardiac surgery with bypass	31
VI	Microfluidic hydro-dynamic focusing device	PDMS	Trisodium citrate	Prior to assay	TF-coated silica particles	50 - 1,000	Platelet deposition, thrombin generation and fibrin formation	Healthy volunteers	58
VII	Side-view device with apertures	PDMS	CTI ± PPACK	Not required	Collagen I + TF	1,00 - 2,000	Thrombus pressure	Healthy volunteers	41
VIII	Hemostasis monitoring micro device	PDMS	Trisodium citrate	Prior to assay	Collagen I	Up to 10,000	Clotting time, thrombus volume	Healthy volunteers	59
IX	Trifurcated device	PDMS	Trisodium citrate + CTI	Mixing during assay	Collagen I ± TF	600	Platelet deposition and fibrin formation	Healthy volunteers	60
X	Badimon cylinder flow chamber	Hard plastic	None (blood directly <i>ex vivo</i>)	Not required	Aorta wall	1,690	Platelet deposition and fibrin formation	Patients with percutaneous coronary intervention	33

Abbreviations: PDMS: polydimethylsiloxane; CTI: corn trypsin inhibitor; PPACK: D-phenylalanyl-L-prolyl-L-arginine chloromethyl ketone; TF: tissue factor; VWD: von Willebrand factor disease.

VWF-dependent platelet deposition. Second, higher blood flow (independent of the shear rate) causes a higher dilution of the locally formed thrombin. Fibrin formation under flow hence is a compromise between high platelet deposition on the one hand and limited thrombin dilution on the other hand.^{5,20} Of note, as a technical artifact, flow stagnation may occur during the experiment, causing fibrin formation independently of the platelet surface, likely due to thrombin diffusion into the surrounding plasma (unpublished data). Common for most microfluidic devices is that they can be used for kinetic measurements or endpoint assessment of the buildup of platelet-fibrin thrombi or clots.

In a specific approach, the so-called side view, ‘leaky’ microfluidic device has been developed by the Philadelphia group operating at a relatively low shear rate, thus mimicking that of vascular leakage or hemostasis.²¹ This device allows a separate control of the trans-thrombus pressure gradient independently of the wall shear rate. It can simulate physiological circumstances, where interstitial permeation of a vessel plays a critical role.

When combined with fluorescence microscopy,²² a whole range of fluorescent labels is available (alone or in combination) to assess: platelet adhesion; granule secretion; integrin activation; exposure of procoagulant phosphatidylserine; binding of fibrinogen, coagulation factors or plasminogen; and/or formation of fibrin fibers (Table II). For adequate measurement of the clot-forming process, high-quality images need to be captured providing sufficiently detailed information. Given the small size of platelets and fibrin fibers, it is essential to maximize both the resolution and the sensitivity of the image capture system. This can be achieved by a highly transparent 40-60x oil immersion objective in combination with a sensitive high pixel density camera (Table II). Confocal microscopy or equivalent is essential to achieve three-dimensional information, *e.g.* for volumetric analyses or co-localization measurements of thrombus components, such as (activated) platelets and fibrin fibers; and for distinction between the thrombus core and shell.²⁰⁻²² If three-dimensional stacks are imaged at multiple colors in time,²⁰ the collected amount of data can be quite extensive. For complete characterization of thrombi formed in microfluidic chambers, advantage can be taken from the morphometric images obtained by enhanced-contrast, transmission illumination in combination with fluorescence imaging.¹⁵

Collected transillumination and fluorescence microscopic images can be analyzed in different ways (Table II). Morphology and specific features of the platelet-fibrin thrombi formed can be assessed by visual inspection of brightfield images. Fluorescence images – whether or not as time series – can precisely be quantified for platelet adhesion, platelet activation markers and fibrin formation, depending on the probes used.²²

Table II. Technical aspects to consider when using microfluidic flow devices in combination with microscopy to measure platelet and coagulation activity under flow. For technical details, see Ref.²².

Feature	Example	Advantages and opportunities
Flow method variable		
Micro-channel design	Rectangular; parallel-plate, stenotic, 'leaky' channels	Custom-made PDMS devices allow precise modeling of the channels, e.g. with stenotic or branched areas. The pouring of soft material can result in channel irregularities, which need to be checked before use.
Anticoagulant	3.2% sodium citrate with re-calcification or CTI	With re-calcified citrate blood: no clot before re-calcification, but residual extrinsic activation. With CTI-treated blood: blocked intrinsic activation, but residual clotting possible.
Intervention	<i>In vivo</i> or <i>in vitro</i>	Platelet function, coagulation activity and fibrinolysis can be assessed simultaneously after antithrombotic therapy <i>in vivo</i> or after additions to blood <i>in vitro</i> .
Thrombogenic surface	Stimulating platelet adhesion vs. coagulation	Allows mimicking of the thrombogenic vessel wall, stimulating platelet adhesion (collagen, laminin, fibrinogen) and triggering coagulation (tissue factor, collagen).
Coagulation pathway	CTI or inactive FVIIa	Blocked intrinsic coagulation with CTI or extrinsic coagulation with active-site inactivated FVIIa.
Shear rate	Venous or arterial	Modeling of either venous (50-500 s ⁻¹) or arterial (1000-5000 s ⁻¹) wall shear rates, possibility of using pulsatile flow patterns.
Fluorescent label	Activity of platelets or coagulation	Measurement of specific processes/reactions by a wide choice of fluorescence labels, e.g. for platelet activation (P-selectin; activated integrins; PS exposure) or coagulant activity (labeled coagulation factors, fibrinogen, fibrin, thrombin substrate).
Microscopic image capture		
Optics	Microscopy	High-magnification, transparent objective (40-60x oil) in combination with a high resolution camera, in order to visualize both single platelets as whole thrombus.
Illumination	White transparent and/or fluorescence light	Capture of brightfield images to visualize whole thrombus, and of fluorescence images to detect specific molecules or processes. Sufficiently high pixel density and bit-size.
3D imaging	Focal plane, z-direction	Advantage of confocal microscopy is the exact localization of platelets, thrombin and fibrin within a thrombus. 3D imaging allows quantification of thrombus volume (see below).
Image data analysis		
Brightfield	Thrombus morphology	Visual inspection and surface-area-coverage analysis of enhanced brightfield images, revealing thrombus features.
Brightfield or fluorescence	Extent of platelet adhesion	Time series of images revealing kinetics of platelet adhesion.
	Platelet activation markers	Images to quantify procoagulant activity, granule secretion, integrin activation, fibrin formation at platelet surface.
	Thrombus growth	Time series of confocal z-stacks revealing growth of platelet-fibrin thrombus.
	Thrombin generation	Time series of images from fluorogenic thrombin substrates: immobilized under flow, soluble under stasis after thrombus is formed.
	Fibrin formation	Images from labeled, cleaved fibrinogen or anti-fibrin antibody.
Thrombus stability		Differential images of time series to assess platelet-adhesive strength and resistance to embolization.

A very different approach for the assessment of platelet-fibrin thrombi is employed in the Total Thrombus-formation Assay (T-TAS) device.^{23,24} This microfluidic device is used for the continuous monitoring of blood flow pressure in time. It allows precise recording of the pressure buildup upon capillary occlusion. The T-TAS device further provides information on thrombus stability, by calculating the area under the flow pressure curve for a given time-period.

Practical approach of microfluidic flow devices to assess platelet-based control of coagulation

The few studies published so far to assess platelet-based coagulation using microfluidic devices, already provide valuable insight into the molecular determinants of this process. As summarized in Table III, main applications are the testing of blood from genetically transformed mice, of pharmacological agents, and of blood from patients with hemostatic insufficiencies.

Using blood from knock out mice, microfluidic devices allowed evaluation of the roles of single genes and proteins in thrombus and fibrin formation *in vitro*. Typical findings are that murine deficiency in the P2Y₁₂ receptor for ADP caused substantial instability of platelet-fibrin thrombi;²⁵ and that deficiency in FVIII or FIX led to reduced platelet procoagulant activity (PS exposure) as well as low fibrin formation. The latter result implicated a key role of the tenase complex in feed-forward mechanisms of platelet activation, thrombin generation and fibrin fiber formation.²⁶ In the presence of TF, it was confirmed that the extrinsic coagulation factor FVII had a rate-limiting role in the buildup of fibrin thrombi.²⁷ In the absence of TF, several groups established that the intrinsic coagulation factors FXII and FXI enhanced the kinetics of fibrin formation and thrombus stabilization.^{18,27,28}

Pharmacological agents with supposed anti-platelet or anticoagulant effects have been tested in flow assays in the presence of coagulation. At high shear rate, inhibition of the thrombin receptor PAR1, but not of the isoform PAR4, was found to play a role in the buildup of occlusive platelet-fibrin thrombi; an inhibitory effect that was enhanced by aspirin and P2Y₁₂ antagonism.²³ Suppression of the intrinsic coagulation pathway with an antibody against FXI lowered platelet activation and aggregation, in particular at the downstream site of formed thrombi.²⁸ Concerning the extrinsic pathway, *in vitro* supplementation of recombinant FVIIa resulted in a restoration of platelet deposition when using blood from patients with FVIIa deficiency, but surprisingly, did not rescue fibrin formation.²⁹ In recent work, direct FXa inhibitors rivaroxaban and apixaban

suppressed fibrin-rich thrombus formation, but left platelet accumulation unaffected.³⁰ Along the same line, the direct thrombin inhibitor argatroban was found to prolong the occlusion time and cause clot instability.²³

Microfluidic flow devices can detect hemostatic insufficiencies in blood from patients with a variety of bleeding disorders (Table III). Using the T-TAS device, it was demonstrated that, in blood from patients with hemodilution, the addition of fibrinogen concentrate normalized thrombus formation, and especially the formation of fibrin fibers.³¹ The same device detected impaired thrombus formation in patients with von

Table III. Different applications of microfluidic devices to study platelet activation and coagulation under flow conditions.

Application	Method (see Table I)	Target	Key findings	Ref.
Genetically modified mice to evaluate thrombus formation <i>in vitro</i>	I-B	P2Y ₁₂	Deficiency of murine P2Y ₁₂ reduces thrombus stability at higher shear rate	25
	I-B	FVIII, FIX	Deficiency of murine FVIII or FIX critically impairs platelet procoagulant activity and ensuing fibrin formation	26
	I-C	FXII	Deficiency of murine FXII reduces thrombus stability and fibrin formation	27
Testing of pharmacological agents in flowed human blood	V-A	PAR1, 4	Antagonist of PAR1, but not of PAR4, impairs thrombin-dependent thrombus formation under flow	61
	(glass capillary)	FXI	Blocking anti-FXI antibody reduces platelet activation and aggregation at downstream site of thrombus	28
	IV-B	FVII	Administration of recombinant FVIIa increases platelet deposition, but unchanged fibrin formation in patients with FVII deficiency	29
	V-A	FXa	Administration of FXa inhibitor, rivaroxaban or apixaban suppresses fibrin rich thrombus formation	30
	V-A	Thrombin	Administration of heparin or argatroban prolongs occlusion time	23
Monitoring hemostasis insufficiencies	V	(Patient)	Hemodilution delays thrombus and thick fibers formation in patients undergoing a cardiopulmonary bypass	31
	V	VWF	Altered buildup of platelet-fibrin thrombus in VWD and after desmopressin treatment	32
	X	$\alpha_{IIb}\beta_3$	Abciximab administration reduced fibrin deposition and thrombus formation in patients with unstable coronary syndrome	33
	X	(Patient)	Increased thrombus formation in blood from patients with major depression	34
	I-A	(Patient)	Impaired platelet-dependent fibrin formation in patients with acquired thrombocytopenia, hemophilia B, Scott syndrome, or hemodilution	20
	I-B	Plasminogen	Diminished fibrinolysis in patients receiving tranexamic acid during cardiothoracic surgery	12

Willebrand disease, an effect that was partly restored by patient treatment with the VWF-releasing agent desmopressin.³² Using the Maastricht flow chamber, fibrin formation was shown to be impaired in blood from patients with several bleeding symptoms, including FIX deficiency.²⁰ Other experiments demonstrated the requirements of platelet adhesion, PS exposure and thrombin generation for appreciable fibrin formation under flow. In patients with unstable coronary syndrome, treatment with the anti-platelet agent abciximab (integrin $\alpha_{\text{IIb}}\beta_3$ antagonist) suppressed both platelet and fibrin accumulation.³³ Even antidepressant treatment targeting serotonin signaling reduced fibrin formation,³⁴ and suppressed thrombus formation on plaque material³⁵. Blood flow was an important factor in the lysis of fibrin fibers around thrombi, in which PS-exposing platelets had a key role in plasminogen activation (the main fibrinolysis mediator).¹²

In the majority of these cases, the thrombogenic surface consisted of collagen with or without TF; and re-calcified/citrated blood was used to allow coagulation (Table III). Blood flow was performed at variable shear rates and, frequently, both platelet deposition and fibrin accumulation are measured in time. These studies indicate that, as long as the flow rate is high enough (*i.e.*, the thrombin formed is sufficiently diluted), adhered and activated platelets are required for a local buildup of fibrin fibers. Interestingly, inability of platelet PS exposure (*e.g.*, blood from Scott patients or anoctamin-6 deficient mice) severely delayed the formation of fibrin.^{20,36} This corresponds with *in vivo* studies,^{37,38} and supports the concept of platelet-based coagulation. The various studies furthermore point out that the precise wall shear and flow rates are important variables for the proper assessment of hemostatic defects.

Mechanisms of platelet-based control of coagulation under flow conditions

Obviously, microfluidic flow devices provide detailed insight into mechanisms of clotting occurring under flow conditions. In a platelet thrombus formed at arterial shear rate, several coagulation factors completely co-localized with PS-exposing platelets, *i.e.* (activated) FV, FIX, FX, and uncleaved prothrombin.^{26,37,39} This indicated that these major components of the tenase and prothrombinase complexes assemble at PS-exposing platelets, and facilitate the local activation of FX into FXa and of prothrombin into thrombin.⁹ Interestingly, the location of (activated) FVIII appeared to be different, in that immunological staining showed a transient presence near PS-exposing membranes, whereas the majority of FVIII co-localized with VWF.²⁶ It was concluded that the VWF in a thrombus acts as a supply site of FVIII, which after its activation (by thrombin) releases and can incorporate into the tenase complex.

Re-localization has also been observed for prothrombin: time series of images of fluorescent-labeled prothrombin indicated a gradual shift from PS-exposing platelets to fibrin fibers, once the prothrombin was cleaved into thrombin.³⁹ This is particularly prominent at lower flow rates, when fibrin fibers grow outside the platelet aggregates. This co-localization of (cleaved) thrombin with fibrin fibers agrees well with earlier evidence that fibrin can act as a main sink for thrombin. A similar rearrangement to fibrin fibers was found for plasminogen, once cleaved into plasmin.¹² Typical fluorescent images obtained with labeled platelets and coagulation factors are shown in Figure 1B.

Recently, the Philadelphia group has shown that the tightly packed platelet thrombi formed at high shear rates also contain a pool of core-localized thrombin, which enhances platelet activation and granule secretion.^{40,41} This was observed from *in vivo* models of thrombus formation as well as from *in vitro* flow studies using the side view microfluidic device.⁴¹ The porous fibrin structures in the thrombus core were found to obstruct the internal transport of thrombin, and provide a trans-clot pressure differential. Recent findings from our group indicate that the so-called 'coated' platelets, with high transglutaminase (FXIII) activity - forming a subpopulation of PS-exposing platelets - play an important role in platelet-dependent fibrin formation.⁴²

The method of nano-indentation was applied to assess the physical properties of a fibrin thrombus produced under coagulant conditions in a flow device.²⁰ The type of thrombogenic surface (*i.e.*, with different densities of collagen and TF) greatly influenced the micro-elasticity of thrombi in a way depending on the shear rate. It could be established that both the fibrin content and the fibrin distribution through a thrombus determined its elastic properties, with luminal-oriented fibrin fibers being most elastic. *In vitro* studies performed under stasis point to a more dense network of highly branched thin fibrin fibers under conditions where platelets are present and thrombin levels are high.⁴³ How this finding extends to thrombi formed under flow conditions is still unclear.

Insight is increasing that fibrin formation is not the end of thrombus buildup (Figure 1C). Various pieces of evidence suggest that fibrin fibers can act as a scaffold for a new cycle of platelet adhesion and activation, and subsequent thrombin generation. For instance, platelet recruitment can be promoted by the binding of VWF to fibrin fibers.⁴⁴ Incorporation of platelets is also enforced by their ability to bind to fibrin via the GPVI receptors, with ensuing increased procoagulant activity.^{45,46} In a developing thrombus, also FXII co-localizes in part with fibrin fibers, pointing to a fibrin-dependent progression of the intrinsic coagulation pathway.^{27,47} An implication of these findings is that, during thrombus buildup with activated platelets and first fibrin fibers, cross-stimulation with

fibrin-dependent platelet stimulation can result in expansion of the fibrin network, until stabilization of the mature thrombus.

Both *in vitro* flow chamber and *in vivo* studies indicate that, mostly, the thrombus-forming process halts within 10-20 minutes. Various processes may contribute to the stopped thrombus growth: the biorheological (flow) conditions, anticoagulation pathways and fibrinolytic activity. *In vivo*, the endothelium is considered to act as a main suppressant of platelet activation and coagulation; this recognition would require inclusion of the relevant endothelial processes in microfluidic measurements. Activated platelets also can support fibrinolysis,¹² although this process is limited by the density of the fibrin network.⁴⁸ Unclear is still which of the possible thrombus termination pathways is most important.

Towards clinical use

There are a number of challenges regarding the use of microfluidic devices under coagulant conditions for clinical assessment of a hemostatic or prothrombotic tendency. One drawback is the still limitedly controlled coagulation - due to continuous thrombin accumulation and its relocation to fibrin fibers -, suggesting that suppressant regulatory mechanisms need to be better incorporated into the flow assays, for instance by mimicking relevant endothelial processes.

The endless combination of variables that can be applied in coagulant flow assays is both a strength and a weakness. This makes it possible to tailor a flow assay for specific clinical questions, namely by changing: *(i)* the type, size and strength of the platelet-activating and coagulation-triggering surface; *(ii)* the flow chamber dimensions; *(iii)* the flow chamber design (*e.g.*, incorporating a shunt or leak-out); *(iv)* the wall shear rate determining platelet deposition; *(v)* the flow rate determining coagulation factor transport; and *(vi)* the flow pattern over time (steadily or pulsatile). Currently, for specific sets of conditions, clinical and research laboratories have been collecting normal values of thrombus parameters with blood samples from healthy volunteers for comparison with patient samples (Table I). The challenge will be to define for each specific clinical question those conditions, where the intra-individual variation of thrombus buildup is limited,⁴⁹ while the difference between normals and the concerning patient group is maximal.⁵⁰ For instance, assessment of thrombus formation in blood from patients with an inherited disease such as hemophilia likely require an assay setup where fibrin formation is less limited than such measurement in blood from patients with hyperlipidemia or atherothrombosis.

From the current state-of-the-art it is clear that microfluidic flow devices can assess platelet and coagulant functions at the same time under defined flow conditions. In principle, this is of advantage in comparison to the clinically used hemostatic assays, which determine either platelet or coagulation functions, or do not operate under flow. Proof-of-principle so far comes from the studies of Table III, showing that microfluidic flow devices can detect the impaired hemostatic activity in blood from patients with platelet defects, coagulation disorders or von Willebrand disease.^{26,31,32,50} Furthermore, microfluidics can be used in the monitoring and treatment of dilution coagulopathy, for instance caused by fluid infusion upon major surgery. Studies indicate that the diminished thrombus formation at dilution can be normalized at high shear rate by VWF replacement and at low shear rate by fibrinogen concentrate, the latter specifically restoring fibrin formation.³¹ Another relevant application is the use of 'coagulation' microfluidics for the monitoring of (combined) anticoagulant and anti-platelet therapy, such as the direct thrombin inhibitor argatroban and the integrin $\alpha_{IIb}\beta_3$ antagonist abciximab.^{23,33} This work is promising for introducing such devices in the clinical laboratory. Yet, the precise assay conditions still need to be defined and subsequently, important assay parameters such as cut-off values, selectivity and sensitivity need to be determined.

Acknowledgements

This study was supported by CTTM / MICRO-BAT; and by the Alexander von Humboldt Stiftung to F.S.

Declaration of interest

The authors declare that no conflicts of interest exist.

References

1. Versteeg HH, Heemskerk JW, Levi M, Reitsma PH. New fundamentals in hemostasis. *Physiol Rev.* 2013;93:327-358.
2. Chiu JJ, Chien S. Effects of disturbed flow on vascular endothelium: pathophysiological basis and clinical perspectives. *Physiol Rev.* 2011;91(1):327-387.
3. Mazepa M, Hoffman M, Monroe D. Superactivated platelets: thrombus regulators, thrombin generators, and potential clinical targets. *Arterioscler Thromb Vasc Biol.* 2013;33:1747-1752.
4. Rittersma SZ, van der Wal AC, Koch KT, *et al.* Plaque instability frequently occurs days or weeks before occlusive coronary thrombosis: a pathological thrombectomy study in primary percutaneous coronary intervention. *Circulation.* 2005;111:1160-1165.
5. Neeves KB, Illing DA, Diamond SL. Thrombin flux and wall shear rate regulate fibrin fiber deposition state during polymerization under flow. *Biophys J.* 2010;98:1344-1352.
6. De Witt SM, Swieringa F, Cavill R, *et al.* Identification of platelet function defects by multi-parameter assessment of thrombus formation. *Nat Commun.* 2014;5:4257.
7. Monroe DM, Hoffman M, Roberts HR. Platelets and thrombin generation. *Arterioscler Thromb Vasc Biol.* 2002;22:1381-1389.

8. Heemskerk JW, Kuijpers MJ, Munnix IC, Siljander PR. Platelet collagen receptors and coagulation. A characteristic platelet response as possible target for antithrombotic treatment. *Trends Cardiovasc Med*. 2005;15:86-92.
9. Heemskerk JW, Mattheij NJ, Cosemans JM. Platelet-based coagulation: different populations, different functions. *J Thromb Haemost*. 2013;11:2-16.
10. Shen F, Kastrop CJ, Liu Y, Ismagilov RF. Threshold response of initiation of blood coagulation by tissue factor in patterned microfluidic capillaries is controlled by shear rate. *Arterioscler Thromb Vasc Biol*. 2008;28:2035-2041.
11. Dejouvencel T, Doeuvre L, Lacroix R, et al. Fibrinolytic cross-talk: a new mechanism for plasmin formation. *Blood*. 2010;115:2048-2056.
12. Whyte CS, Swieringa F, Mastenbroek TG, et al. Plasminogen associates with phosphatidylserine-exposing platelets and contributes to thrombus lysis under flow. *Blood*. 2015;125:2568-2578.
13. Westein E, de Witt S, Lamers M, Cosemans JM, Heemskerk JW. Monitoring in vitro thrombus formation with novel microfluidic devices. *Platelets*. 2012;23:501-509.
14. Zhu S, Herbig BA, Li R, et al. In microfluidico: Recreating in vivo hemodynamics using miniaturized devices. *Biorheology*. 2015;52:303-318.
15. Van Kruchten R, Cosemans JM, Heemskerk JW. Measurement of whole blood thrombus formation using parallel-plate flow chambers - a practical guide. *Platelets*. 2012;23:229-242.
16. Sarvepalli DP, Schmidtke DW, Nollert MU. Design considerations for a microfluidic device to quantify the platelet adhesion to collagen at physiological shear rates. *Ann Biomed Eng*. 2009;37:1331-1341.
17. Roest M, Reininger A, Zwaginga JJ, King MR, Heemskerk JW. Flow chamber-based assays to measure thrombus formation in vitro: requirements for standardization. *J Thromb Haemost*. 2011;9:2322-2324.
18. Van der Meijden PE, Munnix IC, Auger JM, et al. Dual role of collagen in factor XII-dependent thrombus formation. *Blood*. 2009;114:881-890.
19. Colace TV, Jobson J, Diamond SL. Relipidated tissue factor linked to collagen surfaces potentiates platelet adhesion and fibrin formation in a microfluidic model of vessel injury. *Bioconjug Chem*. 2011;22:2104-2109.
20. Swieringa F, Baaten CC, Verdoold R, et al. Platelet control of fibrin distribution and microelasticity in thrombus formation under flow. *Arterioscler Thromb Vasc Biol*. 2016;36:692-699.
21. Muthard RW, Diamond SL. Side view thrombosis microfluidic device with controllable wall shear rate and transthrombus pressure gradient. *Lab Chip*. 2013;13:1883-1891.
22. De Witt S, Swieringa F, Cosemans JM, Heemskerk JW. Multi-parameter assessment of thrombus formation on microspotted arrays of thrombogenic surfaces. *Nat Protocol Exchange*. 2014;2014:3309.
23. Hosokawa K, Ohnishi T, Kondo T, et al. A novel automated microchip flow-chamber system to quantitatively evaluate thrombus formation and antithrombotic agents under blood flow conditions. *J Thromb Haemost*. 2011;9:2029-2037.
24. Yamaguchi Y, Moriki T, Igari A, et al. Studies of a microchip flow-chamber system to characterize whole blood thrombogenicity in healthy individuals. *Thromb Res*. 2013;132:263-270.
25. Nergiz-Unal R, Cosemans JM, Feijge MA, et al. Stabilizing role of platelet P2Y₁₂ receptors in shear-dependent thrombus formation on ruptured plaques. *PLoS One*. 2010;5:e10130.
26. Swieringa F, Kuijpers MJ, Lamers MM, van der Meijden PE, Heemskerk JW. Rate-limiting roles of the tenase complex of factors VIII and IX in platelet procoagulant activity and formation of platelet-fibrin thrombi under flow. *Haematologica*. 2015;100:748-756.
27. Kuijpers MJ, van der Meijden PE, Feijge MA, et al. Factor XII regulates the pathological process of thrombus formation on ruptured plaques. *Arterioscler Thromb Vasc Biol*. 2014;34:1674-1680.
28. Zilberman-Rudenko J, Itakura A, Wiesenekker CP, et al. Coagulation factor XI promotes distal platelet activation and single platelet consumption in the bloodstream under shear flow. *Arterioscler Thromb Vasc Biol*. 2016;36:510-517.
29. Li R, Panckeri KA, Fogarty PF, Diamond SL. Recombinant factor VIIa enhances platelet deposition from flowing haemophilic blood but requires the contact pathway to promote fibrin deposition. *Haemophilia*. 2015;21:266-274.
30. Sugihara H, Idemoto Y, Kuwano T, et al. Evaluation of the antithrombotic effects of rivaroxaban and apixaban using the total thrombus-formation analysis system: *in vitro* and *ex vivo* studies. *J Clin Med Res*. 2016;8:899-907.
31. Ogawa S, Ohnishi T, Hosokawa K, Szlam F, Chen EP, Tanaka KA. Haemodilution-induced changes in coagulation and effects of haemostatic components under flow conditions. *Br J Anaesth*. 2013;111:1013-1023.

32. Ogiwara K, Nogami K, Hosokawa K, Ohnishi T, Matsumoto T, Shima M. Comprehensive evaluation of haemostatic function in von Willebrand disease patients using a microchip-based flow chamber system. *Haemophilia*. 2015;21:71-80.
33. Dangas G, Badimon JJ, Collier BS, et al. Administration of abciximab during percutaneous coronary intervention reduces both ex vivo platelet thrombus formation and fibrin deposition: implications for a potential anticoagulant effect of abciximab. *Arterioscler Thromb Vasc Biol*. 1998;18:1342-1349.
34. Lopez-Vilchez I, Serra-Millas M, Navarro V, et al. Prothrombotic platelet phenotype in major depression: downregulation by antidepressant treatment. *J Affect Disord*. 2014;159:39-45.
35. Bampalis VG, Dwivedi S, Shai E, Brandl R, Varon D, Siess W. Effect of 5-HT_{2A} receptor antagonists on human platelet activation in blood exposed to physiologic stimuli and atherosclerotic plaque. *J Thromb Haemost*. 2011;9:2112-2115.
36. Baig AA, Haining EJ, Geuss E, et al. TMEM16F-mediated platelet membrane phospholipid scrambling is critical for hemostasis and thrombosis but not thromboinflammation in mice. *Arterioscler Thromb Vasc Biol*. 2016;36:2152-2157.
37. Munnix IC, Kuijpers MJ, Auger J, et al. Segregation of platelet aggregatory and procoagulant microdomains in thrombus formation: regulation by transient integrin activation. *Arterioscler Thromb Vasc Biol*. 2007;27:2484-2490.
38. Kuijpers MJ, Munnix IC, Cosemans JM, et al. Key role of platelet procoagulant activity in tissue factor-and collagen-dependent thrombus formation in arterioles and venules in vivo differential sensitivity to thrombin inhibition. *Microcirculation*. 2008;15:269-282.
39. Berny MA, Munnix IC, Auger JM, et al. Spatial distribution of factor Xa, thrombin, and fibrin(ogen) on thrombi at venous shear. *PLoS One*. 2010;5:e10415.
40. Stalker TJ, Welsh JD, Tomaiuolo M, et al. A systems approach to hemostasis: 3. Thrombus consolidation regulates intrathrombus solute transport and local thrombin activity. *Blood*. 2014;124:1824-1831.
41. Muthard RW, Welsh JD, Brass LF, Diamond SL. Fibrin, gamma'-fibrinogen, and transclot pressure gradient control hemostatic clot growth during human blood flow over a collagen/tissue factor wound. *Arterioscler Thromb Vasc Biol*. 2015;35:645-654.
42. Mattheij NJ, Swieringa F, Mastenbroek TG, et al. Coated platelets function in platelet-dependent fibrin formation via integrin $\alpha_{IIb}\beta_3$ and transglutaminase factor XIII. *Haematologica*. 2016;101:427-436.
43. Wolberg AS, Aleman MM, Leiderman K, Machlus KR. Procoagulant activity in hemostasis and thrombosis: Virchow's triad revisited. *Anesth Analg*. 2012;114:275-285.
44. Miszta A, Pelkmans L, Lindhout T, et al. Thrombin-dependent incorporation of von Willebrand factor into a fibrin network. *J Biol Chem*. 2014;289:35979-35986.
45. Alshehri OM, Hughes CE, Montague S, et al. Fibrin activates GPVI in human and mouse platelets. *Blood*. 2015;126:1601-1608.
46. Mammadova-Bach E, Ollivier V, Loyau S, et al. Platelet glycoprotein VI binds to polymerized fibrin and promotes thrombin generation. *Blood*. 2015;126:683-691.
47. Zhu S, Travers RJ, Morrissey JH, Diamond SL. FXIa and platelet polyphosphate as therapeutic targets during human blood clotting on collagen/tissue factor surfaces under flow. *Blood*. 2015;126:1494-1502.
48. Collet JP, Park D, Lesty C, et al. Influence of fibrin network conformation and fibrin fiber diameter on fibrinolysis speed: dynamic and structural approaches by confocal microscopy. *Arterioscler Thromb Vasc Biol*. 2000;20:1354-1361.
49. Kunicki TJ, Nugent DJ. The genetics of normal platelet reactivity. *Blood*. 2010;116:2627-2634.
50. Neeves KB, Onasoga AA, Hansen RR, et al. Sources of variability in platelet accumulation on type 1 fibrillar collagen in microfluidic flow assays. *PLoS One*. 2013;8:e54680.
51. Reininger AJ, Bernlochner I, Penz SM, et al. A 2-step mechanism of arterial thrombus formation induced by human atherosclerotic plaques. *J Am Coll Cardiol*. 2010;55:1147-1158.
52. Onasoga-Jarvis AA, Leiderman K, Fogelson AL, et al. The effect of factor VIII deficiencies and replacement and bypass therapies on thrombus formation under venous flow conditions in microfluidic and computational models. *PLoS One*. 2013;8:e78732.
53. Zhu S, Tomaiuolo M, Diamond SL. Minimum wound size for clotting: flowing blood coagulates on a single collagen fiber presenting tissue factor and von Willebrand factor. *Integr Biol (Camb)*. 2016;8:813-820.
54. Colace TV, Fogarty PF, Panckeri KA, Li R, Diamond SL. Microfluidic assay of hemophilic blood clotting: distinct deficits in platelet and fibrin deposition at low factor levels. *J Thromb Haemost*.

- 2014;12:147-158.
55. Zhu S, Diamond SL. Contact activation of blood coagulation on a defined kaolin/collagen surface in a microfluidic assay. *Thromb Res.* 2014;134:1335-1343.
 56. Welsh JD, Colace TV, Muthard RW, Stalker TJ, Brass LF, Diamond SL. Platelet-targeting sensor reveals thrombin gradients within blood clots forming in microfluidic assays and in mouse. *J Thromb Haemost.* 2012;10:2344-2353.
 57. Nogami K, Ogiwara K, Yada K, *et al.* Assessing the clinical severity of type 1 von Willebrand disease patients with a microchip flow-chamber system. *J Thromb Haemost.* 2016;14:667-674.
 58. Onasoga-Jarvis AA, Puls TJ, O'Brien SK, Kuang L, Liang HJ, Neeves KB. Thrombin generation and fibrin formation under flow on biomimetic tissue factor-rich surfaces. *J Thromb Haemost.* 2014;12:373-382.
 59. Jain A, Graveline A, Waterhouse A, Vernet A, Flaumenhaft R, Ingber DE. A shear gradient-activated microfluidic device for automated monitoring of whole blood haemostasis and platelet function. *Nat Commun.* 2016;7:10176.
 60. Muthard RW, Diamond SL. Rapid on-chip recalcification and drug dosing of citrated whole blood using microfluidic buffer sheath flow. *Biorheology.* 2014;51:227-237.
 61. Hosokawa K, Ohnishi T, Miura N, *et al.* Antithrombotic effects of PAR1 and PAR4 antagonists evaluated under flow and static conditions. *Thromb Res.* 2014;133:66-72.



Chapter 3

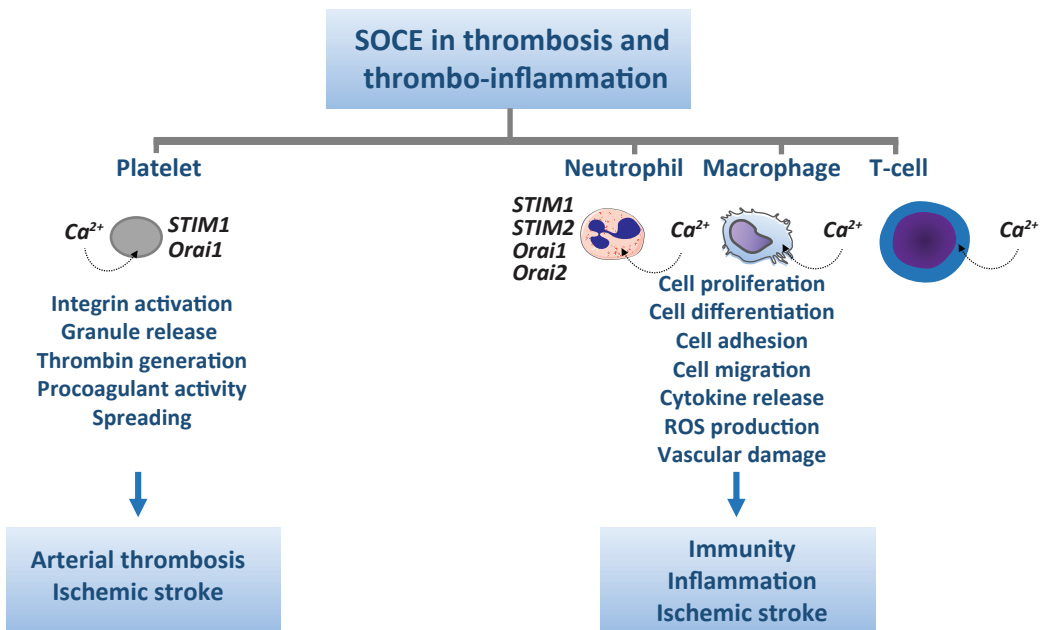
Store-operated calcium entry in thrombosis and thrombo-inflammation

*Mammadova-Bach E, Nagy M, Heemskerk JWM, Nieswandt B,
Braun A*

*Cell Calcium 2019; 77: 39-48
Reprinted with permission*

Abstract

Cytosolic free calcium (Ca^{2+}) is a second messenger regulating a wide variety of functions in blood cells, including adhesion, activation, proliferation and migration. Store-operated Ca^{2+} entry (SOCE), triggered by depletion of Ca^{2+} from the endoplasmic reticulum, provides a main mechanism of regulated Ca^{2+} influx in blood cells. SOCE is mediated and regulated by isoforms of the ion channel proteins ORAI and TRP, and the transmembrane Ca^{2+} sensors stromal interaction molecules (STIMs), respectively. This report provides an overview of the (patho)physiological importance of SOCE in blood cells implicated in thrombosis and thrombo-inflammation, *i.e.* platelets and immune cells. We also discuss the physiological consequences of dysregulated SOCE in platelets and immune cells and the potential of SOCE inhibition as a therapeutic option to prevent or treat arterial thrombosis as well as thrombo-inflammatory disease states such as ischemic stroke.



1. Introduction

Cytosolic free Ca^{2+} ions act as an ubiquitous second messenger that regulates many important functions in platelets and immune cells, including cytoskeletal reorganization, cell adhesion, migration, proliferation and apoptosis.¹ Physiological agonists can increase the cytosolic level of Ca^{2+} by inducing Ca^{2+} release from various intracellular stores as well as by Ca^{2+} entry from the extracellular milieu into the cytosol. In essentially all blood cells, Ca^{2+} entry is regulated by voltage-independent channels, located in the plasma membrane. Both in the anucleated platelets and in nucleated immune cells, several organelles have been described as Ca^{2+} stores, including the dense tubular system or sarco/endoplasmic reticulum, lysosome like acidic organelles and mitochondria.¹⁻⁴ In blood cells, cation channels can be regulated by activation of receptors or by depletion of intracellular Ca^{2+} stores, which then triggers the process of store-operated Ca^{2+} entry (SOCE).⁴⁻⁶ Because of its electrophysiological properties, Ca^{2+} release activated Ca^{2+} current (I_{CRAC}) has been identified as the current facilitating SOCE.⁵

The molecular identity of the Ca^{2+} sensor in the stores responsible for channel opening remained elusive until 2005, when the stromal interaction molecules (STIMs) were identified as reticular membrane located Ca^{2+} sensors.⁷⁻⁹ Shortly afterwards, three isoforms of transmembrane channel protein ORAI (ORAI1-3) were identified as the main Ca^{2+} channels interacting with STIM proteins.¹⁰⁻¹⁵ In platelets and immune cells, transient receptor potential (TRP) channels and ORAI isoforms may form functional units, which are coupled to STIM1 and inositol 1,4,5-trisphosphate (IP_3) receptor channels, thereby enhancing the Ca^{2+} entry.^{4,16-20} For platelets, a role of SOCE has been elucidated in thrombotic processes,^{19,20} while activation of SOCE in immune cells is considered to have a major role in the regulation of inflammation.¹⁸ In the present review, we connected these findings to better understand how the molecular components of SOCE contribute to the whole spectrum of thrombotic and thrombo-inflammatory diseases.

2. Calcium homeostasis in platelets

2.1 Calcium store release

Platelets are anucleated cell fragments, released by megakaryocytes (MKs) into the bone marrow sinusoids, circulating in the blood and safeguarding vascular integrity. Upon vessel wall injury, platelets are recruited to exposed subendothelial extracellular matrix (ECM) proteins and become activated.²¹ The activation process includes fast rearrangement of the platelet cytoskeleton, leading to shape change. Upon

platelet activation, intracellular alpha (α)- and dense (δ) granules containing secondary mediators, such as fibrinogen (FGN), von Willebrand factor (vWF) and adenosine di-, triphosphate (ADP/ATP), serotonin are released, along with the production of short-lived thromboxane A₂ (TxA₂) and hydroxyeicosatetraenoic acid (HETE). These autocrine agents along with locally produced thrombin reinforce the activation process, and cause further recruitment of circulating platelets to the injury site, thereby leading to the formation of thrombi, which can seal the wounded vessel.²¹ If occurring in diseased vessels, such as in atherosclerotic arteries subjected to plaque rupturing, the same reactions can lead to acute vessel occlusion, causing life-threatening disease states such as thromboembolism, myocardial infarction or ischemic stroke.²²⁻²⁵

Signaling-dependent control of Ca²⁺ homeostasis plays a crucial role in the regulation of platelet shape change and adhesion, and also in α - and δ - granule secretion and thrombus growth. The majority of platelet-activating receptors act through stimulation of phospholipase C (PLC) isoforms, which catalyze the hydrolysis of phosphatidyl 4,5-disphosphate (PIP₂) into diacylglycerol (DAG) and inositol 1,4,5-trisphosphate (IP₃) (Figure 1).²⁶⁻²⁸ These second messengers control the processes of receptor- and store-operated Ca²⁺ entry (ROCE and SOCE). Whilst IP₃ induces release of Ca²⁺ through IP₃ receptors located in the endoplasmic reticulum, DAG regulates Ca²⁺ entry through protein kinase C and activation of DAG-sensitive Ca²⁺ channels.²⁶⁻²⁸

Human and mouse platelets express several PLC isoforms, *i.e.* PLC β 2/3 and PLC γ 2. The β -type isoforms are regulated by G-protein coupled receptors (GPCR), including the PAR receptors for thrombin, the purinergic receptors for ADP, and the receptor (TP) for TxA₂, through coupling to the α -subunit of the G-protein, Gq.²⁹ The isoform PLC γ 2 becomes activated via the receptors glycoprotein (GP)VI, C-type lectin-like receptor-2 (CLEC-2), integrins $\alpha_2\beta_1$ and $\alpha_{IIb}\beta_3$, and to a limited extent via the GPIb-V-IX complex, and in human platelets via Fc γ receptor IIA (Fc γ RIIA).²¹

In platelets collagen-dependent activation of GPVI causes tyrosine phosphorylation of the immunoreceptor tyrosine-based activation motif (ITAM) located in the cytoplasmic tail of Fc receptor gamma (Fc γ R γ) chain. Recruitment and activation of Src family kinases is then followed by activation of spleen tyrosine kinase (Syk), phosphorylation of the adaptor molecule linker of activated T cells (LAT), and formation of the LAT signalosome. The latter recruits PLC γ 2 from the cytoplasm to the plasma membrane, where it becomes active.^{30,31} Activation of the various PLC isoforms thus converges in a common pathway of IP₃-mediated Ca²⁺ store depletion.

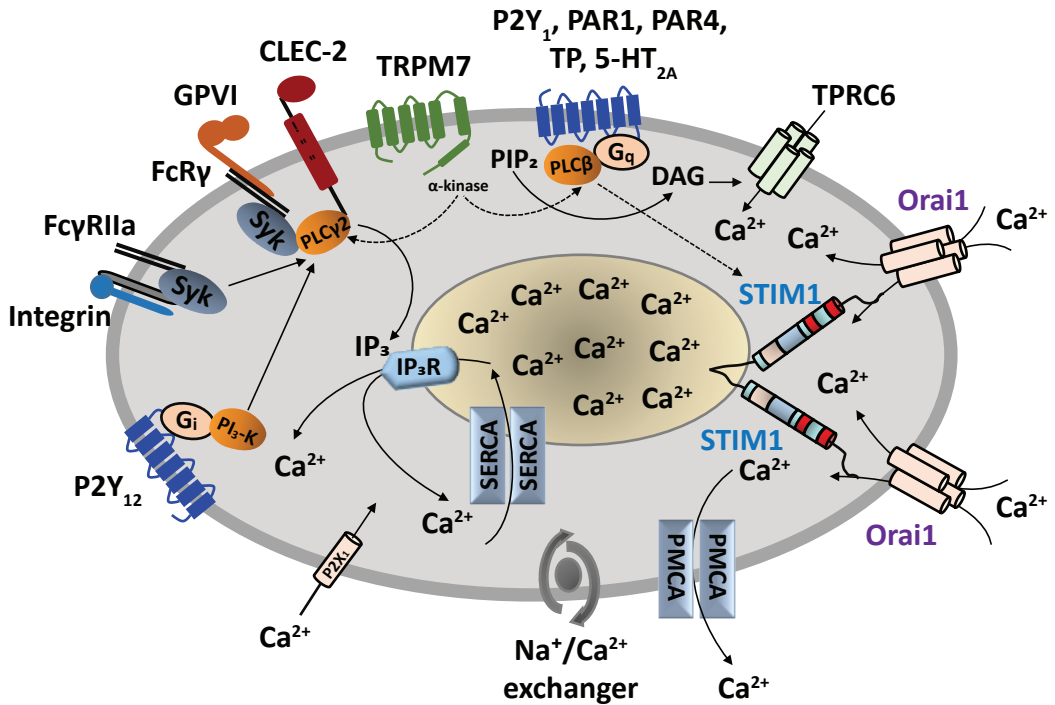


Figure 1: Calcium store release in platelets. After receptor activation, phospholipase C (PLC) isoforms hydrolyse phosphatidylinositol-4,5-bisphosphate (PIP_2) to inositol-1,4,5-trisphosphate IP_3 and diacylglycerol (DAG). IP_3 releases Ca^{2+} from the intracellular stores, in turn STIM1 opens Orai1 channels in the plasma membrane, a process known as store-operated calcium entry (SOCE), whereas DAG mediates non-SOCE through transient receptor potential channel 6 (TRPC6). Direct receptor-operated calcium (ROC) channel, $P2X_1$, and a Na^+/Ca^{2+} exchanger (NCX) contribute to the elevation of intracellular Ca^{2+} [Ca^{2+}_i]. Sarco/endoplasmic reticulum Ca^{2+} ATPases (SERCA) and plasma membrane Ca^{2+} ATPases (PMCA) pump Ca^{2+} back into the stores or through the plasma membrane to outside of the cell, respectively. IP_3R : IP_3 -receptor; GPVI: glycoprotein VI; FcR γ : Fc receptor γ chain; Fc γ RIIIa: Fc γ receptor IIIa; CLEC-2: C-type lectin-like receptor 2; PI3-K: phosphatidylinositol 3-kinase; Syk: spleen tyrosine kinase; $P2Y_1$ and $P2Y_{12}$: purinergic G protein-coupled receptor 1 and 12; PAR1 and 4: protease-activated receptor 1 and 4; TP: thromboxane receptor; $5-HT_{2A}$: serotonin 2A receptor; TRPM7: Transient receptor potential melastanin 7.

2.2. Calcium stores in platelets

In human platelets, at least three separate Ca^{2+} stores have been reported: the dense tubular system (equivalent to the sarco/endoplasmic reticulum), lysosome-like acidic organelles and mitochondria. The existence of distinct Ca^{2+} stores has been proposed based on the different affinities to IP_3 ,⁴ on the expression of two different sarco/endoplasmic reticulum Ca^{2+} ATPase SERCA isoforms^{4,32-34} and on their sensitivity to the thapsigargin (TG). The SERCA2b isoform displaying high sensitivity to TG is expressed on dense tubular system.³⁵ The SERCA3 isoform is expressed in lysosome-like acidic

organelles^{36,37} and less sensitive to TG, but high sensitivity was found to 2,5-di-(tert-butyl)-1,4-benzohydroquinone (TBHQ).³³ Nevertheless, there is a consensus that the major intracellular Ca^{2+} pool in platelets is located in the dense tubular system and the release of Ca^{2+} from this TG-sensitive Ca^{2+} stores is considered to be a key modulator of platelet SOCE.⁴

2.3. Store-operated calcium channels in platelets

It has become clear that SOC channels are major regulators of extracellular Ca^{2+} entry in platelets, similarly as in other electrically non-excitabile cells.^{4,6} In this section, we discuss the molecular composition of the platelet SOC channels.

2.3.1. ORAI1

The ORAI proteins encompass a family of plasma membrane-resident channels with four transmembrane domains and intracellularly located C and N termini.^{10,11} In mammals, the family includes three isoforms: ORAI1-3. ORAI1 is considered to be the main pore-forming unit of SOC channels with the capability to form multimers that make up a highly selective Ca^{2+} channel.^{12,13,38} Studies on genetically engineered mice lacking functional ORAI1 have established its importance in SOCE in many cell types.¹⁸ In mouse and human platelets, all three isoforms of the ORAI channel family have been detected, with ORAI1 being the predominant isoform in both species.³⁹ Messenger ribonucleic acids (mRNAs) of ORAI1 are abundantly expressed in human and mouse platelets, primary murine MKs, and megakaryocytic cell lines, at levels far above those of ORAI2, ORAI3, TRPC1 or other TRP isoforms.^{39,40} In line with this, platelets isolated from *Orai1*^{-/-} bone-marrow chimeric mice showed a strongly decreased SOCE.³⁹

Patients with severe combined immunodeficiency have been identified with an ORAI1^{R93W} missense mutation, resulting in the substitution of a highly conserved arginine residue in the first transmembrane domain of ORAI1.¹¹ Heterozygous expression of the ORAI1^{R93W} mutation appeared to have a dominant negative effect on SOCE, probably inducing abnormal folding of the channel complex, which inhibits channel opening.^{11,41} Platelets from ORAI1^{R93W} mice, similarly to platelets from bone marrow chimeric *Orai1*^{-/-} mice, displayed a strongly reduced SOCE. Yet, specific differences were reported between ORAI1^{R93W}⁴¹ and *Orai1*^{-/-} platelets.^{39,42}

Whereas *Orai1*^{-/-} platelets showed a selective defect in GPVI signaling,^{39,42} ORAI1^{R93W} platelets had a more global defect in integrin activation in response to GPVI as well as GPCR agonists.⁴¹ Such a difference could possibly be explained by increasing expression of other ORAI isoforms (ORAI2 and ORAI3) in *Orai1*^{-/-} platelets, thus partially compensating

for the loss of ORAI1.³⁹ Another explanation for this may be that the R93W mutation not only inactivates the ORAI1 channel, but also modifies the function of the ORAI1 signalosome *e.g.* by triggering a negative feedback signal from the channel to a GPCR. In both ORAI1 mutant platelets, residual Ca²⁺ entry was detected after TG stimulation, suggesting that other Ca²⁺ channels can play an additional role in this process.

2.3.2. TRPC1

The TRP proteins belong to one of the largest ion channel superfamilies and grouped into seven related families, *i.e.* TRPC (canonical), TRPV (vanilloid), TRPM (melastatin), TRPP (polycystin), TRPML (mucolipin), TRPA (ankyrin) and TRPN (no mechanoreceptor potential C (NOMPC)-like); the latter is found only in invertebrates and fish.⁴³ Some members of the canonical TRP subfamily (TRPC1-7) can be activated by SOCE⁴⁴⁻⁴⁶ and appear to be associated to ORAI isoforms.^{4,6} Platelets express two isoforms, *i.e.* TRPC1 and TRPC6.^{44,47,48} Especially the latter is highly expressed in the platelet plasma membrane and mediates non selective-cation influx following binding of DAG.^{48,49}

Before the identification of the ORAI proteins, TRPC1 was considered as a major SOC channel in platelets. A conformational coupling model was proposed, stipulating that TRPC1 mediates SOCE following its interaction with type II IP₃ receptors.^{50,51} Later studies however suggested that TRPC1 is located in the intracellular membranes of human platelets⁴⁸ supporting a different role for the channel rather than activation of SOCE in the plasma membrane. Moreover, TRPC1-deficient mice displayed intact SOCE activity, unaltered Ca²⁺ homeostasis, and unchanged platelet activation responses both *in vitro* and *in vivo* experimental settings.⁵² In addition, studies on human platelets indicated that inhibitory anti-TRPC1 antibodies used in previous studies to demonstrate the function of the channel,^{50,53,54} had no specific effect on SOCE and failed to bind to the protein.⁵² Altogether, these results made it clear that SOCE in platelets involves other Ca²⁺ channels, such as ORAI1 than TRPC1.^{10,11} It has been proposed that TRP channels, including TRPC1 can form heteromeric ion channels together with ORAI channels.^{6,55,56}

2.4. Calcium sensors in platelets

2.4.1. STIM1

The first description of a role for STIM1 in platelet SOCE came from studies using a mouse strain named *Saxcoburggotski* (*Stim1^{Sax}*), which carry a gain of function mutation the EF hand domain of STIM1. The selective amino acid substitution of the EF hand domain of STIM1 showed that this mutation changes the conformation of the sensor to be constitutively active, and hence to mimic Ca²⁺ store depletion without

IP₃-mediated action.^{7,9,57} Strikingly, the homozygous *Stim1*^{Sax} mutation leads to embryonic lethality due to severe hemorrhages in different organs, whereas heterozygous mice are viable but developed severe thrombocytopenia.⁵⁷ Heterozygous mutant mice display splenomegaly, caused by rapid expansion of MKs in the splenic red pulp. Interestingly, the *Stim1*^{Sax/+} MKs showed normal proplatelet formation *in vitro*, suggesting enhanced clearance of the mutant platelets by the reticuloendothelial system in the spleen rather than defective platelet production to be responsible for the low platelet count.⁵⁷ It was confirmed that *Stim1*^{Sax/+} platelets had increased basal levels of cytosolic Ca²⁺, due to a leaky Ca²⁺ store, and showed abnormally activated Ca²⁺ channels, which together led to enhanced phosphatidylserine (PS) exposure and $\alpha_{IIb}\beta_3$ integrin activation in the absence of agonist stimulation.⁵⁷ In the presence of TG, *Stim1*^{Sax/+} platelets showed a faster store depletion, which was accompanied by impaired SOCE. Whereas *Stim1*^{Sax/+} platelets were unresponsive to agonists of (hem)ITAM-linked receptors such as collagen-related peptide or rhodocytin, the Ca²⁺ responses to GPCR agonists (ADP or thrombin) were nearly normal, indicating that the accelerated Ca²⁺ store depletion functionally compensated for the lack of SOCE in integrin $\alpha_{IIb}\beta_3$ activation and degranulation after GPCR stimulation.⁵⁷

Genetic deletion of STIM1 in mice allowed analysis of the role of this Ca²⁺-regulating protein in more detail. Due to perinatal lethality of the constitutive knock-out, bone marrow chimeras needed to be generated, resulting in animals with a deficiency of STIM1 in blood cells, including platelets.⁵⁸⁻⁶⁰ Measurements of cytosolic Ca²⁺ levels showed that *Stim1*^{-/-} platelets still displayed a small residual SOCE in response to TG, but a severely impaired Ca²⁺ increase was observed with all major platelet agonists. The TG-sensitive Ca²⁺ store release was reduced, thus pointing to an essential role of STIM1 in the regulation of Ca²⁺ store refilling.^{42,58} A pronounced defect was observed upon activation of (hem)ITAM receptors, while the platelets displayed only minor defects in integrin $\alpha_{IIb}\beta_3$ activation or in granule release in response to GPCR agonists.⁵⁸

Although both gain (*Stim1*^{Sax}) and loss (*Stim1*^{-/-}) of function mutations of STIM1 led to impaired (hem)ITAM receptor signaling in platelets, the underlying molecular mechanisms remain unclear. Since the Ca²⁺ store content in both mouse strains was abnormal,^{57,58} a hypothesis is that ionic stress in platelets can induce a negative feedback mechanism to (hem)ITAM receptors, which then negatively regulates GPVI- and CLEC-2-induced activation cascades. Alternatively, a dysregulated Ca²⁺ store release and SOCE in both STIM1-mutant platelets no longer amplifies GPVI and CLEC-2 receptor activation through a defective Ca²⁺-dependent phosphorylation or dephosphorylation of the LAT signalosome.

It has been shown that also platelets from serotonin transporter knock-out (*5-Htt^{-/-}*) and granule release defective mice (*Unc13d^{-/-}*) have a strongly reduced SOCE,⁶¹ indicating an essential role of platelet-released secondary agonists to amplify the channel activity of ORAI1. In contrast to *Stim1^{-/-}* platelets, *Orai1^{-/-}* platelets display a normal Ca²⁺ store content and Ca²⁺ store release after TG or agonist stimulation, thus explaining the consistently higher cytoplasmic Ca²⁺ rises in these cells compared to *Stim1^{-/-}* platelets. Studies analyzing platelets from *Orai1^{-/-}* bone marrow chimeras revealed a less severe phenotype than in *Stim1^{-/-}* bone marrow chimeras,^{39,58} *i.e.* milder defects in GPVI-induced integrin activation and platelet degranulation and thrombus formation under flow *in vitro*.

In addition, recently we showed the existence of functional interplay between STIM1 and Transient receptor potential melastanin 7 (TRPM7) channel, which contains a cytosolic domain of serine/threonine α -kinase.⁶² Global deletion of TRPM7 kinase activity in mice (*TRPM7^{R/R}*) resulted in inhibited (hem)ITAM-PLC γ 2 and PAR-PLC β 3-mediated intracellular Ca²⁺ mobilization.⁶² Moreover, activation of STIM1 function with TG-mediated Ca²⁺ store depletion, bypassing receptor-mediated PLC activation, resulted in strongly reduced SOCE in *TRPM7^{R/R}* platelets, suggesting the involvement of TRPM7 kinase activity in the regulation of STIM1-induced SOCE.⁶² Of note, ORAI1 and STIM1 functions are regulated by multiple phosphorylation of serine residues.^{63,64} Future studies are needed to investigate in more details, whether TRPM7 kinase may phosphorylate serine/threonine residues in the protein complex of SOCE.

2.5. Receptor-operated calcium entry

Besides SOCE, also other Ca²⁺ influx mechanisms exist in platelets. These include a ROCE pathway, induced by DAG-mediated TRPC6 activation, and a pathway of Ca²⁺ influx through the ATP-gated purinergic receptor channel P2X₁.

2.5.1. TRPC6

TRPC6, which is abundantly expressed in both mouse and human MKs and platelets, has been proposed as a non-SOC channel.⁴⁸ This was based on the findings that TRPC6 activation is strongly dependent on phospholipase C (PLC) and D (PLD)-mediated DAG production, but independent of Ca²⁺ release from intracellular stores. In addition, TRPC6 is a substrate for cAMP protein kinase and phosphorylation does not affect Ca²⁺ entry through the channel.⁴⁸ TRPC6 contains two sites for cyclic nucleotide kinase action at RRQT and KKLS 48, however it is unknown whether both sites are phosphorylated and their role on TRPC6 function. More recently, Nishida et al., showed that inhibition

of cyclic guanosine 3',5'-monophosphate (cGMP)-selective phosphodiesterase 5 induces phosphorylation of TRPC6 proteins at Thr,^{69,65} leading to inhibition of TRPC6-mediated Ca²⁺ signaling. The authors proposed that cGMP-dependent protein kinase (PKG)-mediated inhibition of TRPC6 channel activity is required for the pathological cardiac hypertrophy.⁶⁵ In addition, PKC also can inhibit TRPC6 activity by phosphorylation of Ser⁴⁴⁸.⁶⁶ Both PKC and TRPC6 are activated by GPCR signaling, suggesting that PKC may act as negative feedback mechanism on TRPC6 activity, thereby to weaken Ca²⁺ entry.⁶⁶

In TRPC6-deficient mouse platelets, TG-induced SOCE was not altered, suggesting that it does not act as a SOC channel or other Ca²⁺ channels compensate for its function. Although TRPC6-mediated Ca²⁺ influx has been described in many studies, contradictory results exist regarding the importance of TRPC6 in platelet physiology. In platelets from *Trpc6*^{-/-} mice or in human platelets in the presence of non-selective TRPC6 blockers, lower aggregation responses were observed.⁶⁷ In contrast, using other *Trpc6*^{-/-} knock-out mouse model, no obvious changes in Ca²⁺ homeostasis or platelet function could be observed, although Ca²⁺ entry induced by the DAG analog 1-oleoyl-2-acetyl-sn-glycerol was virtually abolished.⁶⁸ The latter study also indicated that TRPC6 in mouse platelets provides a major route of DAG-mediated Ca²⁺ entry.⁶⁸ Other authors however suggested that TRPC6 is not only involved in ROCE, but can also contribute to SOCE in platelets.⁴⁹

To further investigate the relations between SOCE and ROCE, mice lacking both ORAI1 and TRPC6 were generated.⁶⁹ *Orai1*^{-/-}*Trpc6*^{-/-} platelets displayed a further reduction in TG-induced SOCE, when compared to *Orai1*^{-/-} platelets, indicating the existence of a crosstalk between the TRPC6 and ORAI1 channels.⁶⁹ However, the crosstalk was independent of biochemical interactions between ORAI1 and TRPC6 in the SOCE complex, since ORAI1-mediated SOCE amplified DAG production through the activation of PLC and PLD isoforms, thereby increasing the channel activity of TRPC6.⁶⁹ Furthermore, the platelets from *Orai1*^{-/-}*Trpc6*^{-/-} mice displayed a severe Ca²⁺ deficit in resting state and upon activation – *i.e.* reduced Ca²⁺ store content and Ca²⁺ levels in the cytosol.⁶⁹

2.5.2. P2X₁

The P2X₁ purinoceptor acts as an ATP-gated ion channel with relatively high Ca²⁺ permeability in the platelet plasma membrane.^{70,71} Activation of the P2X₁ channel causes a rapid Ca²⁺ influx, dense granule centralization, shape change and a low level of platelet aggregation.^{70,72} Moreover, P2X₁ activation enhances platelet responses to thrombin and collagen.^{70,72} Typically, the activation of the P2X₁ channel is transient due to its fast desensitization by released ADP. Therefore, to study the P2X₁ channel *in vitro*, a high concentration of apyrase is required to scavenge ADP.⁷¹

Studies on P2X₁ knock-out mice (*P2X1*^{-/-}) provided most definitive evidence for an important role of this channel in platelet function.⁷³ Bleeding times in *P2X1*^{-/-} mice remained unchanged as compared to wild-type mice, indicating normal hemostasis.⁷³ Under flow conditions, at high shear, however, platelets from *P2X1*^{-/-} mice displayed reduced thrombus formation.⁷³ Moreover, *P2X1*^{-/-} mice were resistant to systemic thromboembolism, induced by the injection of a mixture of collagen and adrenaline, and in a model of arterial thrombosis induced by laser injury.⁷³ In contrast, overexpression of human P2X₁ in transgenic mice resulted in a prothrombotic phenotype.⁷⁴ Therefore, the P2X₁ channel has been proposed as an attractive target for the development of antithrombotic drugs.^{71,75,76} One such drug, NF449, which is an analogue of suramin, a sulfated naphthylamine, was reported to display good selectivity for P2X protein family members and to inhibit thrombus formation *in vivo*.⁷⁷ Studies with NF449 demonstrated a dose-dependent inhibition of systemic thromboembolism in mice, which was accompanied by reduced platelet consumption.⁷⁷ Interestingly, *Orai1*^{-/-} mice were protected also for systemic thromboembolism triggered by intravenous injection of collagen and epinephrine thrombogenic mixture.³⁹

P2X₁ channel activity also induces calmodulin-dependent myosin light chain kinase activity,⁷⁸ which modulates cytoskeletal rearrangements and movement of intracellular granules, thereby triggering platelet shape change. Further studies are necessary to investigate whether ORAI1-mediated SOCE also regulates the channel activity of P2X₁ and downstream responses.

3. Platelet SOCE in arterial thrombosis and hemostasis

Considering that Ca²⁺ signaling is a crucial pathway in platelet activation, regulatory proteins involved in this process could be targets for antithrombotic therapy. In various genetic mouse models, attenuation of intracellular Ca²⁺ signals, in particular SOCE, was found to affect arterial thrombus growth and/or stability. The decreased Ca²⁺ entry in response to (hem)ITAM-linked receptor agonists observed in *Stim1*^{-/-} and *Orai1*^{-/-} platelets resulted in impaired whole blood thrombus formation *ex vivo*. At high shear rates, resembling arterial flow conditions, the overall volume of thrombi formed by *Stim1*^{-/-} and *Orai1*^{-/-} platelets on collagen were reduced by 70% and 46%, respectively, compared to wild-type.^{39,58} In standard aggregometry (*i.e.* stirred suspensions), integrin activation, granule release and aggregation of *Stim1*^{-/-} and *Orai1*^{-/-} platelets were defective in the presence of lower concentrations of GPVI agonists, but not affected in response to GPCR agonists.^{39,79} In line with *ex vivo* flow adhesion assays, *Stim1*^{-/-} and *Orai1*^{-/-} chimeric mice

were found to be protected from arterial thrombosis in different *in vivo* models, albeit to a different extent. The most pronounced protection of both mouse strains was observed in a mechanical injury model of the abdominal aorta, where thrombus formation is triggered predominantly by collagens exposed at the site of endothelial damage.^{39,58} Interestingly, in a chemically induced injury model using topical application of ferric chloride (FeCl₃) on mesenteric arterioles, *Stim1*^{-/-} chimeric mice displayed impaired thrombus formation and vessel occlusion, whilst this process was not affected in *Orai1*^{-/-} chimeric mice. This could be explained by the fact that GPCR-induced Ca²⁺ responses are lower in *Stim1*^{-/-} platelets than in *Orai1*^{-/-} platelets.^{39,58} Accordingly, *Orai1*^{-/-}/*Trpc6*^{-/-} chimeric mice has also normal thrombus formation in the FeCl₃-injured mesenteric arteries highlighting the importance of efficient Ca²⁺ store depletion and contribution of other Ca²⁺ channels to FeCl₃-induced thrombus formation, probably enhancing P2X₁ or other TRP channel activity.⁶⁹

Thrombus formation at high shear rates was also impaired in conditional knock-out mice with a megakaryocyte/platelet specific deletion of *Stim1* gene (*Stim1*^{f/f} PFA-Cre),⁸⁰ however, to less extent than in *Stim1*^{-/-} chimeric mice⁵⁸ in which SOCE of immune cells in addition to platelets SOCE was also defective. However, platelets from both mouse strain displayed a decreased PS exposure. *In vivo* thrombus stability of *Stim1*^{f/f} PFA-Cre mice were correlated with the delayed formation of fibrin at sites of vascular injury,⁸⁰ suggesting that the procoagulant role of STIM1-mediated SOCE in platelets plays an important role in thrombus stability and growth.

Stim1^{Sax/+} mice have been also studied in several models of arterial thrombosis. These mice showed decreased vessel occlusion in the mechanically injured abdominal aorta, but not of FeCl₃-injured mesenteric arterioles.⁵⁷ Of note, *Stim1*^{Sax/+} mice exhibit marked thrombocytopenia which likely contributes to the decreased vessel occlusion in the aorta.⁵⁷

So far, studies in platelets isolated from *Stim2*^{-/-} mice showed no abnormalities and Ca²⁺ responses to common platelet agonists were unaltered compared to wild-type controls.⁴² The unchanged Ca²⁺ store release and SOCE in *Stim2*^{-/-} platelets point to substantial redundancy with the physiological functions of STIM1. Although STIM2 is highly expressed in the MK lineage, platelets from *Stim2*^{-/-} mice did not show defects in platelet production or thrombus formation.⁴²

In humans, rare loss of function mutations in the *ORAI1* and *STIM1* genes have been reported, leading to altered platelet SOCE.⁸¹ These mutations profoundly affect TG-induced SOCE⁸² and seem to be associated with mild thrombocytopenia, but not with a bleeding phenotype. Interestingly, both loss- and gain-of-function mutations in *ORAI1* and *STIM1* are accompanied by a lower platelet count, for reasons that are not

yet clear. A recent report investigated the effect of several mutations in ORAI1 and STIM1 on whole-blood thrombus formation on collagen and non-collagen surface *ex vivo*.⁸² It appeared that both loss-of-function (ORAI1^{R91W}) and gain-of function (ORAI1^{G98S}) variants of ORAI1 lead to decreased thrombus formation on collagen microspots, and in particular to a decreased procoagulant activity indicated by reduced PS exposure. Interestingly, these mutations also decreased platelet aggregation and procoagulant activity on vWF/rhodocytin and vWF/fibrinogen microspots. On the other hand, a heterozygous STIM1^{R429C} mutation, in the STIM1-Orai-activating region did not affect thrombus formation.⁸² It was proposed that depending on the activated signaling pathway, the platelet SOCE defect and the mild thrombocytopenia in different ways might alter the thrombus-forming process.⁸²

The roles of murine STIM1 and ORAI1 have also been studied in hemostasis. Tail bleeding times were normal in *Stim1*^{-/-} or *Orai1*^{-/-} bone marrow chimeric mice. Similarly to patients, loss of STIM1 or ORAI1 has not been associated with a bleeding diathesis.^{39,58} In contrast, the gain-of function mutation of STIM1 in *Stim1*^{Sax/+} mice results in reduced platelet count, dysregulated platelet function and consequently prolonged bleeding.⁵⁷ A similar phenotype was observed in patients with the Stormorken^{83,84} and York syndromes⁸⁵ carrying gain of function mutations in the *STIM1* gene.

4. Platelet SOCE in ischemic stroke

Platelets play a critical role in the progression of ischemic stroke.²³ In mice, the transient middle cerebral artery occlusion (tMCAO) model is widely used to study mechanisms underlying post-ischemic infarct progression in the brain,^{23,86,87} which is also seen in stroke patients where brain infarcts frequently grow despite recanalization of a previously occluded cerebral artery. Platelets are known to contribute to this reperfusion injury but the underlying mechanisms are only poorly understood. Interestingly, in both *Stim1*^{-/-} and *Orai1*^{-/-} bone-marrow chimeras infarct volumes at 24 hours after induction of tMCAO were markedly reduced, when compared to wild-type mice.^{39,58} No intracranial hemorrhages were observed, suggesting a net protective effect on stroke with blood cells lacking STIM1 or ORAI1. Importantly, the reduced infarct sizes were accompanied by significantly improved neurological and motoric functions of the chimeric animals in comparison to the control mice.^{39,58}

When primary neurons isolated from *Orai1*^{-/-} or *Stim1*^{-/-} mice were subjected to ischemia *in vitro*, a similar degree of SOCE was observed as wild-type cells,^{39,58} whereas the neurons from *Stim2*^{-/-} mice showed a reduced Ca²⁺ store content and SOCE.⁸⁸

These results highlight a regulatory role of STIM2 in neuronal SOCE, relevant for the development of experimentally induced ischemic stroke. Taken together, this points to SOCE as a potential target to suppress ischemic insults, *i.e.* by blocking Ca²⁺-induced platelet activation and reducing neuronal cell death. In line with this suggestion, in the tMCAO model, wild-type mice pretreated with the SOCE blocker 2-aminoethoxydiphenyl borate (2APB) were protected from cerebral infarct growth, in a similar manner as seen with *Orai1*^{-/-} bone marrow chimeric mice.⁷⁹ However, the molecular composition of the SOC complex in ischemic neurons has not been elucidated, leaving the possibility that other ORAI and TRP isoforms regulate SOCE in this cell type.

5. Platelets and immune cells in thrombo-inflammation

The current evidence suggests that at ischemic vascular lesions, the rapid intravascular activation of platelets and endothelial cells increases thrombotic events (Figure 2). Collagen–vWF–GPIb platelet activation axis and factor XIIa (FXIIa)-mediated intrinsic coagulation pathways are important players in these events.^{23,87,89} At initial steps, interactions of platelets subendothelial ECM components lead to platelet adhesion, activation, thereby enhancing thrombin generation and fibrin formation, which lead to thrombus formation. This process also involves interactions of platelet GPVI with its ligands, thereby enhancing thrombus growth.^{23,90,91} Recruitment and activation of immune cells from peripheral blood can trigger fibrin formation, which also contribute to thrombotic events.^{23,89,92} In endothelial and immune cells, the increased expression of leukocyte adhesion molecules, such as P-selectin, intercellular adhesion molecule 1 (ICAM-1), vascular cell adhesion molecule 1 (VCAM-1) and platelet-endothelial cell adhesion molecule (PECAM) further stimulate the transmigration of immune cells.^{92,93} At later time points of the stroke event, the ruptured blood-brain barrier exposes ischemic brain tissue to inflammatory molecules, cytokines, proteases, reactive oxygen species (ROS) derived from platelets and different immune cell subsets,^{89,94,95} thereby leading to neuronal damages (Figure 2).

Emerging insights indicate an important link between thrombotic and inflammatory pathways in ischemic stroke. Accordingly, stroke can be redefined as a thrombo-inflammatory disorder.^{23,87,92,96} In this section, we review the role of SOCE in platelets and immune cells in the context of thrombo-inflammation, referring to studies from mice and patients lacking functional STIM or ORAI proteins.

5.1. Role of SOCE in different immune cells

5.1.1. Neutrophils

Neutrophils are first responders of the immune system, which are rapidly recruited into tissues in response to inflammation or infection. Neutrophils recognize antibody-opsonized pathogens and immune complexes containing antigens and antibodies via the Fc γ receptors on their cell surface. This leads to immune complexes in the phagosome and phagocytosis of pathogens, with both processes relying on the production of ROS. Besides the Fc γ receptors, also GPCR and integrins can regulate Ca²⁺ influx in neutrophils, where SOCE is the main mechanism of Ca²⁺ entry.¹⁶ Early studies showed that in the neutrophil-like HL-60 cells, small interfering RNA (siRNA)-mediated knock-down of STIM1 impairs Ca²⁺ entry in response to formyl peptide or TG, resulting in a decreased production of ROS.⁹⁷ Using mice lacking STIM1, STIM2 or both in the myeloid and neutrophil-specific lineage, Clemens and collaborators showed that STIM1 and STIM2 cooperatively regulate neutrophil SOCE. ROS production, neutrophil degranulation and phagocytosis are minimally impaired in the absence of STIM2, suggesting that STIM1 is the major Ca²⁺ sensor required for neutrophil functions.⁹⁸ Interestingly, STIM2-deficient, but not STIM1-deficient, neutrophils display a marked defect in cytokine production and protected in a model of systemic inflammatory response syndrome.⁹⁸

Patients carrying a missense ORAI1 variant have no alteration in leukocyte cell counts, suggesting that SOCE is not required for granulocyte development.¹⁶ However, receptor-induced Ca²⁺ influx was virtually abolished in activated neutrophils from immunodeficient patients with strongly altered ORAI1 functions, indicating that the major route of SOCE triggered by ORAI1 isoform in these cells.⁹⁹⁻¹⁰¹ On other hand, in neutrophil like HL-60 cells, siRNA-mediated knock-down of ORAI1 decreased SOCE and production of ROS in response to stimulation through Fc γ receptors or GPCR by no more than 20-50%,¹⁰²⁻¹⁰⁴ suggesting the presence of an alternative mechanism. Similar results were obtained using *Orai1*^{+/-} murine neutrophils.¹⁰²

Neutrophil recruitment to inflammatory sites involves chemokine release and β_2 -integrin activation, with both events being co-regulated by the cytosolic Ca²⁺ level.¹⁰⁵⁻¹⁰⁷ Inhibition of SOCE in human neutrophils by genetic deletion of ORAI1 delayed integrin β_2 -dependent adhesion and integrin clustering, suggesting a role of SOCE in neutrophil attachment to the endothelium.^{102,108} In contrast to ORAI1, in murine neutrophils STIM1 appeared to be dispensable for cellular migration, indicating a complex sensing mechanism in this cell type.¹⁰⁹

Neutrophils contribute to the disruption of blood brain barrier through the release of proteases and ROS, thereby inducing cerebral edema and neurotoxicity.⁹⁴ It has been also proposed that neutrophils and platelet interaction aggravates ischemic brain damage and causes thrombo-inflammatory injury. This interaction is considered to be important for the extravasation.¹¹⁰ Recently, it has been shown that the migration of neutrophils into the brain is dependent on the platelet GPIb-V-IX complex.¹¹¹ Neutrophil migration also involves TRPM7-channel activity by facilitating Ca^{2+} oscillations. It has been suggested that interplay between TRPM7 and glycoprotein CD147 regulates neutrophil chemotaxis, adhesion and migration in rheumatoid arthritis conditions.¹¹² Recently, using bone marrow chimeric mice, we showed that the kinase activity of TRPM7, which regulates SOCE, is involved in ischemic stroke.⁶² After tMCAO, the protective effects

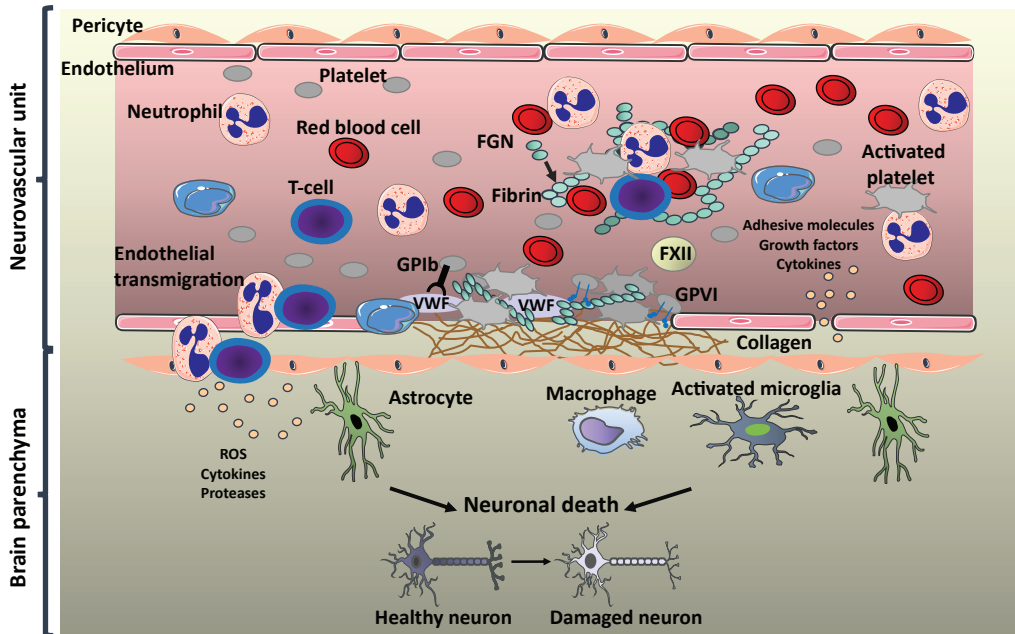


Figure 2: Mechanisms of thrombo-inflammation in brain ischemic stroke. Upon ischemic vascular injury, blood platelets adhere to exposed von Willebrand factor (vWF) through platelet Glycoprotein Ib alpha (GPIb α), thereby enhancing thrombin generation and fibrin formation, which lead to thrombus formation. This process also involves interaction of GPVI with fibrillar collagen and fibrin, leading to the platelet adhesion, activation and subsequently thrombus formation and growth. In addition, activation of intrinsic coagulation pathway and fibrin generation lead to the recruitment of circulating platelets and immune cells, and subsequently to the release of inflammatory cytokines, edema, activation of microglia and finally to neuronal death. During ischemic insults, activated neutrophils and T cells enhance the expression of adhesion molecules and release of growth factors and cytokines in endothelium and immune cells. Crosstalk between neutrophils, platelets and T cells lead to thrombus and fibrin formation, thrombin activation and induction of extrinsic tissue factor pathway. Immune cells may also contribute to ischemic stroke by migrating and infiltrating in brain parenchyma, thereby releasing ROS, inflammatory cytokines and proteases, which also lead to neuronal damage.

observed in different groups of bone marrow chimeric *Trpm7^{R/R}* mice was not only due to the lack of TRPM7 kinase activity in platelets and immune cells⁶², but also suggest the involvement of cells located in the brain vessels and neuronal tissue. However, the detailed role of TRPM7 kinase-mediated SOCE in neutrophils and other immune cells need to be further investigated in ischemic conditions.

Together, these data suggest that SOCE mediates many functions of neutrophils, which may occur in thrombo-inflammatory diseases. Whether SOCE components only in neutrophils or platelets or in bidirectional way could mediate these processes is simulating several questions, which need to be addressed in the future.

5.1.2. Macrophages

Macrophages are phagocytes derived from activated monocytes with central roles in both innate and adaptive immunity.¹¹³ Macrophages play an important role in phagocytosis of cell debris and pathogens, and the production of cytokines such as of interleukin (IL)-1 β , IL-6 and IL-12, which in turn activate other immune cells. The recognition of antibody-opsonized pathogens by macrophages is mediated through Fc gamma (Fc γ) receptors.¹¹³

Initial studies demonstrated that STIM1 and SOCE are essential for Fc γ receptor activation and auto-immune inflammation.¹¹⁴ Upon cross-linking of Fc γ receptors, *Stim1^{-/-}* macrophages displayed markedly reduced phagocytosis of opsonized blood, while the production of inflammatory cytokines, macrophage inflammatory protein-2 (MIP-2) and tumor necrosis factor alpha (TNF α) was only moderately impaired.¹¹⁴ This work further indicated that STIM1 was indispensable for the development of monocytes and their differentiation into macrophages.¹¹⁴ Deficiency in STIM1 also resulted in resistance to experimental IgG-dependent immune thrombocytopenia, anaphylaxis, and acute pneumonitis.¹¹⁴ Later evidence indicated that also STIM2 contributes to Fc γ receptor activation, suggesting a partial functional redundancy between the STIM isoforms in this regulation of inflammation.¹¹⁵

Recently, using *Stim1^{-/-}* and *Stim2^{-/-}* bone marrow chimeras, it was demonstrated that either isoform is dispensable for key effector functions of macrophages and dendritic cells, such as Fc γ receptor-dependent and -independent phagocytosis, phagolysome fusion, cytokine production and NLR family, pyrin domain containing 3 (NLRP3) lammasome activation.¹¹⁶ Altogether, these data indicate that depending of the inflammatory context, SOCE can regulate proinflammatory pathways in macrophages, but not other effector functions.¹¹⁶

TRMP7 channel is also mediator of macrophage functions. TRPM7-deficient macrophages displayed decreased Toll-like receptor 4 (TLR4) internalization and nuclear factor kappa-light-chain-enhancer of activated B cells (NFkB) activation in following lipopolysaccharide (LPS) challenge.¹¹⁷ Interestingly, these defects were due to diminished TRPM7-mediated Ca^{2+} influx.¹¹⁷ In addition, in LPS-induced peritonitis model, *Trpm7^{fl/fl}-LysM-Cre* mice had decreased serum cytokine levels after LPS treatment, preventing pathological inflammation.¹¹⁷ However, whether these functions in macrophages involve TRPM7-mediated SOCE remain still elusive.

After stroke, ischemic brain tissues are abundant in macrophages derived from either resident microglia or infiltrating monocytes.¹¹⁸ Interestingly, it has been shown that expression profile of genes involved in Ca^{2+} signaling enriched in migrating monocytes during ischemic stroke.¹¹⁹ Whether SOCE activity may be involved in the regulation of macrophage function in stroke, future studies needed to establish this process using a wide range of thrombo-inflammatory conditions.

5.1.3. T cells

SOCE regulates many important functions of T cells, including proliferation, differentiation and cytokine production. Activation of the T cell receptor signalosome triggers intracellular Ca^{2+} store depletion and subsequent SOCE, and activates a Ca^{2+} -dependent calcineurin-nuclear factor of activated T cells (NFAT) pathway. T cells isolated from SOCE-defective patients fail to proliferate in response to receptor stimulation, and accordingly, display impaired NFAT signaling thereby blocking downstream cytokine production.^{120,121} In line with these data, murine T cells lacking STIM1 or STIM2 produced less cytokines and displayed reduced nuclear translocation of the transcription factor NFAT.⁵⁹

Homozygous *ORAI1^{R93W}* mice die after birth, but fetal liver chimeras are viable and T cells develop normally, despite defective SOCE. The effector functions of T cells were markedly impaired in these mice, including the production of IL-2, IL-4, IL-17, interferon (IFN)- γ and TNF α ,⁹⁹ indicating a crucial role of ORAI1-mediated SOCE in the regulation of the inflammatory response. In Type 2 T helper (Th2) cells from STIM1 or ORAI1-deficient mice, the activity of CD4⁺ T helper cells is also dependent on SOCE, as apparent from the decreased production of IL-4 and IL-10.⁹⁹ This effect was linked to impaired functions of Type 1 T helper (Th1) and T helper 17 (Th17) cells, and a shortage of IFN- γ and IL-17A production.^{99,122} *Stim1^{-/-}* mice were found to be more resistant to induction of experimental autoimmune encephalomyelitis than *Stim2^{-/-}* mice, which is consistent with only partial involvement of STIM2 in cytokine production and T cell function.^{122,123}

Using conditional knock-out mouse models, it was recently shown that genetic deletion of *Orai1* reduces SOCE in mouse T cells, whereas deletion of *Orai2* increases SOCE. This may suggest that ORAI2 forms heteromeric channels with ORAI1, in which ORAI2 attenuates the function of ORAI1 and limits SOCE.¹²⁴ Interestingly, deletion of *Orai2* enhanced SOCE in naive T cells but not in effector T cells. Combined deletion of *Orai1* and *Orai2* completely abolished SOCE, suggesting that both isoforms mediate SOCE in these cells. Moreover, *Orai1*^{-/-}*Orai2*^{-/-} double knock-out mice displayed severe defects in T cell functions *in vitro*, and impaired T cell-mediated immune responses *in vivo*, such as antibody production after viral infection, colitis or graft-versus-host disease.¹²⁴

Recent studies also highlighted the role of TRPM7 in human T cell proliferation. Pharmacological inhibition of TRPM7 in human T cells leads to growth arrest and reduces cell proliferation.¹²⁵ In addition, TRPM7 was described to be involved in the migration of human T cells.¹²⁶ Consistently, Romagnani et al. showed that TRPM7 kinase activity is essential for T-cell colonization and alloreactivity in the gut.¹²⁷ More recently, it has been shown that the deletion of TRPM kinase activity in mice results in enlarged spleens, reduced T-cell proliferation and decreased SOCE.¹²⁸ In future, it could be important to investigate whether the observed functions of TRPM7-kinase mediated SOCE in mouse cells could be applied to humans.

Rag1^{-/-} mice lacking both mature T and B cells are profoundly protected from experimentally induced focal cerebral ischemia.¹²⁹ Adoptive transfer of T cells, but not of B cells, could fully restore the susceptibility to stroke progression. Importantly, platelet activation pathways were unaltered in *Rag1*^{-/-} mice,¹²⁹ suggesting that the observed effect was not linked to altered thrombus formation. However, adoptive transfer of T cells into platelet-depleted *Rag1*^{-/-} mice did not result in increased infarct sizes,¹²⁹ pointing to a crosstalk between platelets and T cells in the progression of ischemic stroke.

Regulatory T (T_{reg}) cells are a subset of T lymphocytes that regulate immune homeostasis by maintaining immunological self-tolerance. The development of such cells is dependent on the forkhead box P3 (Foxp3) transcription factor.¹³⁰ Kleinschnitz et al. showed that Foxp3⁺ T_{reg} cells can interact with cerebral endothelial cells and platelets, thereby promoting ischemic neurodegeneration after the ischemic insult.¹³¹ In mice, inactivation of the *Stim1*/*Stim2* genes significantly diminished the population of Foxp3⁺ T_{reg} cells in the thymus and lymphoid organs.⁵⁹ However, the T_{reg} cells developed normally in *Stim1*^{-/-} or *Orai1*^{-/-} mice, which may point to a role of STIM2 backing up the SOCE activity for T_{reg} cell development.^{99,132} On other hand, SOCE was shown to regulate T_{reg} suppressive functions. Thus, the few CD4⁺CD25⁺ Foxp3 T_{reg} cells deficient in both STIM1 and STIM2 were unable to suppress the proliferation of wild-

type CD4⁺ T cells.¹⁰¹ T_{reg} cells isolated from STIM1- or ORAI1-deficient animals displayed only a moderate reduction in this suppressive activity.^{99,132} Altogether, these data point on potential crosstalk between STIM1 and STIM2 in the regulation of T_{reg} cell function.

Although T cells are important players of thrombo-inflammatory diseases, the role of SOCE-mediated T-cell functions in such conditions is not established. Moreover, T cell-endothelial cell-platelet interactions may influence thrombo-inflammatory process, it appears interesting whether this cellular crosstalk may be regulated by SOCE.

6. Therapeutic potential of SOCE inhibitors for thrombo-inflammatory diseases

While a range of synthetic pharmacological compounds are known to inhibit the channels responsible for SOCE, several of these can also affect the activities of other, non-SOC channels. One of the most widely studied drugs is 2APB. This compound was discovered as a non-competitive lipophilic antagonist of the reticular IP₃ receptors, inhibiting Ca²⁺ store depletion, but in addition it attenuates SOCE and the TRPC3 channel in the plasma membrane.^{133,134} Subsequently, it appeared that 2APB can also decrease the activities of TRPM6 and TRPM7 channels in various cell types.¹³⁵ Interestingly, at high concentrations, 2APB inhibits ORAI1 and ORAI2, but stimulates ORAI3.¹³⁶ Recently, Wei et al. showed that 2APB has also inhibitory effects on functional coupling between STIM1 and ORAI1.¹³⁷ Treatment with 2APB reduced platelet responses and partially protected mice from cerebral infarct progression in the tMCAO model,⁷⁹ but the target of the compound responsible for these effects has not been established. 2APB may also influence many functions in immune cells. In mast cells, 2APB inhibited cell degranulation and release of inflammatory cytokines, such as TNF α and IL-4.¹³⁸ In addition, in bone marrow-derived macrophages and dendritic cells, 2APB strongly impaired many effector functions, including phagocytosis, inflammasome activation and priming of T-cells.¹¹⁶ In contrast, macrophages and dendritic cells from mice with conditional deletion of *Stim1* and *Stim2* genes displayed no major functional defects,¹¹⁶ suggesting that in these cells 2APB-induced effects occur in SOCE-independent manner.

Another well-studied SOCE blocker is the synthetic estrogen, diethylstilbestrol (DES), which was discovered as an agonist of estrogen receptors.¹³⁹ Initially, DES was used as a therapeutic agent for women, for whom estrogen replacement therapy was indicated. DES was also shown to upregulate IFN γ production in splenic lymphocytes.¹⁴⁰ Later, DES was found to inhibit SOCE in platelets and vascular smooth muscle cells.¹⁴¹

3,5-Bis(trifluoromethyl) pyrazole derivative (BTP2) inhibits SOCE in platelets and macrophages. In primary macrophages, BTP2-inhibited SOCE occurred through the suppression of Fcγ receptor-mediated signaling. Treatment with BTP2 strongly attenuated skin and lung inflammation in mice.¹⁴² The compound was found to suppress anti-CD3 antibody-induced Ca²⁺ mobilization in T cells, thereby affecting cytokine production and cell proliferation,¹⁴³⁻¹⁴⁵ but the underlying molecular mechanisms are still unknown. Besides ORAI, BTP2 may also suppress the channel activity of TRPC3 and TRPC5,¹⁴⁶ although it may activate TRPM4 channels.¹⁴⁷ These diverse actions of BTP2 on cation homeostasis suggest that immunomodulatory effects will depend on the channel composites of the investigated cell types.

A pyrazole derivative, GSK-7975A, has been described to inhibit ORAI-mediated SOCE, likely by blocking the pore-forming unit of the channel.^{148,149} In human embryonic kidney 293 (HEK293) cells expressing the ORAI^{E106D} variant, modifying the structure of the channel pore, it appeared that the inhibitory potency of GSK-7975A on SOCE was significantly reduced.¹⁴⁹ Interestingly, in HEK293 cells, GSK-7975A was also found to inhibit TRPV6 channels.^{148,149} In addition, van Kruchten *et al.* showed that GSK-7975A, like a novel compound Synta66, inhibited platelet-dependent coagulation and thrombus formation as potently as 2APB.⁷⁹

Altogether these studies indicate that SOCE inhibitors influence many functions of platelets and immune cells, which may contribute to thrombo-inflammation. Future studies are needed to investigate the mechanisms induced by SOCE inhibitors in more details.

7. Conclusions

In this review we summarized important aspects of the complex roles of SOCE in platelets and immune cells. In platelets, SOCE is mainly regulated by STIM1 and ORAI1, whereas other isoforms have less prominent roles in these cells in thrombosis and hemostasis. Studies using knock-out mice indicated that in platelets inhibition of ORAI1-mediated SOCE may present an attractive strategy to prevent arterial thrombosis and ischemic stroke. In immune cells, inhibition of SOCE protected mice from various inflammatory diseases. A better understanding of fine-tuning of SOCE in thrombosis and thrombo-inflammation is required to address a large panel of therapeutic strategies for selective SOC channel inhibition in both platelets and immune cells.

Disclosure

The authors report no conflicts of interest.

Acknowledgements

E.M.B., B.N. and A.B. are supported by the Deutsche Forschungsgemeinschaft (SFB/TR 240). M.N. and J.H. acknowledge support from the Cardiovascular Center (HVC), Maastricht University Medical Center⁺, and the 5th Meuse-Rhine Interregional Programme Polyvalve.

References

1. Putney JW. Origins of the concept of store-operated calcium entry. *Front Biosci (Schol Ed)*. 2011; 3: 980-984.
2. Stathopoulos PB, Ikura M. Store operated calcium entry: From concept to structural mechanisms. *Cell Calcium*. 2017; 63: 3-7.
3. Clapham DE. Calcium signaling. *Cell*. 2007; 131: 1047-1058.
4. Varga-Szabo D, Braun A, Nieswandt B. Calcium signaling in platelets. *J Thromb Haemost*. 2009; 7: 1057-1066.
5. Muik M, Schindl R, Fahrner M, Romanin C. Ca²⁺ release-activated Ca²⁺ (CRAC) current, structure, and function. *Cell Mol Life Sci*. 2012; 69: 4163-4176.
6. Parekh AB, Putney JW, Jr. Store-operated calcium channels. *Physiol Rev*. 2005; 85: 757-810.
7. Liou J, Kim ML, Heo WD, et al. STIM1 is a Ca²⁺ sensor essential for Ca²⁺-store-depletion-triggered Ca²⁺ influx. *Curr Biol*. 2005; 15: 1235-1241.
8. Roos J, DiGregorio PJ, Yeromin AV, et al. STIM1, an essential and conserved component of store-operated Ca²⁺ channel function. *J Cell Biol*. 2005; 169: 435-445.
9. Zhang SL, Yu Y, Roos J, et al. STIM1 is a Ca²⁺ sensor that activates CRAC channels and migrates from the Ca²⁺ store to the plasma membrane. *Nature*. 2005; 437: 902-905.
10. Vig M, Peinelt C, Beck A, et al. CRACM1 is a plasma membrane protein essential for store-operated Ca²⁺ entry. *Science*. 2006; 312: 1220-1223.
11. Feske S, Gwack Y, Prakriya M, et al. A mutation in Orai1 causes immune deficiency by abrogating CRAC channel function. *Nature*. 2006; 441: 179-185.
12. Prakriya M, Feske S, Gwack Y, et al. Orai1 is an essential pore subunit of the CRAC channel. *Nature*. 2006; 443: 230-233.
13. Yeromin AV, Zhang SL, Jiang W, et al. Molecular identification of the CRAC channel by altered ion selectivity in a mutant of Orai. *Nature*. 2006; 443: 226-229.
14. Vig M, DeHaven WI, Bird GS, et al. Defective mast cell effector functions in mice lacking the CRACM1 pore subunit of store-operated calcium release-activated calcium channels. *Nat Immunol*. 2008; 9: 89-96.
15. Gwack Y, Srikanth S, Oh-Hora M, et al. Hair loss and defective T- and B-cell function in mice lacking ORAI1. *Mol Cell Biol*. 2008; 28: 5209-5222.
16. Shaw PJ, Feske S. Physiological and pathophysiological functions of SOCE in the immune system. *Front Biosci (Elite Ed)*. 2012; 4: 2253-2268.
17. Bertin S, Raz E. Transient Receptor Potential (TRP) channels in T cells. *Semin Immunopathol*. 2016; 38: 309-319.
18. Feske S. ORAI1 and STIM1 deficiency in human and mice: roles of store-operated Ca²⁺ entry in the immune system and beyond. *Immunol Rev*. 2009; 231: 189-209.
19. Braun A, Vogtle T, Varga-Szabo D, Nieswandt B. STIM and Orai in hemostasis and thrombosis. *Front Biosci (Landmark Ed)*. 2011; 16: 2144-2160.
20. Varga-Szabo D, Braun A, Nieswandt B. STIM and Orai in platelet function. *Cell Calcium*. 2011; 50: 270-278.

21. Versteeg HH, Heemskerk JW, Levi M, Reitsma PH. New fundamentals in hemostasis. *Physiol Rev*. 2013; 93: 327-358.
22. Nieswandt B, Pleines I, Bender M. Platelet adhesion and activation mechanisms in arterial thrombosis and ischaemic stroke. *J Thromb Haemost*. 2011; 9 Suppl 1: 92-104.
23. Nieswandt B, Kleinschnitz C, Stoll G. Ischaemic stroke: a thrombo-inflammatory disease? *J Physiol*. 2011; 589: 4115-4123.
24. Jackson SP. Arterial thrombosis--insidious, unpredictable and deadly. *Nat Med*. 2011; 17: 1423-1436.
25. Vogtle T, Cherpokova D, Bender M, Nieswandt B. Targeting platelet receptors in thrombotic and thrombo-inflammatory disorders. *Hamostaseologie*. 2015; 35: 235-243.
26. Berridge MJ, Bootman MD, Roderick HL. Calcium signaling: dynamics, homeostasis and remodeling. *Nat Rev Mol Cell Biol*. 2003; 4: 517-529.
27. Heemskerk JW, Matheij NJ, Cosemans JM. Platelet-based coagulation: different populations, different functions. *J Thromb Haemost*. 2013; 11: 2-16.
28. Lian L, Wang Y, Draznin J, et al. The relative role of PLC β and PI3K γ in platelet activation. *Blood*. 2005; 106: 110-117.
29. Swieringa F, Kuijpers MJ, Heemskerk JW, van der Meijden PE. Targeting platelet receptor function in thrombus formation: the risk of bleeding. *Blood Rev*. 2014; 28: 9-21.
30. Watson SP, Auger JM, McCarty OJ, Pearce AC. GPVI and integrin $\alpha_{IIb}\beta_3$ signaling in platelets. *J Thromb Haemost*. 2005; 3: 1752-1762.
31. Nieswandt B, Watson SP. Platelet-collagen interaction: is GPVI the central receptor? *Blood*. 2003; 102: 449-461.
32. Brune B, Ullrich V. Different calcium pools in human platelets and their role in thromboxane A₂ formation. *J Biol Chem*. 1991; 266: 19232-19237.
33. Cavallini L, Coassin M, Alexandre A. Two classes of agonist-sensitive Ca²⁺ stores in platelets, as identified by their differential sensitivity to 2,5-di-(tert-butyl)-1,4-benzohydroquinone and thapsigargin. *Biochem J*. 1995; 310 (Pt 2): 449-452.
34. Papp B, Enyedi A, Kovacs T, et al. Demonstration of two forms of calcium pumps by thapsigargin inhibition and radioimmunoblotting in platelet membrane vesicles. *J Biol Chem*. 1991; 266: 14593-14596.
35. Enouf J, Bredoux R, Papp B, et al. Human platelets express the SERCA2- β isoform of Ca²⁺-transport ATPase. *Biochem J*. 1992; 286: 135-140.
36. Wuytack F, Papp B, Verboomen H, et al. A sarco/endoplasmic reticulum Ca²⁺-ATPase 3-type Ca²⁺ pump is expressed in platelets, in lymphoid cells, and in mast cells. *J Biol Chem*. 1994; 269: 1410-1416.
37. Bobe R, Bredoux R, Wuytack F, et al. The rat platelet 97-kDa Ca²⁺ ATPase isoform is the sarcoendoplasmic reticulum Ca²⁺ ATPase 3 protein. *J Biol Chem*. 1994; 269: 1417-1424.
38. Vig M, Beck A, Billingsley JM, et al. CRACM1 multimers form the ion-selective pore of the CRAC channel. *Curr Biol*. 2006; 16: 2073-2079.
39. Braun A, Varga-Szabo D, Kleinschnitz C, et al. Orai1 (CRACM1) is the platelet SOC channel and essential for pathological thrombus formation. *Blood*. 2009; 113: 2056-2063.
40. Tolhurst G, Carter RN, Amisten S, et al. Expression profiling and electrophysiological studies suggest a major role for Orai1 in the store-operated Ca²⁺ influx pathway of platelets and megakaryocytes. *Platelets*. 2008; 19: 308-313.
41. Bergmeier W, Oh-Hora M, McCarl CA, et al. R93W mutation in Orai1 causes impaired calcium influx in platelets. *Blood*. 2009; 113: 675-678.
42. Gilio K, van Kruchten R, Braun A, et al. Roles of platelet STIM1 and Orai1 in glycoprotein VI- and thrombin-dependent procoagulant activity and thrombus formation. *J Biol Chem*. 2010; 285: 23629-23638.
43. Nilius B, Owsianik G. The transient receptor potential family of ion channels. *Genome Biol*. 2011; 12: 218.
44. Carter RN, Tolhurst G, Walmsley G, et al. Molecular and electrophysiological characterization of transient receptor potential ion channels in the primary murine megakaryocyte. *J Physiol*. 2006; 576: 151-162.
45. den Dekker E, Molin DG, Breikers G, et al. Expression of transient receptor potential mRNA isoforms and Ca(2+) influx in differentiating human stem cells and platelets. *Biochim Biophys Acta*. 2001; 1539: 243-255.
46. Authi KS. TRP channels in platelet function. *Handb Exp Pharmacol*. 2007: 425-443.
47. Brownlow SL, Sage SO. Transient receptor potential protein subunit assembly and membrane dis-

- tribution in human platelets. *Thromb Haemost.* 2005; 94: 839-845.
48. Hassock SR, Zhu MX, Trost C, Flockerzi V, Authi KS. Expression and role of TRPC proteins in human platelets: evidence that TRPC6 forms the store-independent calcium entry channel. *Blood.* 2002; 100: 2801-2811.
 49. Jardin I, Redondo PC, Salido GM, Rosado JA. Phosphatidylinositol 4,5-bisphosphate enhances store-operated calcium entry through hTRPC6 channel in human platelets. *Biochim Biophys Acta.* 2008; 1783: 84-97.
 50. Rosado JA, Sage SO. Coupling between inositol 1,4,5-trisphosphate receptors and human transient receptor potential channel 1 when intracellular Ca^{2+} stores are depleted. *Biochem J.* 2000; 350: 631-635.
 51. Rosado JA, Jenner S, Sage SO. A role for the actin cytoskeleton in the initiation and maintenance of store-mediated calcium entry in human platelets. Evidence for conformational coupling. *J Biol Chem.* 2000; 275: 7527-7533.
 52. Varga-Szabo D, Authi KS, Braun A, *et al.* Store-operated Ca^{2+} entry in platelets occurs independently of transient receptor potential (TRP) C1. *Pflugers Arch.* 2008; 457: 377-387.
 53. Rosado JA, Sage SO. Activation of store-mediated calcium entry by secretion-like coupling between the inositol 1,4,5-trisphosphate receptor type II and human transient receptor potential (hTrp1) channels in human platelets. *Biochem J.* 2001; 356: 191-198.
 54. Ong HL, Chen J, Chataway T, *et al.* Specific detection of the endogenous transient receptor potential (TRP)-1 protein in liver and airway smooth muscle cells using immunoprecipitation and Western-blot analysis. *Biochem J.* 2002; 364: 641-648.
 55. Minke B. TRP channels and Ca^{2+} signaling. *Cell Calcium.* 2006; 40: 261-275.
 56. Carafoli E, Santella L, Branca D, Brini M. Generation, control, and processing of cellular calcium signals. *Crit Rev Biochem Mol Biol.* 2001; 36: 107-260.
 57. Grosse J, Braun A, Varga-Szabo D, *et al.* An EF hand mutation in Stim1 causes premature platelet activation and bleeding in mice. *J Clin Invest.* 2007; 117: 3540-3550.
 58. Varga-Szabo D, Braun A, Kleinschnitz C, *et al.* The calcium sensor STIM1 is an essential mediator of arterial thrombosis and ischemic brain infarction. *J Exp Med.* 2008; 205: 1583-1591.
 59. Oh-Hora M, Yamashita M, Hogan PG, *et al.* Dual functions for the endoplasmic reticulum calcium sensors STIM1 and STIM2 in T cell activation and tolerance. *Nat Immunol.* 2008; 9: 432-443.
 60. Baba Y, Nishida K, Fujii Y, *et al.* Essential function for the calcium sensor STIM1 in mast cell activation and anaphylactic responses. *Nat Immunol.* 2008; 9: 81-88.
 61. Wolf K, Braun A, Haining EJ, *et al.* Partially defective store operated calcium entry and hem(ITAM) signaling in platelets of serotonin transporter deficient mice. *PLoS One.* 2016; 11: e0147664.
 62. Gotru SK, Chen W, Kraft P, *et al.* TRPM7 kinase controls calcium responses in arterial thrombosis and stroke in mice. *Arterioscler Thromb Vasc Biol.* 2018; 38: 344-352.
 63. Kawasaki T, Ueyama T, Lange I, Feske S, Saito N. Protein kinase C-induced phosphorylation of Orai1 regulates the intracellular Ca^{2+} level via the store-operated Ca^{2+} channel. *J Biol Chem.* 2010; 285: 25720-25730.
 64. Pozo-Guisado E, Martin-Romero FJ. The regulation of STIM1 by phosphorylation. *Commun Integr Biol.* 2013; 6: e26283.
 65. Nishida M, Watanabe K, Sato Y, *et al.* Phosphorylation of TRPC6 channels at Thr69 is required for anti-hypertrophic effects of phosphodiesterase 5 inhibition. *J Biol Chem.* 2010; 285: 13244-13253.
 66. Bousquet SM, Monet M, Boulay G. Protein kinase C-dependent phosphorylation of transient receptor potential canonical 6 (TRPC6) on serine 448 causes channel inhibition. *J Biol Chem.* 2010; 285: 40534-40543.
 67. Paez Espinosa EV, Murad JP, Ting HJ, Khasawneh FT. Mouse transient receptor potential channel 6: role in hemostasis and thrombogenesis. *Biochem Biophys Res Commun.* 2012; 417: 853-856.
 68. Ramanathan G, Gupta S, Thielmann I, *et al.* Defective diacylglycerol-induced Ca^{2+} entry but normal agonist-induced activation responses in TRPC6-deficient mouse platelets. *J Thromb Haemost.* 2012; 10: 419-429.
 69. Chen W, Thielmann I, Gupta S, *et al.* Orai1-induced store-operated Ca^{2+} entry enhances phospholipase activity and modulates canonical transient receptor potential channel 6 function in murine platelets. *J Thromb Haemost.* 2014; 12: 528-539.
 70. Gachet C. Regulation of platelet functions by P2 receptors. *Annu Rev Pharmacol Toxicol.* 2006; 46: 277-300.
 71. Gachet C. P2 receptors, platelet function and pharmacological implications. *Thromb Haemost.* 2008; 99: 466-472.
 72. Mahaut-Smith MP, Taylor KA, Evans RJ. Calcium signaling through ligand-gated ion channels such

- as P2X1 receptors in the platelet and other non-excitabile cells. *Adv Exp Med Biol.* 2016; 898: 305-329.
73. Hechler B, Lenain N, Marchese P, *et al.* A role of the fast ATP-gated P2X1 cation channel in thrombosis of small arteries in vivo. *J Exp Med.* 2003; 198: 661-667.
 74. Oury C, Kuijpers MJ, Toth-Zsamboki E, *et al.* Overexpression of the platelet P2X1 ion channel in transgenic mice generates a novel prothrombotic phenotype. *Blood.* 2003; 101: 3969-3976.
 75. Hechler B, Gachet C. Purinergic Receptors in thrombosis and inflammation. *Arterioscler Thromb Vasc Biol.* 2015; 35: 2307-2315.
 76. Oury C, Lecut C, Hego A, Wera O, Delierneux C. Purinergic control of inflammation and thrombosis: Role of P2X1 receptors. *Comput Struct Biotechnol J.* 2015; 13: 106-110.
 77. Hechler B, Magnenat S, Zighetti ML, *et al.* Inhibition of platelet functions and thrombosis through selective or nonselective inhibition of the platelet P2 receptors with increasing doses of NF449 [4,4',4'',4'''-(carbonylbis(imino-5,1,3-benzenetriylbis-(carbonylimino))tetrakis -benzene-1,3-disulfonic acid octasodium salt]. *J Pharmacol Exp Ther.* 2005; 314: 232-243.
 78. Toth-Zsamboki E, Oury C, Cornelissen H, *et al.* P2X1-mediated ERK2 activation amplifies the collagen-induced platelet secretion by enhancing myosin light chain kinase activation. *J Biol Chem.* 2003; 278: 46661-46667.
 79. van Kruchten R, Braun A, Feijge MA, *et al.* Antithrombotic potential of blockers of store-operated calcium channels in platelets. *Arterioscler Thromb Vasc Biol.* 2012; 32: 1717-1723.
 80. Ahmad F, Boulaftali Y, Greene TK, *et al.* Relative contributions of stromal interaction molecule 1 and CalDAG-GEFI to calcium-dependent platelet activation and thrombosis. *J Thromb Haemost.* 2011; 9: 2077-2086.
 81. Lacruz RS, Feske S. Diseases caused by mutations in ORAI1 and STIM1. *Ann N Y Acad Sci.* 2015; 1356: 45-79.
 82. Nagy M, Mastenbroek TG, Mattheij NJA, *et al.* Variable impairment of platelet functions in patients with severe, genetically linked immune deficiencies. *Haematologica.* 2018; 103: 540-549.
 83. Misceo D, Holmgren A, Louch WE, *et al.* A dominant STIM1 mutation causes Stormorken syndrome. *Hum Mutat.* 2014; 35: 556-564.
 84. Morin G, Bruechle NO, Singh AR, *et al.* Gain-of-Function Mutation in STIM1 (P.R304W) Is Associated with Stormorken Syndrome. *Hum Mutat.* 2014; 35: 1221-1232.
 85. Markello T, Chen D, Kwan JY, *et al.* York platelet syndrome is a CRAC channelopathy due to gain-of-function mutations in STIM1. *Mol Genet Metab.* 2015; 114: 474-482.
 86. Clark WM, Lessov NS, Dixon MP, Eckenstein F. Monofilament intraluminal middle cerebral artery occlusion in the mouse. *Neurol Res.* 1997; 19: 641-648.
 87. Kraft P, Nieswandt B, Stoll G, Kleinschnitz C. [Acute ischemic stroke. New approaches to antithrombotic treatment]. *Nervenarzt.* 2012; 83: 435-449.
 88. Berna-Erro A, Braun A, Kraft R, *et al.* STIM2 regulates capacitive Ca²⁺ entry in neurons and plays a key role in hypoxic neuronal cell death. *Sci Signal.* 2009; 2: ra67.
 89. De Meyer SF, Denorme F, Langhauser F, *et al.* Thrombo-inflammation in Stroke Brain Damage. *Stroke.* 2016; 47: 1165-1172.
 90. Induruwa I, Jung SM, Warburton EA. Beyond antiplatelets: The role of glycoprotein VI in ischemic stroke. *Int J Stroke.* 2016; 11: 618-625.
 91. Dutting S, Bender M, Nieswandt B. Platelet GPVI: a target for antithrombotic therapy?! *Trends Pharmacol Sci.* 2012; 33: 583-590.
 92. Stoll G, Kleinschnitz C, Nieswandt B. Combating innate inflammation: a new paradigm for acute treatment of stroke? *Ann N Y Acad Sci.* 2010; 1207: 149-154.
 93. Frijns CJ, Kappelle LJ. Inflammatory cell adhesion molecules in ischemic cerebrovascular disease. *Stroke.* 2002; 33: 2115-2122.
 94. Jickling GC, Liu D, Ander BP, *et al.* Targeting neutrophils in ischemic stroke: translational insights from experimental studies. *J Cereb Blood Flow Metab.* 2015; 35: 888-901.
 95. Hermann DM, Kleinschnitz C, Gunzer M. Implications of polymorphonuclear neutrophils for ischemic stroke and intracerebral hemorrhage: Predictive value, pathophysiological consequences and utility as therapeutic target. *J Neuroimmunol.* 2018; 321: 138-143.
 96. Mezger M, Gobel K, Kraft P, *et al.* Platelets and vascular inflammation of the brain. *Hamostaseologie.* 2015; 35: 244-251.
 97. Brechard S, Plancon S, Melchior C, Tschirhart EJ. STIM1 but not STIM2 is an essential regulator of Ca²⁺ influx-mediated NADPH oxidase activity in neutrophil-like HL-60 cells. *Biochem Pharmacol.* 2009; 78: 504-513.
 98. Clemens RA, Chong J, Grimes D, Hu Y, Lowell CA. STIM1 and STIM2 cooperatively regulate mouse

- neutrophil store-operated calcium entry and cytokine production. *Blood*. 2017; 130: 1565-1577.
99. McCarl CA, Khalil S, Ma J, *et al*. Store-operated Ca²⁺ entry through ORAI1 is critical for T cell-mediated autoimmunity and allograft rejection. *J Immunol*. 2010; 185: 5845-5858.
100. Le Deist F, Hivroz C, Partiseti M, *et al*. A primary T-cell immunodeficiency associated with defective transmembrane calcium influx. *Blood*. 1995; 85: 1053-1062.
101. McCarl CA, Picard C, Khalil S, *et al*. ORAI1 deficiency and lack of store-operated Ca²⁺ entry cause immunodeficiency, myopathy, and ectodermal dysplasia. *J Allergy Clin Immunol*. 2009; 124: 1311-1318 e1317.
102. Schaff UY, Dixit N, Procyk E, *et al*. Orai1 regulates intracellular calcium, arrest, and shape polarization during neutrophil recruitment in shear flow. *Blood*. 2010; 115: 657-666.
103. Steinckwich N, Schenten V, Melchior C, Brechard S, Tschirhart EJ. An essential role of STIM1, Orai1, and S100A8-A9 proteins for Ca²⁺ signaling and FcγR-mediated phagosomal oxidative activity. *J Immunol*. 2011; 186: 2182-2191.
104. Brechard S, Melchior C, Plancon S, Schenten V, Tschirhart EJ. Store-operated Ca²⁺ channels formed by TRPC1, TRPC6 and Orai1 and non-store-operated channels formed by TRPC3 are involved in the regulation of NADPH oxidase in HL-60 granulocytes. *Cell Calcium*. 2008; 44: 492-506.
105. Schorr W, Swandulla D, Zeilhofer HU. Mechanisms of IL-8-induced Ca²⁺ signaling in human neutrophil granulocytes. *Eur J Immunol*. 1999; 29: 897-904.
106. Graham DB, Robertson CM, Bautista J, *et al*. Neutrophil-mediated oxidative burst and host defense are controlled by a Vav-PLCγ2 signaling axis in mice. *J Clin Invest*. 2007; 117: 3445-3452.
107. Hellberg C, Molony L, Zheng L, Andersson T. Ca²⁺ signalling mechanisms of the β2 integrin on neutrophils: involvement of phospholipase Cy 2 and Ins(1,4,5) P3. *Biochem J*. 1996; 317 (Pt 2): 403-409.
108. Dixit N, Kim MH, Rossaint J, *et al*. Leukocyte function antigen-1, kindlin-3, and calcium flux orchestrate neutrophil recruitment during inflammation. *J Immunol*. 2012; 189: 5954-5964.
109. Zhang H, Clemens RA, Liu F, *et al*. STIM1 calcium sensor is required for activation of the phagocyte oxidase during inflammation and host defense. *Blood*. 2014; 123: 2238-2249.
110. Koupenova M, Clancy L, Corkrey HA, Freedman JE. Circulating platelets as mediators of immunity, inflammation, and thrombosis. *Circ Res*. 2018; 122: 337-351.
111. Giles JA, Greenhalgh AD, Denes A, *et al*. Neutrophil infiltration to the brain is platelet-dependent, and is reversed by blockade of platelet GPIIb/IIIa. *Immunology*. 2018; 154: 322-328.
112. Wang CH, Rong MY, Wang L, *et al*. CD147 up-regulates calcium-induced chemotaxis, adhesion ability and invasiveness of human neutrophils via a TRPM-7-mediated mechanism. *Rheumatology (Oxford)*. 2014; 53: 2288-2296.
113. Murray PJ, Wynn TA. Protective and pathogenic functions of macrophage subsets. *Nat Rev Immunol*. 2011; 11: 723-737.
114. Braun A, Gessner JE, Varga-Szabo D, *et al*. STIM1 is essential for Fcγ receptor activation and autoimmune inflammation. *Blood*. 2009; 113: 1097-1104.
115. Sogkas G, Stegner D, Syed SN, *et al*. Cooperative and alternate functions for STIM1 and STIM2 in macrophage activation and in the context of inflammation. *Immun Inflamm Dis*. 2015; 3: 154-170.
116. Vaeth M, Zee I, Concepcion AR, *et al*. Ca²⁺ signaling but not store-operated Ca²⁺ entry is required for the function of macrophages and dendritic cells. *J Immunol*. 2015; 195: 1202-1217.
117. Schappe MS, Szteyn K, Stremaska ME, *et al*. Chanzyme TRPM7 mediates the Ca²⁺ influx essential for lipopolysaccharide-induced toll-like receptor 4 endocytosis and macrophage activation. *Immunity*. 2018; 48: 59-74 e55.
118. Fumagalli S, Perego C, Pischiutta F, Zanier ER, De Simoni MG. The ischemic environment drives microglia and macrophage function. *Front Neurol*. 2015; 6: 81.
119. Kronenberg G, Uhlemann R, Richter N, *et al*. Distinguishing features of microglia- and monocyte-derived macrophages after stroke. *Acta Neuropathol*. 2018; 135: 551-568.
120. Feske S, Draeger R, Peter HH, Eichmann K, Rao A. The duration of nuclear residence of NFAT determines the pattern of cytokine expression in human SCID T cells. *J Immunol*. 2000; 165: 297-305.
121. Feske S, Giltner J, Dolmetsch R, Staudt LM, Rao A. Gene regulation mediated by calcium signals in T lymphocytes. *Nat Immunol*. 2001; 2: 316-324.
122. Ma J, McCarl CA, Khalil S, Luthy K, Feske S. T-cell-specific deletion of STIM1 and STIM2 protects mice from EAE by impairing the effector functions of Th1 and Th17 cells. *Eur J Immunol*. 2010; 40: 3028-3042.
123. Schuhmann MK, Stegner D, Berna-Erro A, *et al*. Stromal interaction molecules 1 and 2 are key regulators of autoreactive T cell activation in murine autoimmune central nervous system inflammation. *J Immunol*. 2010; 184: 1536-1542.
124. Vaeth M, Yang J, Yamashita M, *et al*. ORAI2 modulates store-operated calcium entry and T cell-me-

- diated immunity. *Nat Commun.* 2017; 8: 14714.
125. Zierler S, Yao G, Zhang Z, *et al.* Waixenicin A inhibits cell proliferation through magnesium-dependent block of transient receptor potential melastatin 7 (TRPM7) channels. *J Biol Chem.* 2011; 286: 39328-39335.
 126. Kuras Z, Yun YH, Chimote AA, Neumeier L, Conforti L. KCa3.1 and TRPM7 channels at the uropod regulate migration of activated human T cells. *PLoS One.* 2012; 7: e43859.
 127. Romagnani A, Vettore V, Rezzonico-Jost T, *et al.* TRPM7 kinase activity is essential for T cell colonization and alloreactivity in the gut. *Nat Commun.* 2017; 8: 1917.
 128. Beesetty P, Wieczersak KB, Gibson JN, *et al.* Inactivation of TRPM7 kinase in mice results in enlarged spleens, reduced T-cell proliferation and diminished store-operated calcium entry. *Sci Rep.* 2018; 8: 3023.
 129. Kleinschnitz C, Schwab N, Kraft P, *et al.* Early detrimental T-cell effects in experimental cerebral ischemia are neither related to adaptive immunity nor thrombus formation. *Blood.* 2010; 115: 3835-3842.
 130. Sakaguchi S, Miyara M, Costantino CM, Hafler DA. FOXP3+ regulatory T cells in the human immune system. *Nat Rev Immunol.* 2010; 10: 490-500.
 131. Kleinschnitz C, Kraft P, Dreykluft A, *et al.* Regulatory T cells are strong promoters of acute ischemic stroke in mice by inducing dysfunction of the cerebral microvasculature. *Blood.* 2013; 121: 679-691.
 132. Beyersdorf N, Braun A, Vogtle T, *et al.* STIM1-independent T cell development and effector function in vivo. *J Immunol.* 2009; 182: 3390-3397.
 133. Ma HT, Patterson RL, van Rossum DB, *et al.* Requirement of the inositol trisphosphate receptor for activation of store-operated Ca²⁺ channels. *Science.* 2000; 287: 1647-1651.
 134. Ma KT, Guan BC, Yang YQ, Nuttall AL, Jiang ZG. 2-Aminoethoxydiphenyl borate blocks electrical coupling and inhibits voltage-gated K⁺ channels in guinea pig arteriole cells. *Am J Physiol Heart Circ Physiol.* 2011; 300: H335-346.
 135. Li M, Jiang J, Yue L. Functional characterization of homo- and heteromeric channel kinases TRPM6 and TRPM7. *J Gen Physiol.* 2006; 127: 525-537.
 136. Lis A, Peinelt C, Beck A, *et al.* CRACM1, CRACM2, and CRACM3 are store-operated Ca²⁺ channels with distinct functional properties. *Curr Biol.* 2007; 17: 794-800.
 137. Wei M, Zhou Y, Sun A, *et al.* Molecular mechanisms underlying inhibition of STIM1-Orai1-mediated Ca²⁺ entry induced by 2-aminoethoxydiphenyl borate. *Pflugers Arch.* 2016; 468: 2061-2074.
 138. Ng NM, Jiang SP, Zhang W. 2-Aminoethoxydiphenyl borate reduces degranulation and release of cytokines in a rat mast cell line. *Eur Rev Med Pharmacol Sci.* 2012; 16: 1017-1021.
 139. Korach KS, Metzler M, McLachlan JA. Estrogenic activity *in vivo* and *in vitro* of some diethylstilbestrol metabolites and analogs. *Proc Natl Acad Sci U S A.* 1978; 75: 468-471.
 140. Karpuzoglu-Sahin E, Hissong BD, Ansar Ahmed S. Interferon- γ levels are upregulated by 17-beta-estradiol and diethylstilbestrol. *J Reprod Immunol.* 2001; 52: 113-127.
 141. Zakharov SI, Smani T, Dobrydneva Y, *et al.* Diethylstilbestrol is a potent inhibitor of store-operated channels and capacitative Ca²⁺ influx. *Mol Pharmacol.* 2004; 66: 702-707.
 142. Sogkas G, Rau E, Atscheckzei F, Syed SN, Schmidt RE. The pyrazole derivative BTP2 attenuates IgG immune complex-induced inflammation. *Inflammation.* 2018; 41: 42-49.
 143. Ohga K, Takezawa R, Arakida Y, Shimizu Y, Ishikawa J. Characterization of YM-58483/BTP2, a novel store-operated Ca²⁺ entry blocker, on T cell-mediated immune responses *in vivo*. *Int Immunopharmacol.* 2008; 8: 1787-1792.
 144. Yoshino T, Ishikawa J, Ohga K, *et al.* YM-58483, a selective CRAC channel inhibitor, prevents antigen-induced airway eosinophilia and late phase asthmatic responses via Th2 cytokine inhibition in animal models. *Eur J Pharmacol.* 2007; 560: 225-233.
 145. Jara E, Hidalgo MA, Hancke JL, *et al.* Delphinidin activates NFAT and induces IL-2 production through SOCE in T cells. *Cell Biochem Biophys.* 2014; 68: 497-509.
 146. He LP, Hewavitharana T, Soboloff J, Spassova MA, Gill DL. A functional link between store-operated and TRPC channels revealed by the 3,5-bis(trifluoromethyl)pyrazole derivative, BTP2. *J Biol Chem.* 2005; 280: 10997-11006.
 147. Takezawa R, Cheng H, Beck A, *et al.* A pyrazole derivative potently inhibits lymphocyte Ca²⁺ influx and cytokine production by facilitating transient receptor potential melastatin 4 channel activity. *Mol Pharmacol.* 2006; 69: 1413-1420.
 148. Owsianik G, D'Hoedt D, Voets T, Nilius B. Structure-function relationship of the TRP channel superfamily. *Rev Physiol Biochem Pharmacol.* 2006; 156: 61-90.
 149. Derler I, Schindl R, Fritsch R, *et al.* The action of selective CRAC channel blockers is affected by the Orai pore geometry. *Cell Calcium.* 2013; 53: 139-151.

Chapter 4

Variable impairment of platelet functions in patients with severe, genetically linked immune deficiencies

Nagy M, Mastenbroek TG, Mattheij NJA*, de Witt S, Clemetson KJ, Kirschner J, Schulz AS, Vraetz T, Speckmann C, Braun A, Cosemans JMEM, Zieger B*, Heemskerk JWM*
(*Equal contribution)*

*Haematologica 2018;103(3):540-549
Reprinted with permission*

Abstract

In patients with dysfunctions of the Ca^{2+} channel ORAI1, stromal interaction molecule 1 (STIM1) or integrin-regulating kindlin-3 (FERMT3), severe immunodeficiency is frequently linked to abnormal platelet activity. In this paper, we studied in nine rare patients, including relatives, with confirmed genetic mutations of ORAI1, STIM1 or FERMT3, platelet responsiveness by multi-parameter assessment of whole blood thrombus formation under high-shear flow conditions. In platelets isolated from 5 out of 6 patients with ORAI1 or STIM1 mutations, store-operated Ca^{2+} entry (SOCE) was (in)completely defective compared to control platelets. Parameters of platelet adhesion and aggregation on collagen microspots were impaired for 4/6 patients, in part related to a low platelet count. For 4 patients, platelet adhesion/aggregation and procoagulant activity on vWF/rhodocytin and vWF/fibrinogen microspots were impaired, independently of platelet count and partly correlated with SOCE deficiency. Measurement of thrombus formation at low shear rate confirmed a larger impairment of platelet functionality in the ORAI1 patients than in the STIM1 patient. For 3 patients/relatives with a FERMT3 mutation, all parameters of thrombus formation were strongly reduced regardless of the microspot. Bone marrow transplantation, required by two patients, resulted in overall improvement of platelet function. We concluded that multiparameter assessment of whole blood thrombus formation, in a surface-dependent way, can detect: (i) additive effects of low platelet count and impaired platelet functionality; (ii) aberrant ORAI1-mediated Ca^{2+} entry; (iii) differences in platelet activation between patients carrying the same ORAI1 mutation; (iv) severe platelet function impairment linked to a FERMT3 mutation and bleeding history.

Introduction

Severe, genetically linked immunodeficiency can be accompanied by platelet function defects, especially in case of rare mutations in the *ORAI1*, *STIM1* and *FERMT3* genes on platelet properties, in spite of the solid evidence for a role of the mouse orthologous in arterial thrombosis.

In platelets and other blood cells, stromal interaction molecule 1 (STIM1) acts as a major Ca^{2+} sensor located in the endoplasmic reticulum. Upon lowering of the reticular Ca^{2+} concentration, it assembles with the ORAI1 Ca^{2+} (I_{CRAC}) channels in the plasma membrane to mediate store-operated Ca^{2+} entry (SOCE).¹⁻⁴ The conventional test for SOCE (*i.e.*, for STIM1 and ORAI1 activity) hence is to provoke depletion of the STIM1-linked Ca^{2+} store with the endoplasmic Ca^{2+} -ATPase inhibitor thapsigargin, and then measure Ca^{2+} entry through ORAI1 channels upon addition of extracellular CaCl_2 .^{5,6}

Both ORAI1 and STIM1 have non-redundant roles in the patrolling and defense functions of white blood cells. In platelets, ORAI1 as well as STIM1 are considered to enhance the Ca^{2+} signal generation, especially induced by protein tyrosine kinase-linked receptors, such as glycoprotein VI (GPVI). In mouse, both ORAI1 and STIM1 are implicated in hemostasis and arterial thrombus formation.⁷⁻¹⁰ Murine knockout studies have indicated that the ORAI1-STIM1 Ca^{2+} signaling contributes to multiple platelet activation processes, such as adhesiveness via integrin activation, granule release, aggregation of platelets, and procoagulant activity.^{8,11,12} However, in humans, the consequences of defective ORAI1 or STIM1 activity in platelets have only poorly been investigated.

In humans, dysfunctional mutations in the *ORAI1* or *STIM1* genes are very rare.¹³ The patients described with such mutations usually suffer from severe immunodeficiency, congenital myopathy, ectodermal dysplasia or other Ca^{2+} -linked abnormalities.¹⁴⁻¹⁶ The immune deficiency can be attributed to the loss-of-function of leukocyte and lymphocyte subsets. Given the severity of the symptoms often already at a young age, these patients are commonly treated by allogeneic hematopoietic stem cell transplantation. The few patients described do not have an overt bleeding history, although they may periodically show autoimmune thrombocytopenia.¹⁶

Leukocyte adhesion deficiency type III (LAD-III) forms another severe immune disease, in this case accompanied by epistaxis or petechiae. It is associated with dysfunctional mutations in the *FERMT3* gene of the integrin regulation protein, kindlin-3.¹³ LAD-III patients present with normal platelet count, but impaired platelet adhesion, which may explain the bleeding symptoms.^{17,18} Also, these patients may require hematopoietic stem cell transplantation during childhood.¹⁹

Recently, we developed a microspot-based assay for multiparameter assessment of whole blood thrombus formation under flow conditions.²⁰ This assay proved to be valuable to characterize platelet count and function abnormalities in patients with a variety of genetic bleeding disorders. Here, we used this integrative method to investigate overall platelet functions in nine patients with severe immunodeficiencies, including parents, with a confirmed dysfunctional mutation in *ORAI1*, *STIM1* or *FERMT3*. For two patients, we also investigated effects of bone marrow transplantation. The results suggest a variable phenotypic penetrance on platelet properties in patients and relatives carrying those mutations.

Methods

Patients and controls

Blood was drawn from patients and healthy controls after full informed consent (Helsinki declaration). The studies were approved by the local Medical Ethics Committees. Healthy controls had normal blood cell counts, were devoid of anti-platelet medication for at least 2 weeks, and did not have a known history of bleeding or immunodeficiency.

Blood samples from patients with immunodeficiency and their parents (all genotyped) were collected at the Department of Pediatrics and Adolescent Medicine, University Medical Center in Freiburg, and at the Children's Hospital, University of Ulm (Table 1). Simultaneously, blood samples were taken from healthy donors, serving as daily travel controls. Relevant patient characteristics, including identified mutations and the clinical history, are summarized in Table 1. Patient P1 showed homozygosity in the R91W mutation in the *ORAI1*, known to be linked to severe combined immunodeficiency and defective T cell Ca^{2+} signaling.¹ Heterozygosity in this mutation was confirmed for both parents (P2 and P3). Patient P4 carried a heterozygous G98S mutation in *ORAI1*, which was confirmed in the mother (P5). This mutation is reported to be linked to tubular aggregated myopathy-2.²¹ Patient P6 carried a heterozygous R429C mutation of *STIM1*, which is also linked to T cell immunity.²² Patient P7 suffered from severe immunodeficiency, linked to a homozygous R573X mutation in *kindlin-3* encoded by the *FERMT3* gene. The two parents (P8 and P9) were heterozygous for this mutation. Two of the patients with severe immunodeficiency, P1 and P7, were eligible for bone marrow transplantation. Blood samples in these cases were obtained before and at 2 or 3 months after transplantation, respectively. The volumes of blood available for investigation were limited due to the young age of the patients.

Platelet Ca^{2+} responses

Rises in cytosolic $[Ca^{2+}]_i$ were measured in platelets after loading with Fura-2 acetoxymethyl ester (2.5 μ M) by calibrated ratio fluorometry.²³ Data are presented as nM increases in cytosolic $[Ca^{2+}]_i$.²⁴

Multiparameter thrombus formation on microspots under flow

Whole blood thrombus formation was assessed under flow conditions, basically as described before.²⁰ In brief, blood samples (0.5 mL) were re-calcified in the presence of thrombin inhibitors, and perfused over a coverslip coated with three microspots (spot 1: type I collagen, spot 2: vWF/rhodocytin, spot 3: vWF/fibrinogen) in a transparent parallel-plate perfusion chamber. Perfusion was at high wall-shear rate of 1600 s^{-1} for 3.5 min, or at low shear rate of 150 s^{-1} for 6.0 min. The thrombi formed on the microspots were immediately post-stained with FITC-labeled anti-fibrinogen mAb (1:100), FITC-anti-CD62P mAb (25 μ g/mL) and AF647-annexin A5 (0.25 μ g/mL). Representative brightfield and fluorescence images were captured from each microspot in real-time without fixation. Duplicate runs were performed, whenever possible. Analysis of brightfield and fluorescence images, giving 7 parameters per microspot, was performed with predefined scripts in Fiji software.²⁵ (Un)supervised heatmaps using scaled parameters (range 0-10) of thrombus formation were constructed in R.

Statistics

Significance of differences was determined with the paired sample t test (intervention effects) and by principal component analysis (PCA), using the statistical package for social sciences (SPSS, version 11.0).

A detailed description of the methods is available in the *Online Supplementary Appendix*.

Table1. Subjects' characteristics.

Subject	Mutation	Platelet count (x 10 ⁹ /L)	MPV (fL)	Hematocrit (L/L)	Clinical history
HC1-12 (home C)	None assumed	166-390	9.1 - 12.1	0.36 - 0.49	None
C1-5 (travel C)	None assumed	156-291	9.0 - 11.6	0.36 - 0.40	None
P1 (child)	ORAI1 (R91W) W/W [#]	207	n.d.	0.41	Immunodeficiency, myopathy, anhydrosis
P1 (BM)	BM transplanted	74*	8.9*	0.23*	Thrombocytopenia, stabilized myopathy
P2 (mother P1)	ORAI1 (R91W) R/W ^{##}	115*	8.8*	0.36	Mild thrombocytopenia
P3 (father P1)	ORAI1 (R91W) R/W ^{##}	156*	9.2	0.32*	No known history of bleeding
P4 (child)	ORAI1 (G98S) G/S ^{##}	114*	7.7*	0.34*	Thrombocytopenia (recurrent), myopathy with tubular aggregates, anhydrosis
P5 (mother P4)	ORAI1 (G98S) G/S ^{##}	70*	9.2	0.37	Thrombocytopenia, myopathy with tubular aggregates, anhydrosis
P6 (adult)	STIM1 (R429C) R/C ^{##}	150	n.d.	n.d.	No known history of bleeding
P7 (child)	FERMT3 (R573X) X/X [#]	182	7.5*	0.31*	Immunodeficiency, severe vaginal bleeding , leukocytosis
P7 (BM)	BM transplanted	168	6.0*	0.33*	No known clinical symptoms
P8 (father P7)	FERMT3 (R573X) R/X ^{##}	126*	8.3	0.42	No known history of bleeding
P9 (mother P7)	FERMT3 (R573X) R/X ^{##}	142*	6.8*	0.39	No known history of bleeding

HC: home control; C:travel control; n.d.: not determined; MPV: mean platelet volume; P: patient; BM: bone marrow. *Outside of normal range; [#]homozygosity in mutation; ^{##}heterozygosity in mutation.

Results

Variable aberrances in SOCE in platelets from patients with *ORAI1* or *STIM1* mutations

Blood samples were obtained from three patients with a mutation in the Ca^{2+} flux-regulating proteins *ORAI1* or *STIM1*, as well as from parents carrying the same mutation. For comparison, blood samples were also taken from two cohorts of healthy subjects, *i.e.* a group of normal home controls (HC1-12) and a group of normal travel controls (C1-6). Using Fura-2-loaded platelets, we first evaluated the alterations in Ca^{2+} signaling in response to the GPVI receptor agonist convulxin, the PAR receptor agonist thrombin, and the sarco/endoplasmic reticulum Ca^{2+} -ATPase (SERCA) inhibitor thapsigargin. In each case, the platelets were first stimulated with agonist in Ca^{2+} -free medium, after which extracellular CaCl_2 was added to measure secondary Ca^{2+} entry.

In comparison to control platelets, platelets from patient P1, carrying a homozygous *ORAI1*^{91W/W} mutation, responded normally to each agonist, but showed a substantially reduced Ca^{2+} entry following stimulation with convulxin but not thrombin (Figure 1A-B).

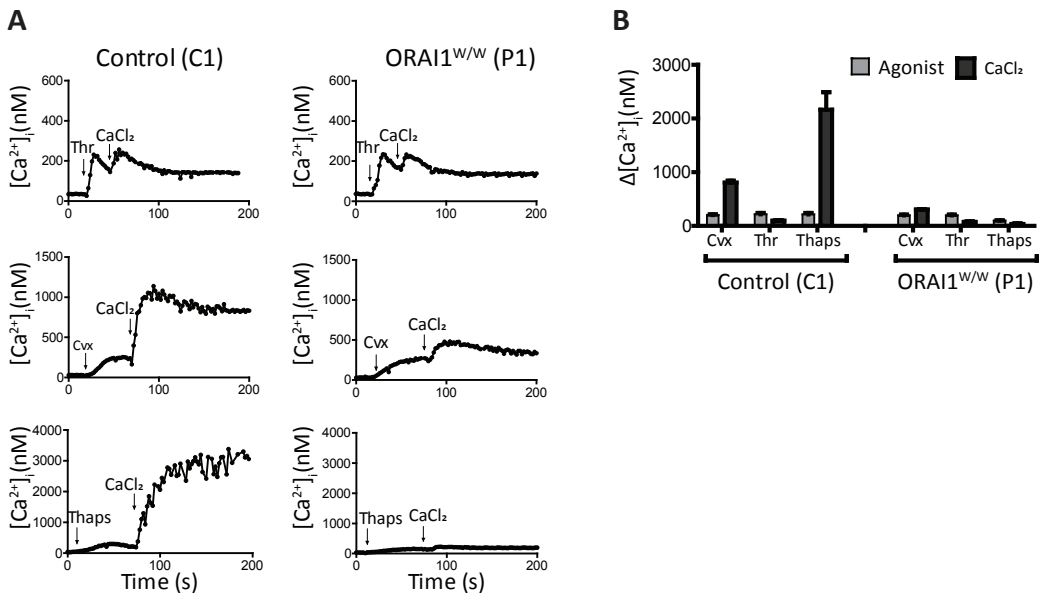


Figure 1. Defective Ca^{2+} entry in platelets from a patient with a homozygous R91W mutation in *ORAI1*. Fura-2-loaded platelets from patient P1 (*ORAI1*^{W/W}) and travel control C1 were used, suspended in HEPES buffer with 0.1 mM EGTA. Rises in cytosolic Ca^{2+} were measured in time upon stimulation with convulxin (Cvx, 50 ng/mL), thrombin (Thr, 4 nM) or thapsigargin (Thaps, 1.0 μM). After a defined time, CaCl_2 (2 mM) was added to induce Ca^{2+} entry. Representative traces (**A**) and quantification (**B**) of Ca^{2+} increases in platelets from control subject and patient P1. Note that the maximal Ca^{2+} rise in response to CaCl_2 following thapsigargin was used as a measure of SOCE capacity.

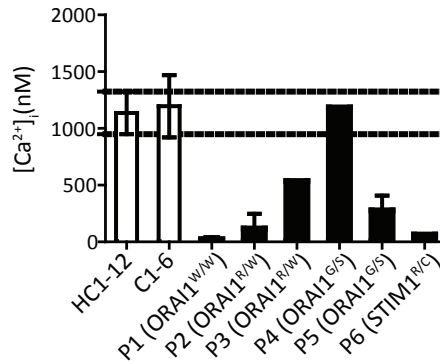


Figure 2. Variably defective Ca^{2+} entry in platelets from patients with ORAI1^{W/W}, ORAI1^{G/S} or STIM1^{R/C} mutations. Fura-2-loaded platelets in Hepes buffer with 0.1 mM EGTA were stimulated with thapsigargin (1.0 μ M), and after a defined time with $CaCl_2$ (2 mM). Platelets were analyzed from 12 healthy home controls (HC1-12), 6 healthy travel controls (C1-6), and the indicated patients/relatives (P1-6). Platelets from patient P1 were also analyzed after bone marrow (BM) transplantation. Shown are maximal increases in Ca^{2+} . Dotted lines indicate range of SOCE levels ($CaCl_2$ -induced Ca^{2+} rise after thapsigargin) for platelets from home controls (mean \pm SD, for HC1-12)

Markedly, in the patient's platelets, Ca^{2+} entry after stimulation with thapsigargin - as a default condition for SOCE - was completely abolished. This pointed to a complete absence of the STIM1-ORAI1 pathway, similarly as established for platelets from STIM1- or ORAI1-deficient mice.^{7,8} Flow cytometric evaluation indicated that convulxin-stimulated platelets from P1 showed a reduced PS exposure ($7 \pm 1\%$ vs. $28 \pm 2\%$ for control platelets, mean \pm SEM, $n=3$, $P < 0.05$), but were not altered in integrin $\alpha_{IIb}\beta_3$ activation or P-selectin expression ($P > 0.10$). Platelets from the patient's parents (both with confirmed heterozygosity) were diminished in SOCE, but to a different extent (Figure 2). Platelets from the mother (P2) showed a nearly annulled Ca^{2+} entry, whereas platelets from the father (P3) were less severely reduced, when compared to platelets from two cohorts of healthy controls. A second blood sample from patient P1 could be obtained at 2 months after bone marrow transplantation. In the platelets, we measured about 50% recovery in SOCE signal after thapsigargin stimulation (SOCE_{P1}: 22 nM vs. SOCE_{P1-BM}: 575 nM).

Platelets from a patient (P4), carrying a heterozygous mutation ORAI1^{89G/S} in the same protein region, responded differently. These platelets displayed a high SOCE signal (Ca^{2+} entry after thapsigargin). In contrast, platelets from parent P5 (also carrying the mutation) were greatly reduced in SOCE (Figure 2). This difference was confirmed for a second set of blood samples (not shown). A different picture was obtained with patient P6 with a heterozygous mutation in STIM1^{429R/C}.²² In these platelets, Ca^{2+} rises evoked by convulxin/ $CaCl_2$ or thrombin/ $CaCl_2$ were in the normal range, whereas SOCE after thapsigargin was completely abolished (Figure 3A-B).

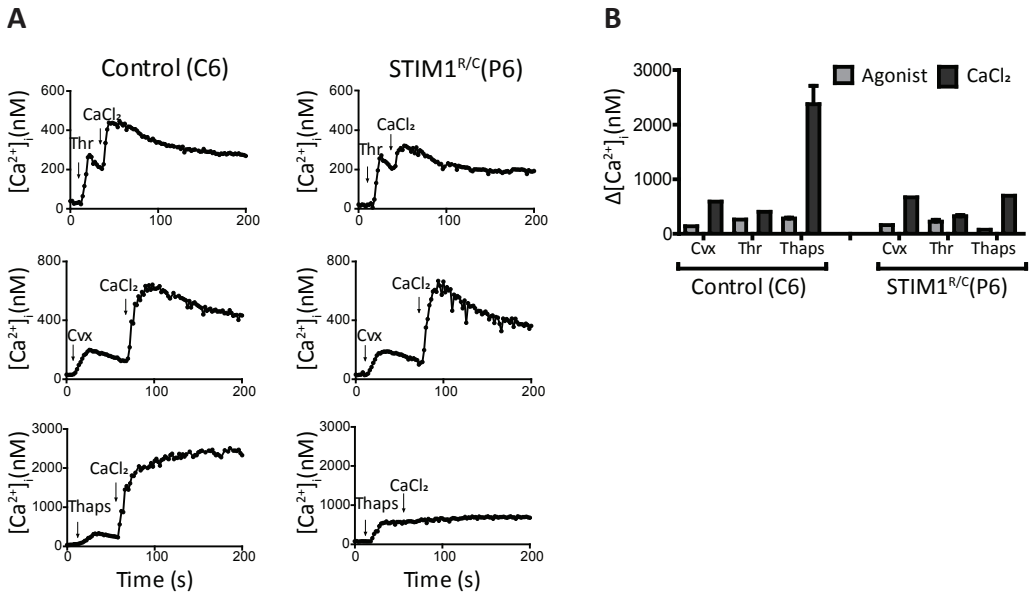


Figure 3. Defective Ca²⁺ entry in platelets from a patient with a heterozygous R429C mutation in STIM1. Fura-2-loaded platelets from patient P6 (STIM1^{R/C}) and travel control C6, suspended in HEPES buffer with 0.1 mM EGTA, were stimulated with convulxin (Cvx, 50 ng/mL), thrombin (Thr, 4 nM) or thapsigargin (Thaps, 1.0 μM), after which CaCl₂ (2 mM) was given to induce Ca²⁺ entry. Representative traces (A) and quantification (B) of Ca²⁺ rises in platelets from control subject and patient P6.

Phenotypic analysis of platelets was also performed of a LAD-III patient (P7), carrying a homozygous FERMT3^{573X/X} mutation, and presenting with immunodeficiency and a history of bleeding.²⁶ Flow cytometry indicated near complete inability of integrin $\alpha_{\text{IIb}}\beta_3$ activation in response to receptor agonists, similarly as described for another patient carrying this mutation.²⁷ In platelets from the two heterozygous parents (P8, P9), $\alpha_{\text{IIb}}\beta_3$ integrin activation was in the normal range (not shown).

Lower range blood cell counts in patients with ORAI1, STIM1 or FERMT3 mutations

Table 1 provides an overview of the clinical histories of patients including P1-9, and furthermore informs on the hematological parameters, determined in freshly isolated blood samples. In all patients, with the exception of P1 and P7, platelet counts were between 70 and 150 × 10⁹/L, which are slightly below the normal ranges as present in both control cohorts. In the majority of patients, also hematocrit levels were in the lower range of normal, *i.e.* between 0.31 and 0.42 L/L. After bone marrow transplantation (2-3 months), platelet count in P1 and P7 was restored to 74 and 168 × 10⁹/L, respectively.

Different patterns between patients of aberrant whole blood thrombus formation at high shear rate

To obtain detailed insight into the hemostatic potential of the patients' platelets, whole blood samples were used for multiparameter assessment of thrombus formation under flow at high wall-shear rate of 1600 s^{-1} . Samples from corresponding control subjects (C1-6) and home control subjects (HC1-12) were again used for comparison. This high-throughput method, previously established,²⁰ allowed simultaneous examination of platelet adhesion, aggregation, and activation at three microspots: spot 1 with coated type I collagen (involving platelet receptors: GPIb-V-IX, GPVI, and integrin $\alpha_2\beta_1$); spot 2 with

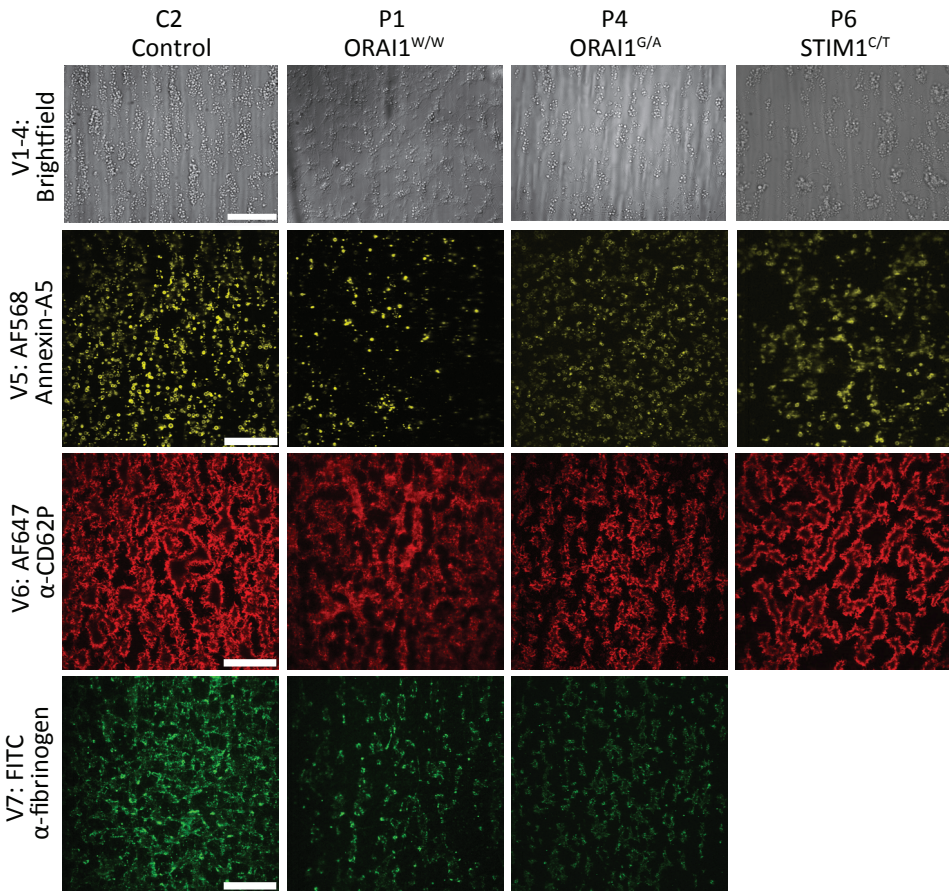


Figure 4. Altered thrombus formation of blood from patients with $ORAI1^{w/w}$, $ORAI1^{G/S}$ or $STIM1^{R/C}$ mutations. Whole blood from indicated control subjects and patients was perfused over three microspots (Sp1, collagen type I; Sp2, VWF/rhodocytin; Sp3, VWF/fibrinogen; downstream \rightarrow upstream) at wall-shear rate of 1600 s^{-1} . After 3.5 min of perfusion, brightfield images were taken from thrombi on all microspots, and platelets were stained for PS exposure (AF568-Annexin A5), P-selectin expression (AF647 anti-CD62P mAb), and integrin $\alpha_{IIb}\beta_3$ activation (FITC anti-fibrinogen mAb). Shown are representative brightfield and fluorescence images at spot 1, obtained with blood from control C2 and patients P1, P4 and P6 (bars, 50 μm).

coated vWF/rhodocytin (receptors GPIb-V-IX and CLEC-2); and spot 3 with coated vWF/fibrinogen (receptors GPIb-V-IX and $\alpha_{IIb}\beta_3$). From each microspot, microscopic brightfield images were recorded to assess platelet adhesion and aggregation (parameters V1-4); in parallel, fluorescence images were recorded in three colors for detection of PS exposure, P-selectin expression, and $\alpha_{IIb}\beta_3$ activation (parameters V5-7).

Representative examples of brightfield and fluorescence images from spot 1 are shown in Figure 4, for blood samples of control C2 and immunodeficient patients with ORAI1 or STIM1 mutation (P1, P4, and P6). Regarding the patient blood samples, the images show patterns of platelet adhesion, aggregation, and activation that vary from normal to reduced. The same holds for spot 2 (vWF/rhodocytin) and spot 3 (vWF/fibrinogen) (see below).

A heatmap was constructed with data from all analyzed images (3 spots \times 7 parameters) for the cohort of 12 normal home controls (HC1-12), the 6 travel controls (C1-6), and the 9 individual patients/relatives with mutations in ORAI1 (P1-5), STIM1 (P6) or FERMT3 (P7-9), in which all values were normalized to a scale of 0-10 per parameter (Figure 5A). In the derived subtraction heatmap of Figure 5B, the patient data were expressed relative to those from the home controls. This subtraction confirmed an overall high similarity between the values of the two control groups (HC1-12 and C1-6), with the exception of a parameter reflecting platelet deposition on spot 2. Datasets for individual subjects C1-6 were within the normal ranges (not shown). This confirmed the usefulness of the multi-parameter test,²⁰ and underscored the quality of the analyzed blood samples. For each patient/relative, we arbitrarily set a relevant effect threshold, *i.e.* when outside the range of mean \pm 2 SD of the control group (HC1-12). This filter produced a ‘relevant’ subtraction heatmap, indicating distinct patterns of altered parameters of thrombus formation for individual patients P1-9 (Figure 5C).

Figure 5C underlines that, overall, multiple parameters on spot 1 were reduced for patients P2-5, whereas especially parameters on spots 2-3 were reduced for patients P1 and P5. Interestingly, patient P4 carrying the assumed gain-of-function mutation ORAI1^{G98S} (but not relative P5 with low SOCE) showed a typical increase in platelet PS exposure. For the patient with homozygous FERMT3 mutation (P7), a more severe reduction on all three spots was seen in comparison to the two heterozygous relatives (P8-9).

Effects of low platelet count

Considering that whole blood thrombus formation can be influenced by not only the inherited platelet disorder, but also a low platelet count,²⁸ the present heatmaps may reflect both platelet-related properties. To examine this in more detail, the subtraction

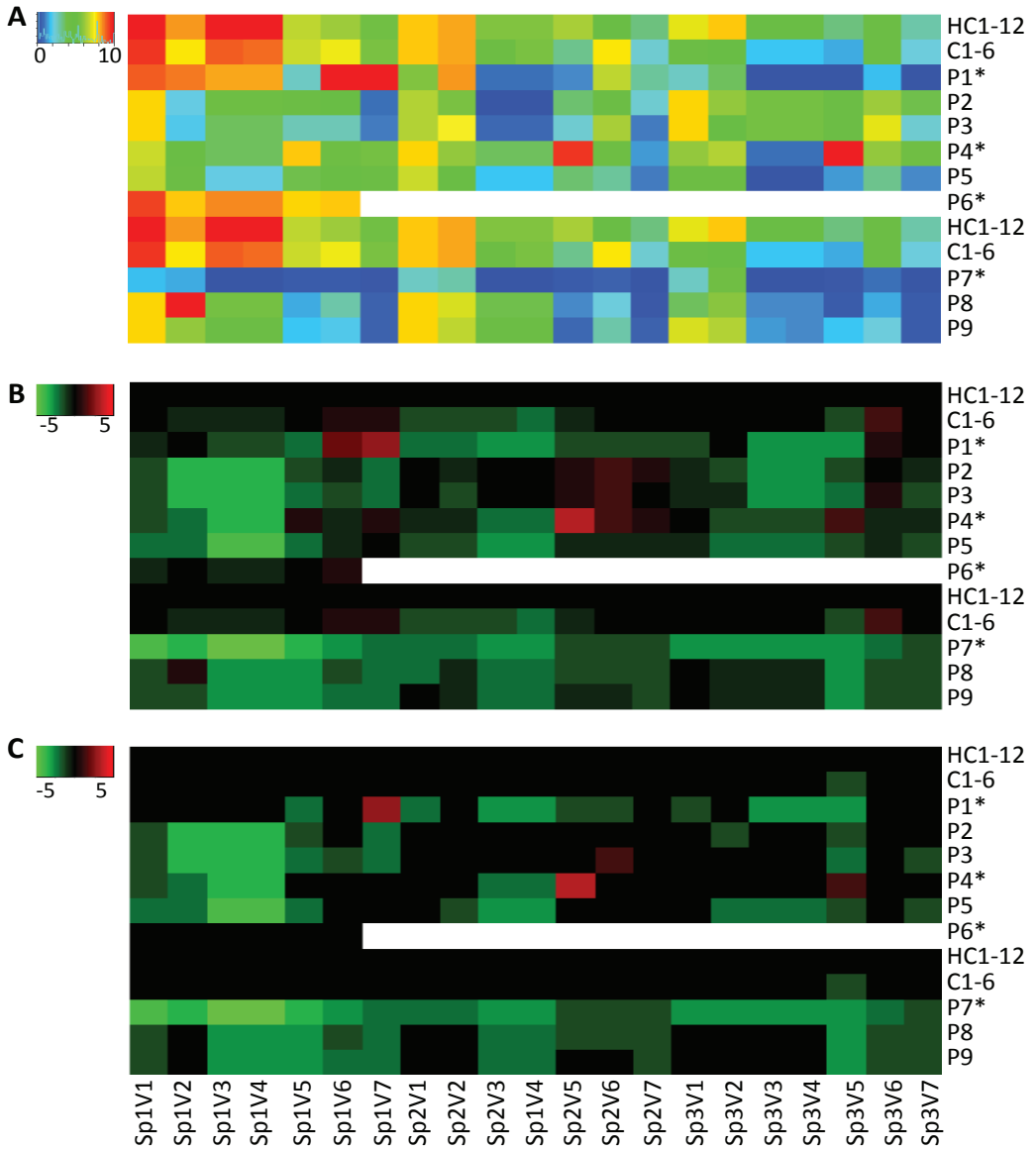


Figure 5. Integrated analysis of thrombus formation for patients with ORAI1, STIM1 or FERMT3 mutations. Thrombus formation on three microspots was measured with blood from home controls (HC1-12), travel controls (C1-6) and indicated patients/relatives with a genetic mutation in ORAI1 (P1-5), STIM1 (P6) or FERMT3 (P7-9), at wall-shear rate of 1600 s^{-1} , as for Figure 4. Coding of microspots: Sp1, collagen type I; Sp2, VWF/rhodocytin; Sp3, VWF/fibrinogen. Coding of outcome parameters: V1, thrombus morphological score (scale 0-5); V2, platelet surface area coverage (% SAC); V3 thrombus contraction score (scale 0-3); V4, thrombus multilayer score (scale 0-3); V5, PS exposure (% SAC); V6, P-selectin expression (% SAC); V7, $\alpha_{\text{IIb}}\beta_3$ activation (% SAC). Data were scaled per parameter from 0-10. **(A)** Heatmap of scaled values for control groups HC1-12 and C1-6 (means), and of scaled values for individual patients (*) and relatives. **(B)** Subtraction heatmap of scaled values, compared to those from HC1-12. **(C)** Subtraction heatmap after filtering for differences considered to be relevant, *i.e.* outside the range of mean \pm 2 SD (HC1-12).

heatmap data were extended with values of platelet count and SOCE. Unsupervised clustering of the extended dataset indicated that in particular spot 1, parameters (V1-4) clustered with platelet count, while spot 2 parameters (V3-5) and PS exposure (Sp1V5, Sp2V5) clustered with altered SOCE (Suppl. Figure 1).

As an alternative approach, we used the primary (non-normalized) data of thrombus formation (Sp1-3, V1-7), platelet count and SOCE for principal component analysis (PCA). This revealed a similar pattern, in that the majority of spot 1 parameters together with platelet count determined component 1, whereas most spot 2 parameters determined component 2 (Suppl. Figure 2A). Statistics (Pearson's regression coefficient) confirmed a correlation of spot 1 parameters with platelet count, and also a correlation of platelet PS exposure (Sp1V5, Sp3V5) with SOCE (Suppl. Figure 2B).

This information was then used to interpret the alterations in thrombus formation for individual patients (see clustered heatmap of Suppl. Figure 1). Concerning the patient (P1) with homozygous R91W mutation in ORA1, with normal platelet count ($207 \times 10^9/L$) and near abolished SOCE, thrombus formation was near normal on spot 1 (collagen), but markedly reduced on spot 2 (vWF/rhodocytin) and spot 3 (vWF/fibrinogen). The impaired Ca^{2+} signal was linked to a low PS exposure on all spots (Suppl. Table 1). On the other hand, for the patients P2 and P3 with heterozygous R91W mutation in ORA1 (relatively low platelet counts of $115-156 \times 10^9/L$, and 20-60% of normal SOCE, respectively), especially parameters for spot 1 were below normal, with a reduced PS exposure.

Concerning patients P4 and P5 heterozygous for the G98S mutation in ORA1 (low platelet counts of 70 and $114 \times 10^9/L$; 100% and 30% of normal SOCE, respectively), thrombus formation on spot 1 was reduced, while parameters of thrombus formation on spots 2-3 (including PS exposure) were only reduced for patient P5. In P4 (but not P5) a gain-of-function of Ca^{2+} channel activity was apparent from an increased PS exposure on spots 2-3. For patient P6, heterozygous for the R429C mutation in STIM1, thrombus formation on spot 1 (collagen) was normal in spite of the abolished SOCE. Together, this underlined the idea that a low platelet count rather than altered SOCE determines the thrombus formation on collagen, but not on the other surfaces.

Control experiments with reconstituted blood confirmed that, for control donors, lowering of the platelet count to $100 \times 10^9/L$ had a minor effect on particular parameters of thrombus formation limited to spot 1, whereas lowering to $50 \times 10^9/L$ affected thrombus formation on all spots (Suppl. Figure 3). Taken together with the predictive effect of platelet count in the principal component analysis, this suggest that a relatively low count affects thrombus formation under flow more severely when combined with a reduced platelet functionality.

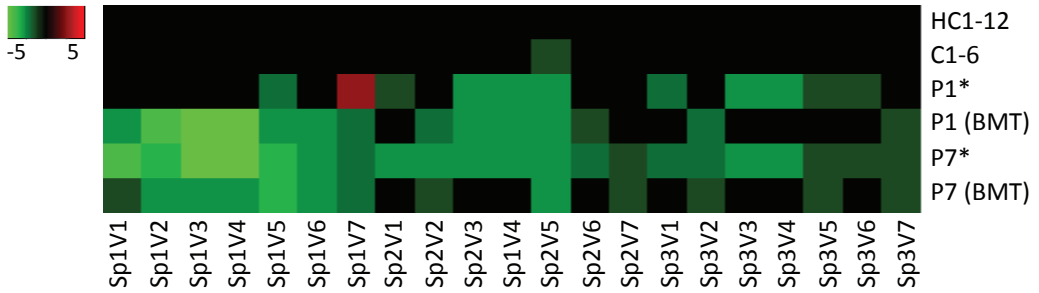


Figure 6. Altered thrombus formation after bone marrow transplantation. Thrombus formation (1600 s^{-1}) on three microspots measured with blood from indicated home controls (HC1-12), travel controls (C1-6) and two patients P1 (ORAI1^{W/W}) and P7 (FERMT3^{R/X}), both before (*) and after bone marrow transplantation (BMT). For description of microspots and parameters, see Figure 4. Subtraction heatmap of scaled values after filtering for differences considered to be relevant, *i.e.* outside the range of mean ± 2 SD (HC1-12).

Patterns of aberrant whole blood thrombus formation at low shear rate

Using remaining samples from patients/relatives P1-6, we further performed whole blood flow measurements at a low shear rate of 150 s^{-1} . Subtraction heatmap analysis of the normalized parameter values, in comparison to control data from HC1-12 cohort, indicated for all patients with ORAI1 mutations (P1-5) a consistent pattern of reduced thrombus formation parameters on spot 1 (Suppl. Figure 4A-C). In particular for patients P2 and P3, markers of platelet activation appeared to be reduced (PS exposure, P-selectin expression and $\alpha_{\text{IIb}}\beta_3$ activation). Again, for patient P6 with STIM1 mutation, most parameters were unchanged.

Principal component analysis of the low shear data again pointed to a linkage of spot 1 parameters with platelet count and a linkage of Sp1V5 (PS exposure) with SOCE activity (Suppl. Figure 5A-B).

Partial recovery of whole blood thrombus formation after bone marrow transplantation

Blood samples from two patients were also obtained after bone marrow transplantation (P1 after 2 months, P7 after 3 months), and employed for platelet activation and thrombus formation studies. Transplantation of patient P1 led to a partially recovered SOCE from 20 to 60% of normal (Table 2). After transplantation, parameters of thrombus formation were particularly reduced on spot 1 (paralleling a reduction in platelet count from 207 to $74 \times 10^9/\text{L}$), but were unchanged for spot 2, and enhanced for spot 3 (Figure 6). Transplantation of patient P7 resulted in an overall improvement of most parameters on all spots (platelet count changing from 182 to $168 \times 10^9/\text{L}$).

Table 2. Overall comparison of defective store-operated Ca²⁺ entry (SOCE) and impairment in thrombus formation of individual patients.

Subject	Mutation	SOCE	Sum	Phase1	Phase2	Phase3
HC1-12	None	0	0	0.00	0.00	0.00
C1-6	None	0	-1	0.00	0.00	-0.33
P1	ORAI1 (R91W) W/W [#]	--	-10	-0.50	-0.17	-1.00
P2	ORAI1 (R91W) R/W ^{##}	--	-8	-0.42	-0.17	-0.67
P3	ORAI1 (R91W) R/W ^{##}	-	-10	-0.50	-0.33	-0.67
P4	ORAI1 (R98S) G/S ^{##}	0	-4	-0.50	0.00	0.67
P5	ORAI1 (R98S) G/S ^{##}	-	-13	-0.83	-0.33	-0.33
P7	FERMT3 (R573X) X/X [#]	n.d.	-21	-1.00	-1.00	-1.00
P8	FERMT3 (R573X) R/X ^{##}	n.d.	-14	-0.50	-0.83	-1.00
P9	FERMT3 (R573X) R/X ^{##}	n.d.	-12	-0.42	-0.83	-0.67

For indicated patients, measurements of store-operated Ca²⁺ entry (SOCE) (see Figure 2) and differential heatmap data relative to control cohort HC1-12 (see Figure 5C) were put in a table to obtain an overview of the changes in platelet function. For thrombi (1600 s⁻¹) formed on the three microspots (Sp1-3), all parameters (V1-7) were scored as within normal range (0), decreased (-1) or increase (+1). Per patient, summed scores are indicated (column 'Sum'). In addition, fractions of altered scores are indicated for three phases of thrombus formation. Color intensity corresponds with the relative changes in parameters. Phase 1 refers to platelet adhesion and aggregation (Sp1-3, V1-4), Phase 2 to platelet integrin activation and granule secretion (Sp1-3, V6-7), and phase 3 to platelet procoagulant activity (Sp1-3, V5). n.d.: not determined; [#]homozygosity in the indicated mutation; ^{##}heterozygosity in the indicated mutation.

Discussion

In the present study, we used a multiparameter test of whole blood thrombus formation under flow conditions, as a proxy measurement of hemostatic activity,²⁰ to characterize quantitative and qualitative platelet abnormalities in rare patients with severe immunodeficiencies and their relatives, linked to signaling protein defects and mutations in the *Orai1*, *Stim1* and *Fermt3* genes. So far, functional effects of the *Orai1* and *Stim1* mutations have only been described for human immune cells or cell lines. Hence, the present data are the first to report on comparative alterations in platelet SOCE and platelet functions in as many as nine genotyped patients/relatives.

Aberrations in SOCE accompanied by mutations in *Orai1* or *Stim1*

Earlier work with bone marrow chimeric mice with megakaryocytic deficiency in *Orai1* or *Stim1* demonstrated a prominent role of these Ca²⁺-entry regulating proteins in platelet calcium homeostasis and activation, including PS exposure.^{11,29} Our human data are compatible with these findings in that SOCE after thapsigargin or GPVI stimulation appeared to be impaired in platelets from patient P1 with homozygous *Orai1*^{W/W} mutation.

A similar impairment of SOCE has been reported in platelets from *Orai1*^{R93W} mice, *i.e.* a loss-of-function mutation orthologous to the human ORAI1 R91W variant.²⁹ Platelets from the latter mice showed a defect in Ca²⁺ fluxes and other responses, when triggered with low concentrations of thrombin or collagen receptor agonists. These platelets displayed normal aggregation under flow conditions, but a decreased procoagulant activity (PS exposure).²⁹

Relatives P2 and P3, heterozygous for the R91W mutation, showed about 20-50% residual SOCE activity, which is compatible with co-expression of the non-mutated allele in the platelets. Interestingly, Ca²⁺ entry after thrombin stimulations remained unaffected in patients/relatives P1-3, which is explained by involvement of the SOCE-independent Ca²⁺ entry mechanism through TRPC6 channels.³⁰

On the other hand, the R98S mutation in ORAI1, with assumed gain-of-function,³¹ carried by patient P4, was not accompanied by altered SOCE activity after thapsigargin or GPVI stimulation, whereas SOCE was substantially reduced in the relative P5 (confirmed in two independent blood samples). The difference in SOCE activity between P4 and P5 might be explained by a different 'penetration' of the mutated allele in ORAI1 expression in megakaryocytes and platelets. However, an alternative explanation is the presence of other modifying genetic or acquired factors between P4 and P5, with possible effects on platelet SOCE activity, on which we can only speculate.

Concerning patient P6 with a heterozygous R429C mutation in STIM1, Ca²⁺ entry in platelets was impaired after thapsigargin, but not after GPVI or PAR1/4 stimulation. In mammalian cell lines, the R429 mutation modulates the C-terminal oligomerization and puncta formation of STIM1 with ORAI1.³² Our results suggest that, in platelets, this mutation strongly inhibits the interaction of STIM1 with ORAI1 after full Ca²⁺-store depletion, such as provoked by thapsigargin.

Altered platelet functions in thrombus formation accompanied by mutations in ORAI1, STIM1 or FERMT3

Previous murine studies have pointed out that deficiency in platelet ORAI1 or STIM1 led to a moderately reduced collagen-dependent thrombus formation with minimal effect on bleeding,^{8,11} whereas murine deficiency in FERMT3 (kindlin-3) resulted in impaired thrombus formation and a clear bleeding phenotype.³³ Furthermore, both ORAI1-deficient and ORAI1^{R93W} mouse platelets were found to be partly defective in procoagulant activity (PS exposure), along with the annulled SOCE activity.^{8,11,29}

In the present study, we observed even more variable platelet phenotypes in the nine patients/relatives with a mutation in ORAI1, STIM1 or FERMT3. Heatmap analysis indicated

extensive but distinct patterns of reduced thrombus formation between patients, compared to blood from cohorts of healthy control subjects. Blood analysis further indicated that most patients/relatives carrying such a mutation had platelet counts below or near the lower range of normal. Low platelet count was found to correlate with low thrombus formation parameters, especially on spot 1. By comparison with flow studies using blood from healthy controls at lower counts, it appears that mild thrombocytopenia can lead to a more severe reduction in thrombus formation if combined with lower platelet functionality. Mild thrombocytopenia for patients with a loss-of-function mutation in ORAI1 or STIM1 has been reported before.¹⁶ So far, published papers on patients with a FERMT3 mutation do not report on thrombocytopenia.^{26,27}

Because of the relatively large number of patients in our study, we were able to separate the thrombus formation parameters linked to qualitative or quantitative platelet defects. Both unsupervised clustering of the heatmap data and principal component analysis of the raw data indicated that mostly thrombus parameters on spot 1 (collagen; platelet receptors GPIb-V-IX, GPVI, $\alpha_2\beta_1$) showed a dependency on platelet count, whereas those of spot 2 (vWF/rhodocytin; platelet receptors GPIb-V-IX, CLEC-2) and spot 3 (vWF/fibrinogen; platelet receptors GPIb-V-IX, $\alpha_{IIb}\beta_3$) were not dependent of platelet count. Markedly, this was true for both the high-shear and low-shear flow tests. An explanation for this finding is that, with collagen as a relatively strong agonist for GPVI, on spot 1, platelet delivery (thus, count) rather than platelet activation is a limiting factor for thrombus-forming parameters. In contrast, the immobilized ligands of spots 2-3, being less platelet-stimulating, may more rely on full platelet activation including normal SOCE and $\alpha_{IIb}\beta_3$ integrin activation. Correlation analysis also indicated that PS exposure was a key parameter linked to SOCE, in agreement with earlier mouse data.^{10,11}

Improved platelet functions after bone marrow transplantation

Bone marrow transplantation of patient P1 (ORAI1^{W/W}), 2 months before, resulted in improved SOCE activity and normalized thrombus formation on spot 3 but not on spot 1 (linked to a low platelet count). Transplantation of P7 (FERMT3^{X/X}), 3 months before, led to an overall improvement of thrombus formation parameters (at normal platelet count). The partial restoration of platelet count at 2 months post-transplantation is compatible with reports that a full normalization can take several months.^{26,34}

Based on the relevant differential analysis of thrombus formation parameters (Figure 5C), Table 2 provides a summative overview for each patient of alterations in: platelet adhesion/aggregation, integrin activation/secretion and procoagulant activity (phases 1-3). This approach is based on the rationale that this whole blood flow assay

senses additive effects of low platelet count and impaired platelet functionality. Table 2 shows for all patients/relatives with ORAI1 (R91W) mutation an overall defect in adhesion/aggregation, as well as a defect in procoagulant activity. It also underlines that the assumed gain-of-function mutation ORAI1 (G98S) in patient P4 is accompanied by a typical increase in procoagulant activity (but not in relative P5 with low SOCE). Furthermore, in patients carrying the FERMT3 (R573X) mutation, all platelet responses appeared to be more severely reduced in case of homozygosity than of heterozygosity. This may be of clinical relevance, since only the homozygous carrier P7 had a history of bleeding (Table 1).

Competing interests

The authors have declared that no competing interests exist.

Author's contribution

MN performed experiments, analyzed data and drafted the manuscript. TM, NM, SdW performed experiments, analyzed data. KC provided essential materials. JK, AS, TV, CS and BZ recruited the patients. JC and AB contributed ideas and corrected the manuscript. BZ and JH designed the study, drafted and finalized the paper.

Funding

Financial support from the Netherlands Centre for Translational Molecular Medicine (CTMM, MICRO-BAT), the Interreg V Euregio Meuse-Rhine program (Poly-Valve), Dutch Heart Foundation (2015T79 to T.G.M., and J.M.E.M.C.) and the Netherlands Organization for Scientific Research (NWO Vidi 91716421 to J.M.E.M.C.).

References

1. Feske S, Gwack Y, Prakriya M, *et al.* A mutation in Orai1 causes immune deficiency by abrogating CRAC channel function. *Nature*. 2006; 441: 179-185.
2. Penna A, Demuro A, Yeromin AV, *et al.* The CRAC channel consists of a tetramer formed by STIM-induced dimerization of Orai dimers. *Nature*. 2008; 456: 116-120.
3. Luik RM, Wang B, Prakriya M, Wu M, Lewis RS. Oligomerization of STIM1 couples ER calcium depletion to CRAC channel activation. *Nature*. 2008; 454: 538-542.
4. Soboloff J, Rothberg BS, Madesh M, Gill DL. STIM proteins: dynamic calcium signal transducers. *Nat. Rev. Mol. Cell Biol.* 2012; 13: 549-565.
5. Varga-Szabo D, Braun A, Nieswandt B. STIM1 and Orai1 in platelet function. *Cell Calcium*. 2011; 50: 70-278.
6. Ambily A, Kaiser WJ, Pierro C, *et al.* The role of plasma membrane STIM1 and Ca²⁺ entry in platelet aggregation. STIM1 binds to novel proteins in human platelets. *Cell Signal*. 2014; 26: 502-511.
7. Varga-Szabo D, Braun A, Kleinschnitz C, *et al.* The calcium sensor STIM1 is an essential mediator of arterial thrombosis and ischemic brain infarction. *J. Exp. Med.* 2008; 205: 1583-1591.
8. Braun A, Varga-Szabo D, Kleinschnitz C, *et al.* Orai1 (CRACM1) is the platelet SOC channel and essential for pathological thrombus formation. *Blood*. 2009; 113: 2056-2063.

9. Gilio K, Harper MT, Cosemans JM, *et al.* Functional divergence of platelet protein kinase C (PKC) isoforms in thrombus formation on collagen. *J. Biol. Chem.* 2010; 285: 23410-23419.
10. Van Kruchten R, Braun A, Feijge MA, *et al.* Antithrombotic potential of blockers of store-operated calcium channels in platelets. *Arterioscler. Thromb. Vasc. Biol.* 2012; 32: 1717-1723.
11. Gilio K, van Kruchten R, Braun A, *et al.* Roles of platelet STIM1 and Orai1 in glycoprotein VI- and thrombin-dependent procoagulant activity and thrombus formation. *J. Biol. Chem.* 2010; 285: 23629-23638.
12. Heemskerk JW, Mattheij NJ, Cosemans JM. Platelet-based coagulation: different populations, different functions. *J. Thromb. Haemost.* 2013; 11: 2-16.
13. Malacards: human disease database. 2016. Available from: www.malacards.org.
14. Shaw PJ, Feske S. Regulation of lymphocyte function by ORAI and STIM proteins in infection and autoimmunity. *J. Physiol.* 2012; 590: 4157-4167.
15. Nakamura L, Sandrock-Lang K, Speckmann C, *et al.* Platelet secretion defect in a patient with stromal interaction molecule 1 deficiency. *Blood.* 2013; 122: 3696-3698.
16. Lacruz RS, Feske S. Diseases caused by mutations in ORAI1 and STIM1. *Ann. N. Y. Acad. Sci.* 2015; 1356: 45-79.
17. Kuijpers TW, van de Vijver E, Weterman MAJ, *et al.* LAD-1/variant syndrome is caused by mutations in FERMT3. *Blood.* 2009; 113: 4740-4746.
18. Van de Vijver E, De Cuyper IM, Gerrits AJ, *et al.* Defects in Glanzmann thrombasthenia and LAD-III (LAD-1/v) syndrome: the role of integrin β 1 and β 3 in platelet adhesion to collagen. *Blood.* 2012; 119: 583-586.
19. Stepensky PY, Wolach B, Gavrieli R, *et al.* Leukocyte adhesion deficiency type III: clinical features and treatment with stem cell transplantation. *J. Pediatr. Hematol. Oncol.* 2015; 37: 264-268.
20. De Witt SM, Lamers MME, Swieringa F, *et al.* Identification of platelet function defects by multi-parameter assessment of thrombus formation. *Nat. Commun.* 2014; 5: 4257.
21. Endo Y, Noguchi S, Hara Y, *et al.* Dominant mutations in ORAI1 cause tubular aggregate myopathy with hypocalcemia via constitutive activation of store-operated Ca^{2+} channels. *Hum. Mol. Genet.* 2015; 24: 637-648.
22. Fuchs S, Rensing-Ehl A, Speckmann C, *et al.* Antiviral and regulatory T cell immunity in a patient with stromal interaction molecule 1 deficiency. *J. Immunol.* 2012; 188: 1523-1533.
23. Feijge MA, van Pampus EC, Lacabaratz-Porret C, *et al.* Inter-individual variability in Ca^{2+} signalling in platelets from healthy volunteers, relation with expression of endomembrane Ca^{2+} -ATPases. *Br. J. Haematol.* 1998; 102: 850-859.
24. Heemskerk JW, Vis P, Feijge MA, *et al.* Roles of phospholipase C and Ca^{2+} -ATPase in calcium responses of single, fibrinogen-bound platelets. *J. Biol. Chem.* 1993; 268: 356-363.
25. Schindelin J, Arganda-Carreras I, Frise E, *et al.* Fiji: an open-source platform for biological-image analysis. *Nat. Meth.* 2012; 9: 676-682.
26. Crazzolara R, Maurer K, Schulze H, *et al.* A new mutation in the KINDLIN-3 gene ablates integrin-dependent leukocyte, platelet, and osteoclast function in a patient with leukocyte adhesion deficiency-III. *Pediatr Blood Cancer.* 2015; 62: 1677-1679.
27. Jurk K, Schulz AS, Kehrel BE, *et al.* Novel integrin-dependent platelet malfunction in siblings with leukocyte adhesion deficiency-III (LAD-III) caused by a point mutation in FERMT3. *Thromb Haemost.* 2010; 103: 1053-1064.
28. Cauwenberghs S, Feijge MA, Theunissen E, *et al.* Novel methodology for the assessment of platelet transfusion therapy by measuring increased thrombus formation and thrombin generation. *Br. J. Haematol.* 2007; 136: 480-490.
29. Bergmeier W, Oh-Hora M, McCarl CA, *et al.* R93W mutation in Orai1 causes impaired calcium influx in platelets. *Blood.* 2009; 113: 675-678.
30. Hassock SR, Zhu MX, Trost C, Flockerzi V, Authi KS. Expression and role of TRPC proteins in human platelets: evidence that TRPC6 forms the store-independent calcium entry channel. *Blood.* 2002; 100: 2801-2811.
31. Bohm J, Bulla M, Urquhart JE, *et al.* ORAI1 mutations with distinct channel gating defects in tubular aggregate myopathy. *Hum Mutat.* 2017; 38: 426-438.
32. Maus M, Jairaman A, Stathopoulos PB, *et al.* Missense mutation in immunodeficient patients shows the multifunctional roles of coiled-coil domain 3 (CC3) in STIM1 activation. *Proc Natl Acad Sci USA.* 2015; 112: 6206-6211.
33. Moser M, Nieswandt B, Ussar S, Pozgajova M, Fassler R. Kindlin-3 is essential for integrin activation and platelet aggregation. *Nat. Med.* . 2008; 14: 325-330.
34. Takami A, Shibayama M, Orito M, *et al.* Immature platelet fraction for prediction of platelet engraftment after allogeneic stem cell transplantation. *Bone Marrow Transplant.* 2007; 39: 501-507.

Supplemental material

Materials

Horm type-I collagen was purchased from Nycomed. Convulxin was purified to homogeneity from the venom of *Crotalus durissus terrificus* (Latoxan). Human α -thrombin came from Kordia Life Science. Thapsigargin was from Santa Cruz Biotechnology. Annexin A5 labeled with Alexa Fluor-568 (AF568) and Fura-2 acetoxymethyl ester were from Invitrogen. FITC-labeled anti-fibrinogen monoclonal antibody (mAb), staining for activated integrin $\alpha_{IIb}\beta_3$, was from BD Bioscience; AF647-labeled anti-human CD62P (P-selectin) mAb was from BioLegend. Other chemicals were obtained from sources, as described.¹

Blood collection and preparation of platelets

Blood was collected in trisodium citrate anticoagulant. Samples from patients and travel controls were collected under sterile conditions and supplemented with 10 mM glucose, to extend the life time of platelets and red blood cells. Transportation within 24 h was in thermal isolation material to avoid temperature changes. A part (1-2 mL) of the samples was used for whole blood flow perfusion experiments. The remaining blood was used for preparation of platelet-rich plasma (PRP) and Ca^{2+} responses.² The platelets were finally suspended in HEPES buffer pH 7.45 (10 mM HEPES, 136 mM NaCl, 2.7 mM KCl, 2 mM $MgCl_2$, 5 mg/mL glucose and 1 mg/mL bovine serum albumin) at a concentration of 2×10^8 /mL. Where indicated, remaining (unloaded) platelets were used for flow cytometry.

Platelet Ca^{2+} responses

To measure changes in cytosolic Ca^{2+} concentration, platelets in plasma were incubated with fluorescent Fura-2 acetoxymethyl ester (2.5 μ M) for 45 min at ambient room temperature under gentle rotation, under standardized conditions as described before.³ Loaded platelets were washed and activated with indicated agonists under magnetic stirring (37 °C). Fluorescence changes were recorded by 340/380 nm calibrated ratio fluorometry, using appropriate settings of R_{max} and R_{min} .³ Calcium responses are presented as nM rises in cytosolic $[Ca^{2+}]_i$.⁴ Agonist-induced changes in $[Ca^{2+}]_i$ were compared of platelets from patients and from two cohorts of healthy control subjects (home controls and travel controls).

Flow cytometry

Washed platelets ($2 \times 10^8/\text{mL}$) were activated in the presence of 2 mM CaCl_2 with agonists for 5-30 min. Multicolor flow cytometry was used for measurements of surface exposure of phosphatidylserine (with AF647Annexin A5), activated integrin $\alpha_{\text{IIb}}\beta_3$ (with FITC-PAC1 mAb), and α -granule secretion (with FITC anti-CD62P mAb), as described before.^{1,5} Analysis was with a FACScan flow cytometer (BD Accuri Cytometers).

Thrombus formation on microspots under flow

Whole blood was assayed for thrombus formation under defined flow conditions, essentially as described before.⁶ In brief, citrate anticoagulated blood samples were recalcified with 3.75 mM MgCl_2 and 7.5 mM CaCl_2 (final concentrations) in the presence of PPACK (40 μM) and fragmin (40 U/mL). Samples were then directly perfused over a glass coverslip coated with 1-3 microspots (spot 1: collagen type I, spot 2: vWF/rhodocytin, spot 3: vWF/fibrinogen), mounted onto a transparent parallel-plate perfusion chamber. Perfusion was at a laminar wall-shear rate of 1600 s^{-1} for 3.5 min. Spot 1 with strongest thrombogenic activity was located most downstream of the flow direction, in order to prevent cross-reactivity between microspots.⁶ Remaining blood samples were recalcified and perfused over microspots at lower shear rate of 150 s^{-1} for 6 min. Thrombi formed on the spotted surfaces were immediately post-stained with a mixture of FITC-anti-fibrinogen mAb (1:100), FITC-anti-CD62P mAb (25 $\mu\text{g}/\text{mL}$) and AF647-Annexin A5 (0.25 $\mu\text{g}/\text{mL}$) in Hepes buffer pH 7.45 containing CaCl_2 (2 mM) and heparin (1 U/mL). Series of phase-contrast and fluorescence images were then captured for analysis of surface area coverage by adhered platelets or by activated platelets (*i.e.*, with integrin $\alpha_{\text{IIb}}\beta_3$ activation, α -granule release or exposed phosphatidylserine).⁷ Three random images were taken per spot and stain. Image analysis was performed blinded to the condition, using Fiji software,⁸ and predefined scripts.

For comparative analysis, average values from 7 thrombus parameters were scaled over a range from 0-10 (over all 3 microspots), and heatmaps were generated. These data were further processed to obtain subtraction heatmaps in comparison to the normalized mean data from a cohort of normal control subjects.⁶ Filtering of the subtraction data was based on differences in comparison to control values outside the range of mean ± 2 SD and a relevance level arbitrarily set at 20%.

Coding of microspots: Sp1, type I collagen; Sp2, vWF/rhodocytin; Sp3, vWF/fibrinogen. Coding of outcome parameters: V1, thrombus morphological score (scale 0-5); V2, platelet surface area coverage (% SAC); V3 thrombus contraction score (scale 0-3); V4, thrombus multilayer score (scale 0-3); V5, PS exposure (% SAC); V6, P-selectin

expression (% SAC); V7, integrin $\alpha_{\text{IIb}}\beta_3$ activation (% SAC). Scoring of V1-3 was based on predefined reference images.

Statistics

The size of control groups (HC1-12, C-16) with $n \geq 6$ was pre-assessed by power analysis, based on expected effects on PS exposure.⁶ Significance of differences was determined with the paired sample *t* test (intervention effects) and principal component analysis (PCA) using the statistical package for social sciences (SPSS, version 11.0).

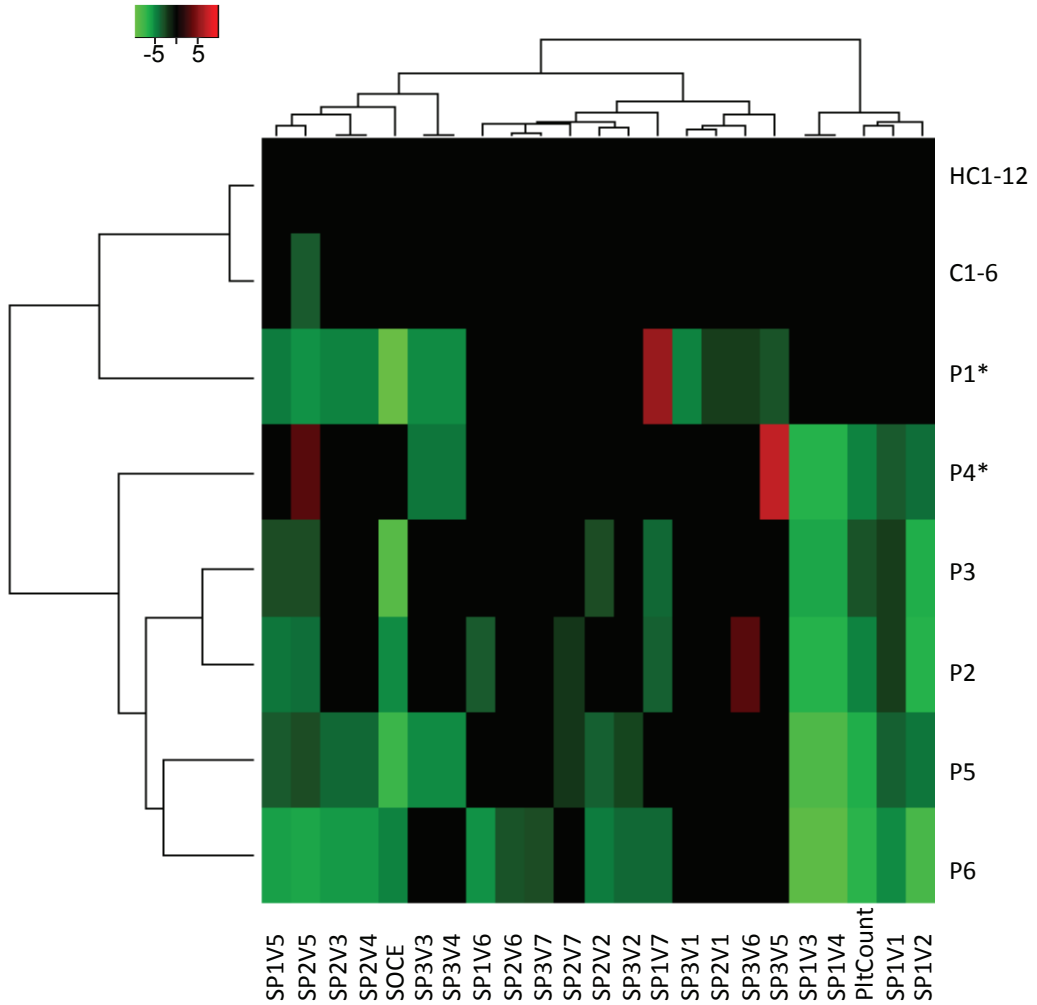
References

1. Gilio K, Harper MT, Cosemans JM, et al. Functional divergence of platelet protein kinase C (PKC) isoforms in thrombus formation on collagen. *J Biol Chem.* 2010;285:23410-9.
2. Van Kruchten R, Braun A, Feijge MA, et al. Antithrombotic potential of blockers of store-operated calcium channels in platelets. *Arterioscler Thromb Vasc Biol.* 2012;32(7):1717-23.
3. Feijge MA, van Pampus EC, Lacabartz-Porret C, et al. Inter-individual variability in Ca^{2+} signalling in platelets from healthy volunteers, relation with expression of endomembrane Ca^{2+} -ATPases. *Br J Haematol.* 1998;102:850-9.
4. Heemskerk JW, Vis P, Feijge MA, et al. Roles of phospholipase C and Ca^{2+} -ATPase in calcium responses of single, fibrinogen-bound platelets. *J Biol Chem.* 1993;268:356-63.
5. Nakamura L, Sandrock-Lang K, Speckmann C, et al. Platelet secretion defect in a patient with stromal interaction molecule 1 deficiency. *Blood.* 2013;122(22):3696-8.
6. De Witt SM, Lamers MME, Swieringa F, et al. Identification of platelet function defects by multi-parameter assessment of thrombus formation. *Nat Commun.* 2014;5:4257.
7. Van Kruchten R, Cosemans JM, Heemskerk JW. Measurement of whole blood thrombus formation using parallel-plate flow chambers: a practical guide. *Platelets.* 2012;23:229-42.
8. Schindelin J, Arganda-Carreras I, Frise E, et al. Fiji: an open-source platform for biological-image analysis. *Nat Meth.* 2012;9:676-82.

Supplemental figures

	Subject	Spot1	Spot2	Spot3
PS exposure (%)	Control	9.4-13.44	6.84-13.88	2.12-8.06
	P1	4.09	1.97	0.09
	P2	7.02	5.69	7.25
	P3	4.53	3.83	7.28

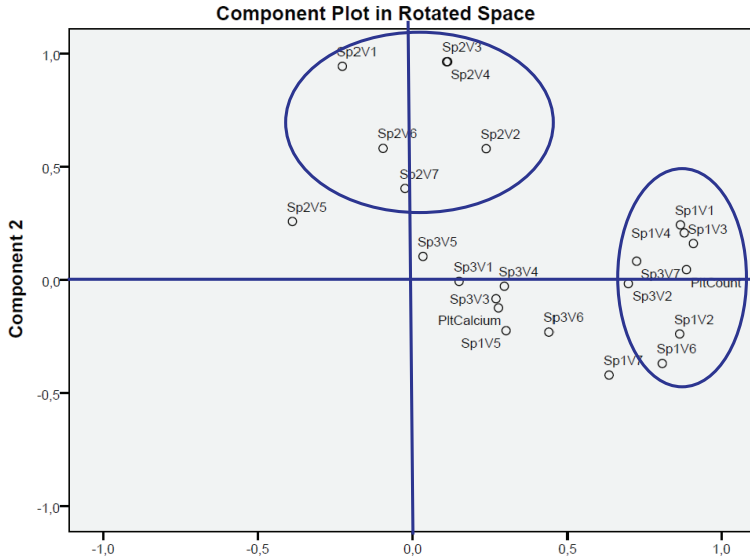
Suppl. Table 1. Reduced PS exposure of platelets from patient P1. Whole blood from control subjects and indicated patients P1-3 was perfused over three microspots, as in Figure. Data are shown of platelet PS exposure (%SAC) at spots 1-3.



4

Suppl. Figure 1. Clustering of parameters of thrombus formation on three microspots with SOCE and platelet count. Unsupervised clustered heatmap for 21 parameters of thrombus formation at high shear rate, SOCE and platelet count (columns) for cohorts of healthy controls (HC1-12 and C1-6) and patients/relatives P1-5 (rows). Clustering reveals a clear distinction between parameters linked to SOCE or platelet count.

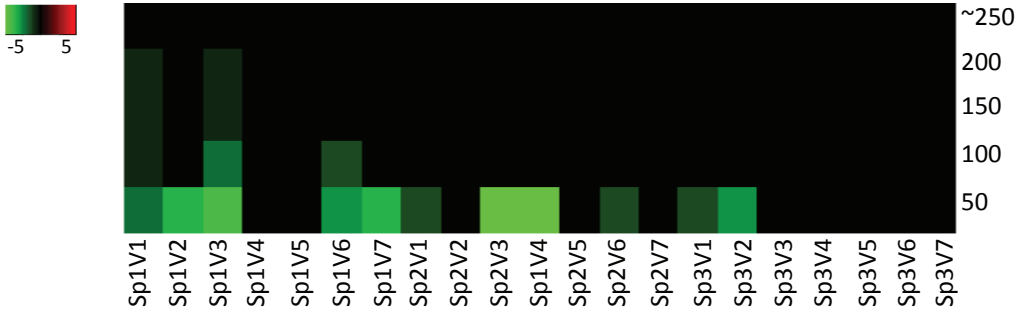
A



B

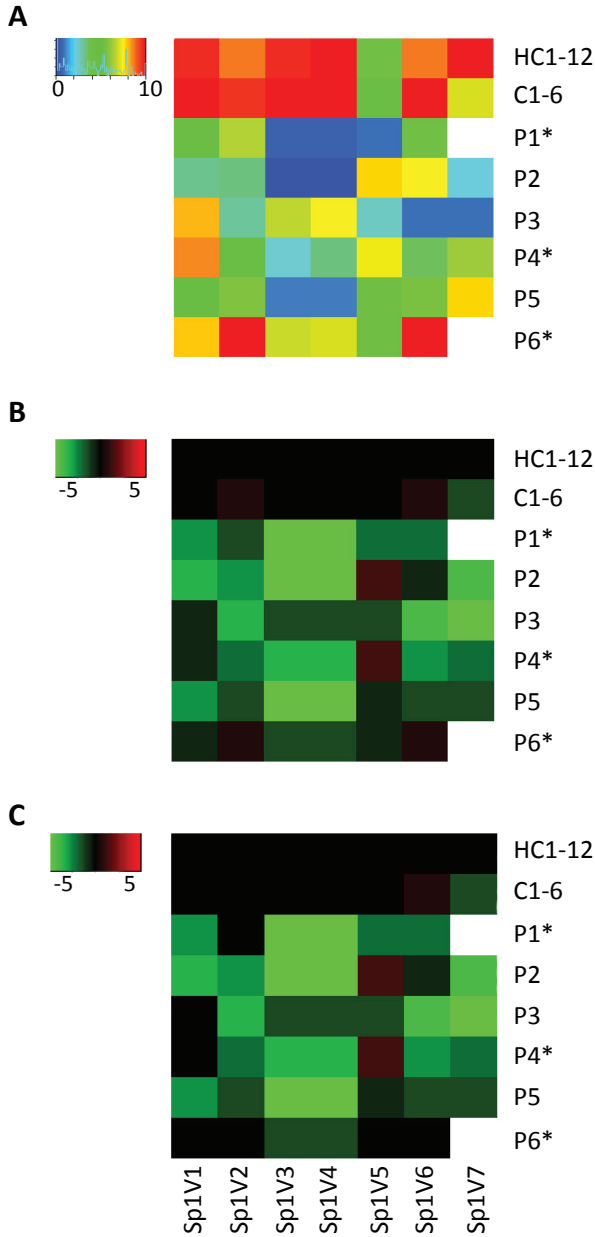
	Parameter	R ²
PltCount	Sp1V1	0.734**
	Sp1V2	0.678**
	Sp1V3	0.796**
	Sp1V4	0.756**
	Sp1V6	0.516**
	Sp3V2	0.611*
	Sp3V7	0.726**
PltCalcium (SOCE)	Sp1V5	0.563*
	Sp3V5	0.577*

Suppl. Figure 2. Principal component analysis (PCA) of parameters of thrombus formation, SOCE and platelet count at high shear rate. (A) PCA biplot with parameter values projecting the first two principal components. **(B)** Tabled R² values (Pearson correlation coefficient) and significance of correlations with platelet count and platelet SOCE. Statistical analysis was performed in SPSS; *P<0.05, **P<0.01.



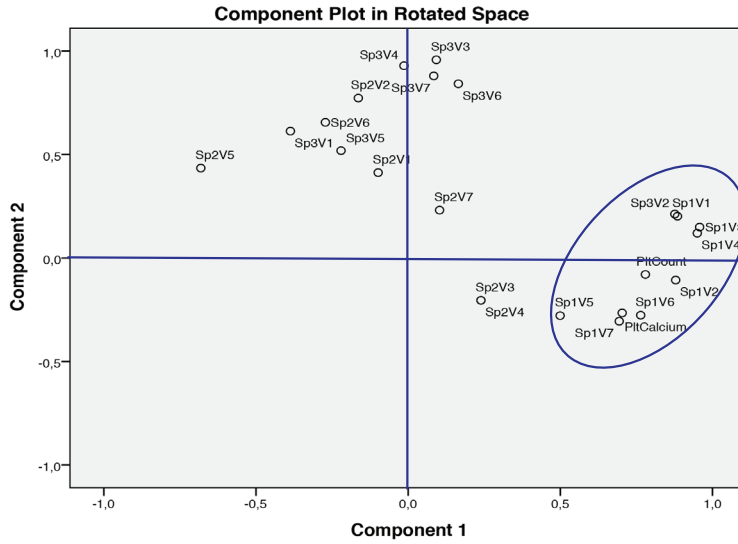
Suppl. Figure 3. Dependency of thrombus formation on platelet count. Blood was reconstituted using washed red blood cells, platelet-rich plasma and platelet-free plasma at hematocrit levels of 0.40 and platelet counts of 50, 100, 150, 200 or 250 x 10⁹/L, as indicated. Samples were perfused over 3 microspots (Sp1-3) at shear rate of 1600 s⁻¹ (n=3-5), as described for Figure 4. Parameters of thrombus formation were determined (V1-7) and scaled for a subtraction heatmap relative to values for 250 x 10⁹ platelets/L, as in Figure 5. Subtracted values were then filtered, based on significant differences in comparison to original platelet count of 250 x 10⁹/L. Note the limited reduction of thrombus parameters on Sp1 at 100 x 10⁹/L and more extended changes on Sp1-3 at the lower count of 50 x 10⁹/L.

4



Suppl. Figure 4. Altered thrombus formation of blood from patients with ORA11 or STIM1 mutations at low shear rate. Whole blood from control subjects or indicated patients was perfused over collagen type I surface at low shear rate of 150 s^{-1} . **(A)** Heatmap of normalized parameters of thrombus formation for control subjects (HC1-12, C1-6) and patients with genetic mutations in ORA11 (P1-5) or in STIM1 (P6). **(B)** Subtraction heatmap of parameters in comparison to control cohort (HC1-12). **(C)** Filtered subtraction data based on differences in comparison to controls outside the range of mean ± 2 SD. *Subject with reduced SOCE.

A



B

	Parameter	R ²
PltCount	Sp1V1	0.609**
	Sp1V2	0.725**
	Sp1V3	0.654**
	Sp1V4	0.643**
	Sp1V6	0.692**
	Sp1V7	0.659*
PltCalcium (SOCE)	Sp1V3	0.704*
	Sp1V5	0.714*
	Sp1V4	0.737**

Suppl. Figure 5. Principal component analysis (PCA) of parameters of thrombus formation, SOCE and platelet count at low shear rate. (A) PCA biplot with parameter values projecting the first two principal components. (B) Tabled R² values (Pearson correlation coefficient) and significance for correlations with platelet count and platelet SOCE. Statistical analysis was performed in SPSS; *P<0.05, **P<0.01

Chapter 5

Thrombus-induced micro-localization and activation of neutrophils: roles of platelet-derived chemokines

Nagy M, Brouns SLN, Montague SJ, Burston JJ, Cosemans JMEM, Jurk K, Koenen RR, Ni Ainle F, O'Donnell VB, Soehnlein O, Watson SP, Heemskerk JWM

To be submitted

Abstract

Neutrophils contribute to pathological thrombus formation at an early stage, by interacting with platelets and the vessel wall. Vice versa, platelets can promote neutrophil activation. However, the spatial and temporal prerequisite for platelet-dependent neutrophil activation is still unclear. Our aim was to unravel the phased interaction mechanisms between human activated platelets and neutrophils in the context of arterial thrombus formation. Stable arterial thrombi of thrombin activated platelets generated in collagen-coated microfluidic devices appeared to incorporate high numbers of neutrophils. These neutrophils, although to some extent heterogeneous in responses, demonstrated directional movements selectivity in: micro-location, secretion of collagenolytic proteases, repetitive transient Ca^{2+} fluxes, granular secretion and production of reactive oxygen species. Post-silencing of the platelets in thrombi by iloprost treatment suppressed the overall Ca^{2+} fluxes in neutrophils and altered pattern of micro-location. Blockage of the platelet-derived chemokines CXCL7 (NAP-2) or CCL5 (RANTES), but not of CXCL4 (platelet factor 4), resulted in similar response alterations. Likewise, 12-lipoxygenase inhibition altered neutrophil Ca^{2+} fluxes as well. Furthermore, platelet integrin $\alpha_{\text{IIb}}\beta_3$ had a regulatory role in platelet-neutrophil interaction. In conclusion, neutrophil attraction to and activation by a highly activated thrombus relies on persistent platelet activation via multiple bioactive mediators. Herein platelet CD62P and CD40L receptors have stimulatory role in neutrophil attachment, whilst $\alpha_{\text{IIb}}\beta_3$ acts as a preventive element. This multi-staged process of neutrophil adhesion, crawling and activation can be suppressed by platelet silencing with iloprost or blockade of the platelet-derived chemokine CXCL7 (NAP-2) or CCL5.

Introduction

The interaction between platelets and leukocytes, in particular polymorphonuclear cells or neutrophils, is recognized as a stimulatory factor contributing to thrombotic and inflammatory processes.^{1,2} Evidence for this is based on findings that both platelets and neutrophils jointly contribute to various diseases including atherosclerotic lesion formation,³⁻⁵ experimental laser-induced microvascular thrombosis,⁶ as well as coronary⁷ and deep venous^{8,9} thrombosis. Supportive evidence also comes from the regular presence of neutrophil extracellular traps (NETs) in atherosclerotic plaques¹⁰ and in arterial and venous thrombi, suggesting that these neutrophil activation contribute to atherothrombosis.¹¹ However, the biochemical pathways by which platelets and neutrophils interact during thrombus formation are still poorly understood.

Mostly investigated so far are the adhesive receptors by which activated platelets adhere to leukocytes. Multiple receptor-ligand pairs are involved, including platelet P-selectin (CD62P) interacting with PSGL-1,¹² CD40L binding leukocyte CD40,^{13,14} and glycoprotein Ib or JAM-C binding integrin $\alpha_{\text{M}}\beta_2$.^{15,16} Interestingly, a polarized distribution of PSGL-1 receptors has been observed on migrating neutrophils, scanning for activated (CD62P-exposing) platelets.¹⁷ In addition, several platelet-derived substances have been described to chemo-attract leukocytes, for example interleukin 8 (IL-8) and chemokines such as platelet factor 4 (CXCL4), NAP-2 (CXCL7) and RANTES (CCL5);¹⁸⁻²⁰ and the compounds platelet-activating factor (PAF) and TREM-1 ligand.^{21,22} The current idea is that the local secretion of these substances leads to a chemotactic gradient that stimulates the directional migration of neutrophils.¹⁷ Indeed, such a migration occurs of neutrophils into arterial thrombi via platelet-derived CXCL4, suggesting a critical role in wound healing and vascular remodeling.^{19,23} However, how all these interactions determine the responsiveness and fate of leukocytes in a thrombotic environment is largely unknown.

In thrombus formation on a collagen surface, platelets accumulate with different activation properties, *i.e.* aggregated platelets showing integrin $\alpha_{\text{IIb}}\beta_3$ activation and fibrinogen binding; platelets undergoing secretion with CD62P expression; and single, ballooned platelets with exposure of the procoagulant phospholipid phosphatidylserine (PS).²⁴⁻²⁶ On the other hand, it has been described that the neutrophils in thrombi release proteases such as cathepsin G and matrix metalloproteinases, which govern their migration to the injured (sub)endothelium.^{23,27} Furthermore, there is evidence that neutrophils undergo NET formation, stimulated by platelet CD62P expression²⁸ and platelet chemokines²⁹ and accompanied by secretion of myeloperoxidase (MPO) and formation of reactive oxygen species.^{30,3}

Neutrophil activation, *e.g.* by PAF, P₂Y₂ or LTB₄ receptors, can proceed via a classical Ca²⁺ signaling pathway, involving Ca²⁺ mobilization, store-operated Ca²⁺ entry and protein kinase C activation.³²⁻³⁴ Such Ca²⁺ fluxes have been implicated in neutrophil migration³⁵ and in the degranulation of different types of storage vesicles.³⁶ Based on this work, we hypothesized that platelet activation during thrombus formation triggers the attraction of neutrophils via adhesive receptors and then stimulates these cells to generate Ca²⁺ fluxes. In the present study, we investigated this by determining the molecular processes by which neutrophils respond to a thrombus generated *in vitro*.

Materials and methods

Materials

Horm-type collagen was obtained from Takeda (Chou-ku, Osaka, Japan). Fluorogenic dye quenched (DQ)-collagen (type I from bovine skin, fluorescein conjugated) was obtained from Life technologies (Carlsbad, CA, USA), as were 4',6-diamidino-2-phenylindole (DAPI), Cell-ROX DeepRed, Alexa Fluor (AF)488- and AF647-labeled annexin A5. From the same source were allophycocyanin (APC)-labeled anti-CD63 mAb, Sytox green nucleic acid stain, and donkey anti-rabbit IgG. N-formyl-methionineleucyl phenylalanine (fMLP) came from Merck (Darmstadt, Germany). Recombinant human Chemokine (C-C motif) ligand 5 (CCL5) was from R&D Systems (Minneapolis, MN, USA). Streptomycin, NCTT-956, histopaque-1077 and histopaque-1119 were from Sigma-Aldrich (St. Louis, MO, USA). Iloprost was from Bayer Schering Pharma (Berlin, Germany); 2-methylthio (Me)-ADP and blocking cluster of differentiation 40 ligand (CD40L) antibody from BioConnect (Huissen, The Netherlands); human recombinant tissue factor from Siemens (Munich, Germany); human thrombin and Gly-Pro-Arg-Pro peptide (GPRP) from Kordia (Leiden, The Netherlands); Thrombin Receptor Activator Peptide 6 (TRAP6 or SFLLRN) from Bachem (Bubendorf, Switzerland); D-Phenylalanyl-prolyl-arginyl Chloromethyl Ketone (PPACK) from VWR (Padnor, PA, USA). Polyclonal rabbit anti-human histone H3-citrulline 2+8+17 antibody, CHIP grade, and blocking antibody against Chemokine (C-X-C motif) ligand 4 (CXCL4) came from Abcam (Cambridge, UK). Fluorescein isothiocyanate (FITC)-labelled anti-CD66b and AF647-labeled anti-CD15 mAb were from BioLegend (San Diego CA, USA) and FITC-labeled anti-CD62P mAb was from Beckman Coulter (Brea, CA, USA). CCL5 was synthesized, as described.²⁰ The cell-permeant 2',7'-dichlorodihydrofluorescein diacetate (H₂DCFDA) was from Thermo-Fisher Scientific (Eindhoven, The Netherlands). Other reagents were obtained from sources indicated before.⁶¹

Human blood collection and blood cell preparation

Blood from healthy volunteers was collected into 10% of 129 mM trisodium citrate. Blood donors gave full informed consent according to the Helsinki declaration. Permission was obtained from the local Medical Ethical Committee. Citrated platelet-rich plasma and washed platelets were prepared, as previously described.⁶¹

Polymorphonuclear leukocytes were enriched from citrated blood using a histopaque-1077 and histopaque-1119 density gradient centrifugation method, essentially as described elsewhere.²¹ A mixture of equal volumes of citrate blood, histopaque-1077 and histopaque-1119 were centrifuged at 700 g for 30 min. The granulocytes layer was removed, washed twice with 10 mL isotonic phosphate-buffered saline (PBS), and centrifuged again at 350 g for 10 min. And the pellets were finally centrifuged at 1500 g for 2 min. The isolated granulocytes were resuspended at a concentration of 1×10^6 cells/mL into Hepes buffer pH 7.45 (10 mM Hepes, 136 mM NaCl, 2.7 mM KCl, 2 mM $MgCl_2$, 0.1% glucose and 0.1% bovine serum albumin). Neutrophil suspensions were supplemented with 2 mM $CaCl_2$ before use. Purity and density of the cell suspensions were assessed with a Sysmex-XP300 hematology analyzer.

Formation of thrombi with differently activated platelets

Thrombus formation was induced in parallel-plate flow chamber,⁶² by perfusion of whole blood over collagen type-I at a wall-shear rate of 1000 s^{-1} during 4 min.^{24,63} For the formation of type I thrombi without coagulation, citrated blood was recalcified (3.75 mM $MgCl_2$ and 7.5 mM $CaCl_2$, f.c.) in the presence of PPACK anticoagulant (40 μM). Type II thrombi were formed similarly with blood that was co-infused with Me-ADP (1 μM , f.c.) to stimulate platelet aggregation. Type III thrombi were by co-infusion of citrated blood with coagulation medium (3.75 mM $MgCl_2$, 7.5 mM $CaCl_2$, 2 pM tissue factor, f.c.). For thrombi of each type, consistent leukocyte adhesion was obtained by 10 s of stasis followed by 2 min of flow continuation, after which residual blood was removed by a 2 min rinse with Hepes buffer pH 7.45, supplemented with 2 mM $CaCl_2$.

Platelet activation in thrombi was verified by dual labeling with FITC-anti CD62P mAb and AF647-Annexin A5, as described before.⁶⁴ From all thrombi on collagen, brightfield and fluorescence microscopic images were recorded with an inverted Zeiss LSM 510 line-scanning confocal microscope, equipped with 488, 532 and a 647 nm laser lines and a 63x oil objective.⁶⁵ Where indicated, an EVOS inverted digital fluorescence microscope (60x oil objective) was used.⁶⁴ Brightfield and fluorescence images were analyzed using scripts written in Fiji/ImageJ software.⁴⁸

Neutrophil activation markers

Neutrophils adhered to type I-III thrombi were stained directly after blood perfusion (6 min), or after rinse and 2-16 h incubation at 37 °C (storage in humid box, streptomycin present). Cells were stained with Alexa Fluor(AF) 647-annexin A5 (1:200), Hoechst (1 µg/mL), Sytox green (1 µM), FITC anti-myeloperoxidase (MPO; 1:100) and/or anti-citrullinated histone-3 Ab (10 µg/mL), as indicated.

Purified suspensions of neutrophils were also stained for activation markers by flow cytometry, using an Accuri C6 flow cytometer and CFlow Plus software (Becton-Dickinson Bioscience). Neutrophils were gated in forward/side scatter plots from a positive coloring with FITC-labeled anti-CD66b mAb (1 µg/mL). Activation was assessed from elevated CD66b expression, MPO expression and ROS staining with CellRox DeepRed, as indicated. Mean fluorescence intensities of gated events were recorded. Where indicated, the neutrophils were stimulated with fMLP (1 µM) or CCL5 (500 nM).

Neutrophil collagenolytic activity

Glass coverslips were spot-coated with a mixture of DQ-collagen (50 µg/mL) and HORM type I collagen (25 µg/mL) in a dark humid box for 1 h. After blocking with HEPES buffer pH 7.45 containing 1% bovine serum albumin, the coverslips were inserted into flow chambers and perfused with blood, as described above. Streptomycin (1:1000) was added to prevent bacterial contamination. The neutrophil containing thrombi in flow chambers were post-incubated in a humid chamber at 37 °C for 2-16 h, and then observed by confocal microscopy at 488 nm excitation. Fluorescent neutrophils with de-quenched and endocytosed DQ-collagen, as a result of collagenase activity, were compared with overlay brightfield microscopic images. Using neutrophils in suspension, degradation and uptake of DQ-quenched-collagen was also assessed by flow cytometry. For the latter, the purified cells were incubated with DQ-collagen (2 µg/mL) at 37 °C for 1 h, and subsequently treated with fMLP (1 µM), CCL5 (500 nM) or iloprost (10 nM). Mean fluorescence intensities were determined.

Calcium signals of and movements of neutrophils in thrombi

For measurement of $[Ca^{2+}]_i$ transients in single neutrophils, buffy coats from blood of healthy donors were incubated with 8 µM Fluo-4 acetoxymethyl ester in presence of pluronic (0.4 mg/mL) for 40 min. Leukocyte count and differentiation was determined with a Sysmex-XP300 hematology analyzer. After centrifugation, the Fluo-4-loaded leukocytes were resuspended in a double volume of HEPES buffer pH 7.45. Autologous Fluo-4-loaded leukocytes (1×10^6 /mL) were then perfused over type III thrombi (treated

as indicated) at shear rate of 200 s^{-1} for 5 min. This resulted in adhesion of the majority of the Fluo-4-loaded cells (>98% neutrophils), after which the non-adhered cells were removed by a 2 min rinse with HEPES buffer pH 7.45. If indicated, thrombi with Fluo-4-loaded platelets were formed that were perfused with unloaded neutrophils. Regarding the latter, blood samples were supplemented with washed, Fluo-4-loaded platelets at 20% of the platelet blood count. Changes in cytosolic $[\text{Ca}^{2+}]$ in fluorescent neutrophils or platelets were recorded for 10 min, using a Zeiss LSM 510 confocal microscope (488 nm excitation). Time series of overlay fluorescence and brightfield images were recorded simultaneously.

Time series of fluorescence images were analyzed for changes in fluorescence intensity in defined regions-of-interest, representing a single neutrophil or thrombus, using Fiji/ImageJ software. Neutrophils were classified, based on the type of oscillatory changes in fluorescence intensity above resting level ($F/F_0 > 1.15$). A score of 4 indicated repetitive, high amplitude rises in $[\text{Ca}^{2+}]_i$; score 3 indicated a single, high amplitude rise in $[\text{Ca}^{2+}]_i$; score 2 indicated short-term, low-amplitude rises in $[\text{Ca}^{2+}]_i$; score 1 indicated no or minimal rises in $[\text{Ca}^{2+}]_i$. Fractions of cells per score were calculated, and converted into an overall weighted score.

Movement patterns of location of neutrophils in thrombi

Time series (10 min) of overlay brightfield and fluorescence images were analyzed for movement patterns of individual neutrophils using scripts in Fiji software. Movement profiles were classified as follows: <20% contact with platelet thrombi, temporary 20-80% contact with thrombi, or persistent >80% contact with thrombi. Regarding directionality of the movement, contacting cells were classified as low fidelity (switching between different thrombi) or high fidelity (staying at or returning to the same thrombus).

Platelet $\alpha_{IIb}\beta_3$ integrin modulation

Whole blood from control subjects and three patients with Glanzmann thrombasthenia was perfused over collagen type I (1000 s^{-1} , 3.5 min) to obtain type I thrombi. Adhered neutrophils in the absence of stasis were analyzed, as described above. In addition, control blood was treated with the clinically used $\alpha_{IIb}\beta_3$ antagonist, tirofiban ($1 \mu\text{g}/\text{mL}$), prior to perfusion over collagen. Fluo-4-loaded neutrophils were post-perfused, and fluxes in Ca^{2+} were recorded.

Mouse experiments

$Alox12^{-/-}$ mice were bred in house in accordance with the United Kingdom Home Office Animals (Scientific Procedures) Act of 1986, under License (PPL 30/3150). Access

to water and standard chow was *ad libitum*. Citrated anticoagulated mouse blood was obtained by cardiac puncture and then used to form type III thrombi, similarly as described for human blood. Mouse neutrophils were characterized by high Ly6G staining using a AF647-labelled antibody.

Statistics

Significance of difference between groups was determined with independent sample t-tests or an ANOVA, as appropriate, using GraphPad Prism 7. Scored fractions were compared by a χ^2 test. Data are expressed as means \pm s.e. Statistical significance was set at $P < 0.05$.

Results

Neutrophil are attracted to thrombi containing highly activated platelets

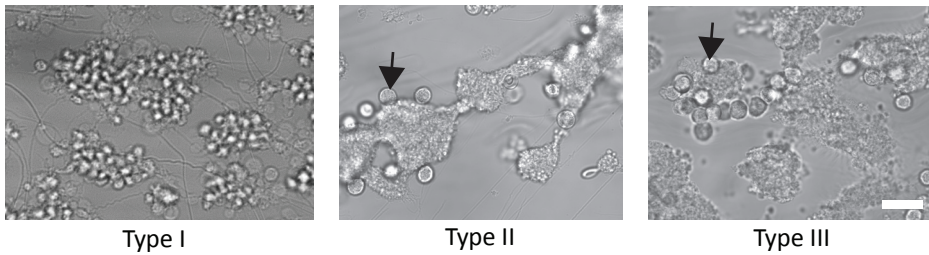
To characterize the interactions of leukocytes with platelets under conditions of thrombus formation, we generated different types of thrombi using microfluidics, by whole-blood perfusion (4 min, arterial wall-shear rate of 1000 s^{-1}) over collagen spots.³⁷ Using PPACK anticoagulated blood, thrombi formed that consisted of loosely aggregated platelets prone to disaggregate³⁸ (Figure 1A), and termed type I thrombi. By co-perfusion with ADP, type II thrombi were formed containing stable platelet aggregates. When initiating coagulation, by using recalcified blood in the presence of tissue factor,²⁴ type III thrombi were formed containing contracted platelet aggregates with no more than traces of fibrin formation during the time of thrombus build-up (Figure 1A).

While the overall deposition of platelets on collagen was similar for types I-III thrombi, their stability during a 2-16 h post-incubation in the microfluidic chamber (37°C) increased from type I to type III as defined by surface area coverage (%SAC) (Figure 1B). In addition, PS exposure, as a marker of high platelet activation, was substantially higher in type II-III than in type I thrombi at all time-point (Figure 1B). During 4 min of blood flow at 1000 s^{-1} with all perfusion conditions, no more than incidental adhesion of leukocytes to the type I-III thrombi was observed. However, a consistent, high incorporation of leukocytes into type II-III thrombi was provoked by a 10 s stasis period, before continuation of the blood flow for another 2 min (data not shown). After stasis, the type II and III thrombi attracted on average 5-7 leukocytes per microscopic field which, by staining for CD15, could be characterized as $>97\%$ neutrophils (Figure 1C). Those neutrophils kept attached to the thrombi upon recapitulating of the flow. In contrast, the unstable, type I thrombi did not attract significant numbers of leukocytes.

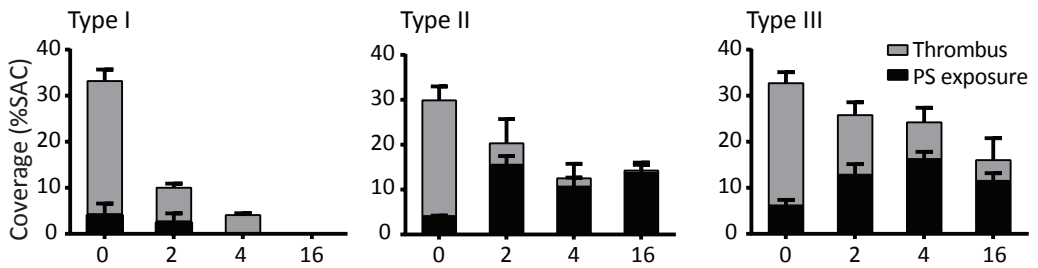
Long term incubation (2-16 h) of the microfluidic chambers at 37 °C demonstrated that the neutrophils stayed to adhere at sites where stable thrombi were present as well (Figure 1C).

Previous studies have shown that platelet activation induces neutrophil extracellular trap (NETs).³⁹ Thus, we quantified this process in type II-III thrombi, at both early time points and after 2-16 h of incubation at 37°C (in presence of antibiotics).

A



B



C

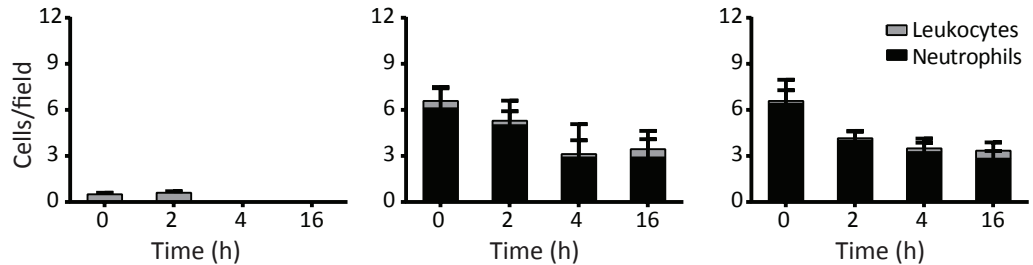
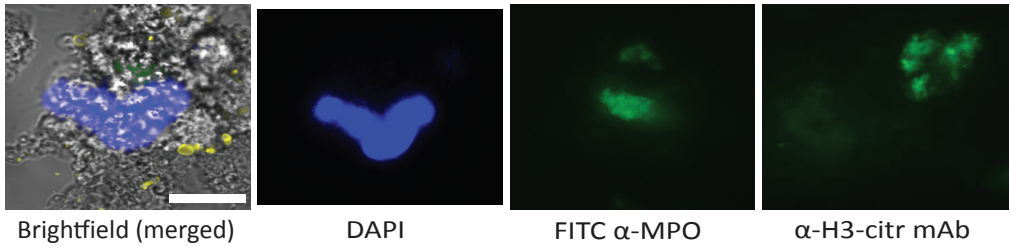


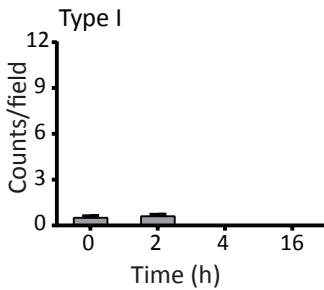
Figure 1. Leukocyte adhesion to different types of thrombi. Whole blood was flowed over collagen in microfluidic chambers at 1000 s^{-1} for 4 min to provoke formation of thrombi of types I-III. Type I: perfusion of PPACK-anticoagulated blood; type II: co-perfusion of PPACK-anticoagulated blood and 2MeS-ADP (1 μM , f.c.); type III: co-perfusion of citrated blood with coagulation medium containing tissue factor and $\text{CaCl}_2/\text{MgCl}_2$. Leukocyte adhesion was induced by 10 s stasis and 2 min of additional flow, after which a rinse of 2 min is applied (is $t=0$ h). Flow chambers were observed by brightfield and fluorescence microscopy at $t=0$ h or incubated for 2-16 h at 37 °C after which 5 random microscopic images were taken. **A**) Representative images of type I-III thrombi at $t=0$ h. Arrows indicate adhered leukocytes (bar, 25 μm). **B**) Surface area coverage (% SAC) of thrombi and PS-exposing platelets (AF647-annexin A5 staining) on collagen. **C**) Counts per microscopic field (213 x 213 μm) of total adhered leukocytes (brightfield) and identified neutrophils (fluorescence, AF647 anti-CD15 mAb). Means \pm S.E. ($n = 4-8$ experiments).

In order to characterize the formation of NETs, three types of staining were used, *i.e.* detecting distorted nuclei (Hoechst stain), extruded DNA filaments (Sytox green stain), and extracellular citrullinated histones (polyclonal anti-histone H3-citrulline antibody) (Figure 2A,B). Remarkably, the large majority of adhered neutrophils failed to form NETs, regardless of thrombus type I-III (Figure 2C,D). Even after 4-16 h incubation, only

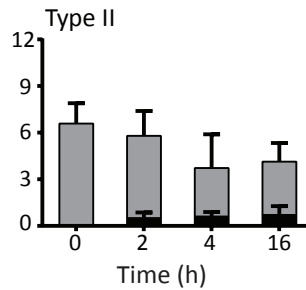
A



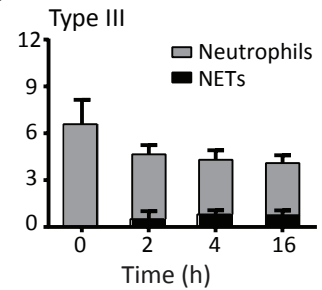
B



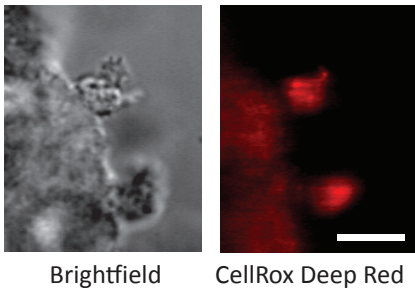
C



D



E



F

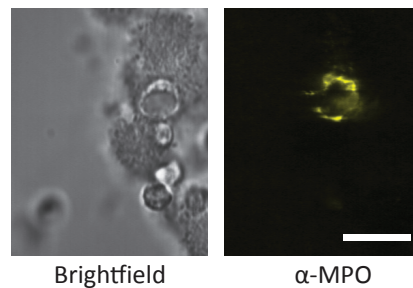


Figure 2. Neutrophil activation at platelet thrombi but restricted NET formation. Thrombi of type I-III with adhered neutrophils were formed in microfluidic chambers, and were then incubated for 2-16 h at 37 °C, as in Fig. 1. **A**) Overlays of microscopic images (type III thrombi, 4 h incubation), characterizing incidentally formed NETs (<1/field). Staining was as indicated by DAPI (distorted nucleus), FITC-anti MPO Ab, or FITC-anti-histone H3-citrulline Ab. Bar = 25 μ m. **B**) Neutrophil counts/field and numbers of NETs formed per microscopic field. Means \pm S.E. (n = 3-8 experiments). **C-D**) Microscopic images characterizing all intact neutrophils without NET formation (T = 0). **E-F**) Overlays of microscopic images indicating activation of neutrophils on type III thrombi, by staining for ROS with CellRox DeepRed (**E**) or using FITC anti-MPO mAb (**F**). Representative images are shown from n = 3 experiments.

rare (<1 per microscopic field) NET-forming structures could be observed, pointing to a rare phenomenon under the present conditions (Figure 2B). This demonstrates that NETs formation is not a common feature of thrombus-associated neutrophils in this model.

Further, characterization of the neutrophil-platelet interaction was then performed for type III thrombi. Multicolor microscopic imaging indicated that thrombi contained aggregated platelets with high secretion of α - and δ -granules as well as many ballooned platelets with PS exposure (Suppl. Figure 1A). The majority of neutrophils interacting with type III thrombi displayed myeloperoxidase secretion (MPO staining) and produced reactive oxygen species (CellRox DeepRed staining) (Figure 2E,F), indicating activation.

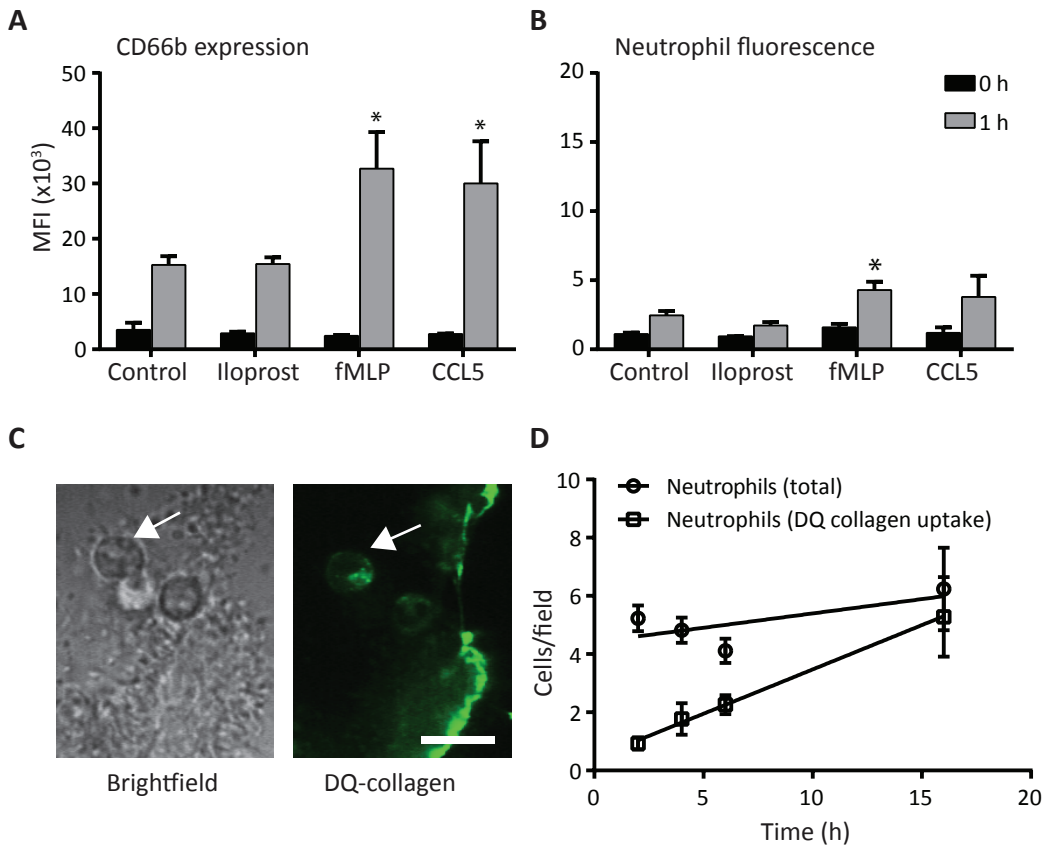
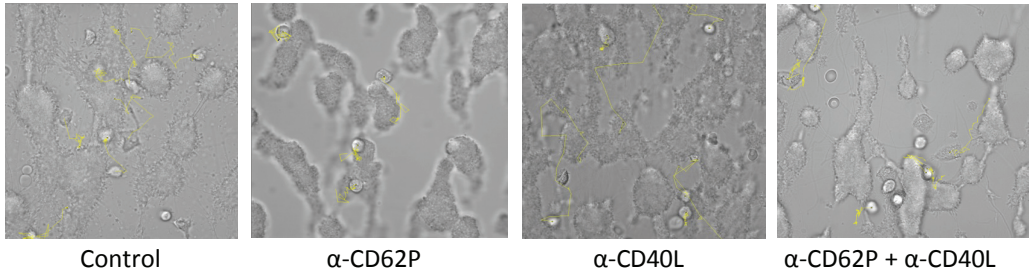
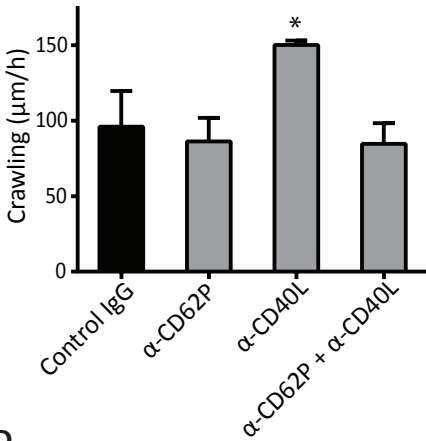


Figure 3. Neutrophil activation and uptake of degraded collagen. A-B) Isolated neutrophils in Hepes buffer pH 7.45 were treated with iloprost (10 nM), fMLP (1 μ M) or CCL5 (500 nM) for 1 h. **A**) Flow cytometric detection of neutrophil activation, indicated by high expression of CD66b. **B**) Samples were incubated with DQ collagen; flow cytometric detection of DQ collagen degradation and uptake (green fluorescence staining). **C-D**) Type III thrombi with adhered neutrophils, formed on a DQ collagen surface, were analyzed for fluorescence due to collagen degradation and uptake at indicated times. Representative image after 16 h with high-fluorescent spots of collagen-degrading neutrophils (**C**, arrow), and low-fluorescent spots by collagen-degrading platelets in thrombi. Quantification of fluorescent neutrophils with collagen uptake per microscopic field. Means \pm S.E. (n=4-7 experiments). * P <0.05, ** P <0.01 vs. control.

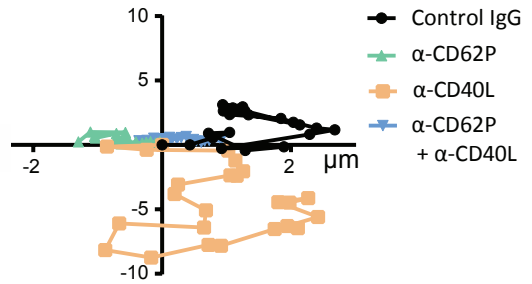
A



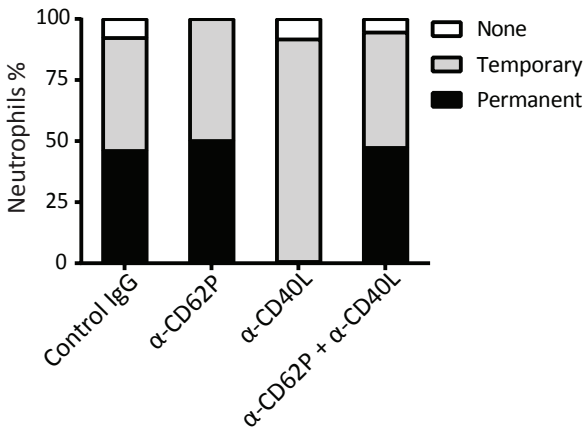
B



C



D



E

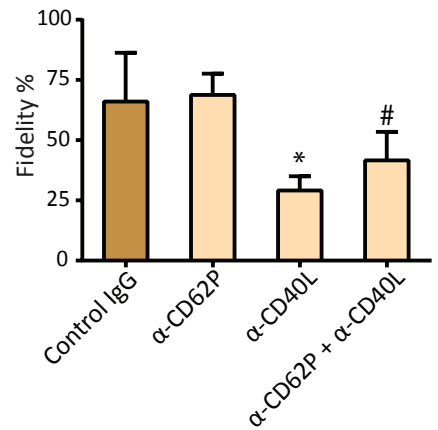


Figure 4. Micro-chemotactic movement and location of neutrophils adhered to thrombi. Type III thrombi were formed, and movements of neutrophils were recorded in brightfield movies during 10 min. Blocking anti-CD62P, anti-CD40L and control antibodies (1 mg/ml) were present, as indicated. **A)** Representative images with movement patterns of single neutrophils (yellow). **B)** Average movement rates of neutrophils per condition. **C-E)** Directionality (**C**), preferred micro-location (**D**) and fidelity (**E**) of neutrophils at thrombus core or edge or distant from thrombi. Means \pm S.E. (n=10-15 cells). *P<0.05 (χ^2 test).

Taken together, these results point to a flow/stasis-induced extensive and continuous interaction of neutrophils with stable thrombi that consist of activated platelets with secretory and procoagulant responses. While neutrophil activation was apparent from MPO secretion and production of reactive oxygen species, NET formation throughout the time-course of the 16 hr was not apparent.

Responsiveness and micro-location of neutrophils on platelet thrombi

To further study the responsiveness of neutrophils, suspensions of isolated neutrophils were stimulated with G-protein coupled receptor agonists, *i.e.* fMLP⁴⁰ or the (platelet-derived) chemokine CCL5.⁴¹ Either agonist stimulated the expression of CD66b, thus indicating cell activation (Figure 3A). In addition, both fMLP and CCL5 triggered the degradation of a dye quenched collagen, leading to the formation of fluorescent collagen fragments, which were attached to the neutrophils (Figure 3B). This fluorescence accumulation was prevented in the presence of a general matrix metalloproteinase inhibitor, GM6001 (data not shown). Incubation of the neutrophils with iloprost did not affect these responses. When neutrophils adhered to type III thrombi on a DQ-collagen surface, this also resulted in time-dependent collagen degradation (Figure 3C,D). This neutrophil response is likely mediated by the release of collagen-degrading matrix metalloproteinases (MMPs) by neutrophils.¹² Confocal images indicated that the

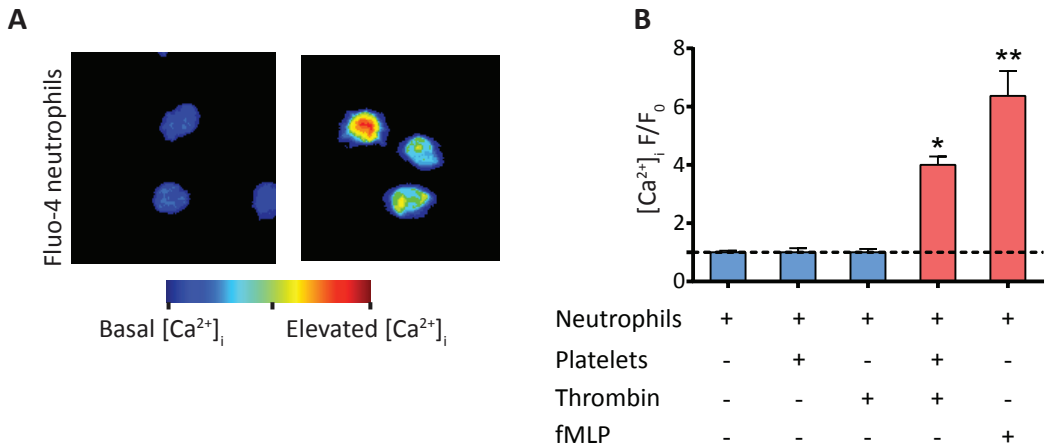
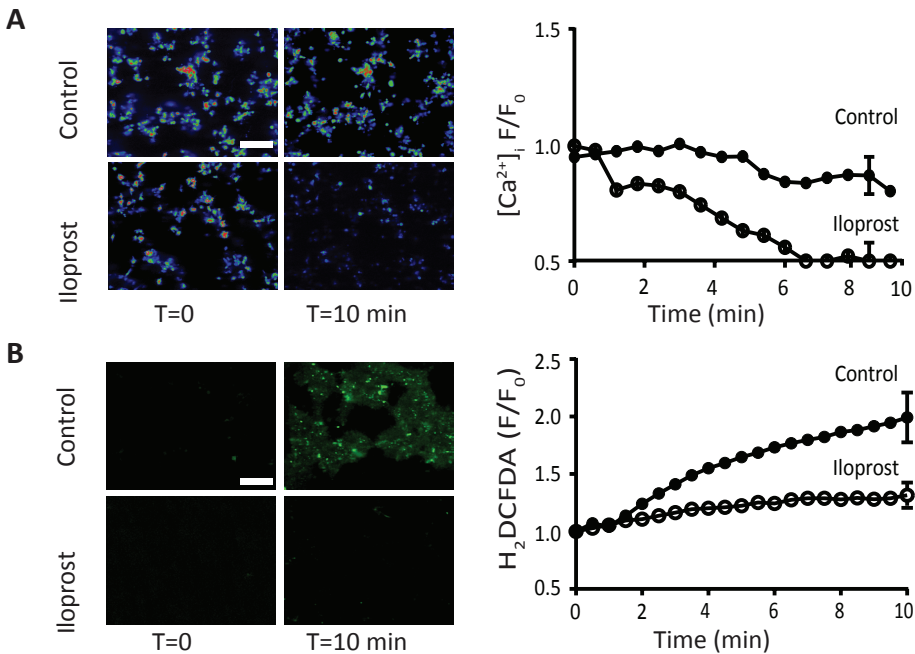


Figure 5. Neutrophil Ca²⁺ fluxes induced by activated platelets. A-B) Fluo-4-loaded neutrophils (1 x 10⁶/ml) in wells were allowed to adhere to BSA-coated coverslips, and rises in [Ca²⁺]_i (F/F₀) were measured by microscopic imaging for 10 min. Added were platelets (10 x 10⁷/ml), iloprost (10 nM), thrombin (4 nM) and/or fMLP (1 μM), as indicated. **A**) Representative microscopic Fluo-4 images with(out) fMLP. **B**) Quantification of maximal rises in [Ca²⁺]_i (>10 cells) per condition. Means ± S.E. (n=3 experiments). *P<0.05, **P<0.01 vs. neutrophils alone.

majority of neutrophils took up fluorescent collagen fragments. In agreement with earlier results,⁴² platelet thrombi also stimulated local MMP-mediated DQ-collagen degradation (Figure 3C).

Given the known ability of neutrophils to migrate in response to gradients of chemokines, *i.e.* chemotaxis, we monitored how single neutrophils moved at or in between type III thrombi. Under control conditions, a mean rate of crawling of 90 $\mu\text{m}/\text{h}$ was seen (Figure 4A,B). This movement was without net directionality, as the majority of neutrophils stayed around the same thrombus, *i.e.* a behavior that was defined as ‘high fidelity’ (Figure 4C). Given the earlier described roles of platelet-expressed CD62P and CD40L in mediating neutrophil interaction,^{13,14} we determined the effects of blocking either or both CD62P and CD40L on neutrophil movements and micro-location. CD40L blockage increased their overall movement rate (Figure 4B,C), thus indicating a weakened neutrophil interaction, which resulted in more cells with a location distant from the thrombi, and hence a lower fidelity (Figure 4D,E). However, these blocking conditions did not affect the numbers of neutrophils present, indicating that CD62P and CD40L were not key factors determining the capturing of neutrophils in our experimental setup.



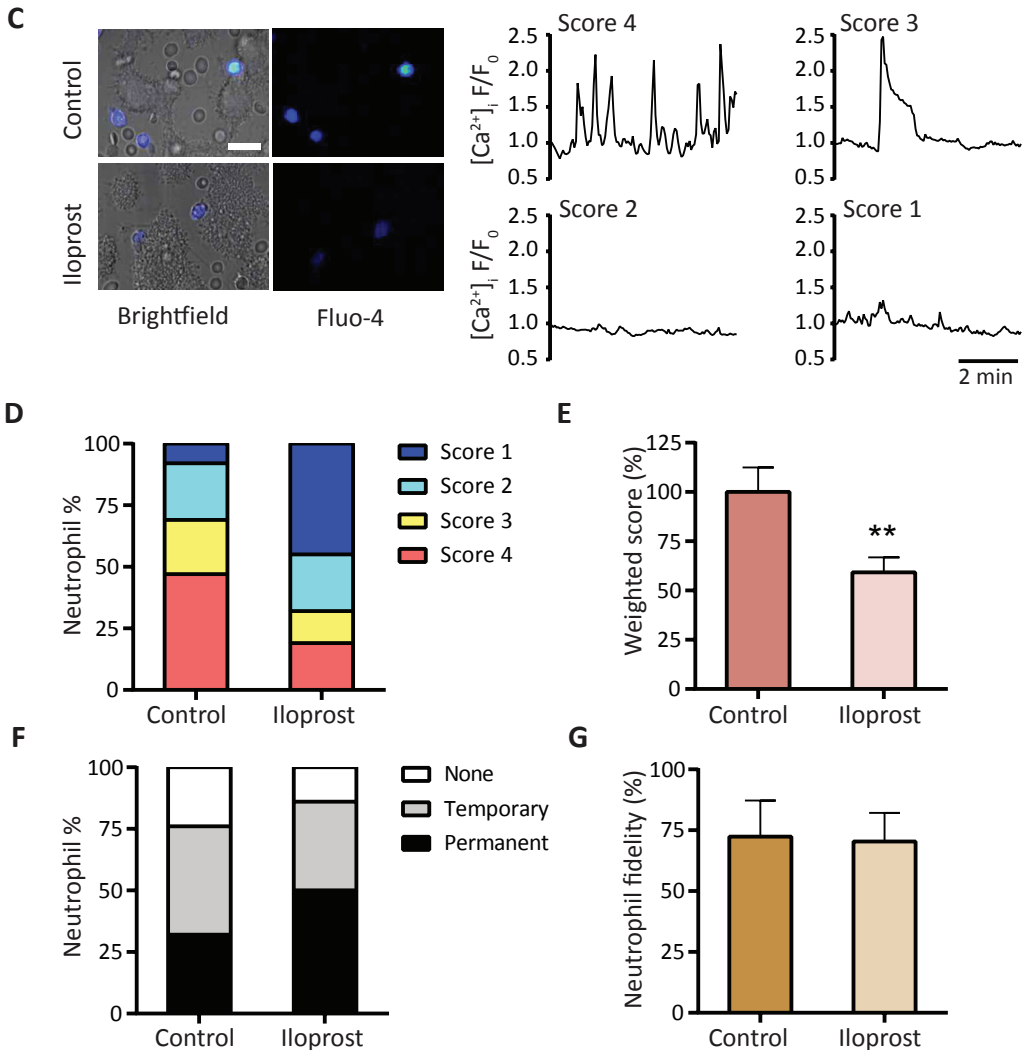


Figure 6. Iloprost-induced post-silencing of thrombi affecting neutrophil activation. **A-D**) Type III thrombi were formed as for Fig. 1, and post-perfused with iloprost (10 nM) for 10 min, as indicated. Autologous platelets in blood (20%) were loaded with Fluo-4; alternatively platelets in thrombi were post-labeled with the ROS probe H_2DCFDA . **A**) Representative confocal images and overall elevation in $[Ca^{2+}]_i$ (F/F_0 , F_0 = basal) of platelets in thrombi. **B**) Representative images and overall rise in ROS production of platelets in thrombi. Note the near-complete silencing of platelets upon iloprost post-treatment. **C-G**) Type III thrombi were formed and post-perfused with iloprost as above. Autologous Fluo-4-loaded neutrophils were post-perfused, and 10-min fluorescence and brightfield movies were recorded to determine rises in $[Ca^{2+}]_i$. Representative images at 10 min, and Ca^{2+} transients of single neutrophils with high $[Ca^{2+}]_i$ (score 4) or lower $[Ca^{2+}]_i$ (score 1-3) scores (**C**). Distribution profiles of neutrophils with different Ca^{2+} scores with(out) iloprost treatment of thrombi (**D**) and calculated weighted Ca^{2+} scores (**E**). **F-G**) Distribution patterns of neutrophils' micro-location (**F**) and fidelity (**G**). Means \pm S.E. ($n=3-5$ experiments). * $P<0.05$, ** $P<0.01$ vs. control.

Neutrophil activation linked to continuous platelet activation

To investigate the inter-cellular cross-talk of neutrophils with platelets in more detail, we assessed the Ca^{2+} fluxes of Fluo-4-loaded neutrophils in mixed suspensions with platelets as a ubiquitous signal of neutrophil activation. Neutrophils on BSA-coated coverslips displayed low levels of $[\text{Ca}^{2+}]_i$, which were markedly increased by the G-protein coupled receptor agonist, fMLP (Figure 5A). Similarly, thrombin stimulation of platelets triggered high $[\text{Ca}^{2+}]_i$ rises in these neutrophils (Figure 5B). In sharp contrast, thrombin in the absence of platelets was completely inactive, thus suggesting that platelet activation processes or products were able to trigger Ca^{2+} fluxes in neutrophils. Control experiments indicated that the platelet/thrombin-induced Ca^{2+} flux in neutrophils was not affected by ATP/ADP-degrading apyrase (not shown), thus arguing against a major role of the neutrophil P2X receptor channels. The platelet inhibitor iloprost (10 nM) by itself did not affect fMLP-induced $[\text{Ca}^{2+}]_i$ rises in the isolated neutrophils (not shown).

Considering that platelet secretion is a continuous process,⁴³ these findings prompted us to determine if post-silencing of the platelets in a thrombus would affect the activation of neutrophils. Therefore, type III thrombi were generated containing Fluo-4-loaded platelets, which were then post-treated with iloprost (10 nM). In comparison to the control condition, iloprost treatment resulted in a marked reduction of the platelet Ca^{2+} signal (Figure 6A). Similarly, the iloprost treatment markedly suppressed the formation of reactive oxygen species produced by platelets (detected with the probe H_2DCFADA) (Figure 6B). Hence, treatment with iloprost seemed to be an effective way to revert the activation state of platelets in a thrombus.

Subsequently, we monitored Ca^{2+} fluxes in neutrophils interacting with the iloprost-treated (silent) thrombi. For this, type III thrombi (no iloprost) were super-fused with autologous Fluo-4-loaded neutrophils, and combined brightfield and fluorescence microscopic images were recorded over a time period of 10 min. A marked heterogeneity was revealed between individual neutrophils attracted to the thrombi (Figure 6C). While about 50% of the cells displayed high and continuous $[\text{Ca}^{2+}]_i$ transients (*i.e.* calcium score 4), other cells showed a single, large $[\text{Ca}^{2+}]_i$ transient (*i.e.* calcium score 3), or multiple low-amplitude $[\text{Ca}^{2+}]_i$ rises (*i.e.* calcium score 2). Less than 10% of the cells were scored as essentially silent (*i.e.* calcium score 1). This distribution, however, substantially changed if thrombi were post-treated with iloprost (10 nM). In this case, <20% of the Fluo-4-loaded neutrophils were scored 4, and over 40% of the cells scored 1. This change was also reflected by a lower value of the weighted Ca^{2+} score (Figure 6D,E). Interestingly, iloprost treatment increased the fraction of neutrophils permanently located at a

thrombus, while fidelity was unchanged. Hence, it seemed that platelet silencing by iloprost reduced the presence at thrombi of neutrophil-activating substances, causing overall lower Ca^{2+} signaling and reduced movement to and from thrombi.

Regulation of neutrophil Ca^{2+} and chemotactic responses

Earlier studies indicated that activated platelets secrete and bind considerable amounts of the chemokines CXCL4 (platelet factor 4), CCL5 (RANTES) and CXCL7 (NAP-2).⁴⁴ For type III thrombi, the extracellular presence of CCL5 and CXCL7 could be confirmed by immuno-staining (Suppl. Fig 1B). We then investigated how these chemokines affected the neutrophil responses using a panel of blocking antibodies. Analysis of Ca^{2+} responses in individual cells indicated that the blockage of CCL5 or CXCL7, but not of CXCL4, resulted in an overall lower Ca^{2+} signal (Figure 7A,B). For CXCL7 blockage, this was accompanied by a significant reduction in neutrophils with permanent location at a given thrombus and a decreased fidelity (Figure 7C,D). For CCL5 blockage, there was a tendency to a decreased fidelity.

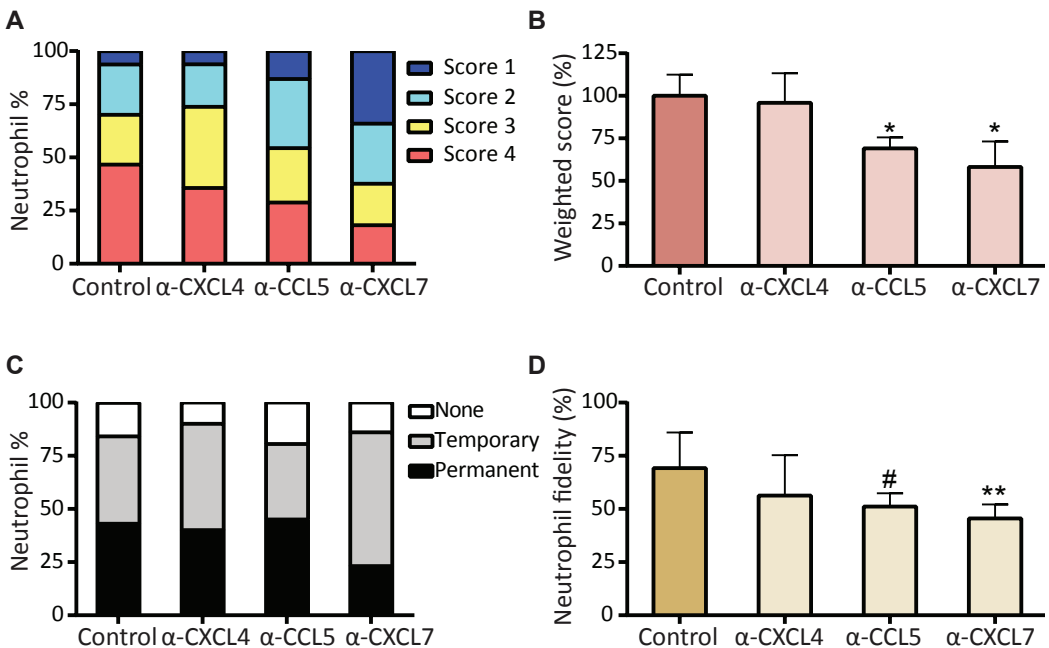


Figure 7. Blocking of platelet-secreted chemokines and effects on neutrophil responses. Type III thrombi were formed, as described for Fig. 1, followed by 2-min perfusion with control IgG (vehicle) or blocking antibody against CXCL4, CCL5 or CXCL7 (1 mg/ml). Calcium fluxes and chemotactic responses were monitored for 10 min in single Fluo-4-loaded neutrophils by combined brightfield and fluorescence microscopy recordings. **A-B**) Distribution profile of neutrophils with different Ca^{2+} scores, and calculated weighted Ca^{2+} score. **C-D**) Quantification of neutrophil micro-location and fidelity for a certain thrombus. Means \pm s.e. (n=3-4). * $P < 0.05$, ** $P < 0.01$ vs. control.

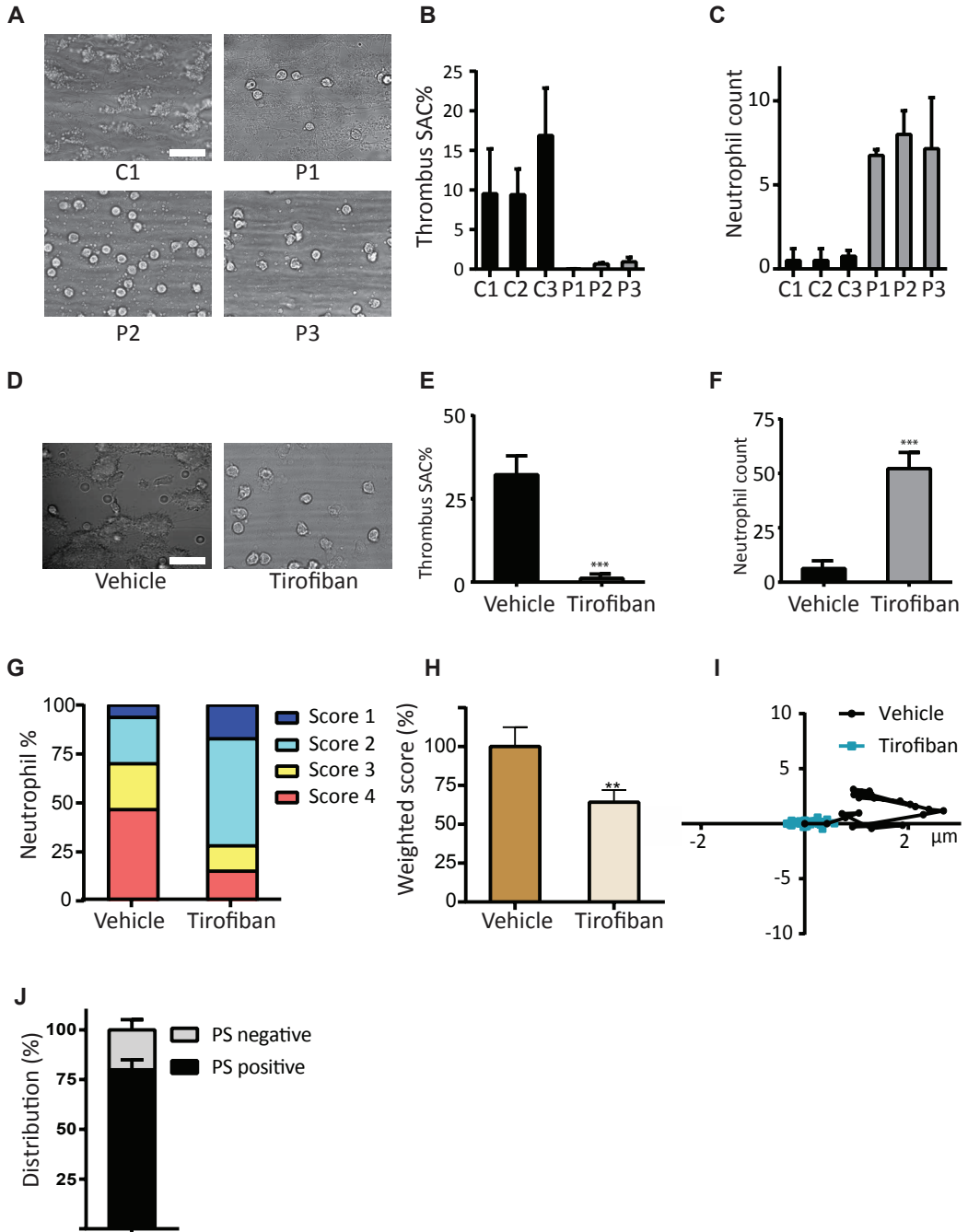


Figure 8. Regulatory role of platelet integrin $\alpha_{IIb}\beta_3$ on neutrophil responses in thrombus formation. A-C) Whole blood from three control subjects (C1-3) and three patients with Glanzmann thrombasthenia (P1-3, with complete deficiency in platelet integrin $\alpha_{IIb}\beta_3$ expression) was flowed over collagen at 1000 s^{-1} . After 4 min of flow (no stasis), brightfield and fluorescence images were captured to characterize thrombi

and neutrophils. Shown are representative images (bar, 25 μm) (A), thrombus surface area coverage (SAC%) (B) and neutrophil counts per field (C). D-I) Control whole-blood containing vehicle or tirofiban (1 $\mu\text{g}/\text{ml}$) was flowed over collagen under conditions of type III thrombus formation, and responses of Fluor-4-loaded neutrophils were monitored. D) Representative brightfield images showing effects of integrin blockage (tirofiban pre-added to the blood) on platelet aggregation and neutrophil abundance (bar, 25 μm). Quantification of thrombus surface area coverage (E) and neutrophil counts (F) with(out) tirofiban treatment. In addition, distribution of neutrophils with different Ca^{2+} scores (G), and calculated weighted Ca^{2+} scores (H). Neutrophils' directionality with(out) tirofiban (I). J) Type III thrombi were stained for PS exposure (FITC annexin A5) and neutrophils interacting with PS-exposing platelets were quantified. Means \pm S.D. (n=3). *P<0.05, **P<0.01 vs. control or vehicle.

Regulation of neutrophil Ca^{2+} and chemotactic responses

Earlier studies indicated that activated platelets secrete and bind considerable amounts of the chemokines CXCL4 (platelet factor 4), CCL5 (RANTES) and CXCL7 (NAP-2).⁴⁴ For type III thrombi, the extracellular presence of CCL5 and CXCL7 could be confirmed by immuno-staining (Suppl. Fig 1B). We then investigated how these chemokines affected the neutrophil responses using a panel of blocking antibodies. Analysis of Ca^{2+} responses in individual cells indicated that the blockage of CCL5 or CXCL7, but not of CXCL4, resulted in an overall lower Ca^{2+} signal (Figure 7A,B). For CXCL7 blockage, this was accompanied by a significant reduction in neutrophils with permanent location at a given thrombus and a decreased fidelity (Figure 7C,D). For CCL5 blockage, there was a tendency to a decreased fidelity.

Human platelets express high 12-lipoxygenase (LOX) activity,⁴⁵ thereby producing the bioactive products 12-HETE and 12-HPETE, which mediators have been shown to stimulate Ca^{2+} release in neutrophils.⁴⁶ To investigate the role of 12-LOX in the present setting, type III thrombi were post-treated with the selective 12-LOX inhibitor, NCTT-956⁴⁷, after which the Ca^{2+} signals in adherent neutrophils were measured. This treatment resulted in a consistent lowering of neutrophils with calcium score 4, along with a significantly reduced weighted score (Suppl. Figure 2A,B). While NCTT-956 treatment of platelets reduced the number of adhered neutrophils, their micro-location and thrombus fidelity remained unchanged (Suppl. Figure 2C-E). In contrast, inhibition of platelet cyclooxygenase by post-treatment of thrombi with indomethacin did not influence the neutrophil Ca^{2+} signals or movement (not shown). Further proof of a role for 12-LOX came from experiments with blood from *Alox12^{-/-}* mice (deficient in 12-LOX), which again resulted in a diminished adhesion of neutrophils (characterized by high Ly6G expression) to thrombi, when compared to wildtype blood (Suppl. Figure 2F,H). In terms of location, the neutrophils showed a trend to be more in permanent contact with the *Alox12^{-/-}* thrombi (Suppl. Figure 2G).

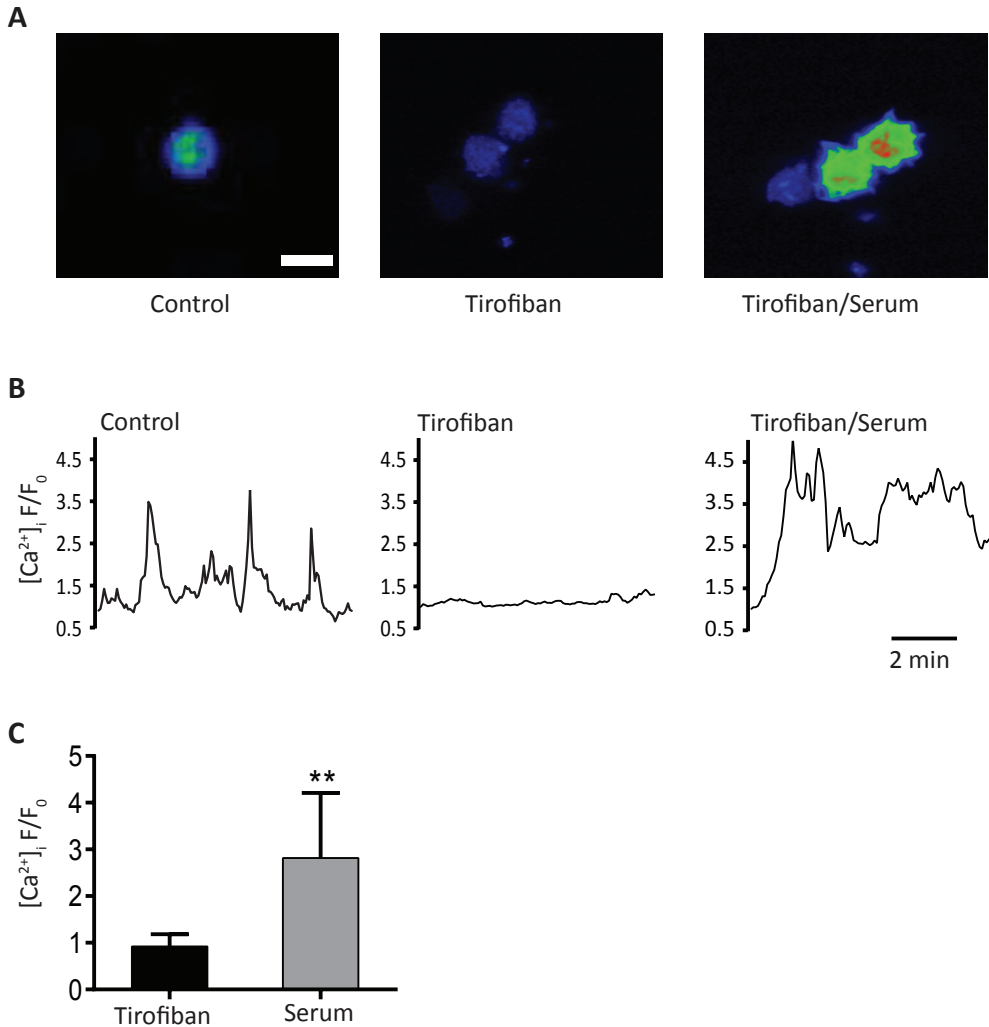


Figure 9. Platelet-derived substances overrule the inhibitory effect of platelet integrin $\alpha_{IIb}\beta_3$. Platelet thrombi formed in the presence of tirofiban (Fig. 8), containing Fluo-4-loaded neutrophils, were post-perfused with buffer medium or autologous serum (10 min, 200 s^{-1}). Shown are (A) representative fluorescence images (bar, $50\ \mu\text{m}$), (B) representative Ca^{2+} transients of single neutrophils, (C) quantification of rises in neutrophil $[Ca^{2+}]_i$. Means \pm S.D. ($n=3$). ** $P<0.01$ vs. tirofiban.

Platelet integrin $\alpha_{IIb}\beta_3$ activation suppresses neutrophil adhesion under flow

In screening studies using blood from three unrelated patients with Glanzmann thrombasthenia, characterized by the absence on platelets of integrin $\alpha_{IIb}\beta_3$.⁴⁸ Here, a marked increase was seen in neutrophil attachment during thrombus build-up on collagen, in the presence of high-shear blood flow (1000 s^{-1}). Thus, while flowing blood from control subjects, multilayered thrombi with aggregated platelets formed that were

devoid of neutrophils. However, when using blood from the Glanzmann patients, a single layer of activated platelets formed that attracted a large fraction of the flowing neutrophils (Figure 8A-C).

To further explore the role of integrin $\alpha_{\text{IIb}}\beta_3$ in platelet-neutrophil interactions, blood from control subjects was treated with the (clinically used) integrin inhibitor tirofiban, and flowed over collagen while forming type III thrombi. Tirofiban treatment prevented platelet aggregation, but a dramatic increase in neutrophil count due to the single layer of activated platelets was seen of flow (Figure 8D-F). Analysis of the Ca^{2+} fluxes in the adhered neutrophils with tirofiban demonstrated a markedly low Ca^{2+} signal and score, when compared to the controls (Figure 8G,H). In addition, the blockage of $\alpha_{\text{IIb}}\beta_3$ markedly reduced the movement of adhered neutrophils (Figure 8I).

Considering that procoagulant, PS-exposing platelets are characterized by $\alpha_{\text{IIb}}\beta_3$ inactivation,⁴⁹ we examined if these platelets in a thrombus preferentially interact with neutrophils. Labeling studies using FITC-annexin A5 indeed indicated that the majority of neutrophils in thrombi were in contact with PS-exposing platelets (Figure 8J). This is in agreement with an earlier finding showing platelet factor 4 (CXCL4) release by PS-exposing platelets to explain neutrophil interactions,²¹ and it further supports the inhibitory role of $\alpha_{\text{IIb}}\beta_3$ in platelet-neutrophil contacts.

We hypothesized that, in the presence of tirofiban, the absence of platelet accumulation into aggregates limits the release of neutrophil-activating substances, thus explaining the low Ca^{2+} signals. To evaluate this, Fluo-4-loaded neutrophils on thrombi generated in the presence of tirofiban were post-perfused with freshly prepared autologous serum – highly enriched in platelet secretion products. This greatly increased the Ca^{2+} signals in the neutrophils (Figure 9A-C).

Discussion

In the present paper, we determined the interactions and responses of autologous human neutrophils with thrombi formed under flow by platelets. The data show that thrombi consisting of platelets with a high activation state -i.e. continuously secreting platelets- most effectively direct neutrophil attachment, micro-location and activation responses. Strikingly, regardless of the type of thrombus and the extent of platelet activation, neutrophils incidentally formed NETs in a time interval for up to 16 h. In initial papers, NETs were considered as a mechanism of neutrophils for scavenging bacteria as in sepsis.^{50,51} It has been suggested that platelets can induce NET formation via CD62P expression²⁸ or Toll-like receptors,^{51,52} and furthermore that platelets may have a role in

NET formation in animal models of deep venous thrombosis.^{8,53} However, our findings indicate that additional factors than activated platelets alone need to be present to stimulate NET formation in activated neutrophils.

A new finding was that the neutrophils in thrombi formed on a collagen surface contribute to the degradation of collagen fibers and can internalize the degraded collagen fragments. This extends earlier reports that activated neutrophils as well as platelets secrete collagen-degrading MMP isoforms, in case of the neutrophils supposedly supported by CD62P-PSGL-1 interactions.^{12,54} In addition, the results are compatible with the recognition that collagen matrix degradation via MMPs is critical for neutrophil extravasation.²⁷

As active secretory cells, neutrophils rely for their responsiveness on agonist-induced $[Ca^{2+}]_i$ rises, mediated by the process of store-operated Ca^{2+} entry.³⁴ The neutrophil chemokine receptors, in particular CXCR2, are considered to mediate such Ca^{2+} responses,⁵⁵ with as a consequence degranulation.^{32,36} Pharmacological intervention experiments indicated clear roles of platelet-released CXCL7 and CCL5, but not of CXCL4, on neutrophil Ca^{2+} fluxes and hence activation. This is in accordance with earlier work describing a reducing rather than stimulating effect of CXCL4 on neutrophil apoptosis.¹⁸ Furthermore, a role of CCL5 agrees with published effects of this chemokine on neutrophil activation under conditions of chronic obstructive pulmonary disease or experimental colitis.^{56,57} The chemokine CXCL7, acting via the receptors CXCR1/2, has been shown to promote directional intravascular leukocyte migration through platelet thrombi,¹⁹ which is in accordance with its identified contribution to neutrophil Ca^{2+} fluxes.

In mouse models, a role of the platelet thrombin receptors have been postulated in the trafficking of leukocytes towards sites of vascular injury, with a negative regulation by GPIIb and fibrin.⁵⁸ Integrin $\alpha_{IIb}\beta_3$ as a fibrin receptor⁵⁹ was not investigated. Our results with human platelets and neutrophils extend this work with the concept emerging that activated $\alpha_{IIb}\beta_3$ acts as a check-point mechanism determining the interactions of neutrophils with a thrombus under flow, in the development of thrombo-inflammatory disorders. Our data point to a promotion of neutrophil incorporation by thrombin-induced platelet activation and a suppression by activated integrin $\alpha_{IIb}\beta_3$. This finding implies a difference between platelet integrins (inhibitory) and undisclosed neutrophil integrins (stimulatory)⁶⁰ in the recruitment of neutrophils to thrombotic wound sites.

Detailed comparison of the micro-location of neutrophils in and at thrombi, their crawling movements and Ca^{2+} fluxes pointed to a multifactorial regulation of platelet-neutrophil cross-talk under flow, with as contributing factors (Figure 10): (i) platelet

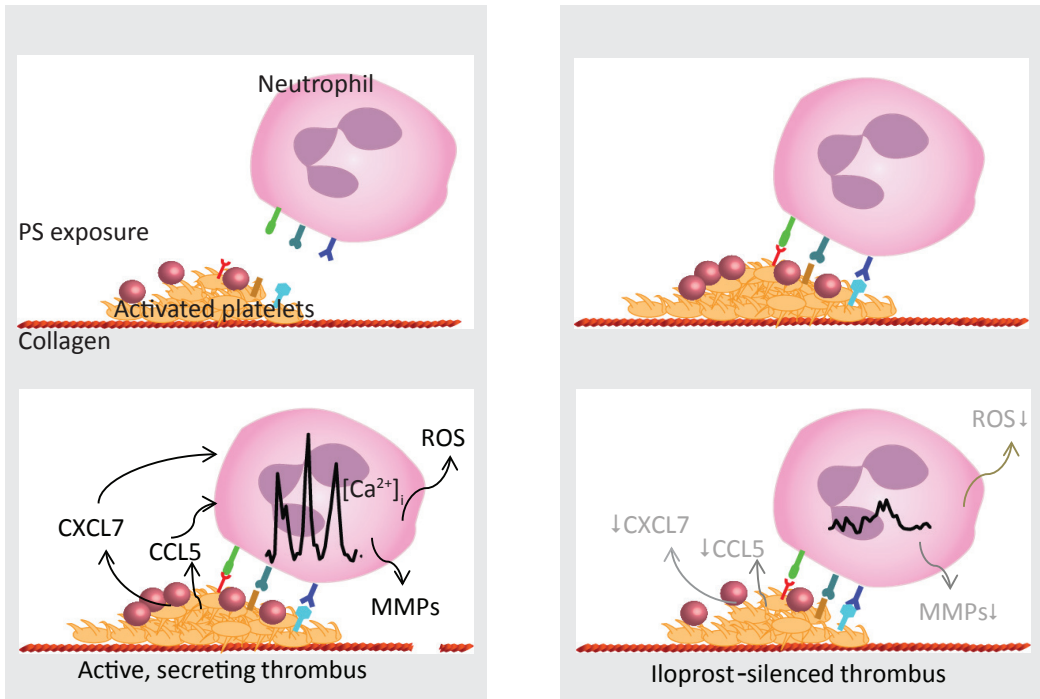


Figure 10. Model of phased platelet-dependent neutrophil activation on thrombi. For explanation, see text.

activation-dependent receptor expression controlling neutrophil adhesion (CD40L and CD62P acting stimulatory; activated $\alpha_{IIb}\beta_3$ acting inhibitory); (ii) persistent (thrombin-induced) secretion of platelet activation products (CCL5, CXCL7, LOX-12) triggering neutrophil $[Ca^{2+}]_i$ rises; (iii) heterogeneity in microthrombus structures influencing directional movement and fidelity (patches of aggregated and PS-exposing platelets).

Acknowledgements

Support for this work was obtained from the Cardiovascular Centre (HVC), Maastricht University Medical Centre⁺, the Interreg programme Euregio Meuse-Rhin (Polyvalve) (to MN, SLNB and JWMH), and the Center for Translational Molecular Medicine (Incoag/ Microbat to MN, JMEMC and JWMH), the Dutch Heart Foundation (2015T79 to JMEMC) and the Netherlands Organization for Scientific Research (NWO Vidi 91716421 to JMEMC).

Authors contributions

MN performed experiments, analyzed and interpreted data, wrote the manuscript. SLNB and SM performed experiments and analyzed data. JJB and VBO provided mice and revised the manuscript. RRK provided essential materials, contributed with ideas and revised the manuscript. FNA provided essential material. KJ recruited patients and revised manuscript. OS revised the manuscript. JMEMC designed the research, interpreted data and revised the manuscript. SPW contributed with ideas and revised manuscript. JWMH designed and coordinated the research, interpreted data and wrote the manuscript.

Conflicts of interest

JWMH is a co-founder and shareholder of FlowChamber. The other authors indicate that no relevant conflict of interest exists.

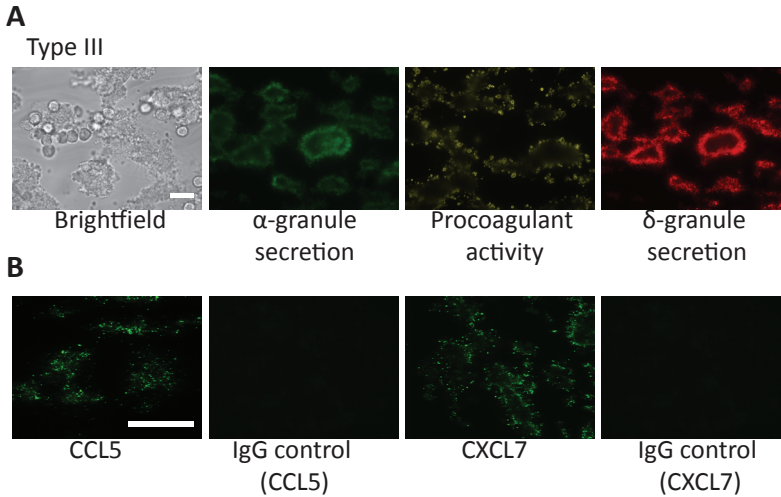
References

1. Deppermann C, Kubes P. Start a fire, kill the bug: The role of platelets in inflammation and infection. *Innate Immun.* 2018; 24: 335-348.
2. Ley K, Hoffman HM, Kubes P, *et al.* Neutrophils: new insights and open questions. *Sci. Immunol.* 2018; 3: eaat4579.
3. Zarbock A, Polanowska-Grabowska RK, Ley K. Platelet-neutrophil-interactions: linking hemostasis and inflammation. *Blood Rev.* 2007; 21: 99-111.
4. Gawaz M, Langer H, May AE. Platelets in inflammation and atherogenesis. *J. Clin. Invest.* 2005; 115: 3378-3384.
5. Mastenbroek TG, van Geffen JP, Heemskerk JW, Cosemans JM. Acute and persistent platelet and coagulant activities in atherothrombosis. *J. Thromb. Haemost.* 2015; 13 (Suppl. 1): S272-280.
6. Darbousset R, Thomas GM, Mezouar S, *et al.* Tissue factor-positive neutrophils bind to injured endothelial wall and initiate thrombus formation. *Blood.* 2012; 120: 2133-2143.
7. Naruko T, Ueda M, Haze K, *et al.* Neutrophil infiltration of culprit lesions in acute coronary syndromes. *Circulation.* 2002; 106: 2894-2900.
8. Fuchs TA, Brill A, Duerschmied D, *et al.* Extracellular DNA traps promote thrombosis. *Proc. Natl. Acad. Sci. USA.* 2010; 107: 15880-15885.
9. Von Bruhl ML, Stark K, Steinhart A, *et al.* Monocytes, neutrophils, and platelets cooperate to initiate and propagate venous thrombosis in mice in vivo. *J. Exp. Med.* 2012; 209: 819-835.
10. Silvestre-Roig C, Braster Q, Wichapong K, *et al.* Externalized histone H4 orchestrates chronic inflammation by inducing lytic cell death. *Nature.* 2019; 569: 236-240.
11. Döring Y, Soehnlein O, Weber C. Neutrophil extracellular traps in atherosclerosis and atherothrombosis. *Circ. Res.* 2017; 120: 736-743.
12. Abou-Saleh H, Theoret JF, Yacoub D, Merhi Y. Neutrophil P-selectin-glycoprotein-ligand-1 binding to platelet P-selectin enhances metalloproteinase 2 secretion and platelet-neutrophil aggregation. *Thromb. Haemost.* 2005; 94: 1230-1235.
13. Lievens D, Zerneck A, Seijkens T, *et al.* Platelet CD40L mediates thrombotic and inflammatory processes in atherosclerosis. *Blood.* 2010; 116: 4317-4327.
14. Gerdes N, Seijkens T, Lievens D, *et al.* Platelet CD40 exacerbates atherosclerosis by transcellular activation of endothelial cells and leukocytes. *Arterioscler. Thromb. Vasc. Biol.* 2016; 36: 482-490.
15. Wang Y, Sakuma M, Chen Z, *et al.* Leukocyte engagement of platelet glycoprotein Iba via the integrin Mac-1 is critical for the biological response to vascular injury. *Circulation.* 2005; 112: 2993-3000.
16. Santoso S, Sachs UJ, Kroll H, *et al.* The junctional adhesion molecule 3 (JAM-3) on human platelets is a counterreceptor for the leukocyte integrin Mac-1. *J. Exp. Med.* 2002; 196: 679-691.
17. Sreeramkumar V, Adrover JM, Ballesteros I, *et al.* Neutrophils scan for activated platelets to initiate

- inflammation. *Science*. 2014; 346: 1234-1238.
18. Hartwig H, Drechsler M, Lievens D, *et al*. Platelet-derived PF4 reduces neutrophil apoptosis following arterial occlusion. *Thromb. Haemost.* 2014; 111: 562-564.
 19. Ghasemzadeh M, Kaplan ZS, Alwis I, *et al*. The CXCR1/2 ligand NAP-2 promotes directed intravascular leukocyte migration through platelet thrombi. *Blood*. 2013; 121: 4555-4566.
 20. Koenen RR, von Hundelshausen P, Nesmelova IV, *et al*. Disrupting functional interactions between platelet chemokines inhibits atherosclerosis in hyperlipidemic mice. *Nat. Med.* 2009; 15: 97-103.
 21. Kulkarni S, Woollard KJ, Thomas S, Oxley D, Jackson SP. Conversion of platelets from a proaggregatory to a proinflammatory adhesive phenotype: role of PAF in spatially regulating neutrophil adhesion and spreading. *Blood*. 2007; 110: 1879-1886.
 22. Haselmayer P, Grosse-Hovest L, von Landenberg P, Schild H, Radsak MP. TREM-1 ligand expression on platelets enhances neutrophil activation. *Blood*. 2007; 110: 1029-1035.
 23. Ghasemzadeh M, Hosseini E. Intravascular leukocyte migration through platelet thrombi: directing leukocytes to sites of vascular injury. *Thromb. Haemost.* 2015; 113: 1224-1235.
 24. Munnix IC, Strehl A, Kuijpers MJ, *et al*. The glycoprotein VI-phospholipase Cy2 signaling pathway controls thrombus formation induced by collagen and tissue factor in vitro and in vivo. *Arterioscler. Thromb. Vasc. Biol.* 2005; 25: 2673-2678.
 25. Cosemans JM, Mattheij NJ, Angelillo-Scherrer A, Heemskerk JW. The effects of arterial flow on platelet activation, thrombus growth and stabilization. *Cardiovasc. Res.* 2013; 99: 342-352.
 26. Versteeg HH, Heemskerk JW, Levi M, Reitsma PS. New fundamentals in hemostasis. *Physiol. Rev.* 2013; 93: 327-358.
 27. Lerchenberger M, Uhl B, Stark K, *et al*. Matrix metalloproteinases modulate ameboid-like migration of neutrophils through inflamed interstitial tissue. *Blood*. 2013; 122: 770-780.
 28. Etulain J, Martinod K, Wong SL, *et al*. P-selectin promotes neutrophil extracellular trap formation in mice. *Blood*. 2015; 126: 242-246.
 29. Rossaint J, Herter JM, Van Aken H, *et al*. Synchronized integrin engagement and chemokine activation is crucial in neutrophil extracellular trap-mediated sterile inflammation. *Blood*. 2014; 123: 2573-2584.
 30. Metzler KD, Fuchs TA, Nauseef WM, *et al*. Myeloperoxidase is required for neutrophil extracellular trap formation: implications for innate immunity. *Blood*. 2011; 117: 953-959.
 31. Papayannopoulos V, Metzler KD, Hakkim A, Zychlinsky A. Neutrophil elastase and myeloperoxidase regulate the formation of neutrophil extracellular traps. *J. Cell Biol.* 2010; 191: 677-691.
 32. Sage SO, Pintado E, Mahaut-Smith MP, Merritt JE. Rapid kinetics of agonist-evoked changes in cytosolic free Ca²⁺ concentration in Fura-2-loaded human neutrophils. *Biochem. J.* 1990; 265: 915-918.
 33. Salmon MD, Ahluwalia J. Discrimination between receptor- and store-operated Ca²⁺ influx in human neutrophils. *Cell. Immunol.* 2010; 265: 1-5.
 34. Mammadova-Bach E, Nagy M, Heemskerk JW, Nieswandt N, Braun A. Store-operated calcium entry in blood cells in thrombo-inflammation *Cell Calcium*. 2019; 77: 39-48.
 35. Lawson MA, Maxfield FR. Ca²⁺- and calcineurin-dependent recycling of an integrin to the front of migrating neutrophils. *Nature*. 1995; 377: 75-79.
 36. Richter J, Olsson I, Andersson T. Correlation between spontaneous oscillations of cytosolic free Ca²⁺ and tumor necrosis factor-induced degranulation in adherent human neutrophils. *J. Biol. Chem.* 1990; 265: 14358-14363.
 37. Kuijpers MJ, Mattheij NJ, Cipolla L, *et al*. Platelet CD40L modulates thrombus growth via phosphatidylinositol 3-kinase β , and not via CD40 and I κ B kinase α . *Arterioscler. Thromb. Vasc. Biol.* 2015; 35: 1374-1381.
 38. Cosemans JM, Munnix IC, Wetzker R, *et al*. Continuous signaling via phosphoinositide 3-kinase isoforms β and γ is required for platelet ADP receptor function in dynamic thrombus stabilization. *Blood*. 2006; 108: 3045-3052.
 39. Carestia A, Kaufman T, Schattner M. Platelets: New bricks in the building of neutrophil extracellular traps. *Front Immunol.* 2016; 7: 271.
 40. Forsman H, Dahlgren C. The FPR2-induced rise in cytosolic calcium in human neutrophils relies on an emptying of intracellular calcium stores and is inhibited by a gelsolin-derived PIP2-binding peptide. *BMC Cell Biol.* 2010; 11: 52.
 41. Bednar F, Song C, Bardi G, Cornwell W, Rogers TJ. Cross-desensitization of CCR1, but not CCR2, following activation of the formyl peptide receptor FPR1. *J. Immunol.* 2014; 192: 5305-5313.
 42. Mastenbroek TG, Feijge MA, Kremers RM, *et al*. Platelet-associated matrix metalloproteinases regulate thrombus formation and exert local collagenolytic activity. *Arterioscler. Thromb. Vasc. Biol.* 2015; 35: 2554-2561.

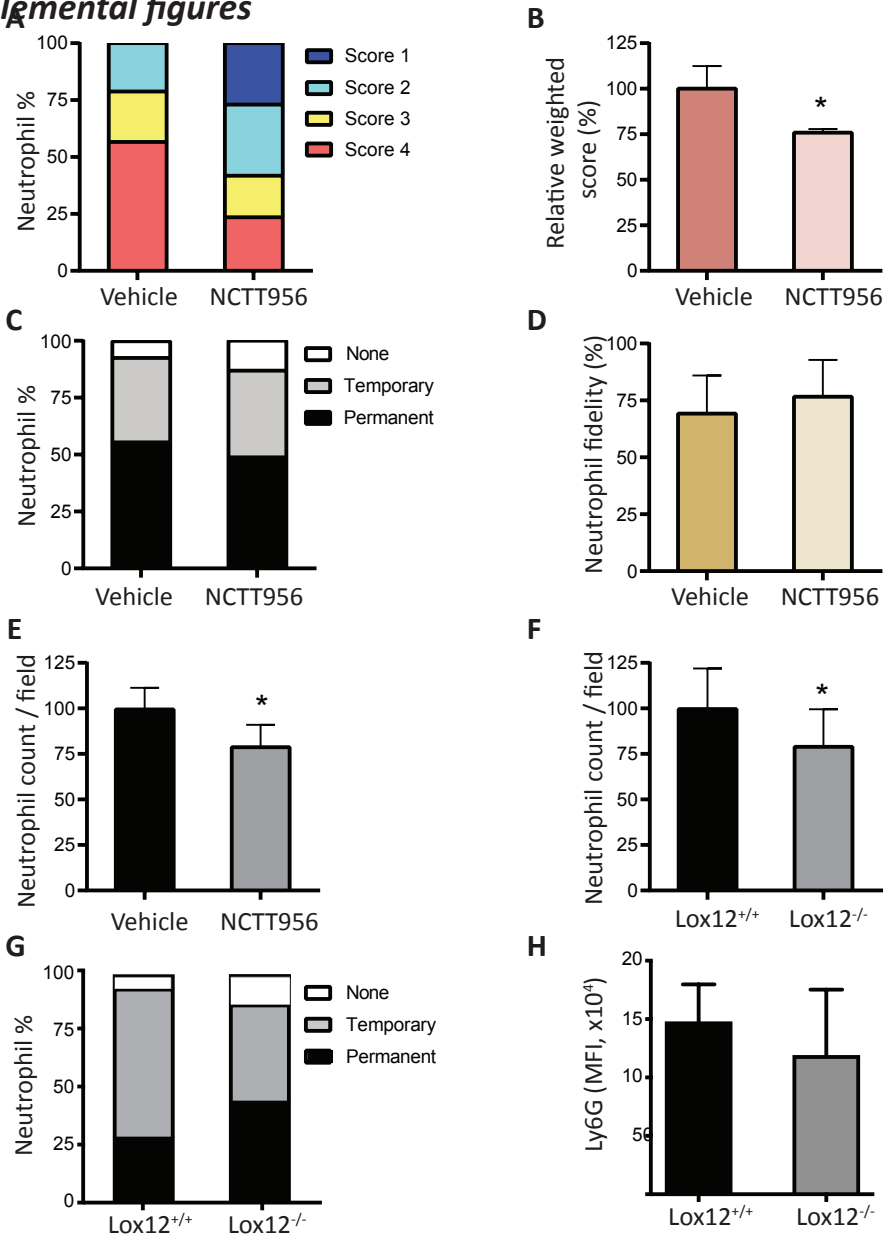
43. Golebiewska EM, Poole AW. Platelet secretion: From haemostasis to wound healing and beyond. *Blood Rev.* 2015; 29: 153-162.
44. Von Hundelshausen P, Schmitt MM. Platelets and their chemokines in atherosclerosis-clinical applications. *Front. Physiol.* 2014; 5: 294.
45. Morgan LT, Thomas CP, Kühn H, O'Donnell VB. Thrombin-activated human platelets acutely generate oxidized docosahexaenoic-acid-containing phospholipids via 12-lipoxygenase. *Biochem. J.* 2010; 431: 141-148.
46. Reynaud D, Pace-Asciak CR. 12-HETE and 12-HPETE potently stimulate intracellular release of calcium in intact human neutrophils. *Prostaglandins Leukot. Essent. Fatty Acids.* 1997; 56: 9-12.
47. Yeung J, Apopa PL, Vesci J, et al. Protein kinase C regulation of 12-lipoxygenase-mediated human platelet activation. *Mol Pharmacol.* 2012; 81: 420-430.
48. Van Geffen JP, Brouns S, Batista J, et al. High-throughput elucidation of thrombus formation reveals sources of platelet function variability. *Haematologica.* 2019; in press.
49. Mattheij NJ, Gilio K, van Kruchten R, et al. Dual mechanism of integrin $\alpha_{IIb}\beta_3$ closure in procoagulant platelets. *J Biol Chem.* 2013; 288: 13325-13336.
50. Brinkmann V, Reichard U, Goosmann C, et al. Neutrophil extracellular traps kill bacteria. *Science.* 2004; 303: 1532-1535.
51. Clark SR, Ma AC, Tavener SA, et al. Platelet TLR4 activates neutrophil extracellular traps to ensnare bacteria in septic blood. *Nat. Med.* 2007; 13: 463-469.
52. Caudrillier A, Kessenbrock K, Gilliss BM, et al. Platelets induce neutrophil extracellular traps in transfusion-related acute lung injury. *J. Clin. Invest.* 2012; 122: 2661-2671.
53. Brill A, Fuchs TA, Savchenko AS, et al. Neutrophil extracellular traps promote deep vein thrombosis in mice. *J. Thromb. Haemost.* 2012; 10: 136-144.
54. Owen CA, Hu Z, Lopez-Otin C, Shapiro SD. Membrane-bound matrix metalloproteinase-8 on activated polymorphonuclear cells is a potent, tissue inhibitor of metalloproteinase-resistant collagenase and serpinase. *J. Immunol.* 2004; 172: 7791-7803.
55. Kuwano Y, Adler M, Zhang H, Groisman A, Ley K. Gai2 and Gai3 differentially regulate arrest from flow and chemotaxis in mouse neutrophils. *J. Immunol.* 2016; 196: 3828-3833.
56. Yu C, Zhang S, Wang Y, et al. Platelet-derived CCL5 regulates CXC chemokine formation and neutrophil recruitment in acute experimental colitis. *J Cell Physiol.* 2016; 231: 370-376.
57. Di Stefano A, Caramori G, Gnemmi I, et al. Association of increased CCL5 and CXCL7 chemokine expression with neutrophil activation in severe stable COPD. *Thorax.* 2009; 64: 968-975.
58. Kaplan ZS, Zarpellon A, Alwis I, et al. Thrombin-dependent intravascular leukocyte trafficking regulated by fibrin and the platelet receptors GPIb and PAR4. *Nat. Commun.* 2015; 6: 7835.
59. Mattheij NJ, Swieringa F, Mastenbroek TG, et al. Coated platelets function in platelet-dependent fibrin formation via integrin $\alpha_{IIb}\beta_3$ and transglutaminase factor XIII. *Haematologica.* 2016; 101: 427-436.
60. Lämmermann T, Afonso PV, Angermann BR, et al. Neutrophil swarms require LTB4 and integrins at sites of cell death in vivo. *Nature.* 2013; 498.
61. Gilio K, Munnix IC, Mangin P, et al. Non-redundant roles of phosphoinositide 3-kinase isoforms a and b in glycoprotein VI-induced platelet signaling and thrombus formation. *J. Biol. Chem.* 2009; 285: 33750-33762.
62. Van Kruchten R, Cosemans JM, Heemskerk JW. Measurement of whole blood thrombus formation using parallel-plate flow chambers: a practical guide. *Platelets.* 2012; 23: 229-242.
63. Swieringa F, Kuijpers MJ, Lamers MM, van der Meijden PE, Heemskerk JW. Rate-limiting roles of tenase complex of factors VIII and IX in platelet procoagulant activity and formation of platelet-fibrin thrombi under flow. *Haematologica.* 2015; 100: 748-756.
64. De Witt SM, Lamers MM, Swieringa F, et al. Identification of platelet function defects by multi-parameter assessment of thrombus formation. *Nat. Commun.* 2014; 5: 4257.
65. Westein E, van der Meer AD, Kuijpers MJ, et al. Atherosclerotic geometries spatially confine and exacerbate pathological thrombus formation poststenosis in a von Willebrand factor-dependent manner. *Proc. Natl. Acad. Sci. USA.* 2013; 110: 1357-1362.

Supplemental figures



Suppl. Figure 1. Activation state and chemokine expression of platelets in type III thrombi. Whole blood was flowed over collagen at 1000 s^{-1} for 4 min to induce formation of type III thrombi as in Fig. 1. **A)** Representative brightfield and confocal fluorescence images (overlays), staining for secretion of α -granules (FITC anti-CD62P mAb), secretion of δ -granules (AF647 anti-CD63 mAb), and for PS exposure (AF568-annexin A5). Note distinction between aggregated platelets with high granule secretion and single PS-exposing platelets, concentrated around edges of the aggregates. **B)** Representative confocal fluorescence images after staining of thrombi for released CCL5 or CXCL7, and control staining with irrelevant IgG ($n=3$). Bars = $25 \mu\text{m}$.

Supplemental figures



Suppl. Figure 2. Blocking of platelet lipoxygenase-12 affects neutrophil responses. A-E) Type III thrombi were formed and post-treated with vehicle or lipoxygenase-12 inhibitor, NCCT-956 (10 mM). Fluo-4-loaded neutrophils on thrombi were imaged by brightfield and confocal fluorescence microscopy during 10 min. A-B) Distribution profiles of neutrophils with different Ca²⁺ scores and calculated weighted Ca²⁺ score. C-E) Quantification of neutrophils per field, of neutrophil micro-location and of fidelity upon NCCT-956 treatment. Means \pm S.E. (n=3-4), *P<0.05, **P<0.01 vs. vehicle. F-G) Blood from *Lox12*^{-/-} and corresponding *Lox12*^{+/+} mice was flowed over collagen to form type III thrombi, and interaction of neutrophils (staining for Ly6g) was monitored for 10 min. Quantification of neutrophils per field (F), of neutrophil micro-location (G) and of Ly6g fluorescence intensity (H). Means \pm S.E. (n=3).

Chapter 6

Comparative analysis of microfluidics thrombus formation in multiple genetically modified mice: link to thrombosis and hemostasis

Nagy M, van Geffen JP, Stegner D, Adams DJ, Braun A, de Witt SM, Elvers M, Geer MJ, Kuijpers MJE, Kunzelmann K, Mori J, Oury C, Pircher J, Pleines I, Poole AW, Senis YA, Verdoold R, Weber C, Nieswandt B, Heemskerk JWM, Baaten CCFMJ

*Frontiers in Cardiovascular Medicine 2019; 6:99
Reprinted with permission*

Abstract

Genetically modified mice are indispensable for establishing the roles of platelets in arterial thrombosis and hemostasis. Microfluidics assays using anticoagulated whole blood are commonly used as integrative proxy tests for platelet function in mice. In the present study, we quantified the changes in collagen-dependent thrombus formation for 38 different strains of (genetically) modified mice, all measured with the same microfluidics chamber. The mice included were deficient in platelet receptors, protein kinases or phosphatases, small GTPases or other signaling or scaffold proteins. By standardized re-analysis of high-resolution microscopic images, detailed information was obtained on altered platelet adhesion, aggregation and/or activation. For a subset of 11 mouse strains, these platelet functions were further evaluated in rhodocytin- and laminin-dependent thrombus formation, thus allowing a comparison of glycoprotein VI (GPVI), C-type lectin-like receptor 2 (CLEC2) and integrin $\alpha_6\beta_1$ pathways. High homogeneity was found between wild-type mice datasets concerning adhesion and aggregation parameters. Quantitative comparison for the 38 modified mouse strains resulted in a matrix visualizing the impact of the respective (genetic) deficiency on thrombus formation with detailed insight into the type and extent of altered thrombus signatures. Network analysis revealed strong clusters of genes involved in GPVI signaling and Ca^{2+} homeostasis. The majority of mice demonstrating an antithrombotic phenotype *in vivo* displayed with a larger or smaller reduction in multi-parameter analysis of collagen-dependent thrombus formation *in vitro*. Remarkably, in only approximately half of the mouse strains that displayed reduced arterial thrombosis *in vivo*, this was accompanied by impaired hemostasis. This was also reflected by comparing *in vitro* thrombus formation (by microfluidics) with alterations *in vivo* bleeding time.

In conclusion, the presently developed multi-parameter analysis of thrombus formation using microfluidics can be used to: (i) determine the severity of platelet abnormalities; (ii) distinguish between altered platelet adhesion, aggregation and activation; and (iii) elucidate both collagen and non-collagen dependent alterations of thrombus formation. This approach may thereby aid in the better understanding and better assessment of genetic variation that affect *in vivo* arterial thrombosis and hemostasis.

Introduction

Current concepts of platelet activation pathways in thrombosis and hemostasis rely to a large extent on the summation of single observations. Frequently, the role of a particular protein or signaling pathway is deduced from the consequences of a genetic knockout in mice on platelet responses, such as in comparison to changes in experimental arterial thrombosis and tail bleeding. A large set of such studies has resulted in the concept of collagen-induced arterial thrombus formation.¹⁻⁴ Herein, it is stipulated that the exposure of subendothelial collagen to flowing blood is a key trigger to start shear-dependent thrombus formation. Collagen causes platelet adhesion and furthermore binds von Willebrand factor (VWF), which can decelerate flowing platelets at high shear rate. Firm VWF/collagen-mediated adhesion and subsequent platelet activation requires synergy between the VWF receptor, glycoprotein (GP)Ib-V-IX, and the collagen receptors, GPVI and integrin $\alpha_2\beta_1$.⁵⁻⁸

Collagen is known to induce a number of stimulating pathways via GPVI, in particular: (i) activation of Src-family and Syk tyrosine kinases, resulting in phospholipase C (PLC) γ 2 activation and intracellular Ca^{2+} mobilization;^{2,9} (ii) additional Ca^{2+} influx via ORAI1 channels which couple to the calcium sensor STIM1 in the reticular membrane;¹⁰ (iii) activation of several isoforms of protein kinase C (PKC),¹¹ phosphoinositide 3-kinases (PI3K),¹² and small GTPases, the latter including CDC42, RAC1 and RHOA.¹³ Additional modifying signaling pathways include: (iv) activation of phospholipase D, augmenting flow-dependent platelet activation;¹⁴ and (v) activation of multiple (tyrosine) phosphatases, a part of which act downstream of immunoreceptor tyrosine-based inhibition motif (ITIM)-containing receptors. Such phosphatases can have a direct or indirect platelet-stimulating (*e.g.* CD148, DUSP) or a platelet-inhibiting effect (PECAM1, G6b-B) in response to collagen.¹⁵ Together, these signaling routes co-operate to control the activation state of the platelet fibrinogen receptor, integrin $\alpha_{IIb}\beta_3$, the secretion of granular contents, and the release of thromboxane- A_2 . Locally secreted or generated soluble agonists, acting via G-protein coupled receptors (GPCR) ensure the capture and incorporation of passing platelets into an aggregate or thrombus.²⁻⁴ In a subset of platelets in the thrombus, procoagulant activity is generated by Ca^{2+} -dependent activation of the anoctamin-6 (TMEM16F) channel,¹⁶ regulating phosphatidylserine (PS) exposure and platelet ballooning.¹⁷⁻¹⁹

Although all these signaling components are known to play a certain role in collagen-dependent thrombus formation, there is still limited insight into the relative contribution of individual proteins. In addition, it is unclear to which extent C-type lectin-

like receptor-2 (CLEC2), another receptor that signals via tyrosine kinases,^{20,21} is capable to regulate the process of thrombus formation. The same holds for integrin $\alpha_6\beta_1$, an adhesive receptor, which mediates flow-dependent adhesion of platelets to the matrix protein laminin.²²

In a recent synthesis approach, a quantitative evaluation was made of the contribution of 431 mouse genes to experimental arterial thrombosis and hemostasis *in vivo*, thereby revealing several genes with a role in thrombosis without affecting bleeding.²³ For the total cohort of studies and mouse genes, it appeared that microfluidics assays where thrombus formation is measured *in vitro* – by whole blood perfusion over a collagen surface – predict the consequences of a gene knockout on thrombosis models *in vivo*.²³ However, the standard microfluidics tests only report on changes in platelet adhesion (surface-area-coverage, SAC%), which is a limitation given that the recorded microscopic images also contain information on platelet aggregate formation.^{4,25} In comparison, for human blood samples from a large cohort of healthy subjects, it could be shown that a multi-parameter image analysis can provide detailed information on the sub-processes of platelet adhesion, aggregation and activation at the same time.²⁶

To better understand the alterations in thrombus phenotypes using microfluidics, we applied a similar multi-parameter approach to quantitatively compare the effects of deficiency of 37 signaling proteins on collagen-induced pathways. We therefore re-analyzed earlier recorded microscopic images, in all cases from thrombi generated using the same microfluidics flow chamber setup.

Materials and methods

Mice

Mice were included from 38 strains, in each case with a monogenetic or antibody-induced deficiency, as well as 22 sets of corresponding wild-type or control mice, as described in the original publications (see Table 1). As a selection criterion for inclusion, microscopic images needed to be available from $n \geq 3$ animals per modified group and $n \geq 4$ for wild-types. Scaled effects on *in vivo* arterial thrombosis and tail bleeding are for the majority of strains described previously.²³

In all cases, mouse blood was collected into anticoagulant medium, consisting of PPACK (40 μ M), unfractionated heparin (5 U/ml) and low molecular weight heparin (fragmin, 50 U/ml). Samples were immediately processed. Experiments were approved by the local Animal Experimental Committees (see references in Table 1).

Whole blood thrombus formation under flow

For all data sets, thrombus formation in whole blood under flow was assessed with the Maastricht flow chamber (depth 50 μm , width 3 mm, length 30 mm).²⁴ In short, PPACK/heparin anticoagulated blood (400-500 μl) was perfused for 3.5-4.0 min at room temperature at a wall shear rate of 1000 s^{-1} (where indicated 1700 s^{-1}) over (i) Horm-type collagen (100 $\mu\text{g}/\text{ml}$, Nycomed Pharma, Munich, Germany), allowing platelet interaction via GPIb, GPVI and integrin $\alpha_2\beta_1$.

Where specified, two additional surfaces were used, similarly as described before:²⁴ (ii) VWF-binding peptide (VWF-BP, 12.5 $\mu\text{g}/\text{ml}$, obtained from Prof. Dr. R. Farndale, Cambridge University, UK) + laminin (50 $\mu\text{g}/\text{ml}$, from human plasma, Sigma-Aldrich, St. Louis MO, USA; binding integrin $\alpha_6\beta_1$)²², and (iii) VWF-BP + laminin + rhodocytin (250 $\mu\text{g}/\text{ml}$, activating CLEC2).²⁷ Rhodocytin purified from *Calloselasma rhodostoma*,²⁸ was a kind gift of Prof. Dr. K. Clemetson (Bern University, Switzerland).

After blood perfusion, platelet thrombi were rinsed with modified Tyrode's Hepes buffer (pH 7.45, 5 mM Hepes, 136 mM NaCl, 2.7 mM KCl, 0.42 mM NaH_2PO_4 , 1 mg/ml glucose, 1 mg/ml bovine serum albumin, 2 mM CaCl_2 , 2 mM MgCl_2 and 1 U/ml heparin), and then stained during 1.5 min flow with one to three fluorescently labeled platelet activation markers. These were: Alexa Fluor (AF)647 (or FITC) conjugated annexin A5 (AF647: 1:200, Invitrogen Life Technologies, Carlsbad, CA, USA/FITC: 1:1000, PharmaTarget, Maastricht, The Netherlands); FITC anti-mouse CD62P mAb (1:40, rat-anti-mouse, Emfret Analytics, Würzburg, Germany); and phycoerythrin (PE)-labeled JON/A mAb (1:20, Emfret Analytics); all diluted in modified Tyrode's Hepes buffer. Residual labels were removed by another perfusion for 2 min with label-free Tyrode's Hepes buffer. Multiple brightfield and (if applicable) fluorescence microscopic images were captured per surface, of which three representative images were re-analyzed in a systematic way.²⁶

For image recording, different fluorescence microscopic systems were used (see references in Table 1), but always containing a 60/63x oil objective and a sensitive CCD camera for capturing enhanced-contrast, brightfield images.

Microscopic image analysis

For all mouse strains, the recorded 16-bit or 8-bit brightfield and fluorescence images were re-analyzed using the same newly developed scripts (one per image type), written in Fiji.²⁹ Scripts always opened a series of images one-by-one with a loop. In each loop run, background illumination was corrected using a fast Fourier transform bandpass filter, followed by manual setting of a threshold and measurement of the surface area

coverage. For brightfield images, a series of Gray morphology conversions was applied to reduce striping and to improve the detection quality. Image conversion steps were as follows: a diamond large sized close, followed by a medium sized circle close and a small circle shaped dilate. Note that the first step increased the pixels that were stronger in regions with many neighboring pixels, the second step then rounded the shapes and additionally reduced straight lines, while the final step (allowing alteration by user-interface) served to obtain a best match with the original image. The Fourier transform filter served to flatten the background areas sufficiently for good analysis, with a minimal impact on the structures. For brightfield images, large structures were filtered down to 60 pixels, for the fluorescence images of annexin A5, integrin and P-selectin images large structures were filtered down to 65 pixels. Small structures were not filtered down, as these contained structures of interest within the adhered platelets (Figure S1).

Using these scripts and by visually scoring the unprocessed brightfield images, the following parameters of thrombus formation were obtained (Table 2): surface area coverage of adhered platelets ($P1$, %SAC); platelet aggregate coverage ($P2$, %SAC); thrombus morphology score ($P3$, scale 0-5); thrombus multilayer score ($P4$, scale 0-3); and thrombus contraction score ($P5$, scale 0-3). Scoring was performed in comparison to a set of predefined standard images (Figure S1). For the assessment of platelet activation, fluorescence images were analyzed for PS exposure ($P6$, %SAC), P-selectin expression ($P7$, %SAC) and integrin $\alpha_{IIb}\beta_3$ activation ($P8$, %SAC).²⁴

Regardless of the image type, parameter values from three images per experiment were averaged, thus resulting in a single value per parameter and experiment. The image analysis and scoring parameters were verified by different observers, who were blinded to the experimental condition. Parameters of experiments from the same mouse strain were combined as proxy measures of platelet adhesion ($P1$), thrombus signature ($P2-5$), and platelet activation ($P6-8$), as described before for human platelets.²⁶

Network analysis

A network of protein-protein interactions was built based on 37 investigated genes, using the STRING database,³⁰ taking into consideration the following settings: 1st shell interactors: <20 interactors, 2nd shell interactors: <60 interactors, confidence level: medium to high. Networks were visualized in Cytoscape version 3.7.0.³¹

Network clustering analysis was performed with the Cytoscape app, MCODE to identify highly interacting nodes using the following settings: degree cutoff: 2, node score cutoff: 0.2, K-core: 2 and maximum depth: 100.^{32,33}

Data processing and statistical analysis

For each genetically modified strain and corresponding wild-types, image data were averaged to obtain one parameter per surface, of which mean and SD values were calculated. For heatmap representation, mean values were univariate scaled from 0 to 10 per parameter.²⁴ Gene effect heatmaps were constructed by subtracting scaled average values of the wild-type (control) strain from those of the modified strain. For statistical evaluation, a filter was applied, considering changes outside the range of composite mean \pm SD as a relevant difference between modification and wild-type.²⁶ Heatmap data were visualized by (unsupervised hierarchical) cluster analysis using the program R.³⁴ For comparison of raw parameter values, a Kendall's tau-b correlation analysis was performed using SPSS (IBM SPSS version 24, Armonk, NY, USA).

Results

Microfluidics analysis of thrombus formation on collagen of multiple wild-type mouse datasets

Microscopic brightfield and (annexin A5 fluorescence) images were collected from earlier performed whole blood perfusion experiments with blood from 38 different strains of modified mice and 22 corresponding wild-types (Table 1). Included were experiments with strains (in majority published), that were judged to be of sufficiently high quality and power to allow re-analysis by newly developed image analysis scripts (Figure S1). From each experiment, five parameters of thrombus formation were obtained (Table 2). Platelet adhesion was quantified by the conventional analysis of platelet SAC% (P1). Thrombus signature (26) was composed of four parameters related to the thrombus buildup (Σ P2-5), *i.e.* platelet aggregate SAC% (P2), thrombus morphology score (P3), thrombus multilayer score (P4), and thrombus contraction score (P5). As far as available, platelet activation was assessed from fluorescence images of PS exposure (P6) (see Figure S1).

To establish the overall consistency of the combined databases of the whole blood experiments, we compared the mean values plus variation for each of the image analysis parameters P1-5 for the 22 wild-type control datasets. The calculated coefficients of variation of means across the wild-type datasets ranged from <12% (P3-5) to 23-25% (P1,2) (Table S1). For heatmap presentation, mean values for all wild-types (and corresponding transgenic animals) were univariate scaled from 0-10 (Figure 1A).

Table 1. Overview of re-analyzed data sets on thrombus formation using the Maastricht flow chamber. Shown are published changes in platelet deposition (SAC%) on collagen for mice with indicated genetic deficiencies in comparison to wild-type mice. Where indicated, GPVI and/or CLEC2 were rendered non-functional by injection of antibodies. Further indicated are published effects of the gene deficiency (same mouse strain) on *in vivo* arterial thrombosis, pulmonary thromboembolism and/or (tail) bleeding.

Gene	Protein	Genetic modification	Background	DB	ΔSAC%	Thrombosis phenotype	Bleeding phenotype	Remarks	Ref(s)
<i>Ano1</i>	anoctamin-1	PF4-Cre <i>Ano1</i>	C57Bl/6	07	o	n.d.	n.d.	-	18
<i>Ano6</i>	anoctamin-6	<i>Ano6</i> ^{St(AW0382)}	C57Bl/6	07	o	n.d.	↑	prolonged bleeding	18
<i>Anxa1</i>	annexin A1	PF4-Cre <i>Anxa1</i>	C57Bl/6	22	o	n.d.	n.d.	-	23***
<i>Apoe</i>	apolipoprotein E	<i>Apoe</i> ^{tm1Unc}	C57Bl/6	22	↑	n.d.	n.d.	-	23***
<i>Brip2</i>	BCL2-interacting protein	<i>Brip2</i> ^{tm1a}	C57Bl/6N	21	o	n.d.	n.d.	-	23***
<i>Capn1</i>	calpain-1	<i>Capn1</i> ^{tm1Ahc}	C57Bl/6	10	↑	↓	n.d.	delayed vessel occlusion	37,38
<i>Cd36</i>	CD36	<i>Cd36</i> ^{tm1Mfe}	C57Bl/6	14	o	↓	o	delayed thrombus formation, increased embolization	36,47
<i>Cdc42</i>	small GTPase CDC42	PF4-Cre <i>Cdc42</i>	C57Bl/6 x 129SV	20	o	↑	↑	accelerated vessel occlusion, prolonged bleeding	48
<i>Clec1b</i>	CLEC2	INU1 Ab*	C57Bl/6	19	↓	↓	↑	delayed thrombus formation, increased embolization	20
<i>Csk</i>	tyrosine kinase CSK	PF4-Cre <i>Csk</i> ^{tm2Tara}	C57Bl/6	23	↓	↓	↑	moderately reduces thrombus formation	49
<i>Dlg4</i>	scaffold protein DLG4	<i>Dlg4</i> ^{tm1a}	C57Bl/6N	21	o	n.d.	n.d.	-	23***
<i>Dusp3</i>	protein phosphatase DUSP3	<i>Dusp3</i> ^{tm15Tah}	C57Bl/6	11	↓	↓	o	decreased pulmonary embolism, small thrombus volume	50

Table 1. (continued)

Gene	Protein	Genetic modification	Background	DB	ΔSAC%	Thrombosis phenotype	Bleeding phenotype	Remarks	Ref(s)
<i>Fcer1g</i>	FCR γ-chain	<i>Fcer1g</i> ^{tmRaw}	C57Bl/6 x 129SV	04	↓	↓	n.d.	delayed and reduced thrombus formation	51,52
<i>Fpr2</i>	formyl peptide receptor-2	<i>Fpr2</i> ^{Tg(ActB)tmw}	C57Bl/6	22	↑	n.d.	n.d.	-	23***
<i>Gnaq</i>	Gq α-subunit	<i>Gnaq</i> ^{tm1Sof}	C57Bl/6 x 129SV	04	↓	↓	↑	intra-abdominal bleeding frequent postnatal death, protection thromboembolism	51,53
<i>Gp6</i>	GPVI	<i>Gp6</i> ^{tm1Beni}	C57Bl/6	03	↓	↓	o	reduced thrombus stability, enhanced embolization	42,43
<i>Gp6/Clec1b</i>	GPVI/CLEC2	JAQ1+INU1 ab*	C57Bl/6	03	n.d	↓	↑	delayed thrombus formation, smaller thrombus volume	43**
<i>Grm8</i>	glutamate metabotropic receptor 8	<i>Grm8</i> ^{tm1a}	C57Bl/6N	21	o	n.d.	n.d.	-	23***
<i>Ifnar1</i>	interferon receptor 1	<i>Ifnar1</i> ^{tm1a}	C57Bl/6N	21	↓	n.d.	n.d.	-	23***
<i>Itga2</i>	integrin α2	LoxP-Cre <i>Itga2</i>	C57Bl/6 x 129SV	05	↓	↓	o	reduced thrombus formation, increased embolization	5,54
<i>Itgb1</i>	integrin β1	Mx-Cre <i>Itgb1</i>	C57Bl/6 x 129SV	04	↓	o	o	unchanged thrombus formation	5,51,55
<i>Kcnn4</i>	K-activated Ca channel-4	<i>Kcnn4</i> ^{tm1Rkr}	C57Bl/6 x 129SV	16	o	n.d.	n.d.	-	18
<i>Mpig6b</i>	receptor G6B-b	<i>Mpig6b</i> ^{tm1,tm2re}	C57Bl/6	24	↓	n.d.	↑	prolonged bleeding	56
<i>Orai1</i>	calcium channel ORAI1	BMC <i>Orai1</i> ^{-/-}	C57Bl/6	01	↓	↓	o/↑	reduced thrombus formation and stability	57,58
<i>Plk3cg</i>	PI 3 kinase-γ	<i>Plk3cg</i> ^{tm1Wym}	129SV	13	↓	↓	o	protected from thromboembolic vascular occlusion	59,60

Table 1. (continued)

Gene	Protein	Genetic modification	Background	DB	ASAC%	Thrombosis phenotype	Bleeding phenotype	Remarks	Ref(s)
<i>Plcg2</i> (GOF)	phospholipase C- γ 2 (GOF)	<i>Plcg2</i> ^{all5}	C3HeB/Fej	12	↑	↑	n.d.	increased pulmonary thromboembolism	35
<i>Plid1</i>	phospholipase D1	<i>Plid1</i> ^{tm3Mafr}	C57Bl/6	06	↓	↓	o	reduced thromboembolism, reduced thrombus stability	14
<i>Prkca</i>	protein kinase C- α	<i>Prkca</i> ^{Mvh6/hero/Lmk}	C57Bl/6	06	↓	↓	o	delayed thrombus formation, on fecal occult blood	61;62
<i>Prkcd</i>	protein kinase C- δ	<i>Prkcd</i> ^{tm1kin}	C57Bl/6	06	↑	o	n.d.	unchanged thrombus formation	61;63
<i>Prkcg</i>	protein kinase C- θ	<i>Prkcg</i> ^{tm1utt}	C57Bl/6	17	↑	n.d.	n.d.	limited occlusion, thrombus instability	61
<i>Prkd2</i>	protein kinase D2	<i>Prkd2</i> ^{tm1.1Dca}	C57Bl/6	17	↓	n.d.	o	unchanged bleeding	64
<i>Ptprj</i>	phosphatase CD148	PF4-Cre <i>Ptprj</i> ^{tm1.1Weis}	C57Bl/6	23	↓	↓	o	severely compromised thrombus formation	49
<i>Rac1</i>	small GTPase RAC1	Mx-Cre <i>Rac1</i>	C57Bl/6	08	↓	↓	↑	reduced thrombus formation and volume, variable but prolonged bleeding	65
<i>Rhoa</i>	small GTPase Rho-A	PF4-Cre <i>Rhoa</i>	C57Bl/6 x 129SV	08	o	↓	↑	unstable thrombus formation, increased embolization	13**
<i>Stim1</i>	regulator STIM1	BMC <i>Stim1</i> ^{-/-}	C57Bl/6	01	↓	↓	↑	reduced thrombus stability, no vessel occlusion	57;66
<i>Stim2</i>	regulator STIM2	<i>Stim2</i> ^{tm1Ben1}	C57Bl/6	01	o	n.d.	n.d.	-	57
<i>Syk</i>	tyrosine kinase SYK	PF4-Cre <i>Syk</i> ^{tm1.1SykSpwa}	C57Bl/6	09	n.d.	↓	↑	blood-filled lymphatics, impaired thrombus formation	67**
<i>Vps13a</i>	vacuolar sorting protein VPS13A	<i>Vps13a</i> ^{tm1a}	C57Bl/6	21	↓	n.d.	n.d.	-	23***

Abbreviations: BMC, bone-marrow chimera; DB, database; GOF, gain-of-function; n.d., not determined. * Antibody mediated deficiency of CLEC2 and/or GPVI; **microfluidics data not included in reference; ***only data for M1 published.

The obtained heatmap illustrated an overall high cohesion of the data, yet also suggesting that wild-type strains with mixed C57Bl/6 x 129SV background (databases 04, 05, 08, 16, 20) had a tendency for smaller *P3-5* values. Overall, these findings point to a high degree of comparability between the various wild-type datasets.

To determine how the different parameters of collagen-mediated thrombus formation correlated within our dataset of wild-type and genetically modified mice, a correlation matrix was constructed based on the Kendall's tau-b correlation analysis (Figure 1). All parameters showed a significant moderate to strong correlation to each other (Kendall's tau-b: 0.424-0.829). Platelet adhesion (*P1*) correlated strongly to platelet aggregation (*P2*), while it correlated moderately to thrombus morphology (*P3*), multilayer (*P4*) and contraction (*P5*) (Kendall's tau-b: 0.424-0.572). Strongest associations were observed between platelet aggregation (*P2*) and the thrombus scores (*P3-5*) (Kendall's tau-b 0.55-0.65, $p < 0.001$). Furthermore, even stronger correlations were seen between *P3-5*, *i.e.* the thrombus morphology, multilayer and contraction scores (Kendall's tau-b 0.76-0.83, $p < 10^{-10}$).

Table 2. Overview of microspotted surfaces (*M*) and parameters of image analysis (*P*) for the assessment of thrombus formation

<i>M</i>	<i>Microspot surface</i>		<i>Platelet receptors involved</i>	
<i>M1</i>	collagen type I (VWF)*		GPIb, GPVI, $\alpha_2\beta_1$	
<i>M2</i>	rhodocytin + laminin + VWF-BP		GPIb, CLEC2, $\alpha_v\beta_1$	
<i>M3</i>	laminin + VWF-BP		GPIb, $\alpha_v\beta_1$	
<i>P</i>	<i>Parameter of analysis</i>	<i>Image</i>	<i>Range</i>	<i>Scaling</i>
<i>Platelet adhesion</i>				
<i>P1</i>	platelet surface area coverage (%SAC)	BF**	0 - 93.67	0 - 10
<i>Thrombus signature</i>				
<i>P2</i>	platelet aggregate coverage (%SAC)	BF	0 - 49.17	0 - 10
<i>P3</i>	thrombus morphology score	BF	0 - 5.0	0 - 10
<i>P4</i>	thrombus multilayer score	BF	0 - 3.0	0 - 10
<i>P5</i>	thrombus contraction score	BF	0 - 3.0	0 - 10
<i>Platelet activation</i>				
<i>P6</i>	PS exposure (%SAC)	FL	0 - 12.23	0 - 10
<i>P7</i>	P-selectin expression (%SAC)	FL	0 - 29.70	0 - 10
<i>P8</i>	integrin $\alpha_{IIb}\beta_3$ activation (%SAC)	FL	0 - 28.25	0 - 10

*binds VWF from plasma. **Abbreviations: BF; brightfield; FL, fluorescence.

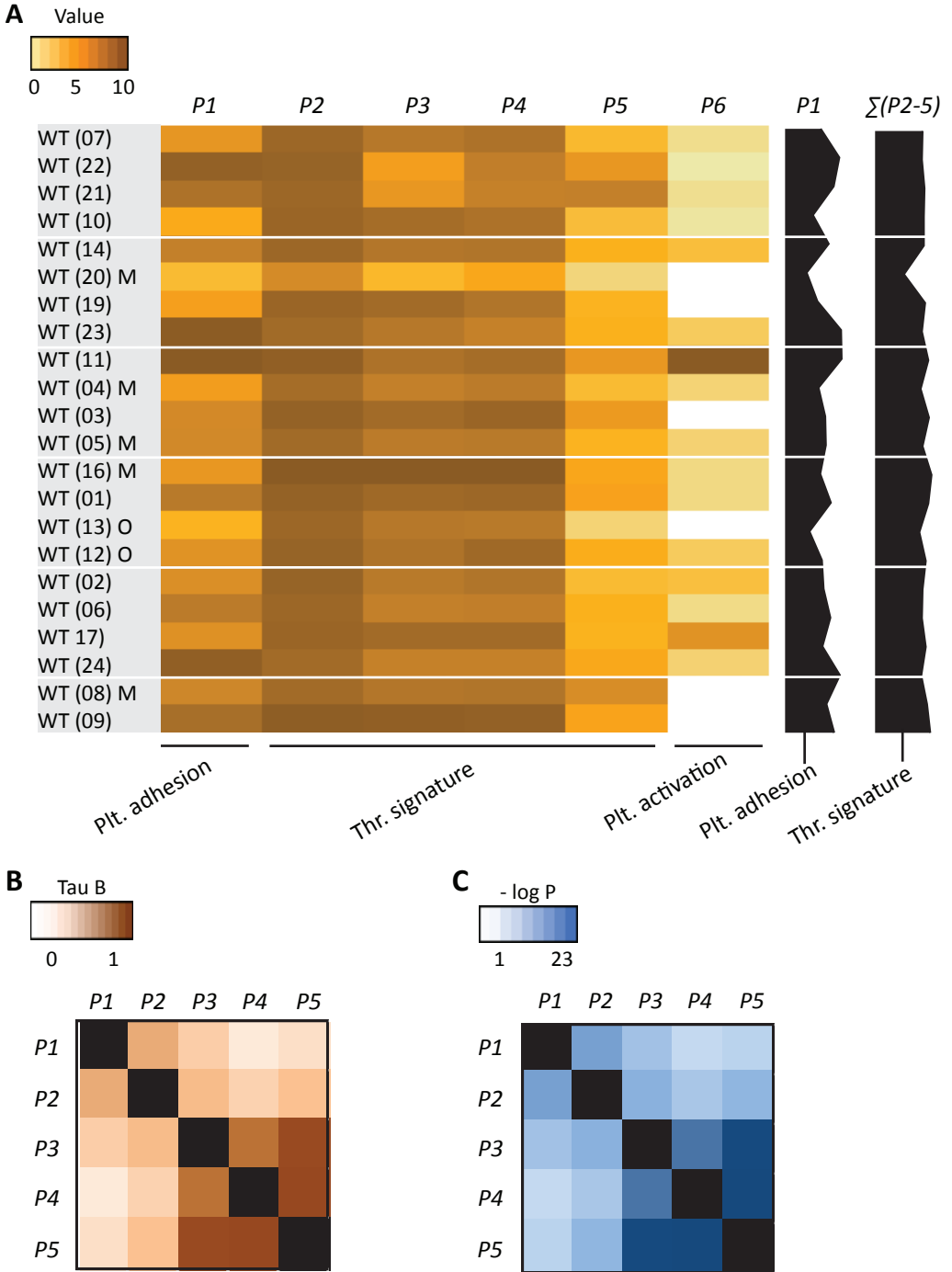


Figure 1. Consistency of collagen-dependent thrombus formation between multiple wild-type mouse datasets. Blood from wild-type (WT) mice (databases as indicated in brackets) was perfused over collagen at shear rate of 1000 s^{-1} (in two cases 1700 s^{-1}), and parameters of thrombus formation were obtained by

reanalysis of random brightfield images. Investigated wild-type mice (n = 22) had a C57Bl6 genetic background or, where indicated, a mixed C57Bl6 x 129SV background (M) or other background (O). For full details, see Table 1. **A)** Heatmap of mean parameters, univariate scaled (0-10) across all mouse strains. Parameter clustering was as follows: platelet adhesion: *P1* (platelet SAC%); thrombus signature: *P2* (platelet aggregate SAC%), *P3* (thrombus morphology score), *P4* (thrombus multilayer score), *P5* (thrombus contraction score); and platelet activation: *P6* (PS exposure). Also indicated (black bars on the right) are the overall scaled values of platelet adhesion (*P1*) and thrombus signature ($\Sigma P2-5$). The wild-type datasets were arranged based on the alphabetical order of the (genetically) modified mice. **B-C)** Correlations between parameters of thrombus formation for all cohorts of mice strains. Shown are Kendall's tau-b correlation coefficients (**B**) and corresponding p-values (**C**).

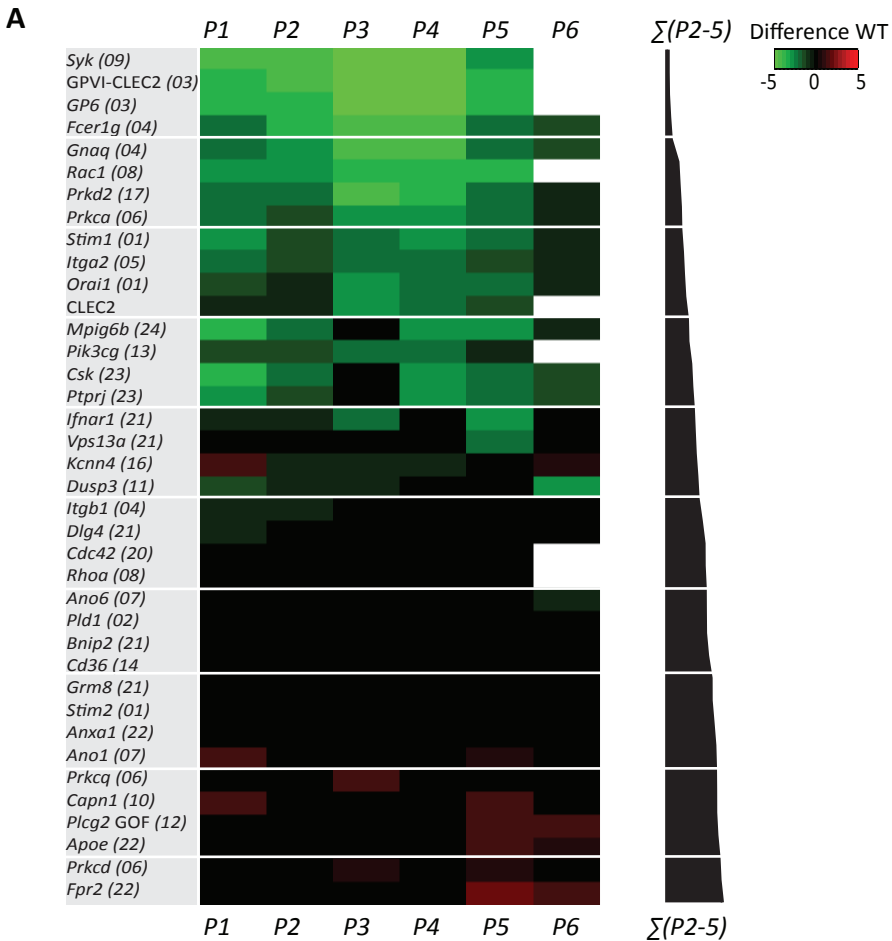
Comparing thrombus formation on collagen in multiple genetically modified mice

As detailed in Table 1, the included 38 modified mouse strains concern animals with defects of single genes, encoding for proteins implicated in GPVI- and/or GPCR-related platelet activation pathways, *i.e.*, *Csk*, *Fcer1g* (FcR γ -chain), *Gnaq* ($G\alpha_q$), *Orai1*, *Pik3cg* (PI3K γ), *Pld1* (PLD1), *Prkca* (PKC α), *Prkcd* (PKC δ), *Prkcq* (PKC θ), *Prkd2* (PKD2), *Stim1*, *Stim2* or *Syk*. In addition, the list contains mice with genetic deficiencies of the small GTPases, *Cdc42*, *Rhoa* or *Rac1*; deficiencies of protein (tyrosine) phosphatases *Dusp3*, *Mpig6b* (G6b-B) or *Ptprj* (CD148); deficiencies of other adhesive receptors, such as *Itga2* (integrin α_2), *Itgb1* (integrin β_1) or *Cd36* (GPIV); defects linked to altered PS exposure, *i.e.* *Ano1* (TMEM16A), *Ano6* (TMEM16F), *Capn1* (calpain-1) or *Kcnn4*. Other mice with single gene deficiencies came from an earlier undertaking to find novel proteins implicated in thrombosis and hemostasis,²³ namely *Anxa1* (annexin 1), *ApoE* (plasma lipoprotein component), *Bnip2* (CBL2-interacting protein), *Dlg4* (scaffold protein), *Fpr2* (formyl peptide receptor), *Grm8* (glutamate receptor), *Ifnar1* (interferon receptor) or *Vps13a* (vacuolar sorting protein). In addition, a mutated mouse strain with a *Plcg2* gain-of-function (GOF, constitutive active PLC γ 2) was incorporated.³⁵ Given the ability of antibodies JAQ1 and INU1 to specifically cause platelet depletion from GPVI or CLEC2, respectively, after *in vivo* injection into mice,⁵ we also included strains with such antibody-induced GPVI and/or CLEC2 deficiencies.

For assessment of the effects of (genetic) deficiency, scaled values per parameter were calculated for each of the 38 modified mouse strains and compared to those of the corresponding wild-types (Figure S2). A subtraction heatmap was generated to pinpoint the effects of genetic modification, in which differences outside the range of (composite) means \pm SD were considered as being relevant. The heatmap data could be ranked based on alterations in thrombus signature (Figure 2A) or on differences in platelet adhesion (Figure 2B). With either way of ranking, profound quantitative differences were observed in the majority of the thrombus formation parameters, when comparing the 38 modified mouse strains. Thrombus signatures were suppressed, in a decreasing order (Figure 2A), by deficiencies in *Syk*, GPVI/CLEC2, GPVI, *Fcer1g*, *Gnaq*, *Rac1*, *Prkd2*, *Prkca*, *Stim1*,

Itga2, *Orai1*, *CLEC2*, *Mpig6b*, *Pik3cg*, *Csk* and *Ptpr*. In contrast, this thrombus marker was elevated, in an increasing order, by deficiencies in *Prkca*, *Capn1*, *Plcg2* (gain-of-function mutation), *ApoE*, *Prkcd* and *Fpr2*.

The ranking based on altered platelet adhesion revealed several similarities, but also marked differences. Defects in *Syk*, GPVI, *Rac1*, *Stim1* and *Itga2* resulted in a strong suppression of both platelet adhesion and thrombus signature. Relative larger effects on thrombus signature - in comparison to platelet adhesion - were apparent for mice with defects in *Fcer1g*, *Prkd2* and *Prkca* (reduced thrombus formation), as well as for mice with defective members of the PKC family, *Prkcd* and *Prkca* (increased thrombus formation). Relative increases in platelet adhesion were only seen for mice with deficiencies in *Kcnn4*, *Ano1* and *Capn1*.



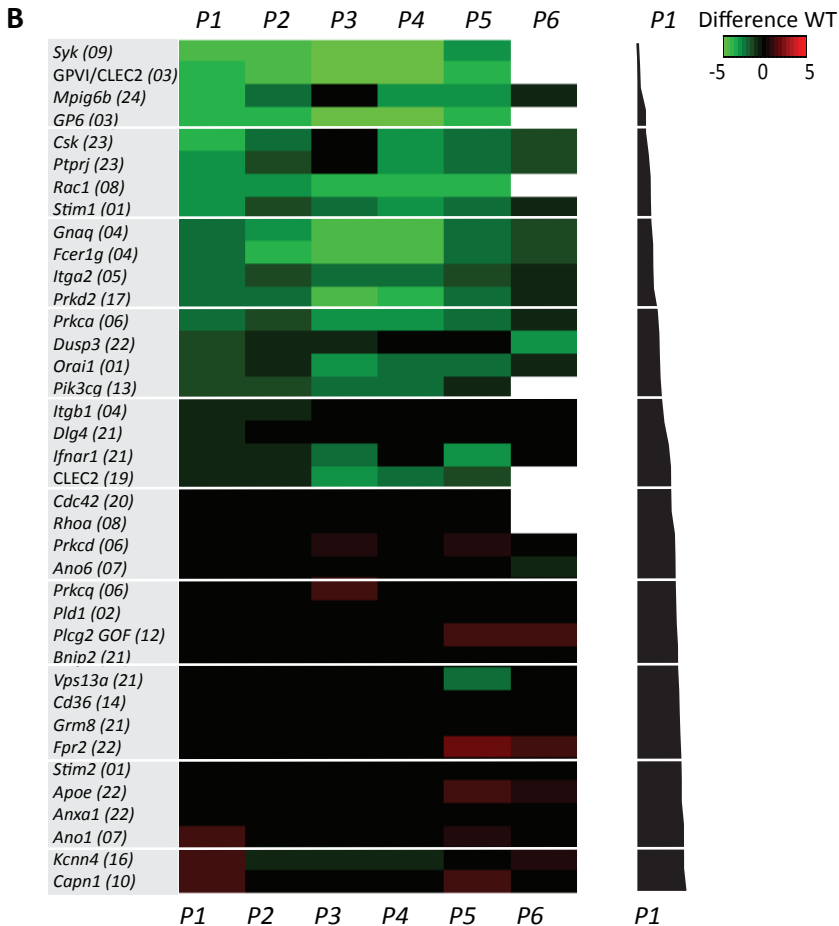


Figure 2. Multi-parameter comparison of collagen-dependent thrombus formation for 38 (genetically) deficient mice. Whole blood from mice with indicated genetic or antibody-induced defects as well as from corresponding wild-type mice was perfused over collagen-I. Parameters of thrombus formation were as indicated in Figure 1. For detailed information on mouse strains, see Table 1. Mean parameters per strain were scaled (0-10) across all wild-types ($n = 22$) and defects ($n = 38$), as for Figure 1. Subtraction heatmaps showing differences between indicated genetic (or antibody-mediated) deficiency in comparison to wild-type, after filtering for differences outside the range of (composite) mean \pm SD, to select relevant changes. **A**) Ranking of genes based on effect on thrombus signature ($\Sigma P2-5$), as shown in black bars on the right. Colors indicate unchanged (black), decreased (green) or increased (red) parameters. **B**) Ranking of genes based on effect on platelet adhesion ($P1$), as indicated in black bars. Colors represent unchanged (black), decreased (green) or increased (red) parameters. Non-subtracted heatmap values are provided in Figure S2.

In general, these heatmaps demonstrated that the ranking based on changes in thrombus signature (Figure 2A) can provide additional insight into the ‘thrombogenic’ consequences of a gene defect, in comparison to a ranking based on altered platelet adhesion (Figure 2B).

Microfluidics analysis of thrombus formation on collagen and other surfaces

For a subset of 11 genetically modified mice strains, the same microfluidic device was used to assess whole blood thrombus formation on collagen-I (*M1*) plus two additional microspots, *i.e.* rhodocytin/laminin (*M2*) and laminin (*M3*), both co-coated with VWF-BP to induce shear-dependent platelet adhesion (Table 2). As clarified before, immobilized rhodocytin triggers CLEC2-induced platelet activation,^{26,27} whereas laminin surfaces allow platelet adhesion via integrin $\alpha_6\beta_1$.²² For the same subset of mice, the formed thrombi were post-stained in three colors to quantify PS exposure (*P6*), P-selectin expression (*P7*) and integrin $\alpha_{IIb}\beta_3$ activation (*P8*), using procedures previously established for human platelet thrombi.²⁶ Representative images from each of the microspots using wild-type blood are depicted in Figure 3. In comparison to collagen-I (*M1*), rhodocytin/laminin (*M2*) was less thrombogenic, with only moderately activated platelets that formed small aggregates. The laminin microspot (*M3*) only triggered adhesion of a monolayer of spreading platelets. For these 11 genetically modified mouse strains plus corresponding wild-type mice, we again listed the scaled parameters (*P1-8*) for each microspot (*M1-3*) (Figure S3). The ensuing subtraction heatmap revealed major reductions in platelet

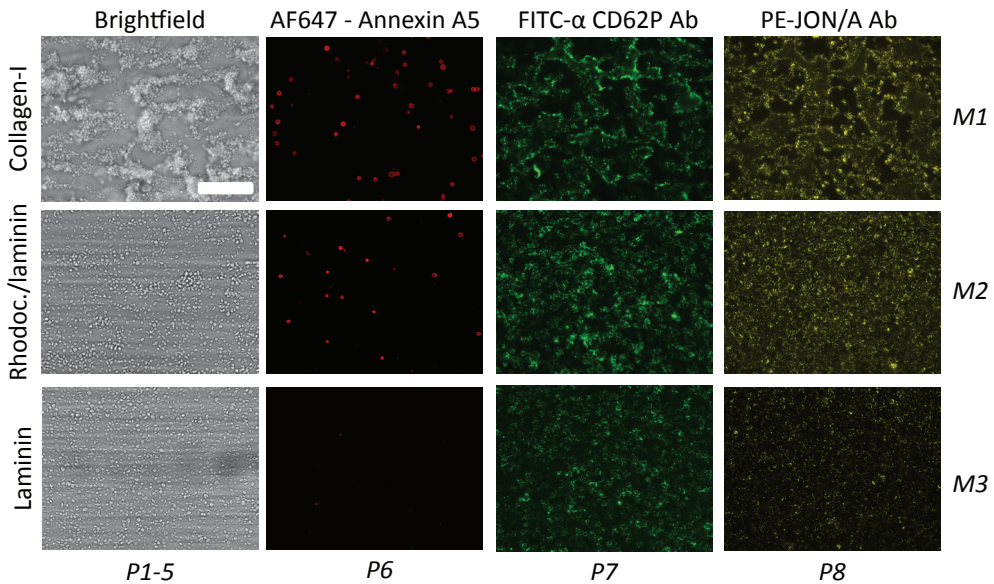


Figure 3. Microscopic imaging of whole blood thrombus formation on adjacent microspots. Whole blood from wild-type mice (DB 24) was flowed for 3.5 min at 1000 s^{-1} over three consecutive microspots of collagen-I (*M1*, upper row), rhodocytin/laminin/VWF-BP (*M2*, middle row), and laminin/VWF-BP (*M3*, lower row). Shown are representative brightfield and fluorescence microscopic images of the thrombi formed. Triple staining was performed with AF647-annexin A5, FITC anti-CD62P Ab, and PE-Jon/A Ab. Also indicated are the types of parameters (*P1-8*) taken from the image sets. Bar 50 μm .

adhesion and thrombus signature at surface *M1* for the animals with deficiencies in *Csk*, *Ptprj*, *Mpig6b* (tyrosine protein kinase and phosphatases, respectively); and, to a clearly lesser extent, for deficiencies in *Ifnar1*, *Vps13a* and *Anxa1* (Figure 4). For the kinase and phosphatase knockouts, this extended to a reduction in platelet activation parameters (*P6-8*) at *M1*, and furthermore to lower *P1-2* values at the other microspots *M2-3*.

Markedly, for several of these mice, also gain-of-platelet-functions could be detected. In this case, increased parameters *P4-6* were distributed over *M1* (deficiencies in *ApoE* and *Fpr2*) and *M2* (deficiency in *Grm8*). Another remarkable finding was that, for the majority of mice, parameters at the laminin surface (*M3*) were unchanged. This suggested that laminin-platelet interactions are relatively insensitive to these genetic modifications. Next to the ranking based on changes in platelet adhesion (Figure 4B), the ranking of genes according to changes in overall thrombus signature (Figure 4A) appeared to be a valuable addition in the description of the alterations in platelet properties.

Linking microfluidics outcomes to thrombosis and hemostasis *in vivo*

Recently, we described a systematic procedure to compare the consequences of genetic knockout in mice for experimentally induced (collagen-dependent) arterial thrombosis and hemostasis.²³ For the 38 deficiencies, it was thus of interest to compare the results of the current extended microfluidic assay (*M1*, *P1-5*) with the previously reported changes in arterial thrombosis tendency and tail bleeding *in vivo*. Hence, per modified mouse strain, the recorded changes (Table 1) were listed as being a reduced/unchanged/increased thrombosis phenotype and as a prolonged/unchanged/shortened bleeding time. Figure 5 gives the comparison of these *in vivo* effects with altered parameters of *in vitro* thrombus formation using microfluidics.

Strikingly, the majority of mice demonstrating an antithrombotic phenotype *in vivo* manifested with a larger or smaller reduction in collagen-dependent thrombus formation *in vitro* (Figure 5). We noted only a few exceptions: (i) mice deficient in *Cdc42* with an apparently prothrombotic phenotype, but for unknown reasons no effect *in vitro*; (ii) mice deficient in *Pld1* (where *in vitro* thrombus formation was only impaired at a higher shear rate of 1700 s^{-1});¹⁴ and (iii) *Cd36*-deficient mice (requiring a thrombospondin surface for altered *in vitro* thrombus formation).³⁶ Also, the impaired arterial thrombosis reported for *Capn1*^{-/-} mice³⁷ did not match with a measured higher platelet adhesion under flow, although it should be noted that the latter mice showed a complex pattern of increased and decreased platelet activation parameters *in vitro*.³⁸

Markedly, in the mouse strains with a reduced arterial thrombosis tendency *in vivo*, only approximately half of these were accompanied with hemostatic defect (Figure 5).

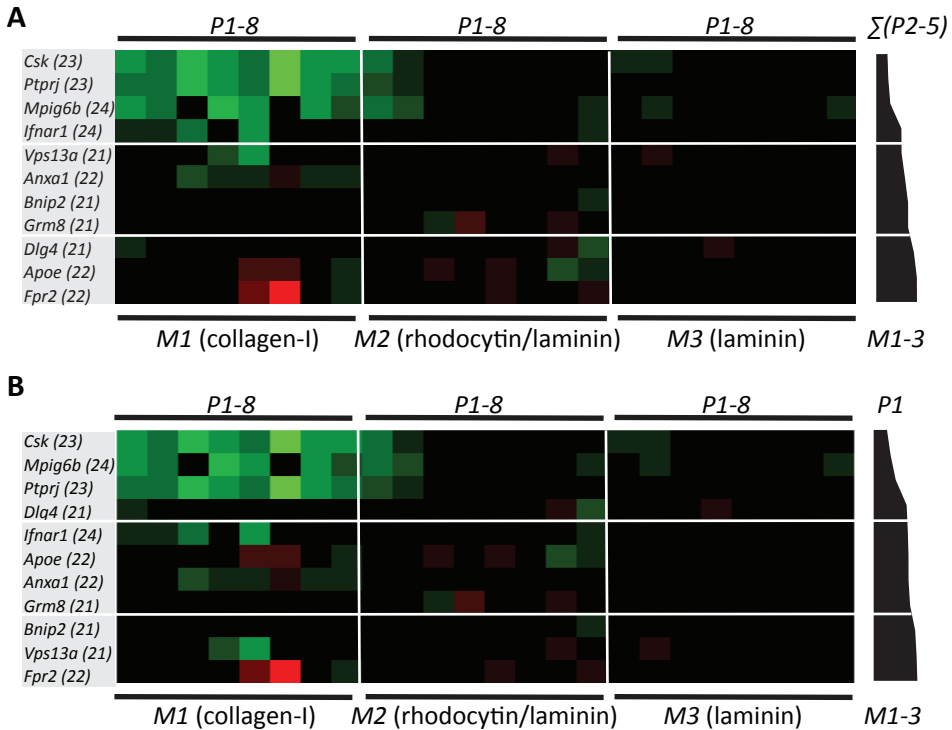


Figure 4. Multi-parameter comparison of thrombus formation on three microspots for 11 mouse strains with genetic deficiencies. Whole blood from mice with indicated genetic defects or corresponding wild-types was perfused over three microspots (*M1-3*), as for Figure 3. Brightfield images (*P1-5*) and fluorescence images (*P6*, AF647-annexin A5; *P7*, FITC anti-CD62P Ab; *P8*, PE-JON/A Ab) were analyzed for each microspot. Per microspot, parameter values were univariate scaled (0-10) across all mouse strains. **A**) Subtraction heatmap of differences between deficient and wild-type strains, filtered for changes outside the range of (composite) mean \pm SD, to select relevant changes. Genes were ranked based on effects on thrombus signature ($\Sigma P2-5$) across microspots *M1-3*, as shown in black bars. Colors represent unchanged (black), decreased (green) or increased (red) parameters. **B**) Subtraction heatmap with ranking based on gene effects on platelet adhesion (*P1*), as indicated in right black bars.

This was also reflected by comparing *in vitro* thrombus formation (by microfluidics) with alterations in bleeding time. Mice with reduced *in vitro* thrombus formation, but unchanged or slightly prolonged bleeding times, included animals with deficiencies in the collagen receptors *Gp6* and *Itga2*; the protein kinases *Prkd2* and *Prkca*; and the protein phosphatases *Ptprj* and *Dusp3*. This may suggest that the collagen receptors (and hence collagen itself) and the (de)phosphorylating proteins within the downstream signaling pathways are not essential for hemostasis. This may suggest that the collagen receptors (and hence collagen itself) and the (de)phosphorylating proteins are not uniquely – perhaps redundantly – required for platelet functions at lower shear rates such as during hemostasis. The same mouse genes were also previously characterized as having a distinct role in arterial thrombosis and hemostasis.²³

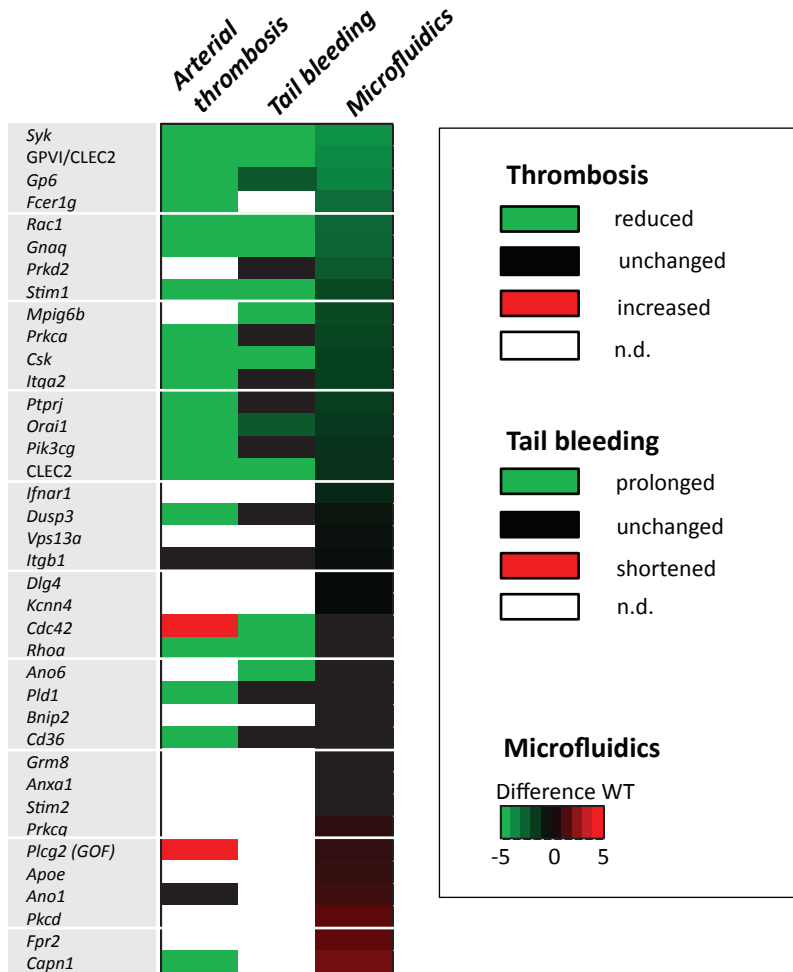


Figure 5. Effects of genetic modification on arterial thrombosis and tail bleeding in comparison to collagen-dependent thrombus formation using microfluidics. Effects of genetic or antibody-induced defects of concerning mouse strains on arterial thrombosis and tail bleeding was obtained from the literature (see Table 1). Effects were classified as being unchanged (black), antithrombotic/prolonged bleeding (green) or prothrombotic/shortened bleeding (red), according to procedures described before²³. White color indicates that information is lacking. Heat mapped data were ranked based on summative effects on all thrombus formation parameters ($\Sigma P1-5$) from surface *M1*.

Network modeling to predict novel proteins implicated in mouse platelet functions

Based on the 37 different mouse genes/proteins that were analyzed for effects on collagen-dependent whole blood thrombus formation, we constructed a network using the biological STRING (Search Tool for the Retrieval of Interacting Genes/Proteins) database, in order to be capable to depict additional protein-protein interactions.

Accordingly, a network was established containing in total 117 nodes (37 core and 80 novel nodes) and 1142 edges (interaction score: medium to highest confidence: 0.40-0.99). Reactome pathways that were highly represented in the network were: platelet activation, signaling and aggregation (count in gene set: 37 of 242; false discovery rate: $3.25e^{-39}$), hemostasis (count in gene set: 44 of 489; false discovery rate: $1.5e^{-38}$),

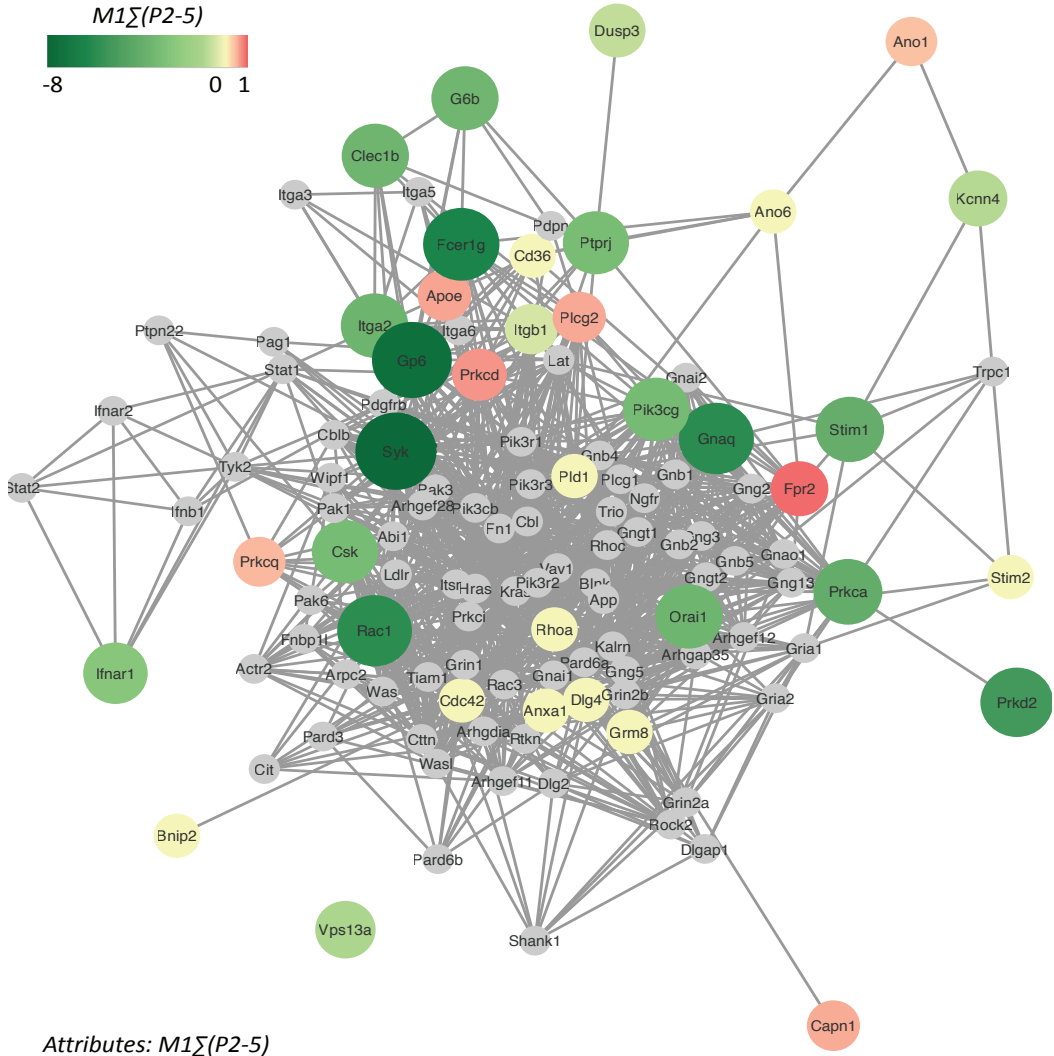


Figure 6. Network of protein-protein interactions in collagen-dependent thrombus formation. Network, constructed from the STRING database and visualized in Cytoscape, of murine protein-protein interactions with as seed the 37 investigated core genes. The network contained 117 nodes (37 core nodes, 80 novel nodes) and 1142 edges. Core nodes of the network were color- and size-coded based on altered thrombus signature ($\Sigma P2-5$) at surface *M1*. Green color intensity (larger size) of nodes points to a stronger reducing effect, and red color intensity (large size) to a stronger stimulating effect in comparison to wild-type. Novel nodes are indicated in gray.

signal transduction (count in gene set: 68 of 2430; false discovery rate: $2.14e^{-32}$), GPVI-mediated activation cascade (count in gene set: 18 of 34; false discovery rate: $2.07e^{-26}$) and G alpha (12/13) signaling events (count in gene set: 18 of 68; false discovery rate: $2.64e^{-22}$). The 37 core nodes were color- and size-coded, based on the established gene effects on thrombus signature *M1PΣ(2-5)*, and then indicated three typical clusters of genes/proteins with large size effects (Figure 6): (i) *Gp6* with associated receptors *Fcgr1g* and kinase *Syk* (cluster score: 7; #nodes: 19; #edges: 63); (ii) the low-molecular weight GTPases *Rac1* and *Cdc42* together with *Itga2* and *Itgb1* (cluster score: 5.24; #nodes: 22; #edges: 55); and (iii) Ca^{2+} -regulating signaling components, *Stim1*, *Stim2* and *Orai1* (cluster score: 4; #nodes: 4; #edges: 6). Out of the 80 novel nodes, 12 genes have been previously shown to modify *in vivo* arterial thrombosis and/or bleeding (*Cblb*, *Cttn*, *Gnai2*, *Gria1*, *Itga6*, *Lat*, *Lcp2*, *Ldlr*, *Pik3cb*, *Pik3r1*, *Rock2*, *Vav1*).²³ Color-coding of the same network nodes for gene effects on platelet adhesion revealed as most notable changes the above-mentioned gain-of-function effects of *Ano1*, *Kcnn4* and *Capn1* (Figure S4).

Discussion

In this paper, we applied standardized analysis procedures in order to allow detailed and quantitative comparison of the changes in platelet functions in multiple genetically modified mice, using microfluidic methods of collagen-dependent thrombus formation under shear conditions. For this purpose, we re-analyzed sets of microscopic brightfield and fluorescence images, using defined semi-automated scripts, resulting in quantitative parameters of platelet adhesion, platelet aggregation (defined as thrombus signature),²⁶ and platelet activation. The underlying rationale was that earlier captured images provide more relevant information than only a platelet surface area coverage, and thus can provide additional insight into the complex process of thrombus formation. For a subset of mice, it was also possible to extend this complex phenotyping of thrombus formation to other, non-collagen surfaces with additional parameters of platelet activation.

Recent work has shown that multiple platelet function assessment by whole blood microfluidic assays provides novel insights, for instance into the changes in human platelets linked to normal genetic variation^{26,39} and in mouse platelets due to co-activation by interacting chemokines.⁴⁰ The present comparative quantitative analysis of changes in thrombus formation in multiple genetically or antibody-induced modified mice also allows to evaluate the assay outcomes for changes in specific platelet functions. Here, we could identify a partial distinction between genes/proteins affecting platelet adhesion and those altering platelet aggregation properties (collectively termed as thrombus

signature). For instance, it seems that the murine platelet protein kinases and phosphatases *Csk*, *Mpig6b* and *Ptprj* have a relatively large role in flow-dependent platelet adhesion. Markedly, for *Csk*, *Mpig6b* and *Ptprj* this effect is extended to also a reduced adhesion at the non-collagen surface *M2*. On the other hand, the processes of platelet adhesion and aggregate formation are also related, as shown by an overall consistent correlation between adhesion and aggregation parameters (Kendall's tau-b = 0.42-0.68). A similar conclusion was drawn earlier from the analysis of thrombus formation in blood samples from 94 healthy subjects, also pointing to the existence of a subject-dependent thrombus signature.²⁶

In comparison to the collagen surface (*M1*), for the 11 mouse strains analyzed, we observed in general smaller gene effects at the two other surfaces (*M2-3*), which mediate platelet adhesion via GPIb-V-IX and $\alpha_6\beta_1$ with or without CLEC2 (rhodocytin). Accordingly, it seems that, at least in part, distinct sets of genes/proteins are implicated in the platelet adhesion to non-collagen surfaces than to the collagen surface. Clearly *in vivo* thrombus formation is not purely mediated by collagen, but rather is the result of platelet interactions with a mixture of different extracellular matrix proteins.

The present data set also includes new findings with unpublished blood samples from mice deficient in *Rhoa* and *Syk*. The *Rhoa* defect did not appear to influence platelet adhesion nor thrombus signature parameters at the shear rate of 1000 s⁻¹, which is in support of the earlier conclusion that platelet RHO-A becomes relevant for thrombus formation at high (pathological) shear rates.¹³ In contrast, genetic deficiency in *Syk* resulted in a strong reduction of all platelet and thrombus parameters on collagen. This highlights the importance of SYK signaling in collagen-dependent thrombus formation

Given the earlier established correlation between the outcome of microfluidic tests (in terms of platelet surface area coverage) and experimental arterial thrombosis in mice,²³ it was of interest to evaluate for the current mouse strains how a more detailed analysis (considering more thrombus parameters) contributes to this relationship. Such a comparison clearly has limitations, such as the wide variety of methods and test outcomes of the *in vivo* thrombosis measurements, making a clear differentiation between moderate and strong phenotypes difficult;²³ and furthermore, the absence of coagulation and vessel wall components other than collagen in the *in vitro* approach. Nevertheless, a ranking of the investigated mouse strains according to overall changes in thrombus parameters (including platelet adhesion and aggregation) showed a good reflection with published changes in arterial thrombosis *in vivo*. On the other hand, for a considerable set of genes, a changed thrombus formation *in vitro* (and mostly *in vivo*) was not associated with an altered bleeding time. In several cases, a discrepancy is

well explainable. For instance, defects in platelet *Clec1b* (as a non-collagen receptor)⁴¹ or in *Ano6* (an isolated defect of platelet-dependent coagulation),¹⁸ will not be picked up by flow assays over collagen with anticoagulated blood. A striking example is *Gp6*. Whereas GPVI deficiency overall impairs thrombus formation *in vitro* as well as arterial thrombosis *in vivo*, mouse tail bleeding times are only moderately prolonged.^{42,43} In line with that, mild bleeding symptoms have been reported in patients with a defect in the *GP6* gene.^{44,45} Hence, this gene does likely have a restricted role, which is in line with the constructed network indicating multiple GPVI-linked proteins that contribute to both thrombosis and hemostasis.

Translation of the current evaluation of genes in murine thrombus formation to human pathophysiology can – taking into account the above – provide better insight into the genetic background of human platelet function abnormalities and how these can relate to thrombotic and bleeding disorders. Indeed, for orthologs of several of the genes analyzed in this paper, *e.g.* human *ORAI1* and *STIM1*, mutations have been identified that link to defective collagen-dependent thrombus formation *in vitro*.⁴⁶ By applying an extended image analysis, a detailed description of the formed thrombi can be generated. This can aid in the identification of the defective part (platelet adhesion, aggregation or procoagulant response) of the process of thrombus formation in patients with an unexplained increased risk for either thrombosis or bleeding. Extended analysis of the available mouse data and summation in the form of a network can also contribute to a more targeted approach to select novel candidate genes and proteins, possibly affecting platelet functions in a positive or negative way. Moreover, by applying new knowledge and techniques, in the present paper, new insights were gained from previously performed mouse experiments. In such a manner, our study may contribute to the 3R approaches by reducing, refining and replacing animal experiments.

Taken together, we conclude that the presently developed multi-parameter analysis of thrombus formation on microspots using microfluidics can be used to: *(i)* determine the severity of platelet abnormalities; *(ii)* distinguish between altered platelet adhesion, aggregation and activation; and *(iii)* elucidate both collagen and non-collagen dependent platelet changes. This approach may thereby aid in the better understanding and better assessment of the changes in platelets that affect arterial thrombosis and hemostasis.

Conflict of interest statement

JWMH is a co-founder and shareholder of FlowChamber. The other authors indicate that no relevant conflict of interest exists.

Author contributions

MN and JPVG analyzed and interpreted data and wrote the manuscript. SMDW and MJEK analyzed data. RV created scripts used for image analysis. DA, AB, ME, KK, CO, JP, IP, AWP, JM, MJG, YAS and CW provided mice and other tools and revised the manuscript. DS and BN provided mice, original published and unpublished images and revised the manuscript. JWMH and CCFMJB provided expert supervision, analyzed and interpreted data and wrote the manuscript.

Acknowledgements

MN, MJEK, and JWMH have received funding from the Cardiovascular Centre (HVC) MUMC⁺ Maastricht, the Interreg V Euregio Meuse-Rhine program (Poly-Valve). DS, AB, IP and BN were supported by the Deutsche Forschungsgemeinschaft (project-number 374031971 – TRR240). CO is Senior Research Associate at the Belgian Fund for Scientific Research (F.R.S.-FNRS). YAS received founding from a BHF Fellowship (FS/13/1/29894) and a Programme Grant RG/15/13/31673. CCFMJB is supported by the Alexander von Humboldt Foundation.

References

1. Ruggeri ZM, Mendolicchio GL. Adhesion mechanisms in platelet function. *Circ Res.* 2007; 100: 1673-1685.
2. Stegner D, Nieswandt B. Platelet receptor signaling in thrombus formation. *J Mol Med.* 2011; 89: 109-121.
3. Versteeg HH, Heemskerk JW, Levi M, Reitsma PH. New fundamentals in hemostasis. *Physiol.Rev.* 2013; 93: 327-358.
4. Van der Meijden PE, Heemskerk JW. Platelet biology and functions: new concepts and future clinical perspectives. *Nat Rev Cardiol.* 2019; 16: 166-179.
5. Nieswandt B, Brakebusch C, Bergmeier W, *et al.* Glycoprotein VI but not $\alpha_2\beta_1$ integrin is essential for platelet interaction with collagen. *EMBO J.* 2001; 20: 2120-2130.
6. Siljander PR, Munnix IC, Smethurst PA, *et al.* Platelet receptor interplay regulates collagen-induced thrombus formation in flowing human blood. *Blood.* 2004; 103: 1333-1341.
7. Auger JM, Kuijpers MJ, Senis YA, Watson SP, Heemskerk JW. Adhesion of human and mouse platelets to collagen under shear: a unifying model. *FASEB J.* 2005; 19: 825-827.
8. Varga-Szabo D, Pleines I, Nieswandt B. Cell adhesion mechanisms in platelets. *Arterioscler Thromb Vasc. Biol.* 2008; 28: 403-412.
9. Senis YA, Mazharian A, Mori J. Src family kinases: at the forefront of platelet activation. *Blood.* 2014; 124: 2013-2024.
10. Mammadova-Bach E, Nagy M, Heemskerk JW, Nieswandt N, Braun A. Store-operated calcium entry in blood cells in thrombo-inflammation. *Cell Calcium.* 2019; 77: 39-48.
11. Harper MT, Poole AW. Diverse functions of protein kinase C isoforms in platelet activation and thrombus formation. *J Thromb Haemost.* 2010; 8: 454-462.
12. Guidetti GF, Canobbio I, Torti M. PI3K/Akt in platelet integrin signaling and implications in thrombosis. *Adv Biol Regul.* 2015; 59: 36-52.
13. Pleines I, Hagedorn I, Gupta S, *et al.* Megakaryocyte-specific RhoA deficiency causes macrothrombocytopenia and defective platelet activation in hemostasis and thrombosis. *Blood.* 2012; 119: 1054-1063.
14. Elvers M, Stegner D, Hagedorn I, *et al.* Impaired $\alpha_{IIb}\beta_3$ integrin activation and shear-dependent thrombus formation in mice lacking phospholipase D1. *Sci Signal.* 2010; 3: ra1.

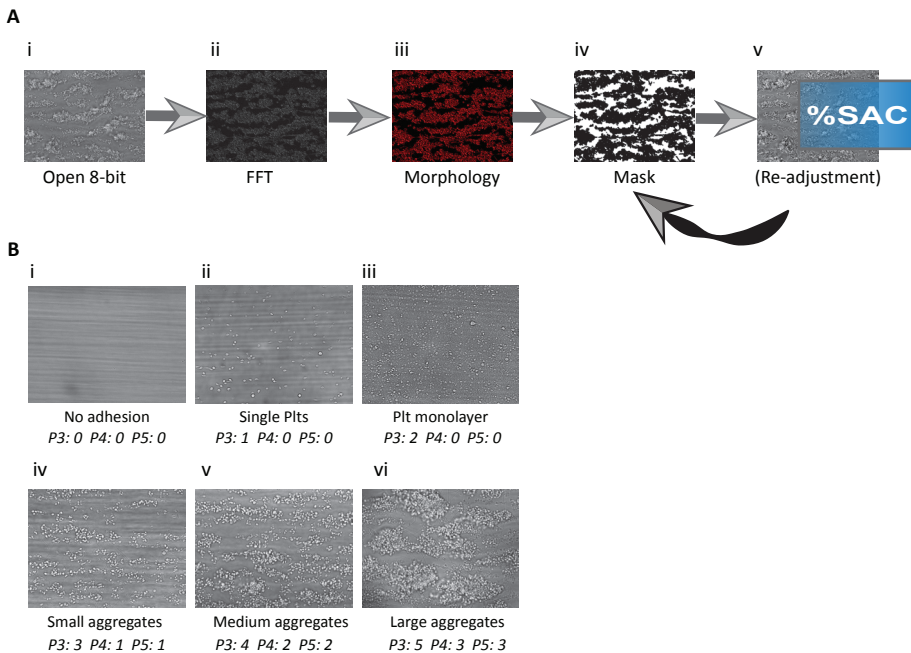
15. Coxon CH, Geer MJ, Senis YA. ITIM receptors: more than just inhibitors of platelet activation. *Blood*. 2017; 129: 3407-3418.
16. Kunzelmann K, Nilius B, Owsianik G, *et al*. Molecular functions of anoctamin 6 (TMEM16F): a chloride channel, cation channel, or phospholipid scramblase? *Pflugers Arch*. 2014; 466: 407-414.
17. De Witt SM, Verdood R, Cosemans JM, Heemskerk JW. Insights into platelet-based control of coagulation. *Thromb. Res*. 2014; 133: S139-148.
18. Mattheij NJ, Braun A, van Kruchten R, *et al*. Survival protein anoctamin-6 controls multiple platelet responses including phospholipid scrambling, swelling, and protein cleavage. *FASEB J*. 2016; 30: 727-737.
19. Agbani EO, Poole AW. Procoagulant platelets: generation, function, and therapeutic targeting in thrombosis. *Blood*. 2017; 130: 2171-2179.
20. May F, Hagedorn I, Pleines I, *et al*. CLEC-2 is an essential platelet-activating receptor in hemostasis and thrombosis. *Blood*. 2009; 114: 3464-3472.
21. Watson SP, Herbert JM, Pollitt AY. GPVI and CLEC-2 in hemostasis and vascular integrity. *J Thromb Haemost*. 2010; 8: 1457-1467.
22. Schaff M, Tang C, Maurer E, *et al*. Integrin $\alpha_6\beta_3$ is the main receptor for vascular laminins and plays a role in platelet adhesion, activation, and arterial thrombosis. *Circulation*. 2013; 128: 541-552.
23. Baaten CC, Meacham S, de Witt SM, *et al*. A synthesis approach of mouse studies to identify genes and proteins in arterial thrombosis and bleeding. *Blood*. 2018; 132: e35-46.
24. De Witt SM, Swieringa F, Cavill R, *et al*. Identification of platelet function defects by multi-parameter assessment of thrombus formation. *Nat Commun*. 2014; 5: 4257.
25. Brouns S, van Geffen JP, Heemskerk JW. High throughput measurement of platelet aggregation under flow. *Platelets*. 2018; 29: 662-669.
26. Van Geffen JP, Brouns S, Batista J, *et al*. High-throughput elucidation of thrombus formation reveals sources of platelet function variability. *Haematologica*. 2019; In press.
27. Suzuki-Inoue K, Kato Y, Inoue O, *et al*. Involvement of the snake toxin receptor CLEC-2, in podoplanin-mediated platelet activation, by cancer cells. *J Biol Chem*. 2007; 282: 25993-26001.
28. Hooley E, Papagrigoriou E, Navdaev A, *et al*. The crystal structure of the platelet activator aggretin reveals a novel (ab)₂ dimeric structure. *Biochemistry*. 2008; 47: 7831-7837.
29. Schindelin J, Arganda-Carreras I, Frise E, *et al*. Fiji: an open-source platform for biological-image analysis. *Nat Methods*. 2012; 9: 676-682.
30. Szklarczyk D, Franceschini A, Wyder S, *et al*. STRING v10: protein-protein interaction networks, integrated over the tree of life. *Nucleic Acids Res*. 2015; 43: D447-D452.
31. Shannon P, Markiel A, Ozier O, *et al*. Cytoscape: a software environment for integrated models of biomolecular interaction networks. *Genome Res*. 2003; 13: 2498-2504.
32. Bader GD, Hogue CW. An automated method for finding molecular complexes in large protein interaction networks. *BMC Bioinformatics*. 2003; 4: 2.
33. Miryala SK, Anbarasu A, Ramaiah S. Discerning molecular interactions: A comprehensive review on biomolecular interaction databases and network analysis tools. *Gene*. 2018; 642: 84-94.
34. R Core Team. R: A language and environment for statistical computing. Foundation for Statistical Computing, Vienna, Austria. (ed. Computing, F.f.S.) (Vienna, Austria, 2018).
35. Elvers M, Pozgai R, Varga-Szabo D, *et al*. Platelet hyperactivity and a prothrombotic phenotype in mice with a gain-of-function mutation in phospholipase C γ 2. *J Thromb Haemost*. 2010; 8: 1353-1363.
36. Kuijpers MJ, de Witt S, Nergiz-Unal R, *et al*. Supporting roles of platelet thrombospondin-1 and CD36 in thrombus formation on collagen. *Arterioscler Thromb Vasc Biol*. 2014; 34: 1187-1192.
37. Kuchay SM, Kim N, Grunz EA, Fay WP, Chishti AH. Double knockouts reveal that protein tyrosine phosphatase 1B is a physiological target of calpain-1 in platelets. *Mol Cell Biol*. 2007; 27: 6038-6052.
38. Mattheij NJ, Gilio K, van Kruchten R, *et al*. Dual mechanism of integrin $\alpha_{IIb}\beta_3$ closure in procoagulant platelets. *J Biol Chem*. 2013; 288: 13325-13336.
39. Petersen R, Lambourne JJ, Javierre BM, *et al*. Platelet function is modified by common sequence variation in megakaryocyte super enhancers. *Nat Commun*. 2017; 8: 16058.
40. Von Hundelshausen P, Agten SM, Eckardt V, *et al*. Chemokine interactome mapping enables tailored intervention in acute and chronic inflammation. *Sci Transl Med*. 2017; 9.
41. Suzuki-Inoue K, Inoue O, Ozaki Y. Novel platelet activation receptor CLEC-2: from discovery to prospects. *J Thromb Haemost*. 2011; 9: 44-55.
42. Nieswandt B, Schulte V, Bergmeier W, *et al*. Long-term antithrombotic protection by *in vivo* deple-

- tion of platelet glycoprotein VI in mice. *J Exp Med.* 2001; 193: 459-469.
43. Bender M, May F, Lorenz V, *et al.* Combined *in vivo* depletion of glycoprotein VI and C-type lectin-like receptor 2 severely compromises hemostasis and abrogates arterial thrombosis in mice. *Arterioscler Thromb Vasc Biol.* 2013; 33: 926-934.
 44. Matus V, Valenzuela G, Sáez CG, *et al.* An adenine insertion in exon 6 of human GP6 generates a truncated protein associated with a bleeding disorder in four Chilean families. *J Thromb Haemost.* 2013; 11: 1751-1759.
 45. Dumont B, Lasne D, Rothschild C, *et al.* Absence of collagen-induced platelet activation caused by compound heterozygous GPVI mutations. *Blood* 2009; 114: 1900-1903.
 46. Nagy M, Mastenbroek TG, Mattheij NJ, *et al.* Variable impairment of platelet functions in patients with severe, genetically linked immune deficiencies. *Haematologica.* 2018; 103: 540-549.
 47. Podrez EA, Byzova TV, Febbraio M, *et al.* Platelet CD36 links hyperlipidemia, oxidant stress and a prothrombotic phenotype. *Nat Med.* 2007; 13: 1086-1095.
 48. Pleines I, Eckly A, Elvers M, *et al.* Multiple alterations of platelet functions dominated by increased secretion in mice lacking Cdc42 in platelets. *Blood.* 2010; 115: 3364-3373.
 49. Mori J, Nagy Z, Di Nunzio G, *et al.* Maintenance of murine platelet homeostasis by the kinase Csk and phosphatase CD148. *Blood.* 2018; 131: 1122-1144.
 50. Musumeci L, Kuijpers MJ, Gilio K, *et al.* Dual-specificity phosphatase 3 deficiency or inhibition limits platelet activation and arterial thrombosis. *Circulation.* 2015; 131: 656-668.
 51. Kuijpers MJ, Schulte V, Bergmeier W, *et al.* Complementary roles of glycoprotein VI and $\alpha_2\beta_1$ integrin in collagen-induced thrombus formation in flowing whole blood *ex vivo*. *Faseb J.* 2003; 17: 685-687.
 52. Munnix IC, Strehl A, Kuijpers MJ, *et al.* The glycoprotein VI-phospholipase C γ 2 signaling pathway controls thrombus formation induced by collagen and tissue factor *in vitro* and *in vivo*. *Arterioscler Thromb Vasc Biol.* 2005; 25: 2673-2678.
 53. Offermanns S, Toombs CF, Hu YH, Simon MI. Defective platelet-activation in *Gaq*-deficient mice. *Nature.* 1997; 389: 183-186.
 54. Kuijpers MJ, Pozgajova M, Cosemans JM, *et al.* Role of murine integrin $\alpha_2\beta_1$ in thrombus stabilization and embolization: contribution of thromboxane A $_2$. *Thromb Haemost.* 2007; 98: 1072-1080.
 55. Grüner S, Prostedna M, Schulte V, *et al.* Multiple integrin-ligand interactions synergize in shear-resistant platelet adhesion at sites of arterial injury *in vivo*. *Blood* 2003; 102: 4021-4027.
 56. Hofmann I, Geer MJ, Vögtle T, *et al.* Congenital macrothrombocytopenia with focal myelofibrosis due to mutations in human G6b-B is rescued in humanized mice. *Blood.* 2018; 132: 1399-1412.
 57. Gilio K, van Kruchten R, Braun A, *et al.* Roles of platelet STIM1 and Orai1 in glycoprotein VI- and thrombin-dependent procoagulant activity and thrombus formation. *J Biol Chem.* 2010; 285: 23629-23638.
 58. Braun A, Varga-Szabo D, Kleinschnitz C, *et al.* Orai1 (CRACM1) is the platelet SOC channel and essential for pathological thrombus formation. *Blood.* 2009; 113: 2056-2063.
 59. Cosemans JM, Munnix IC, Wetzker R, *et al.* Continuous signaling via PI3K isoforms β and γ is required for platelet ADP receptor function in dynamic thrombus stabilization. *Blood.* 2006; 108: 3045-3052.
 60. Hirsch E, Bosco O, Tropel P, *et al.* Resistance to thromboembolism in PI3K γ -deficient mice. *FASEB J.* 2001; 15: 2019-2021.
 61. Gilio K, Harper MT, Cosemans JM, *et al.* Functional divergence of platelet protein kinase C (PKC) isoforms in thrombus formation on collagen. *J Biol Chem.* 2010; 285: 23410-23419.
 62. Konopatskaya O, Gilio K, Harper MT, *et al.* PKC α regulates platelet granule secretion and thrombus formation in mice. *J Clin Invest.* 2009; 119: 399-407.
 63. Chari R, Getz T, Nagy B, Jr., *et al.* Protein kinase C δ differentially regulates platelet functional responses. *Arterioscler Thromb Vasc Biol.* 2009; 29: 699-705.
 64. Konopatskaya O, Matthews SA, Harper MT, *et al.* Protein kinase C mediates platelet secretion and thrombus formation through protein kinase D2. *Blood.* 2011; 118: 416-424.
 65. Pleines I, Elvers M, Strehl A, *et al.* Rac1 is essential for phospholipase C- γ 2 activation in platelets. *Pflugers Arch.* 2009; 457: 1173-1185.
 66. Varga-Szabo D, Braun A, Kleinschnitz C, *et al.* The calcium sensor STIM1 is an essential mediator of arterial thrombosis and ischemic brain infarction. *J Exp Med.* 2008; 205: 1583-1591.
 67. Hughes CE, Finney BA, Koentgen F, Lowe KL, Watson SP. The N-terminal SH2 domain of Syk is required for (hem)ITAM, but not integrin, signaling in mouse platelets. *Blood.* 2015; 125: 144-154.

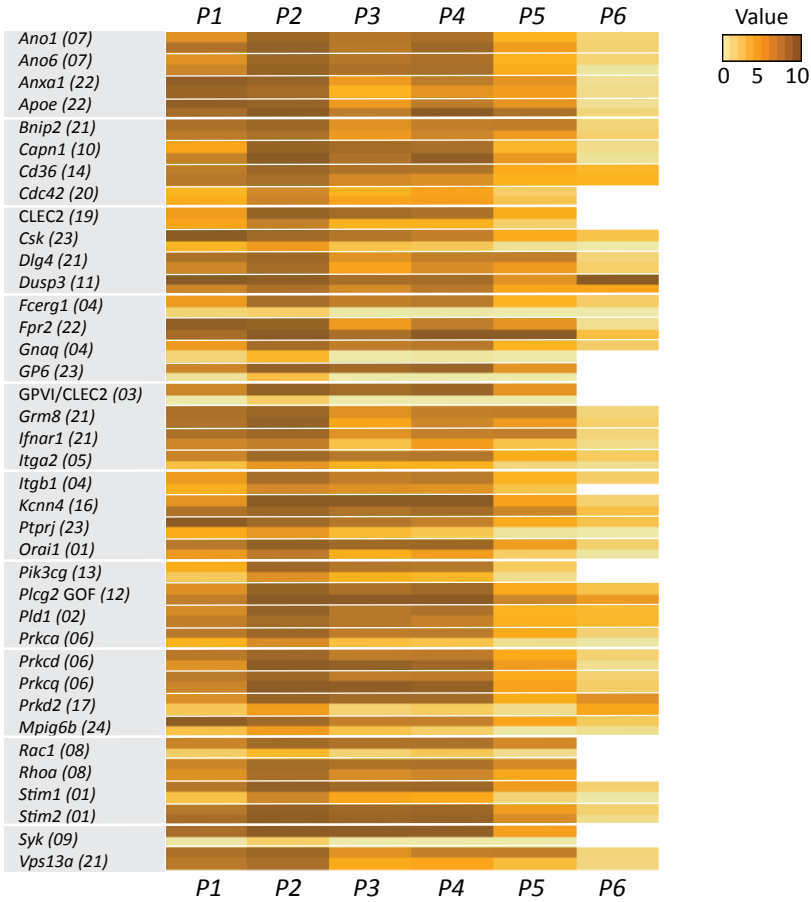
Supplemental data

Supplemental Table 1. Mean coefficient of variation (CV%) of parameters P1-5 for collagen dependent thrombus formation, comparing the results from 22 wild-type mice datasets (for databases see Figure 1).

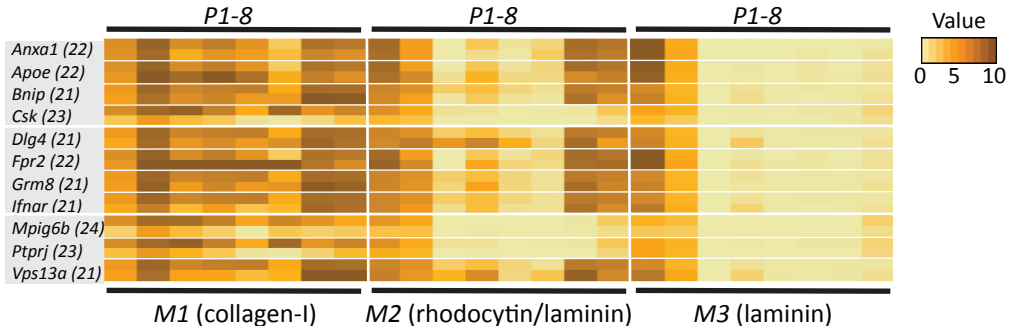
<i>Parameter</i>	<i>CV%</i>
<i>Platelet adhesion</i>	
<i>P1</i> , platelet surface area coverage (%SAC)	23.01
<i>Thrombus signature</i>	
<i>P2</i> , platelet aggregate coverage (%SAC)	24.88
<i>P3</i> , thrombus morphology score	3.40
<i>P4</i> , thrombus multilayer score	8.19
<i>P5</i> , thrombus contraction score	11.84



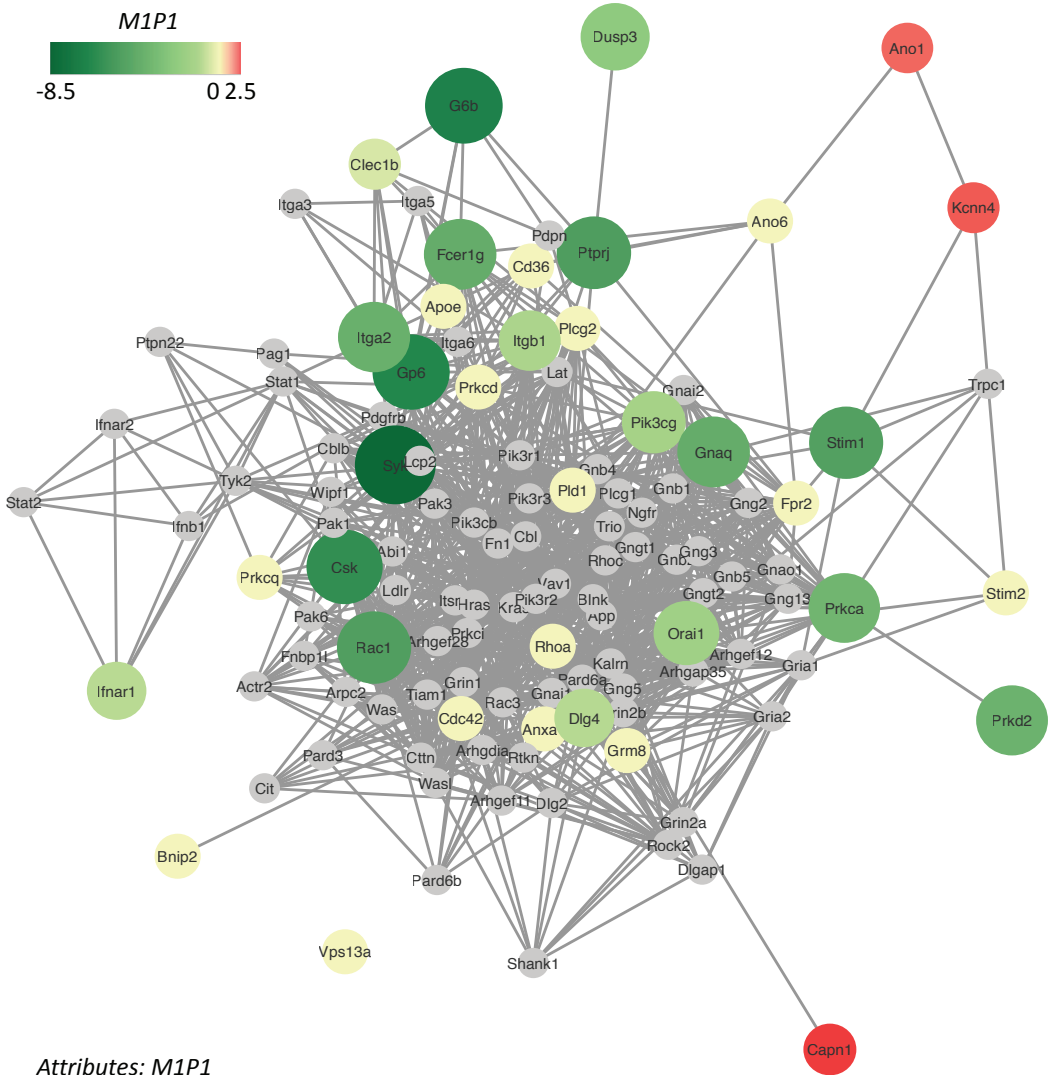
Supplemental Figure 1. Flow-chart of image analysis procedures. A) Brightfield and fluorescence microscopic images were analyzed for surface area coverage (SAC%) using scripts written in Fiji. Separate analysis steps were: (i) opened image in 8-bit; (ii) fast Fourier transformation (FFT) to correct for background noise; (iii) morphology filter with vertical/horizontal dilate and erode steps to enhance relevant structures; (iv) thresholding and conversion to mask overlays; (v) back-loop of manual re-adjustment of threshold, if not adequately set. Different scripts were used per image type and fluorescent label. **B)** Reference brightfield images for scoring of parameters *P3* (thrombus morphology score, scale 0-5), *P4* (thrombus multilayer score, scale 0-3), and *P5* (thrombus contraction score, scale 0-3).



Supplemental Figure 2. Overall effect of genetic modification or antibody treatment on parameters of collagen-dependent thrombus formation per gene and parameter. Blood from 22 corresponding wild-type (upper rows) and 38 modified (lower rows) mouse strains (databases as indicated in brackets) was perfused over collagen at a shear rate of 1000 s^{-1} (in two cases 1700 s^{-1}). For full details, see Table 1. Heatmap is shown of mean parameters is shown, after scaling (0-10) across all mouse strains. Parameters: platelet adhesion: *P1* (platelet SAC%); thrombus signature: *P2* (platelet aggregate SAC%), *P3* (thrombus morphology score), *P4* (thrombus multilayer score), *P5* (thrombus contraction score); and platelet activation: *P6* (phosphatidylserine exposure).



Supplemental Figure 3. Multi-parameter comparison of thrombus formation on three microspots for 11 genetically modified mouse strains. Blood from corresponding wild-type (upper rows) and 11 modified (lower rows) mouse strains (databases as indicated in brackets) was perfused over microspots M1-3 at a shear rate of 1000 s^{-1} . Mouse strains were arranged based on alphabetical order. For full details, see Table 1. Heatmap of mean parameters, scaled (0-10) across all mouse strains.



Attributes: M1P1

Supplemental Figure 4. Network of protein-protein interactions in collagen-dependent thrombus formation: platelet adhesion attributes. Network, constructed as in Figure 6, but with the core nodes color- and size-coded, based on altered platelet adhesion (*P1*) at surface M1.

Chapter 7

Comparison of the GPVI inhibitors losartan and honokiol

*Onselaer M-B, Nagy M, Pallini C, Pike JA, Perrella G, Quintanilla LG,
Eble JA, Poulter NS, Heemskerk JWM, Watson SP*

*Platelets: 2019; 8:1-11
Reprinted with permission*

Abstract

Losartan and honokiol are small molecules which have been described to inhibit aggregation of platelets by collagen. Losartan has been proposed to block clustering of GPVI but not to affect binding of collagen. Honokiol has been reported to bind directly to GPVI but only at a concentration that is three orders of magnitude higher than that needed for inhibition of aggregation. The mechanism of action of both inhibitors is so far unclear. In the present study, we confirm the inhibitory effects of both agents on platelet aggregation by collagen and show that both also block the aggregation induced by the activation of CLEC-2 or the low affinity immune receptor FcγRIIa at similar concentrations. For GPVI and CLEC-2, this inhibition is associated with a reduction in protein tyrosine phosphorylation of multiple proteins including Syk. In contrast, on a collagen surface, spreading of platelets and clustering of GPVI (measured by single molecule localization microscopy) was not altered by losartan or honokiol. Furthermore, in whole- blood, both inhibitors suppressed the formation of multi-layered platelet thrombi at arteriolar shear rates at concentrations that hardly affect collagen-induced platelet aggregation in platelet rich plasma. Together, these results demonstrate that losartan and honokiol have multiple effects on platelets which should be considered in the use of these compounds as anti-platelet agents.

Introduction

Hemostasis is a finely regulated process triggered after vessel wall injury serving to curtail blood loss and to restore vascular integrity. One of the key components of hemostasis are platelets, which rapidly adhere and aggregate at sites of a lesion.¹ Glycoprotein VI (GPVI), a member of the immunoglobulin superfamily, is the major signaling receptor for collagen and fibrin.²⁻⁵ GPVI is expressed on the surface membrane in complex with the FcRγ chain which contains an immunoreceptor tyrosine activation motif (ITAM) characterized by two YxxL/I sequences (where x is any amino acid) separated by 12 amino acids. Src kinases associated with the cytoplasmic tail of GPVI initiate phosphorylation of two conserved tyrosines in the ITAM of the FcRγ chain.^{6,7} This leads to the recruitment and activation of Syk via its SH2 domains, and triggering of a phosphorylation complex consisting of adapter and signaling proteins that culminates in Ca²⁺ mobilization and platelet activation.^{8,9}

The C-type lectin-like receptor, CLEC-2, has a single copy of a YxxL sequence known as a hemITAM. Phosphorylation of two CLEC-2 receptors leads to binding of Syk and initiation of a signaling cascade that is similar to that driven by the GPVI- FcRγ-chain.¹⁰⁻¹²

To date, podoplanin is the only established endogenous ligand for CLEC-2. Podoplanin is expressed on the surface of a variety of cells including epithelial and stromal cells but is absent from vascular endothelial cells. Although its function in hemostasis is not clear, there is evidence that CLEC-2 play a pivotal role in arterial and venous thrombosis.^{13,14}

Losartan, an angiotensin II receptor antagonist, has been proposed to inhibit clustering but not binding of GPVI to collagen,^{15,16} leading to inhibition of platelet activation *in vitro* and reduced platelet accumulation after carotid injury in mice.¹⁷⁻²⁰ Honokiol is a natural bioactive molecule isolated from *Magnolia* species, which is used in traditional Chinese medicine. Honokiol is a multi functional compound with many potential therapeutic properties, including anti-oxidant, anti-inflammatory, anti-cancer, anti-depressant and anti-neurodegenerative activities.²¹⁻²³ Honokiol also has anti-thrombotic effect, and has been shown to bind to GPVI at concentrations that are three orders of magnitude higher than those required for inhibition of platelet aggregation, suggesting an alternative mechanism of inhibition.^{24,25} In the present study, we have further interrogated the mechanism of action for both inhibitors.

Material and methods

Reagents

Horm collagen and collagen diluent were purchased from Nycomed (Munich, Germany). CRP (ten glycine-proline-hydroxyproline [GPO] repeats) was crosslinked as described.²⁶ Rhodocytin was purified in the Eble lab (University of Münster, Germany) from the crude venom of *Calloselasma rhodostoma*. The mouse monoclonal antibodies (mAbs) anti-phosphotyrosine clone 4G10 (05–321) and rabbit polyclonal anti-FcR γ -chain (06–727) were purchased from Merck Millipore (Watford, UK). The rabbit polyclonal antibody anti-Syk (sc-1077), the mouse mAbs anti-Syk 4D10 (sc-1240) and anti-FcR γ -chain (sc-390222) were purchased from Santa Cruz (Wembley, UK). All other reagents including losartan, honokiol and the anti-mouse IgG (Fc specific) F(ab')₂ fragment antibody were purchased from Sigma-Aldrich (Poole, UK), or came from described sources.³ Losartan was dissolved in water and honokiol in DMSO. The mouse monoclonal mAb IV.3 against the low affinity immune receptor Fc γ RIIA was purified from the hybridoma obtained from the American Type Culture Collection. 1G5-Fab against Pan-GPVI was gift from Elizabeth Gardiner (Australian National University, Canberra, Australia).

Platelet isolation

Venous blood was taken from healthy volunteer using 3.8% (v/v) sodium citrate (1:9) as the anticoagulant with informed consent according to the guidelines of the local ethics committee (ERN_11-0175). All steps of this study complied with the ethical principles according to the Declaration of Helsinki. Acid Citrate Dextrose (ACD, 1:10) was added to the blood. Platelet-rich plasma (PRP) was obtained by centrifugation at 200 g for 20 min at room temperature. Washed platelets were obtained by centrifugation at 1000 g for 10 min at room temperature using prostacyclin (2.8 μ M) and resuspended in modified Tyrode's-HEPES buffer (134 mM NaCl, 0.34 mM Na₂HPO₄, 2.9 mM KCl, 12 mM NaHCO₃, 20 mM HEPES, 5 mM glucose, 1 mM MgCl₂; pH7.3) Washed platelets were used at 2×10^7 /mL for static adhesion or 5×10^8 /mL for other studies.

Platelet aggregation

Washed platelets at 5×10^8 /mL were pretreated for 5 min with different concentrations of losartan, honokiol or solvent controls prior to stimulation by collagen, rhodocytin, thrombin or mAb IV.3 cross-linked with F(ab')₂. Light transmission was recorded at 37°C with stirring (1200 rpm) in an aggregometer (Chrono-Log Stago, Havertown, Pennsylvania, USA). ATP secretion was monitored in washed platelets in parallel with platelet aggregation by adding firefly luciferase and luciferin (2 μ M) and comparing the luminescence generated by platelet ATP release with an ATP standard.

Platelet spreading

Glass coverslips were coated in the presence of 10 μ g/mL of collagen or fibrin generated as described previously.⁵ Following washing with PBS, the coverslips were blocked with 5 mg/mL heat-inactivated bovine serum albumin (BSA) in PBS for 60 min. Washed platelets 2×10^7 /mL were incubated with honokiol (25 μ M), losartan (25 μ M) or solvent controls prior to be allowed to spread for 30 or 45 min, for human or mouse platelets respectively, at 37°C. The cells were then washed with PBS followed by fixation with paraformaldehyde (3.7%) for 10 min. For actin staining, the platelets were permeabilized with 0.1% Triton X-100 for 5 min and stained with Alexa-488-labeled phalloidin for 45 min in the dark. Platelets were imaged on a Zeiss Axiovert 200 M microscope. Fluorescence from platelets was analyzed using ImageJ (NIH, Bethesda, USA). In each independent experiment, 5 random fields of view per condition were analyzed, with at least 100 platelets in total per condition.

Protein phosphorylation study

In presence of eptifibatide (9 μM), washed platelets $5 \times 10^8/\text{mL}$ were pretreated for 5 min with honokiol (25 μM), losartan (25 μM) or solvent controls prior to activation by collagen (3 $\mu\text{g}/\text{mL}$), rhodocytin (150 μM) or thrombin (1 U/mL) with or without fibrinogen (200 $\mu\text{g}/\text{mL}$) at 37°C with stirring (1200 rpm) in an aggregometer for 60 sec. Activation was terminated with 2x ice-cold lysis buffer (300 mM NaCl, 20 mM Tris, 2 mM EGTA, 2 mM EDTA, and 2% IGEPAL CA630 [NP-40 equivalent], pH 7.4, plus 2. mM Na_3VO_4 , 100 mg/mL AEBSF [4-{2-aminoethyl} benzenesulfonyl fluoride hydrochloride], 5 mg/mL leupeptin, 5 mg/mL aprotinin, and 0.5 mg/mL pepstatin). Whole cell lysates (WCLs) were prepared by boiling a sample of lysate with sodium dodecyl sulfate (SDS) sample buffer. Syk was immunoprecipitated with 2 μg of Syk antibody (4D10) and incubated protein A-Sepharose beads overnight at 4°C. The beads were then washed, and proteins were eluted by boiling in SDS sample buffer. Immunoprecipitates (IPs) and WCLs were separated by SDS-polyacrylamide gel electrophoresis, electrotransferred, and western blotted. All primary antibodies were used diluted at 1/1,000 in TBS-Tween-BSA 5% for overnight at 4°C. The secondary antibodies were used diluted at 1/10,000 in TBS-Tween for 1 h at room temperature. Western blots were imaged with autoradiographic film.

Cell/NFAT assay

The following constructs and plasmids were used for GPVI transfections into cells for NFAT-luciferase assays as previously described.²⁷ Human GPVI subcloned into pcDNA3 with a C-terminal Myc tag and human FcR γ (untagged) in pEF6 were generated. The nuclear factor of activated T cells (NFAT)- luciferase reporter containing three copies of the distal NFAT site from the IL-2 promoter as described previously.²⁸ In brief, indicated amounts of DNA of each construct and 15 μg of NFAT- luciferase reporter construct were transfected by electroporation at 350 V and 500 μF microfarads into 2×10^7 DT40 cells. The transfected cells were incubated with losartan at 25 μM or 250 μM and stimulated by collagen at 10 $\mu\text{g}/\text{mL}$ for 6 h at 37°C. Luciferase activity was measured with a Centro LB960 microplate luminometer (Berthold Technologies, Germany).

Platelet spreading and staining for STORM imaging

For STORM imaging, 35 mm #1.5 (0.17 mm) glass bottomed MatTek dishes (MatTek Corporation, USA) were coated with 10 $\mu\text{g}/\text{mL}$ Horm collagen diluted in manufacturer-supplied diluent or in 10 $\mu\text{g}/\text{mL}$ cross-linked collagen related peptide (CRP-XL) using phosphate-buffered saline (PBS) and stored overnight at 4°C. Dishes were blocked with 5 mg/mL BSA for 1 h at room temperature then washed with PBS. Washed and rested human

platelets, diluted to 2×10^7 /mL in modified Tyrode's buffer were incubated with 2 μ g/mL 1G5-Fab against Pan-GPVI for 5 min at 37°C. The labeled platelets were then incubated with 25 μ M losartan or 25 μ M honokiol or vehicle (PBS for losartan or DMSO for honokiol) for another 5 min at 37°C before being transferred onto the coated MatTek dishes. Platelets were allowed to spread for 45 min at 37 °C and rinsed once with PBS to remove unbound platelets. Adhered platelets were fixed for 10 min with 10% neutral buffered formalin solution (Sigma, Poole, UK), followed by 5 min permeabilization with 0.1% Triton X-100 in PBS. After PBS washes, the platelets were blocked for 1 h at room temperature with 1% BSA + 2% goat serum (in PBS). 1G5-Fab-labeled platelets were secondary labeled with anti-mouse-Alexa647 antibody and stained for actin with Alexa488- phalloidin (both from ThermoFisherScientific; 1:300 dilution in block buffer) for 1 h at room temperature. Platelet samples were washed at least three times with PBS prior to imaging.

STORM imaging

Single-molecule images of platelet GPVI were acquired using a 100×1.49 N.A. TIRF objective lens on a Nikon N-STORM system in TIRF and dSTORM mode. The system was equipped with a Ti-E stand with Perfect Focus, Agilent Ultra High Power Dual Output Laser bed (containing a 170 mW 647-nm laser and a 20 mW 405 laser) and an Andor IXON Ultra 897 EMCCD camera. Fluorophore blinking was achieved by imaging the samples in a PBS-based buffer containing 100 mM MEA-HCl, 50 μ g/mL glucose oxidase and 1 μ g/mL catalase as detailed in Metcalf et al.²⁹ Single color (Alexa647) imaging was performed using the N-STORM emission cube with reactivation of fluorophore blinking achieved by increasing the 405 nm laser power by 5% every 30 sec. For each image, 20,000 frames were acquired using the Nikon NIS Elements v4.5 software with an exposure time of 9.2 ms, gain 300 and conversion gain 3.

Image reconstruction to obtain localization coordinates for each identified fluorescence blink was undertaken with the Nikon STORM analysis module 3.2 using drift correction and Gaussian rendering. For each condition, 5 different fields of view (FOV) from 3 independent experiments were captured. Only data points with a photon count > 500 were included in the cluster analysis.

For the analysis of dSTORM data, localized data points within each FOV were grouped into clusters using density-based clustering of applications with noise (DBSCAN). The clustering was executed using the open-source software KNIME and the R package 'dbscan' (work flow available on request).³⁰ The radius of local neighborhood was set to 40 nm and 50 nm, and the minimum number of directly reachable points was set to 15 and 10, for CRP and collagen respectively. Cluster area was calculated by placing a circle

of radius 30 nm over every detection in a cluster and calculating the union of these circles. This was estimated using a grid with pixel size 5 nm and image based dilation. The analysis was performed on whole FOVs and the quantitative cluster data was outputted as a spreadsheet. Graphs and statistics of the clustering data were calculated in GraphPad Prism 7.

Whole blood thrombus formation

Whole blood thrombus formation was assessed under flow conditions as described elsewhere.³¹ In brief, glass coverslips were coated with 2 μl of 50 $\mu\text{g}/\text{mL}$ collagen type I and mounted onto a transparent parallel-plate flow chamber. Blood samples treated with honokiol or losartan or vehicle were re-calcified with 3.75 mM MgCl_2 and 7.5 mM CaCl_2 in the presence of 40 μM active-site thrombin inhibitor PPACK, prior to experiment. Re-calcified blood samples were perfused for 6 min at wall shear rate of 1000 s^{-1} over the microspot surface. Representative phase-contrast microscopic images were captured using a fast line-scanning Zeiss LSM7 microscope equipped with 63x oil-immersion objective. Images were analyzed using Fiji software.³² Four outcome parameters were assessed: platelet surface area coverage, thrombus morphological score (0–5), thrombus contraction score (0–3) and platelet multilayer score (0–3) as previously explained.^{31,33} Scoring was done by visual inspection of brightfield images based on a predefined score system. Morphological score indicates the aggregate formation by using a 5-point scale: 0: no platelet adhesion; 1: single platelet (>15) adhesion, 2: platelet monolayer; 3: small aggregates; 4: medium size aggregates; 5: large aggregates respectively. Thrombus contractility is appreciated based on a 3-point scale, where 0: no aggregate formation, 1: loose aggregates; 2: aggregates started to contract; 3: tightly packed, dense aggregates respectively. Multilayer score refers to thrombus volume on a 3-point scale, where 0: monolayer of platelets; 1: 2 layers of platelets; 2: multiple layer of platelets; 3: large, really high thrombi respectively.

Data analysis

Statistical analysis was realized by ANOVA with Turkey post-test. A P value of <0.05 was considered to be significant.

Results

Comparison of losartan and honokiol in platelet aggregation

In a previous study, platelet aggregation induced by 10 $\mu\text{g}/\text{mL}$ of collagen was found to be inhibited by losartan with an IC_{50} of 6.3 μM ²¹ and by honokiol with an IC_{50} of 0.6 μM .²⁶ In Figure 1, we demonstrate, by comparing the two compounds, that losartan

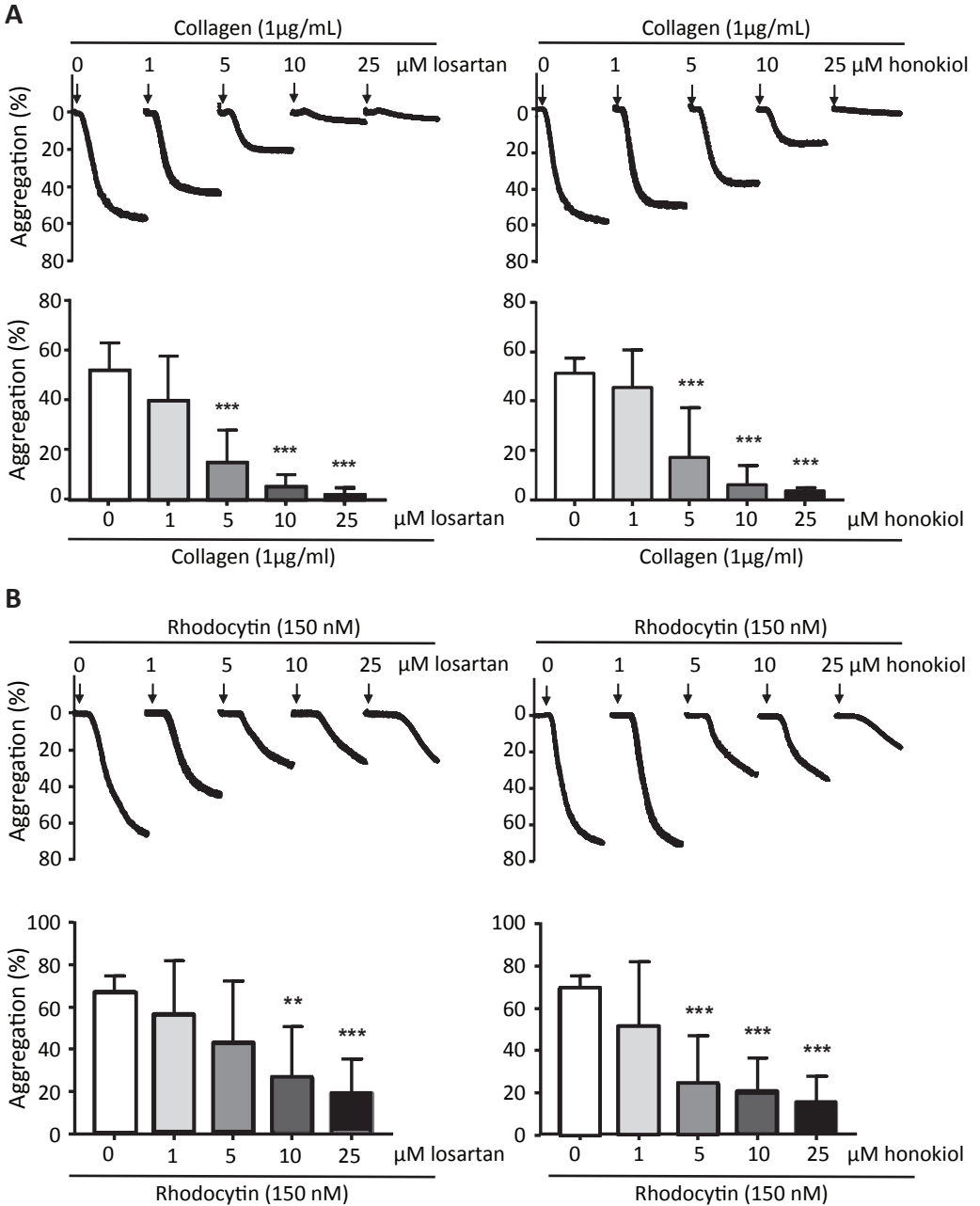
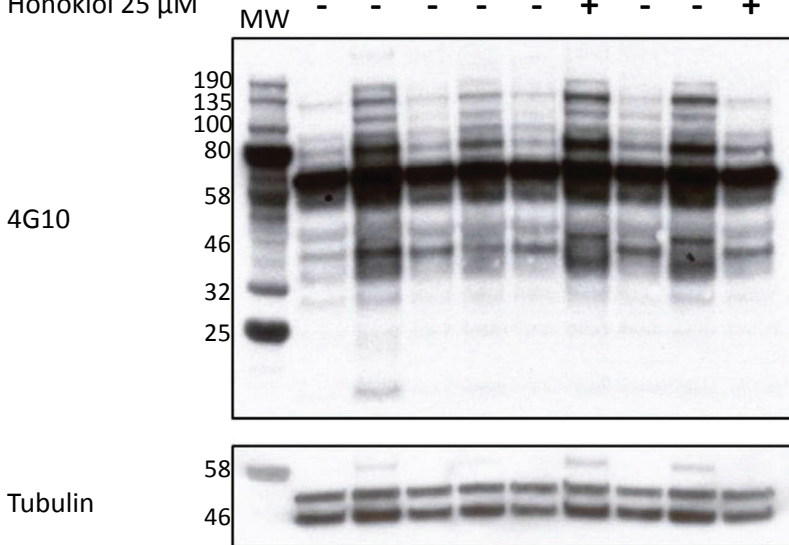


Figure 1. Losartan and honokiol dose-dependently reduce aggregation of washed platelets induced by collagen or rhodocytin. Washed platelets were pretreated with different concentrations of losartan or honokiol for 3 min before stimulation with (A) collagen 1µg/mL or (B) rhodocytin 150 nM. Bar graphs represent results from a total of 5 independent experiments and results are shown as mean ± SD **P < 0.01, ***P < 0.001.

and honokiol dose-dependently inhibited aggregation of washed platelets induced by 1 $\mu\text{g}/\text{mL}$ collagen with an IC_{50} of 3.7 μM for losartan and of 4.6 μM for honokiol. At these concentrations, neither inhibitor had an effect on platelet activation by thrombin or the thromboxane mimetic U46619 (data not shown). On the other hand, both losartan and honokiol delayed and reduced aggregation to the CLEC-2 agonist rhodocytin with IC_{50} values of 3.5 μM and 2.1 μM , respectively (Figure 1) and furthermore inhibited the platelet response to the low affinity immune receptor $\text{Fc}\gamma\text{RIIA}$ over the same

A

Collagen 3 $\mu\text{g}/\text{mL}$	-	+	+	+	+	-	-	-	-
Rhodocytin 150 nm	-	-	-	-	-	+	+	+	+
Losartan 25 μM	-	-	+	-	-	-	+	-	-
Honokiol 25 μM	-	-	-	-	-	+	-	-	+



B

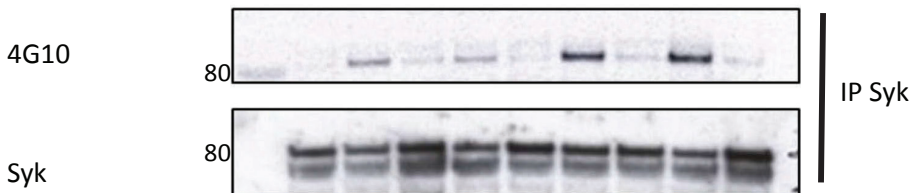


Figure 2. Losartan and honokiol inhibit platelet protein tyrosine phosphorylation, including Syk, induced by collagen or rhodocytin. Washed platelets were pre-treated with 25 μM of losartan or honokiol for 3 min before stimulation with collagen 3 $\mu\text{g}/\text{mL}$ or rhodocytin 150 nM. Stimulations were stopped with addition of lysis buffer. (A) whole-cell lysate (WCL) and (B) immunoprecipitate (IP) of Syk. WCL and IP were separated by SDS-polyacrylamide gel electrophoresis and Western blotted for pTyr and Syk, respectively. The first lane shows the molecular weight markers (MW).The results are representative of 3 independent experiments.

concentration range (Supplemental Figure 1). Collagen and rhodocytin induce a similar pattern of increase in tyrosine phosphorylation, which was abrogated by losartan or honokiol at approximately 10x their IC_{50} values (Figure 2). In addition, both inhibitors blocked tyrosine phosphorylation of the tyrosine kinase Syk (Figure 2).

Losartan and honokiol were less potent in the presence of plasma, due to protein binding, requiring a concentration of 250 μ M to achieve inhibition of aggregation (Supplemental Figure 2).³² At this concentration, losartan inhibited NFAT activation by GPVI and CLEC-2 in a transfected cell line model in the presence of serum (Figure 3A), but did not have an effect on constitutive signaling (*i.e.* ligand independent signaling) of either receptor (Figure 3B). Honokiol could not be tested in the cell line model due to the effects of vehicle DMSO on NFAT activity.

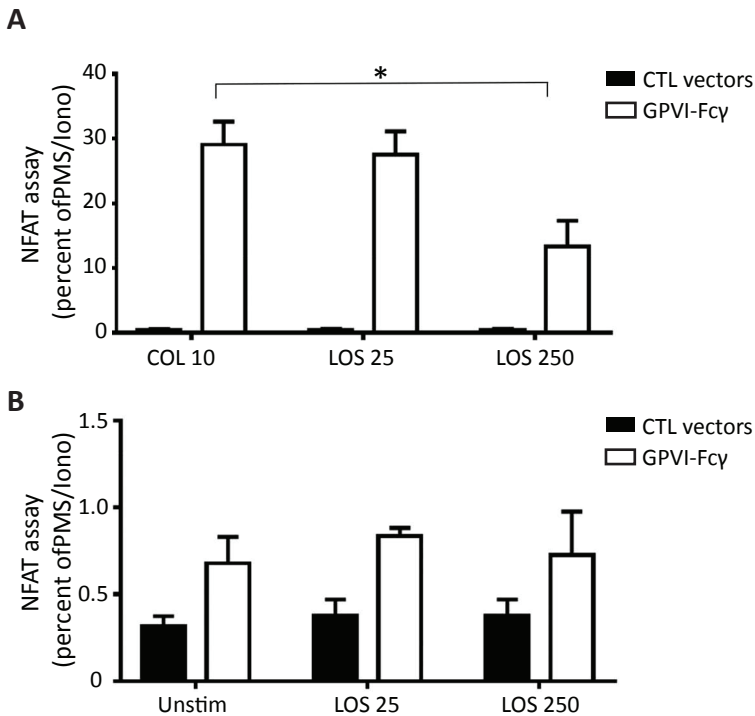


Figure 3. Losartan reduces signaling induced by collagen in transfected DT40 cells. DT40 B-cells were transfected with a NFAT-luciferase reporter construct, a β -galactosidase construct to control for transfection efficiency, and two GPVI and FcR γ -chain(Fc γ) expression constructs or empty control (CTL) vectors. Sixteen hours post-transfection, expression of GPVI was confirmed by flow cytometry (data not shown). The transfected cells were pre-treated with losartan (LOS) at 25 μ M or 250 μ M. They were either (A) stimulated with collagen (10 μ g/mL) or PMA (50 ng/mL) plus ionomycin (1 μ M) or (B) unstimulated. Six hours later, cells were lysed and assayed for luciferase and β -galactosidase. Luciferase data were normalized for β -galactosidase expression. Error bars represent the SEM from three independent experiments. * $P < 0.001$

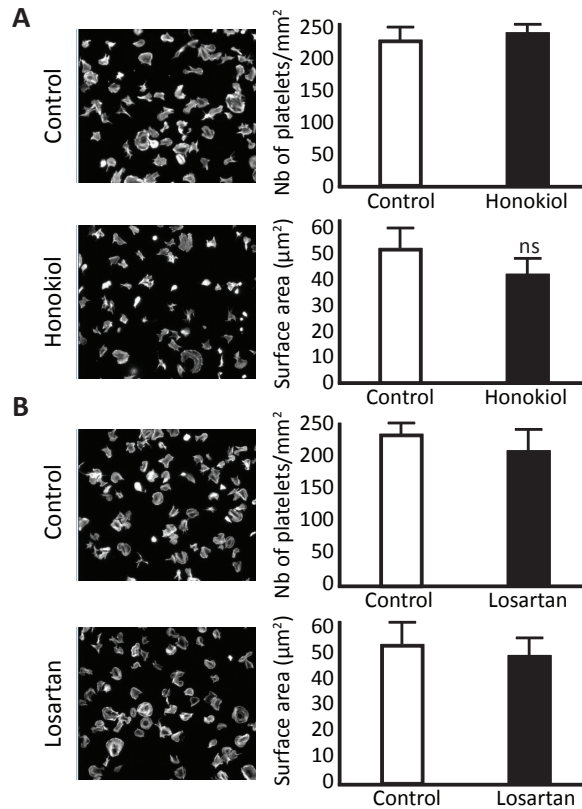


Figure 4. Losartan and honokiol do not affect platelet spreading on collagen. Glass coverslips were coated with collagen. Washed platelets were pre-treated with 25 μM of (A) losartan or (B) honokiol before spreading on collagen, followed by fixation and staining for actin with Alexa-488 phalloidin. Scale bar, 5 μm. Bar graphs illustrate quantification of the surface area covered with platelets per field, and the numbers of platelets counted per field. Data are shown as mean ± SD and are representative of three experiments.

Losartan and honokiol do not block platelet spreading or ligand binding to GPVI

Losartan and honokiol (both used at 25 μM in Tyrode's buffer) did not have significant effects on the adhesion or spreading of platelets on collagen (Figure 4). Similar results were observed at 100 μM (data not shown). Further, neither compound altered clustering of GPVI by CRP (Figure 5) or by collagen (not shown) as measured by single molecule localization microscopy (dSTORM). This result is consistent with the lack of interference of either compound with GPVI-collagen binding, in an ELISA competitive binding assay using recombinant GPVI (Supplemental Figure 3).²¹

Losartan and honokiol inhibit thrombus formation

Whole blood perfusion experiments were performed on collagen coated microspots to assess the effects of platelet pretreatment with losartan or honokiol (25–100 μM). Thrombi were analyzed for platelet deposition (% surface area coverage) and

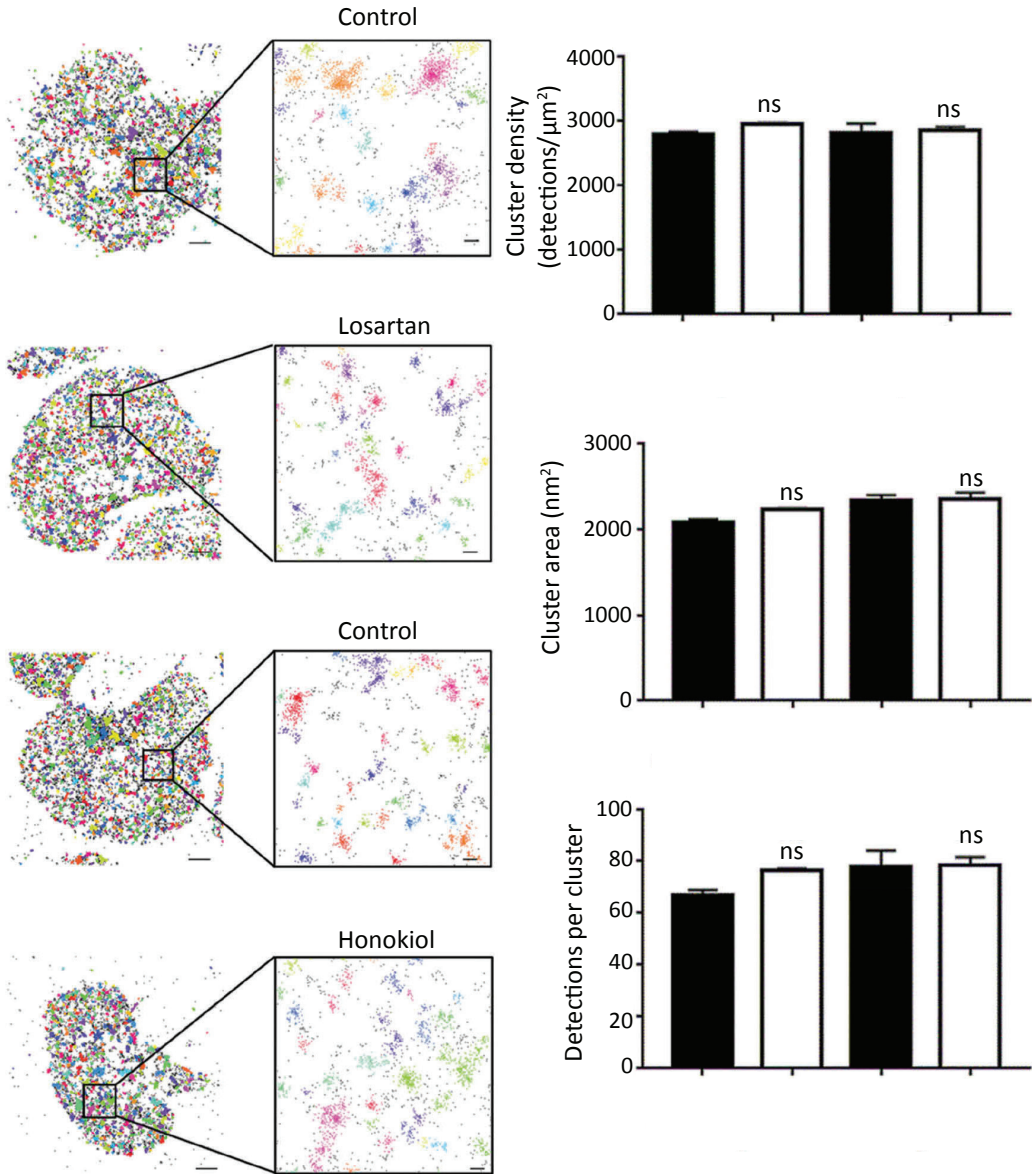


Figure 5. Losartan and honokiol do not affect clustering of GPVI. Glass coverslips were coated with CRP. Washed platelets were pre-incubated with 1G5 Fab (pan-GPVI), then pretreated with 25 μM losartan, 25 μM honokiol or vehicle before spreading on CRP. Following fixation, GPVI was secondary labeled with mouse-Alexa647 and actin was labeled with Alexa488-phalloidin. The single molecule localization data acquired by STORM was analyzed for clustering using DBSCAN. Different colors represent different clusters (with black dots representing noise). For each condition, 5 different fields of view (FOV) from 3 independent experiments were captured. Representative cropped scatter plots for each condition show the output of the DBSCAN clustering algorithm (left panel). Scale bars: 1 μm and 0.1 μm . Bar graphs show quantification of cluster density, cluster area and number of detections per cluster. Mean+SEM ($n=3$) (right panel).

visual inspection using a predefined score system (morphological, contraction and multilayer score).³³ Losartan treatment did not affect platelet deposition (Figure 6B) but decreased thrombus contraction and multilayer scores (Figure 6D,E) as an indication of lower thrombus integrity and the presence of loose platelet aggregates. In contrast, honokiol pretreatment resulted in a dose-dependent decrease in platelet adhesion (lower surface area coverage of platelets) to collagen and significantly decreases the contraction and multilayer scores (Figure 7), pointing to a suppressed formation of tightly packed thrombi. These results show that both losartan and honokiol affect formation of thrombi in whole blood but in different ways. These concentrations of the two inhibitors have little effect however on the response to GPVI activation of platelets in platelet rich plasma due to protein binding (see above).

Discussion

This work provides new information on the platelet inhibition mechanisms of losartan and honokiol. We confirmed that losartan and honokiol inhibit platelet aggregation by collagen. However, while the IC₅₀ for losartan was similar to that previously reported,²⁰ the IC₅₀ for honokiol is almost one order of magnitude higher than in the original report.²¹ The explanation for this difference is unclear. Interestingly, both losartan and honokiol inhibited platelet activation by the (hem)ITAM receptors rhodocytin and FcγRIIA at similar concentrations to those for inhibition by collagen. This effect was mediated by inhibition of tyrosine phosphorylation, including Syk which plays a proximal role in signaling by all three receptors. Inhibition of the response to GPVI was not due to a direct competition with collagen since losartan did not block binding of recombinant GPVI to collagen¹⁵ and honokiol inhibited this binding at a concentration that is three orders of magnitude greater than required for inhibition of aggregation.²⁵

Although both losartan and honokiol inhibited platelet aggregation and Syk phosphorylation, they were unable to prevent clustering of GPVI or spreading on collagen at concentrations up to 100 μM. This may be related to the relatively high concentration of collagen on the surface thus overcoming the inhibitory effect of the two reagents. Alternatively, neither agent may be able to inhibit clustering of GPVI on a surface and therefore inhibit activation, in contrast to previous results in suspension using an antibody that recognizes the dimeric form of GPVI (9E18) conjugated with Duolink PLA probes.¹⁵ Losartan had no effect on constitutive signaling by GPVI in transfected DT40 cells, which may be a functional readout for clustering of the immunoglobulin receptor.

Losartan and honokiol are highly protein bound in plasma^{18,32,34} necessitating use of higher concentrations in the presence of plasma to achieve the same level of inhibition as seen in washed platelets. Unexpectedly however, both inhibitors suppressed collagen-dependent platelet aggregation in whole blood under flow conditions at concentrations

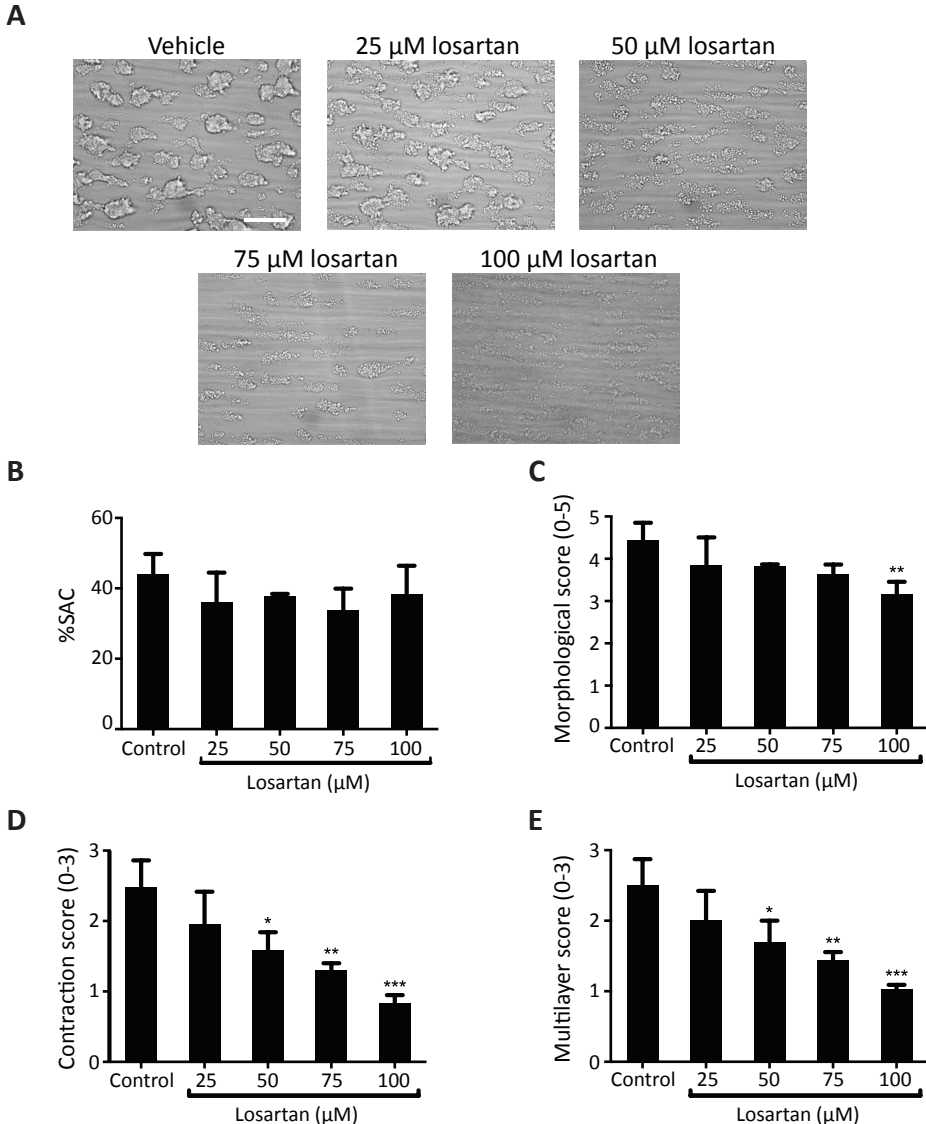


Figure 6. Losartan inhibits the formation of contracted, multilayered platelet thrombi under flow. Whole blood treated with vehicle solution or losartan was perfused over collagen surface for 6 min at wall shear rate of 1000 s^{-1} . Phase contrast images were captured and shown as representative images (A). Platelet surface area coverage (% SAC), thrombus morphological score (range 0-5), thrombus contraction score (0-3) and platelet multilayer score (0-3) were determined (B-E). Data are presented as mean \pm SEM (n=4). *P < .05, **P < 0.01, ***P < 0.001.

that hardly affect platelet aggregation in plasma as measured by light transmission aggregometry. Furthermore, the mode of inhibition under flow was distinct for the two inhibitors: while both suppressed the formation of tight platelet thrombi, honokiol also interfered with platelet adhesion. One explanation for the inhibition observed in whole blood could be based on their lipophilic characteristic causing disruption of lipid-to-lipid or lipid-protein interactions^{35,36} or blocking protein-protein interactions.

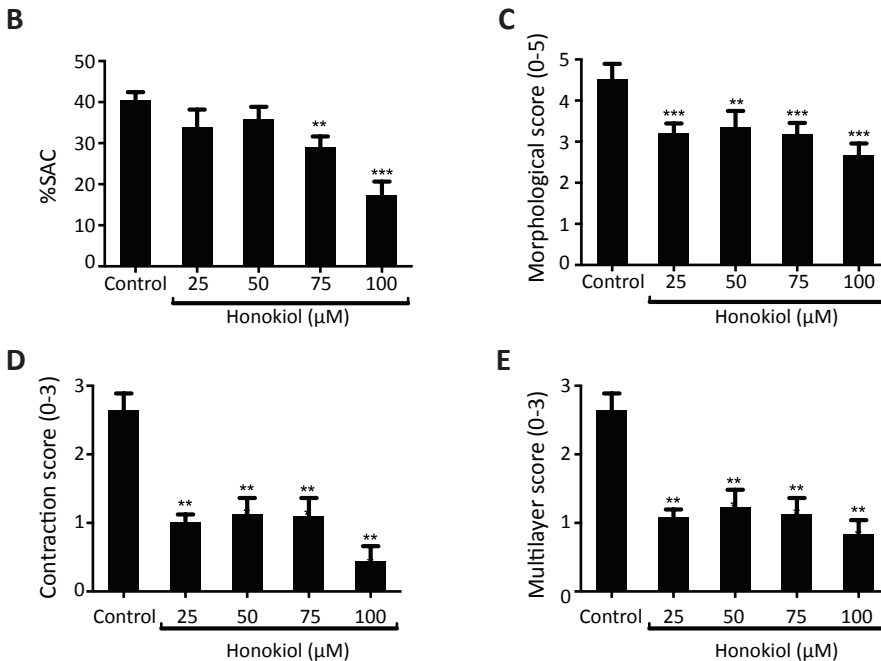
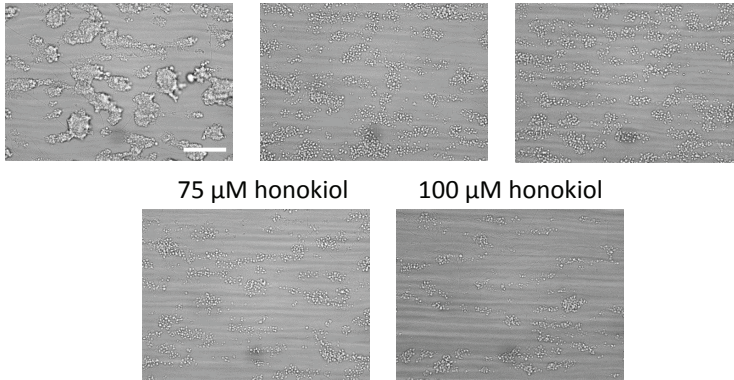


Figure 7. Honokiol inhibits both platelet adhesion and formation of multilayered platelet thrombi under flow. Whole blood treated with vehicle solution or honokiol was perfused over collagen type I for 6 min at wall shear rate of 1000 s⁻¹. Phase contrast images were captured and shown as representative images (A). Platelet surface area coverage (% SAC), thrombus morphological score (range 0-5), thrombus contraction score (0-3) and platelet multilayer score (0-3) were determined (B-E). Data are presented as mean ± SEM (n=4). *P < 0.05, **P < 0.01, ***P < 0.001.

In addition, honokiol has been reported to disrupt the integrity of the inner membrane of mitochondria.³⁷ These data could explain the pleiotropic impacts on various cells in different pathologies.³⁸

In this study, we compared two small molecules described as specific inhibitors for GPVI on different aspects of platelets activation and function. Although both compounds were able to inhibit platelet aggregation induced by collagen, we could not confirm the original potency of honokiol on this response and we found that neither agent inhibited spreading of platelets on collagen. The likely explanation is that both compounds are unable to inhibit clustering of GPVI of platelets on a surface. Both inhibitors also blocked rhodocytin and FcγRIIA-induced CLEC-2 activation demonstrating that they are not specific to GPVI at the concentrations used. This is illustrated by the inhibition of platelet aggregation on whole blood under flow conditions at concentrations that have a minimal effect on platelet activation by collagen in plasma. The multiplicity of effects of the two inhibitors should be considered in the context of their use as anti-platelet agents.

Acknowledgements

SPW holds a BHF Chair (CH03/003) and ATH holds a BHF Studentship (FS/15/71/31677). JAE is supported by Deutsche Forschungsgemeinschaft (DFG grant: Eb177/13-1).

Authorship Contributions

M-B.O. designed and performed research, analyzed and interpreted data, made the figures and wrote the manuscript; M.N., C.P., and J.A. P. performed experiments, analyzed and interpreted data, and made figures; G.P., L.G.C. and N.S.P. performed experiments; J.A.E. purified rhodocytin and edited the manuscript; J.M.W.H. designed research, interpreted data and edited the manuscript; S.P.W. supervised research, analyzed and interpreted data, wrote the manuscript. All authors read and approved the final manuscript.

Disclosure Statement

The authors declare no competing financial interests.

Funding

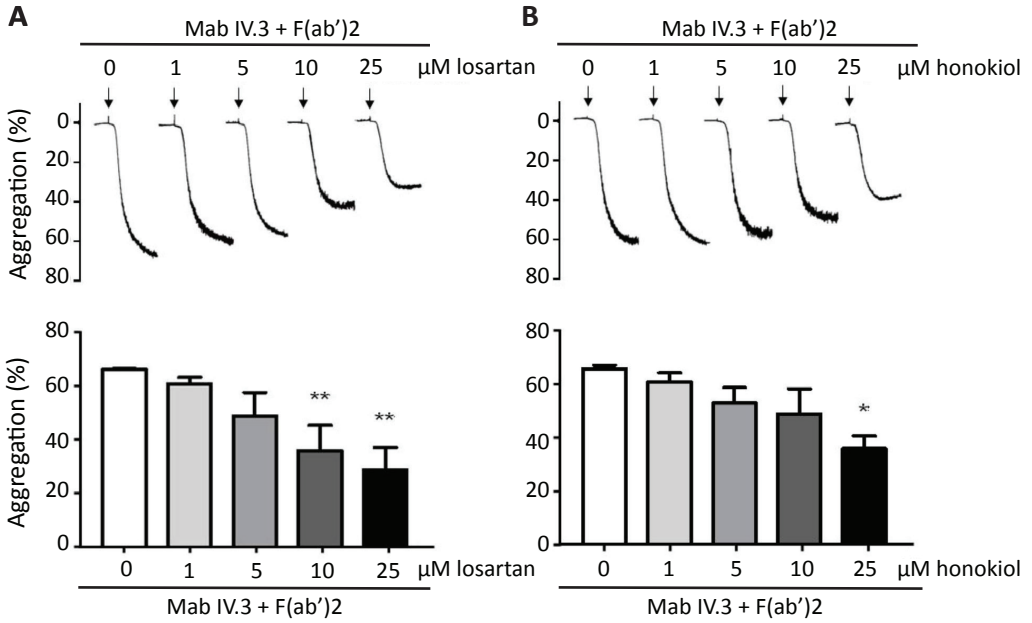
This work was supported by the British Heart Foundation [RG/13/18/30563].

References

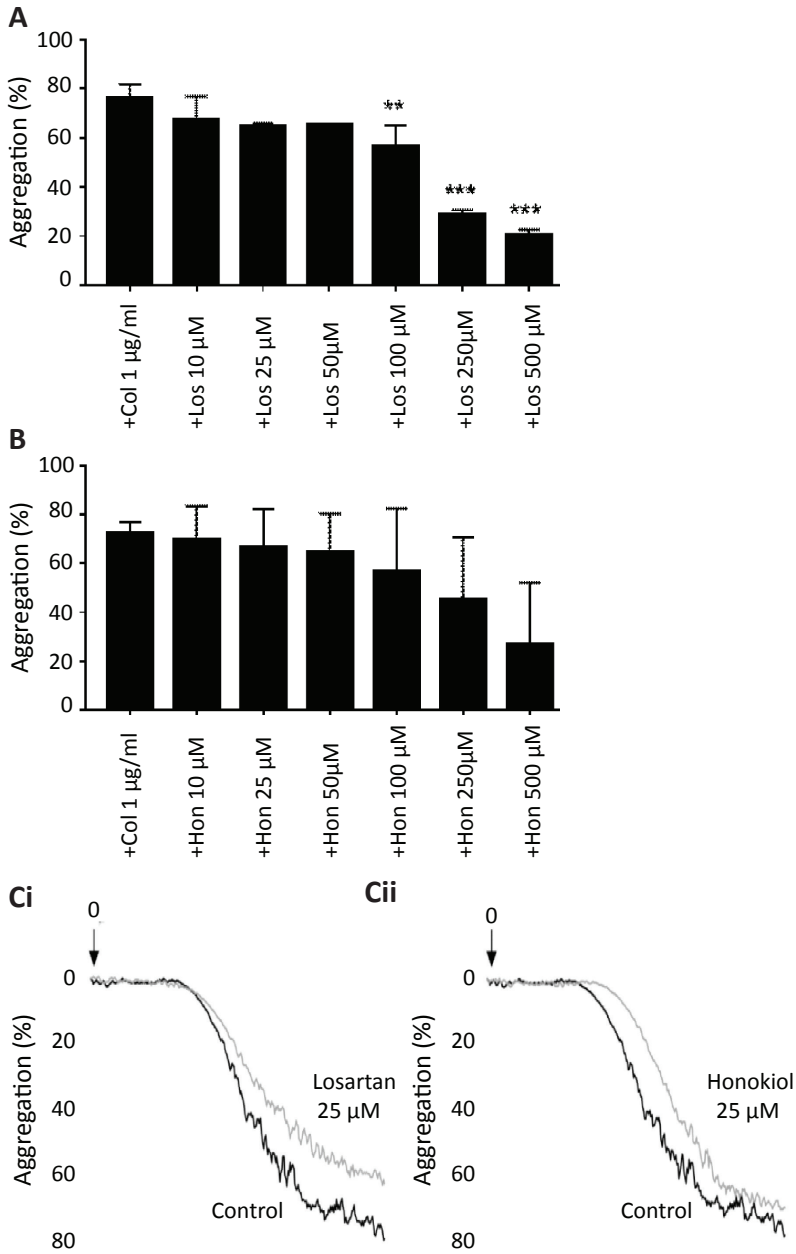
1. Clemetson KJ. Platelets and primary haemostasis. *Thromb Res* 2012;129:220–224.
2. Tomlinson MG, Calaminus SD, Berlanga O, *et al*. Collagen promotes sustained glycoprotein VI signaling in platelets and cell lines. *J Thromb Haemost*. 2007;5:2274–2283.
3. Alshehri OM, Hughes CE, Montague S, *et al*. Fibrin activates GPVI in human and mouse platelets. *Blood*. 2015;126:1601–1608.
4. Mammadova-Bach E, Ollivier V, Loyau S, *et al*. Platelet glycoprotein VI binds to polymerized fibrin and promotes thrombin generation. *Blood*. 2015;126(5):683–691.
5. Onselaer MB, Hardy AT, Wilson C, Sanchez X, Babar AK. Fibrin and D-dimer bind to monomeric GPVI. *Blood*. Adv 2017;1:1495–1504.
6. Nieswandt B, Bergmeier W, Schulte V, *et al*. Expression and function of the mouse collagen receptor glycoprotein VI is strictly dependent on its association with the FcR γ chain. *J Biol Chem*. 2000;275:23998–24002.
7. Moroi M, Jung SM. Platelet glycoprotein VI: its structure and function. *Thromb Res* 2004;114(4):221–233.
8. Watson SP, Auger JM, McCarty OJ, Pearce AC. GPVI and integrin $\alpha_{IIb}\beta_3$ signaling in platelets. *J Thromb Haemost*. 2005;3(8):1752–1762.
9. Bergmeier W, Stefanini L. Platelet ITAM signaling. *Curr Opin Hematol*. 2013;20(5):445–450.
10. Pollitt AY, Poulter NS, Gitz E, *et al*. Syk and Src family kinases regulate C-type lectin receptor 2 (CLEC-2)-mediated clustering of podoplanin and platelet adhesion to lymphatic endothelial cells. *J Biol Chem*. 2014;289(52):35695–35710.
11. Suzuki-Inoue K, Fuller GL, Garcia A, *et al*. A novel Syk-dependent mechanism of platelet activation by the C-type lectin receptor CLEC-2. *Blood*. 2006;107(2):542–549.
12. Watson AA, Christou CM, James JR, *et al*. The platelet receptor CLEC-2 is active as a dimer. *Biochemistry*. 2009;48(46):10988–10996.
13. Rayes J, Lax S, Wichaiyo S, Watson SK, *et al*. The podoplanin-CLEC-2 axis inhibits inflammation in sepsis. *Nat Commun*. 2017;8:2239.
14. Payne H, Ponomaryov T, Watson SP, Brill A. Mice with a deficiency in CLEC-2 are protected against deep vein thrombosis. *Blood*. 2017;129:2013–2020.
15. Jiang P, Loyau S, Tchitchinadze M, *et al*. Ropers J, Jondeau G, Jandrot-Perrus M. Inhibition of glycoprotein VI clustering by collagen as a mechanism of inhibiting collagen-induced platelet responses: the example of losartan. *PLoS One*. 2015;10:e0128744.
16. McIntyre M, Caffè SE, Michalak RA, Reid JL. Losartan, an orally active angiotensin (AT1) receptor antagonist: a review of its efficacy and safety in essential hypertension. *Pharmacol Ther*. 1997;74:181–194.
17. Xu F, Mao C, Hu Y, Rui C, Xu Z, Zhang L. Cardiovascular effects of losartan and its relevant clinical application. *Curr Med Chem*. 2009;16:3841–3857.
18. Grothusen C, Umbreen S, Konrad I, *et al*. EXP3179 inhibits collagen-dependent platelet activation via glycoprotein receptor-VI independent of AT1-receptor antagonism: potential impact on atherothrombosis. *Arterioscler Thromb Vasc Biol*. 2007;27:1184–1190.
19. Murad JP, Espinosa EV, Ting HJ, Khasawneh FT. Characterization of the in vivo antiplatelet activity of the antihypertensive agent losartan. *J Cardiovasc Pharmacol Ther*. 2012;17:308–314.
20. Taylor L, Vasudevan SR, Jones CI, *et al*. Discovery of novel GPVI receptor antagonists by structure-based repurposing. *PLoS One*. 2014;9:e01209.
21. Kumar A, Kumar Singh U, Chaudhary A. Honokiol analogs: a novel class of anticancer agents targeting cell signaling pathways and other bioactivities. *Future Med Chem*. 2013;5:809–829.
22. Rios JL, Francini F, Schinella GR. Natural products for the treatment of type 2 diabetes mellitus. *Planta Med*. 2015;81:975–994.
23. Talarek S, Listos J, Barreca D, *et al*. Neuroprotective effects of honokiol: from chemistry to medicine. *Biofactors*. 2017;43:760–769.
24. Hu H, Zhang XX, Wang YY, Chen SZ. Honokiol inhibits arterial thrombosis through endothelial cell protection and stimulation of prostacyclin. *Acta Pharmacol Sin*. 2005;26:1063–1068.
25. Lee TY, Chang CC, Lu WJ, *et al*. Honokiol as a specific collagen receptor glycoprotein VI antagonist on human platelets: functional *ex vivo* and *in vivo* studies. *Sci Rep*. 2017;7:40002.
26. Raynal N, Hamaia SW, Siljander PR, *et al*. Use of synthetic peptides to locate novel integrin $\alpha_2\beta_1$ -binding motifs in human collagen III. *J Biol Chem*. 2006;281:3821–3831.
27. Berlanga O, Bori-Sanz T, James JR, Frampton J, Davis SJ, Tomlinson MG, Watson SP. Glycoprotein VI oligomerization in cell lines and platelets. *J Thromb Haemost*. 2007;5:1026–1033.

28. Shapiro VS, Truitt KE, Imboden JB, Weiss A. CD28 mediates transcriptional upregulation of the interleukin-2 (IL-2) promoter through a composite element containing the CD28RE and NF-IL-2B AP-1 sites. *Mol Cell Biol*. 1997;17:4051–4058.
29. Metcalf DJ, Edwards R, Kumarswami N, Knight AE. Test samples for optimizing STORM super-resolution microscopy. *J Vis Exp*. 2013;79:50579.
30. Berthold MR, Cebron N, Dill F, et al. KNIME-the Konstanz information miner: version 2.0 and beyond. *SIGKDD Explor*. 2009;11:26–31.
31. De Witt SM, Swieringa F, Cavill R, Wuestner S, Hess O. Identification of platelet function defects by multi-parameter assessment of thrombus formation. *Nat Commun*. 2014;5:4257.
32. Schindelin J, Arganda-Carreras I, Frise E, et al. Fiji: an open-source platform for biological-image analysis. *Nat Methods* 2012;9(7):676–682.
33. Geffen JPV, Brouns SLN, McKinney H, et al. High-throughput elucidation of thrombus formation reveals sources of platelet function variability. *Haematologica*. 2019; *In print*
34. Al-Majed AR, Assiri E, Khalil NY, Abdel-Aziz HA. Losartan: comprehensive profile. *Profiles Drug Subst Excip Relat Methodol*. 2015;40:159–194.
35. Zoumpoulakis P, Daliani I, Zervou M, et al. Losartan's molecular basis of interaction with membranes and AT1 receptor. *Chem Phys Lipids*. 2003;125:13–25.
36. Fotakis C, Christodouleas D, Zoumpoulakis P, et al. Comparative biophysical studies of sartan class drug molecules losartan and candesartan (CV-11974) with membrane bilayers. *J Phys Chem B*. 2011;115:6180–6192.
37. Dong JX, Zhao GY, Yu QL, Li R, Yuan L, Chen J, Liu Y. Mitochondrial dysfunction induced by honokiol. *J Membr Biol*. 2013;246:375–381.
38. Chrysant SG, Chrysant GS. The pleiotropic effects of angiotensin receptor blockers. *J Clin Hypertens*. (Greenwich) 2006;8:261–268.

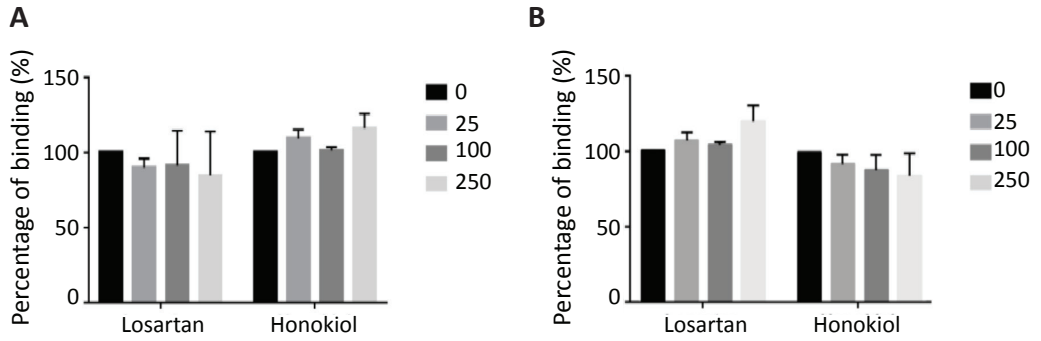
Supplemental figures



Supplemental Figure 1. Losartan and honokiol dose-dependently reduce aggregation of washed platelets induced by Fc γ RIIA activation. Washed platelets were pretreated with different concentrations of losartan (A) or honokiol (B) for 3 min before addition of mab IV.3 (1 μ g/ml) for 60 sec followed by stimulation with F(ab')₂ (30 μ g/ml). Bar graphs represent a total of 3 independent experiments and results are shown as mean \pm SD. *P < .05, **P < .01.



Supplemental Figure 2. Losartan and honokiol dose-dependently reduce platelet aggregation in plasma, induced by collagen. Platelet rich plasma was pretreated with different concentrations of losartan (A) or honokiol (B) for 3 minutes before stimulation with collagen 1 $\mu\text{g/ml}$. The bar graphs represent a total of 5 independent experiments. The results are shown as mean \pm SD. ** $P < .01$, *** $P < .001$. Aggregation traces are representative for the effect of 25 μM of losartan (Ci) or honokiol (Cii) on collagen-induced platelet stimulation. The slight delay in aggregation onset observed in the presence of honokiol was not seen in all experiments.



Supplemental Figure 3. Losartan and honokiol do not inhibit binding of monomeric GPVI to collagen. Recombinant GPVI monomeric protein (A) or GPVI dimeric protein (B) was incubated with different concentrations of losartan or honokiol (in μM) before addition onto a collagen coated-surface ($10 \mu\text{M}$). The bar graph represents the binding of the recombinant GPVI to collagen from an ELISA inhibition assay ($n = 4$). Data are shown as mean \pm SD.

EMBARGOED

Chapter 8

Tight junction-like structures in platelet-platelet interactions

Nagy M, Baaten CCF, Vrijnschauren SLN, Koenen RR, Bender M, Poulter NS, Heemskerk JWM (*Equal contribution)*

Preliminary report

Chapter 9

Bioactive glucagon-like peptide 1 suppresses thrombus growth under flow: beneficial antithrombotic effect of dipeptidyl peptidase 4 inhibition

Sternkopf M, Nagy M*, Baaten CCFMJ, Wirth J, Theelen W, Mastenbroek TG, Lehrke M, Winnerling B, Baerts L, Marx N, Cosemans JMEM, De Meester I, Daiber A, Steven S, Jankowski J, Heemskerk JWM, Noels H
(*Equal contribution)*

Under revision

Abstract

Objective: Dipeptidyl peptidase 4 (DPP4) inhibitors are frequently used for diabetes treatment to improve the glucagon-like peptide-1 (GLP1)-regulated glucose metabolism. Limited evidence suggests that DPP4 influences platelets via GLP1-dependent effects. We characterized the role of bioactive GLP1 and DPP4 on flow-dependent thrombus formation in mouse and human blood.

Approach and Results: An *ex vivo* whole blood microfluidics model was applied to approach *in vivo* thrombosis and study collagen-dependent platelet adhesion, activation and thrombus formation under shear flow conditions by multi-parameter analyses. In hyperlipidemic and hyperglycemic *ApoE^{-/-}* mice, treatment with the DPP4 inhibitor linagliptin strongly reduced platelet adhesion ($38.87 \pm 8.07\%$ vs $24.23 \pm 7.15\%$) and platelet multilayer formation ($30.88 \pm 8.12\%$ vs $15.05 \pm 7.72\%$). Similarly, genetic deficiency of mouse DPP4 (*Dpp4^{-/-}*), but not of GLP1 receptors (*Glp1r^{-/-}*), suppressed flow-dependent platelet aggregation and activation, although to a lesser degree. In human blood, bioactive GLP1(7-36), but not the DPP4-cleaved inactive GLP1(9-36) form, impaired thrombus formation parameters at both low/venous and high/arterial wall-shear rates, effects that were enforced in the presence of ADP co-stimulation. As for DPP4 interference, a consistent inhibitory effect of GLP1(7-36) was observed on thrombus volume, with GLP1(7-36) significantly reducing thrombus volume by 31%. In contrast, GLP1(7-36) did not inhibit collagen-induced aggregation in slowly stirred suspensions of platelets with(out) plasma (inducing a fold change of 1.13 ± 0.12 (washed platelets) and 0.94 ± 0.04 (platelet-rich plasma) vs 0.74 ± 0.03 (whole blood)), suggesting a strictly flow and shear-dependent effect.

Conclusions: DPP4 inhibition and elevated bioactive GLP1 levels suppress platelet aggregation under physiological flow conditions, resulting in the formation of smaller sized thrombi.

Introduction

Dipeptidyl peptidases (DPP) consist of a family of intra- or extracellular exopeptidases that cleave X-proline dipeptides from the polypeptide N-terminus. Since dipeptidyl peptidase 4 (DPP4 or CD26) cleaves the incretin hormone glucagon-like peptide 1 (GLP1), thereby regulating the glucose metabolism,¹ this enzyme has been highly investigated in the context of type 2 diabetes mellitus. Enhanced secretion of GLP1 upon food uptake activates the GLP1 receptors (GLP1R) on pancreatic beta cells, triggering insulin release and thereby reducing the blood glucose level. DPP4 rapidly cleaves the bioactive GLP1 forms, *i.e.* GLP1(7-36)amide and GLP1(7-37), into the inactive forms, GLP1(9-36)amide and GLP1(9-37), both of which are incapable of stimulating GLP1R.² Accordingly, inhibitors of DPP4, such as linagliptin and sitagliptin, markedly prolong the half-life of bioactive GLP1, and are being successfully applied to reduce hyperglycemia in patients with diabetes.^{1,3}

Patients with diabetes mellitus have a two- to four-fold higher risk to develop cardiovascular diseases (CVD) and, at least in some cohorts, encounter a mortality rate as high as patients with a previous myocardial infarction.^{4,5} In diabetes, increased platelet reactivity was found to be a strong independent predictor of major adverse cardiac events.^{4,5} In line with the platelet hyperactivity, diabetes is also associated with increased atherosclerosis and thrombosis as underlying pathologies of CVD.⁶⁻⁹ Antiplatelet therapy in diabetes has proven to be beneficial for secondary prevention of atherothrombotic recurrences¹⁰ and can also reduce vascular events in diabetic patients without prior evidence of cardiovascular disease.¹¹

First indications that DPP4 activity can affect platelet activation came from a study, revealing that diabetic patients treated with the DPP4 inhibitor sitagliptin displayed reduced platelet aggregation *in vitro*.¹² A later study showed increased aggregation in platelet-rich plasma from *Glp1r*-deficient mice, along with increased cAMP-mediated signaling in platelets stimulated with the GLP1R agonist exendin-4.¹³ Furthermore, the GLP1R agonist exenatide (with sequence similarity to exendin-4) was found to suppress aggregation responses of human and mouse platelets, paralleled by cAMP changes.¹⁴ Together, these observations supported a concept that DPP4 and GLP1R activation can alter platelet responsiveness. However, mechanistic insights how DPP4 inhibition affects platelet properties in the context of thrombosis is still missing. Further, with previous studies focusing on GLP1-mimetics (exendin-4 and exenatide, sharing only ~50% sequence identity with native GLP1¹⁵), the effects of native (DPP4-cleaved) forms of GLP1 on platelet responses have not yet been investigated. Given the frequent clinical

application of DPP4 inhibitors, this study aimed to characterize the possible antiplatelet effects of *i*) DPP4 inhibition and *ii*) physiological bioactive vs. DPP4-cleaved GLP1 forms. Considering that *ex vivo* measurements of collagen-dependent thrombus formation under flow can be used as a validated proxy measure of arterial thrombosis *in vivo*,¹⁶ we used a validated whole blood microfluidics assay in a multi-parameter setting¹⁷ for detailed assessment of alterations in thrombus formation.

Materials and Methods

Materials

Collagen I was from Nycomed Pharma (Berlin, Germany), ionomycin was from Merck (Darmstadt, Germany), and prostacyclin from Cayman (Hamburg, Germany). Human recombinant DPP4, apyrase, heparin, exendin fragment 9-39 (exendin-9) and thrombin from human plasma were from Sigma Aldrich (Darmstadt, Germany), DPP8 from USBiological (Salem, USA) and DPP9 from BPS Bioscience (Hamburg, Germany). Sitagliptin phosphate monohydrate was from Carbolution Chemicals (Saarbrücken, Germany); 1G244 inhibitor and HRP-labeled goat anti-rabbit IgG were from Santa Cruz (Heidelberg, Germany). FITC-labeled anti-mAb P-selectin mAb and phycoerythrin (PE)-labeled JON/A mAb (recognizing activated $\alpha_{IIb}\beta_3$) were from Emfret Analytics (Eibelstadt, Germany), Alexa-Fluor (AF)647-labeled, AF488-labeled fibrinogen and AF546-labeled annexin A5 cam from Thermo-Fisher Scientific (Bleiswijk, The Netherlands), anti-P-selectin PE from e-Bioscience (Dreieich, Germany). Synthetized human/mouse GLP1(7-36) amide and GLP1(9-36) amide came from Bachem (Weil am Rhein, Germany). 2-methyl thioadenosine diphosphate trisodium salt (2MeADP) was from Tocris (Wiesbaden-Nordenstadt, Germany), and antibodies against AKT, ERK, pERK and pAKT were from Cell Signaling Technologies (Frankfurt am Main, Germany). Phospho STOP and protease inhibitor cocktail were from Roche (Mannheim, Germany). The protease DPPiV-Glo assay was purchased from Promega (Mannheim, Germany), and CRP-XL was from Cambcol (University of Cambridge, Cambridge, United Kingdom). PPACK came from VWR (Amsterdam, The Netherlands), fragmin was purchased from Pfizer (New York, NY, USA), iloprost (ilomedine) from Bayer (Leverkusen, Germany), human type III collagen from Bio-Connect Life Sciences (Huissen, The Netherlands), and DiOC6 from Tebu-bio (Heerhugowaard, The Netherlands).

Human blood and platelet isolation

Experiments were approved by the local Medical Ethics Committees (Nr. EK191/14, University Hospital Aachen; and METC 10-3-023, Maastricht University). Human blood

was drawn from healthy volunteers after full informed consent, conform the Declaration of Helsinki. Blood was collected into 3.2% trisodium citrate; the first 3 mL were discarded. Washed platelets were isolated from citrated blood, as described before.¹⁸ In brief, platelet-rich plasma (PRP) was obtained by centrifuging citrate-anticoagulated blood at 250 g for 15 min, and platelet-free plasma was collected by centrifuging twice at 2150 g for 10 min. Washed platelets were then suspended into HEPES buffer (10 mM HEPES, 136 mM NaCl, 2.7 mM KCl, 2 mM MgCl₂, 1 mg/mL glucose, 1 mg/mL BSA, pH 7.45).

Mouse blood for platelet studies

All animal experiments were approved by the local authorities (Landesamt für Natur, Umwelt und Verbraucherschutz Nordrhein-Westfalen, Germany, approval number 81-02.04.2017.A413; and by the Landesuntersuchungsamt Koblenz, approval numbers G17-1-050 and G14-1-039) and complied with the German animal protection law. To study platelet activation, blood was obtained from mice with deficiencies in *Glp1r*, *ApoE* or *Dpp4*,¹⁹⁻²¹ all on a C57BL/6 genetic background. DPP4 knockout mice (*Dpp4*^{-/-}) were bred in Mainz; they were originally a kind gift of Dirk Reinhold (Otto-von-Guericke-University Magdeburg, Magdeburg, Germany) and generated by Didier Marguet (Centre d'Immunologie de Marseille-Luminy, Marseille, France).¹⁹ GLP1R knockout mice (*Glp1r*^{-/-}) were bred in Mainz; they were originally obtained from Charles River (Sulzfeld, Germany) and generated by Daniel Drucker (Mt. Sinai Hospital, Toronto, Canada).²⁰ Mice deficient in Apolipoprotein E (*ApoE*^{-/-}) were bred in Aachen and were generated by N. Maeda.²¹ Wildtype control mice of the same background came from the same breeding program. All experiments were performed using age- and sex-matched littermates. Before blood withdrawal, the *ApoE*^{-/-} mice were fed a Western-type diet (Sniff EF T/M TD88137 mod, containing 21.2% fat, 0.2% cholesterol and 32.8% sugar), which was supplemented or not with linagliptin (83 mg/kg diet) for five days. The mice were anesthetized by an intraperitoneal injection of 100 mg/kg per bodyweight ketamine and 10 mg/kg xylazine. Blood from *ApoE*^{-/-}, *Glp1r*^{-/-} or wildtype control mice was collected into 40 μM PPACK, 5 U/mL heparin and 40 U/mL fragmin by retro orbital puncture. Blood from *Dpp4*^{-/-} or corresponding wildtype mice was collected on trisodium citrate.

DPP activity measurements

DPP4 activity was measured in lysates and releasates from stimulated human platelets. Therefore, washed platelets (1×10⁷/mL) were stimulated with thrombin (1 U/mL), ionomycin (10 μM) or CRP-XL (5 μg/mL) in the presence of 2 mM CaCl₂ for 45 min at 37 °C. As a negative control, unstimulated platelets were treated with prostacyclin

(0.1 $\mu\text{g}/\text{mL}$) in the presence of 2 mM CaCl_2 . In all cases, platelet releasates and pelleted platelets were analyzed. The pelleted platelets (1×10^6) were lysed with 360 μL cell lysis buffer, as described.²² DPP activity was measured using the DPPIV-Glo protease assay (Promega) according to the manufacturer's instructions; per test 25 μL releasate or lysate was used plus 25 μL assay reagent. The activity of DPP4 plus that of its closest family members DPP8 and DPP9 (containing similar cleavage recognition motif and pH optimum) contribute to the luminescent read out in this assay; this is referred to as DPP4-like activity. Specific quantification of DPP4 or DPP8/9 activities was performed by addition of the DPP8/9 inhibitor 1G244 or the DPP4 inhibitor sitagliptin, respectively, at final concentrations of 7 μM in the assay (30 min treatments). Measurements gave total DPP4-like activity as well as specific DPP4 and DPP8/9 activity in platelets and platelet-free plasma.²³

Whole blood thrombus formation

An established whole blood microfluidics assay in a multi-parameter setting was applied for a detailed assessment of alterations in thrombus formation under physiological flow conditions, as described.¹⁷ Glass coverslips were coated with 2 μL microspots of collagen type I (100 $\mu\text{g}/\text{mL}$) and collagen type III (100 $\mu\text{g}/\text{mL}$), and were subsequently blocked with 1% BSA. Citrated mouse blood was recalcified (3.75 mM MgCl_2 , 7.5 mM CaCl_2) in the presence of PPACK (40 μM) and subsequently, perfused over the coated surfaces for 3.5 min at a wall shear rate of 1000 s^{-1} . Mouse blood collected into PPACK anticoagulant medium did not require recalcification. Where indicated, blood samples were pretreated with iloprost (0.55 μM) or exendin-9 (10 nM) for 30 min; or alternatively with sitagliptin (7 μM) in combination with GLP1(7-36) (50 nM) or vehicle for 10 min before perfusion. Thrombi formed after 3.5 min of flow were directly post-labeled with a mixture of FITC-conjugated anti-P-selectin mAb (1:40), PE-labeled JON/A mAb (1:20; to analyze integrin activation) and AF647-annexin A5 (1:200; to analyze exposure of phosphatidylserine (PS)) in modified Tyrode's buffer (136 mM NaCl, 2.7 mM KCl, 0.42 mM NaH_2PO_4 , 5 mM HEPES, 2 mM MgCl_2 , 1 mg/mL glucose and 1 mg/mL BSA, pH 7.45) containing CaCl_2 (2 mM) and heparin (1 U/mL).

For formation of human platelet thrombi, citrated blood from healthy subjects was recalcified (3.75 mM MgCl_2 ; 7.5 mM CaCl_2) in the presence of PPACK (40 μM), and perfused over collagen I surface at given wall-shear rates (6 min at 150 s^{-1} ; 3.5 min at 1000 s^{-1} or 1700 s^{-1}).²⁴ Where indicated, blood samples were pre-incubated with sitagliptin for 10 min (7 μM) plus GLP1(7-36) (50 nM), GLP1(9-36) (50 nM) or vehicle, and/or co-perfused with 2MeADP (1 μM , f.c.). Human thrombi formed on the surfaces were stained with

AF647-conjugated anti-P-selectin mAb (2 $\mu\text{g}/\text{mL}$), FITC-labeled anti-fibrinogen mAb (1:100; to quantify fibrinogen binding as read-out for integrin activation), and AF568-annexin A5 (1:200) in HEPES buffer (10 mM HEPES, 136 mM NaCl, 2.7 mM KCl, 2 mM MgCl_2 , 1 mg/mL glucose and 1 mg/mL BSA) containing CaCl_2 (2 mM) and heparin (1 U/mL).

Per flow run, series of representative brightfield and fluorescence images were captured for analysis of surface area coverage (SAC) by adhered platelets (platelet SAC) as well as for analysis of platelet activation markers (PS exposure, P-selectin expression, integrin activation) using scripts written in Fiji software, as described.^{17,25} Furthermore, based on the brightfield images of adhered platelets, effects on platelet aggregation and thrombus formation were assessed by quantifying the multilayer SAC as well as by determining a morphological score, contraction score and multilayer score. These scores were determined by visual inspection of the platelet features per microspot in comparison to preset reference images, using the following criteria:¹⁷ morphological score [range 0-5]: 0, no or hardly any adhered platelets; 1, multiple single-adhered platelets; 2, extensive coverage of single-adhered platelets; 3, small platelet aggregates, 4, intermediate platelet aggregates; 5, thrombi with large-size platelet aggregates. Contraction score [range 0-3]: 0, no contraction; 3, close contraction. Multilayer score [range 0-3]: 0, no platelet layers; 3, multilayered aggregates.²⁶ Observers were blinded to the experimental condition.

For quantification of thrombus volume and height, blood samples were incubated with sitagliptin (7 μM) in combination with vehicle, GLP1(7-36) (50 nM) or GLP1(9-36) (50 nM) for 10 min at room temperature. The membrane probe DiOC₆ (0.5 $\mu\text{g}/\text{ml}$) was added to the blood samples prior to recalcification to label the platelets. After blood perfusion for 3.5 min at 1000 s^{-1} , z-stacks of confocal fluorescence images were recorded with a spacing of 0.5 μm using a fast line-scanning Zeiss LSM7 system (Oberkochen, Germany), equipped with a 63x oil immersion objective.

Light transmission aggregometry

Washed platelets ($25 \times 10^7/\text{mL}$, 2 mM CaCl_2) or PRP were preincubated with sitagliptin (7 μM) in combination with GLP1(7-36) (50 nM) or vehicle for 10 min at room temperature. Platelet aggregation was induced by a submaximal concentration of collagen type I, and measured under constant stirring at 37 °C using a lumi-aggregometer (Chronolog Corporation; Havertown, USA).

Western blot analysis

Washed platelets (1×10^7 /mL) were incubated with sitagliptin (7 μ M) in combination with GLP1(7-36) (50 nM), GLP1(9-36) (50 nM) or vehicle; and were subsequently stimulated with CRP-XL (5 μ g/mL), 2MeADP (10 μ M) or thrombin (1 U/mL) in the presence of 2 mM CaCl_2 for 15 min at 37 °C, as indicated. After stimulation, platelets were lysed with 1x lysis buffer (25 mM Tris-HCl, 150 mM NaCl, 1% NP-40, 1% sodium deoxycholate, 0.1 % sodium dodecyl sulfate, 1x Phospho stop, 1x protease inhibitor complex). Protein amounts in lysates were quantified with a BioRad DC protein kit. Lysates with equal protein amounts, dissolved in 4x Laemmli sample buffer, were separated by 10% sodium dodecyl sulfate-polyacrylamide gel electrophoresis (SDS-PAGE), and were transferred to PVDF membranes (GE Healthcare; Freiburg, Germany). The membranes were stained for phosphorylated ERK and AKT with an anti-p-ERK Ab (1:1000) and an anti-p-AKT Ab (1:1000), respectively; followed by secondary HRP-conjugated secondary Ab (1:10,000). Total ERK and AKT were determined by re-probing the blots with an anti-ERK Ab (1:2000) and an anti-AKT Ab (1:1000). After incubation with Luminol Enhancer solution (GE Healthcare; Freiburg, Germany), protein bands were visualized using a ChemiDoc XRS+ (BioRad, Munich; Germany).

Statistics and heat mapping

Data were analyzed as appropriate, using a one-sample Wilcoxon signed rank test with a Bonferroni correction for multiple comparisons, a Wilcoxon matched pairs signed rank test with a Bonferroni correction for multiple comparisons, a one-way ANOVA with Bonferroni's multiple comparisons test or two-way ANOVA with Sidak's multiple comparisons test; GraphPad Prism 6 Software was used throughout. P-values <0.05 were considered to be statistically significant.

Mean values of whole blood thrombus formation assays were averaged per parameter and per surface and scaled over a range from 0-10 per parameter. Univariate scaled heatmaps were generated using the program R.^{17,27} Where indicated, data were transformed into subtraction heatmaps to compare to control conditions. Filtering of the subtraction arrays was according to conventional large effect sizes (Cohen's $d \geq 0.8$).²⁸

Results

Platelets harbor high DPP8/9 and minimal DPP4 activity compared to plasma

We first determined DPP4-like enzyme activity in whole platelet lysates and in releasates of activated platelets using the DPPIV-Glo protease assay. This assay quantifies DPP4-like N-terminal X-Pro dipeptide cleavage at a defined pH, which can be caused by

DPP4 or by the related DASH (DPP4 activity and/or structure homologue) proteases, DPP8 and DPP9. As assessed in lysates as well as platelet releasates, platelet stimulation with thrombin, ionomycin or CRP-XL could not trigger an increase in DPP4-like activity (Figure 1A,B). To identify the active DPP enzyme, enzymatic measurements were repeated in the presence of sitagliptin (to block DPP4) or 1G244 inhibitor (to block DPP8/DPP9) at concentrations optimized for enzyme selectivity (Suppl. Figure 1A-B). This analysis revealed that the DPP activity in lysed platelets was due to DPP8/9 and not to DPP4 (Figure 1A). In platelet releasates, DPP4-like activity was due to DPP4, with only minor levels of DPP8/9 activity measurable (Figure 1B). Absolute quantification demonstrated in washed platelets a DPP8/9 activity of 82 ± 6 mU/g protein, whereas the DPP4 activity was limited to 3 ± 1 mU/g (Figure 1C). In contrast, plasma (depleted from platelets) revealed a high enzyme activity of DPP4 (113 ± 16 mU/g), but no enzymatically active DPP8/9.

Together, these results indicate that the DPP4-like activity in platelets derives from DPP8/9 and not DPP4, whereas platelet-free plasma displays high DPP4 but no DPP8/9 activity. Thus, in subsequent experiments, we characterized in more detail the effect of plasma-derived DPP4 on thrombus formation.

Linagliptin-mediated DPP4 inhibition in ApoE^{-/-} mice reduces thrombus formation under hyperlipidemic and hyperglycemic conditions

In order to investigate the consequences of DPP4 inhibition on platelet function in hyperlipidemic and hyperglycemic conditions, ApoE^{-/-} mice were fed a Western-type diet enriched in fat and sugar for 5 days, which was supplemented with linagliptin at a dose previously established to efficiently inhibit DPP4 in animal models.^{29,30} In whole blood samples perfused *ex vivo* over collagen-I at arterial wall-shear rate, platelet activation and characteristics of thrombus formation were assessed by multicolor microscopic imaging (Figure 2A). Linagliptin treatment resulted in a marked reduction of platelet deposition (quantified as platelet surface area coverage (SAC): $38.87 \pm 8.07\%$ (control) vs $24.23 \pm 7.15\%$ (linagliptin)) and platelet multilayer formation ($30.88 \pm 8.12\%$ vs $15.05 \pm 7.72\%$) and also reduced platelet activation parameters, such as integrin $\alpha_{IIb}\beta_3$ activation ($29.36 \pm 6.75\%$ vs $19.06 \pm 8.16\%$) and phosphatidylserine (PS) exposure ($1.79 \pm 0.24\%$ vs $0.76 \pm 0.57\%$). Based on the microscopic images, a heatmap consisting of scaled values of eight parameters of thrombus formation revealed a substantial overall reduction of the thrombotic process upon linagliptin administration (Figure 2B). This was even more apparent from a subtraction heatmap filtered for large effect sizes (Cohen's $d > 0.8$), which revealed reductions also for thrombus morphology (4.76 ± 0.23

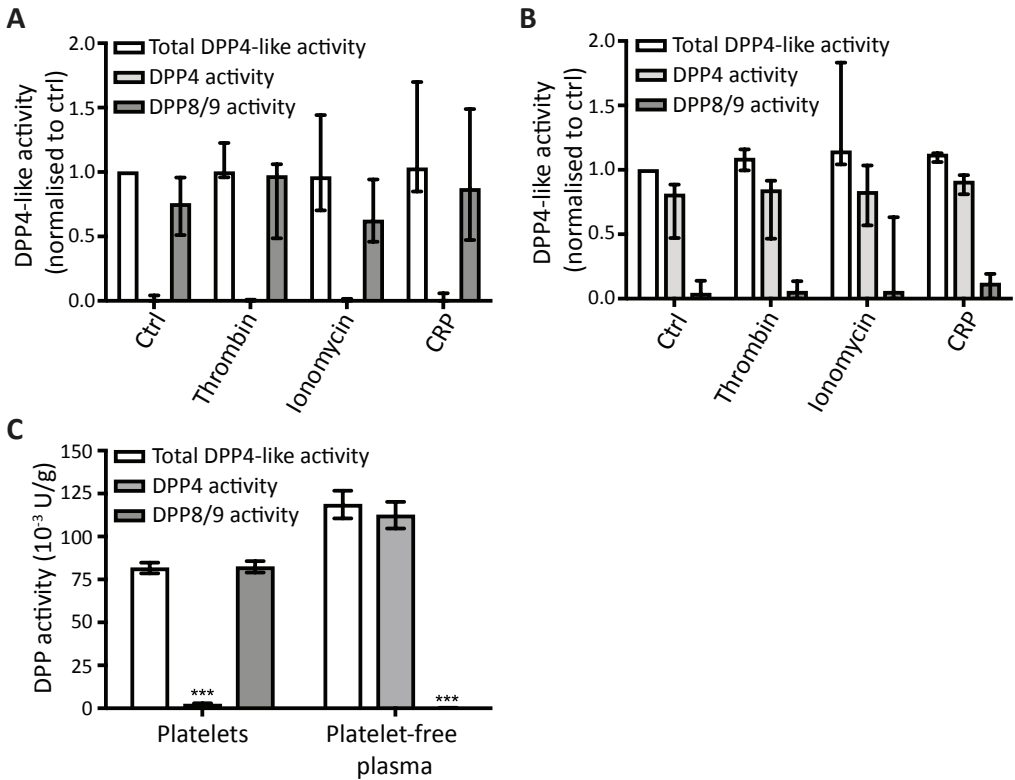


Figure 1. High DPP8/9 activity in platelets and high DPP4 activity in plasma. A-B) Washed human platelets ($1 \times 10^7/\text{mL}$) were stimulated with thrombin (1 U/mL), ionomycin (10 μM) or CRP-XL (5 $\mu\text{g}/\text{mL}$) at 37 $^\circ\text{C}$ for 45 min, as indicated. As a negative control, platelets were treated with prostacyclin (0.1 $\mu\text{g}/\text{mL}$). DPP4-like activity, specific DPP4 activity (in the presence of DPP8/9 inhibitor 1G244, 7 μM), and DPP8/9 activity (in presence of DPP4 inhibitor sitagliptin, 7 μM). Activity measurement in (A) platelet lysates and (B) platelet releasates using the DPP-IV-Glo protease assay. DPP activity was expressed relative to total DPP4-like activity in prostacyclin-treated platelets (ctrl), and displayed as medians with IQR; $n=6-8$. Wilcoxon matched pairs signed rank test (stimulated vs. ctrl), with Bonferroni correction for multiple comparisons. C, DPP4-like activity and specific DPP8/9 and DPP4 activities in lysates from resting platelets and in platelet-free plasma, quantified as described²³; $n=5-6$. Data are displayed as means \pm SEM; two-way ANOVA with Sidak's multiple comparisons test, *** $P < 0.001$.

vs 3.99 ± 0.87), contraction (2.79 ± 0.24 vs 2.11 ± 0.77) and multilayer scores (2.82 ± 0.25 vs 2.07 ± 0.80) (Figure 2C). Hence, these results indicated that, in hyperlipidemic and hyperglycemic conditions, long-term inhibition of DPP4 activity by linagliptin reduces collagen-dependent platelet adhesion, aggregation and activation responses under high-shear flow conditions.

Deficiency in *Dpp4* but not *Glp1r* in mice suppresses thrombus formation

To examine more specifically the role of DPP4 under normolipidemic conditions, we studied thrombus formation in flowed blood from *Dpp4*^{-/-} mice in comparison to corresponding wildtype mice. The platelets from *Dpp4*^{-/-} mice displayed reduced

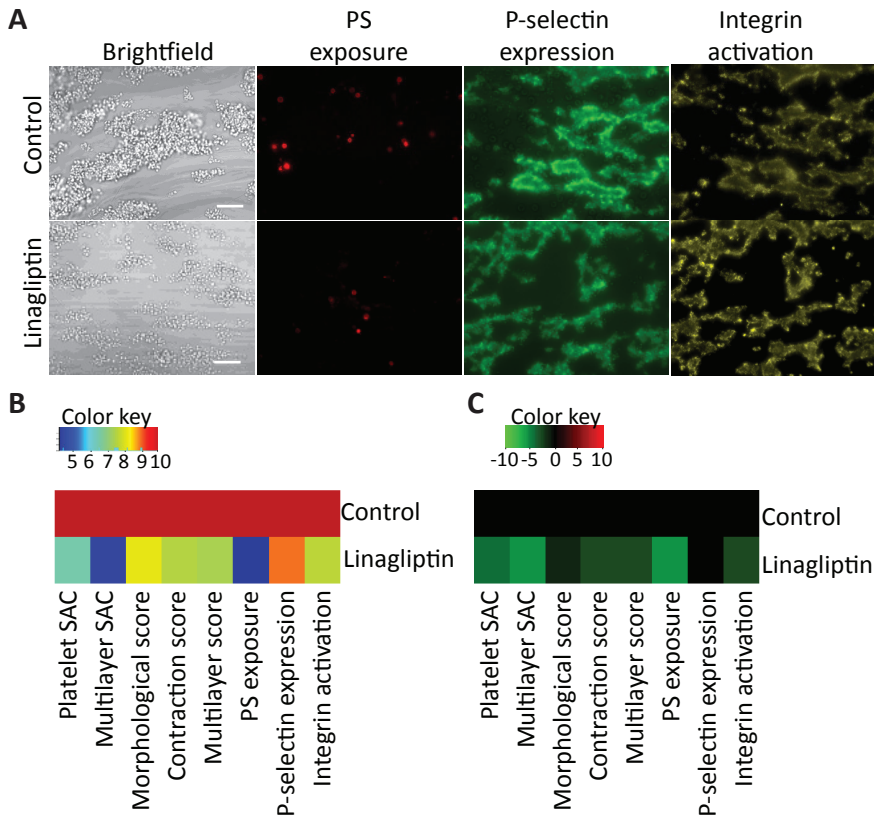


Figure 2. *In vivo* treatment of DPP4 with linagliptin impairs thrombus formation in hyperlipidemic *ApoE*^{-/-} mice. Blood was collected from *ApoE*^{-/-} mice, fed with Western-type diet (high fat and sugar content); linagliptin was supplemented for five days, as indicated. Blood samples were perfused over collagen-I microspots at wall-shear rate of 1000 s⁻¹ for 4 min. Thrombi formed were post-stained with FITC-labeled anti-P-selectin mAb (secretion), PE-labeled JON/A mAb (integrin activation) and AF647-annexin A5 (PS exposure). **A**, Representative brightfield and fluorescence images. Scale bar = 20 μ m. **B**, Heatmap of univariate scaled (0-10) values for control and linagliptin-fed mice. **C**, Subtraction heatmap of scaled values, compared to means of control mice, filtered for differences with large effect size (Cohen's *d*>0.8); *n*=7.

adhesion and aggregation on collagen I, as indicated by decreased parameters of platelet deposition (platelet SAC) and aggregation (multilayer SAC, morphological and multilayer scores). No differences in thrombus formation were observed on a less activating collagen III surface (Figure 3A-B, Suppl. Figure 2A/C-D). As previous research suggested that GLP1R activation reduces platelet activation at least partially by raising cAMP levels,¹³ we determined the effect of DPP4 deficiency on thrombus formation in the presence of the stable prostacyclin analog iloprost, the latter efficiently elevating platelet cAMP levels via Gs stimulation.³¹

Compared to DPP4 deficiency, iloprost pretreatment led to a more severe reduction in essentially all parameters of thrombus formation. Upon additional DPP4 deficiency,

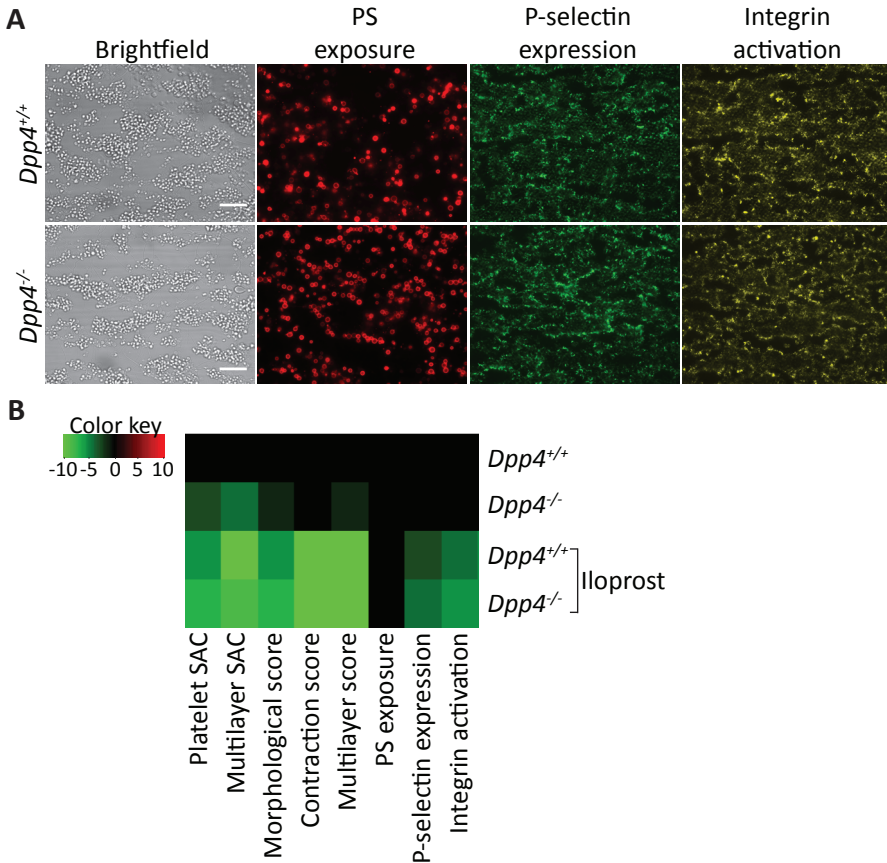


Figure 3. Murine DPP4 deficiency impairs thrombus formation under flow. Whole blood from *Dpp4*^{-/-} or corresponding wildtype mice was perfused over collagen-I microspots at 1000 s⁻¹. Where indicated, blood samples were pretreated 30 min with iloprost (0.55 μM). Thrombi formed were post-stained, as described for Figure 2. A, Representative brightfield and fluorescence images for *Dpp4*^{-/-} and *Dpp4*^{+/+} blood. Scale bar = 20 μm. B, Subtraction heatmap of scaled values, compared to *Dpp4*^{+/+} without treatment, filtered for differences with large effect size (Cohen's d>0.8); n=10. Suppl. Figure 2 shows representative images in the presence of iloprost.

we observed a minor further decrease in platelet adhesion and integrin activation on collagen I, but not collagen III (Figure 3B, Suppl. Figure 2B-D). Together, these results indicate that genetic absence of DPP4 leads to a reduction in collagen I-dependent thrombus formation, but to a lesser degree than caused by cAMP elevation with iloprost

With the GLP1R agonist exendin-4 previously shown to reduce platelet aggregation,^{13,14} we next assessed whether GLP1R blocking with exendin-9 could reverse the observed effects of DPP4 deficiency on thrombus formation under flow: in these conditions, *Dpp4*^{-/-} mice showed comparable platelet deposition (39.45±8.70 (*Dpp4*^{-/-}) vs 43.03±15.02 (*Dpp4*^{-/-} + exendin-9), P=0.39, n=10) and multilayer thrombus formation (14.44±6.83 (*Dpp4*^{-/-}) vs 16.86±11.16 (*Dpp4*^{-/-} + exendin-9), P=0.36, n=10) (mean±SD).

Also, different than observed for *Dpp4*^{-/-} mice, GLP1R deficiency did not alter platelet adhesion, aggregation, activation or thrombus structure parameters on collagen-I, but only induced a minor increase in PS exposure (Suppl. Figure 3A-C). Also, on collagen-III, only minor increases were observed for thrombus scores, though without significant effects on platelet deposition (platelet SAC) or aggregation (multilayer SAC) (Suppl. Figure 3A-C). Furthermore, the addition of GLP1(7-36) did not affect thrombus formation in wildtype mice, though it could abolish the minor effects of GLP1R deficiency on collagen-III induced thrombus formation (Suppl. Figure 3A-C).

In summary, these data indicate that, in line with the observed effects upon linagliptin treatment, deficiency of DPP4 but not GLP1R reduces thrombus formation under flow in mouse blood.

GLP1(7-36) reduces platelet aggregation in human whole blood under flow, but not in isolated human platelets

Next, we tested the effects of a short-term treatment of human blood samples with the DPP4 inhibitor sitagliptin and the DPP8/9 inhibitor 1G244, respectively. These enzyme inhibitors did not affect collagen-I induced thrombus formation under flow (Suppl. Figure 4), although DPP4, respectively, DPP8/9 enzyme activity were efficiently inhibited under the investigated conditions (data not shown). These results hence raised the hypothesis that the reduced thrombus formation, observed by *in vivo* DPP4 inhibition with linagliptin, are due to an accumulation of non-cleaved over cleaved DPP4 substrates, rather than by a direct DPP4-mediated enzymatic effect on the thrombus formation parameters.

As the clinically applied DPP4 inhibitors aim to increase the ratio of bioactive GLP1(7-36) over inactive (DPP4-cleaved) GLP1(9-36), we next directly compared the effects of GLP1(7-36) vs. GLP1(9-36) peptides on human thrombus formation under a variety of flow conditions, *i.e.* low (venous), intermediate (large arterial) as well as high wall-shear rates. The heatmap of 'active' GLP1(7-36) and 'inactive' GLP1(9-36) effects on parameters of thrombus formation, obtained from series of microscopic images, indicated a substantial overall reduction of thrombus formation by GLP1(7-36) under flow. Notably, this reduction was seen at all shear flow conditions, from low (150 s^{-1}) and intermediate (1000 s^{-1}) to high (1700 s^{-1}) (Figure 4A, Suppl. Figure 5). For quantification, subtraction heatmaps were generated in which the changes were filtered for large effect sizes (Cohen's $d > 0.8$), thus revealing reductions in aggregation-related parameters (multilayer thrombus SAC, multilayer, morphological and contraction scores) (Figure 4B).

In addition, we investigated the effects of GLP1(7-36) on thrombus formation upon co-infusion with stable ADP. This resulted in a reduction in platelet deposition

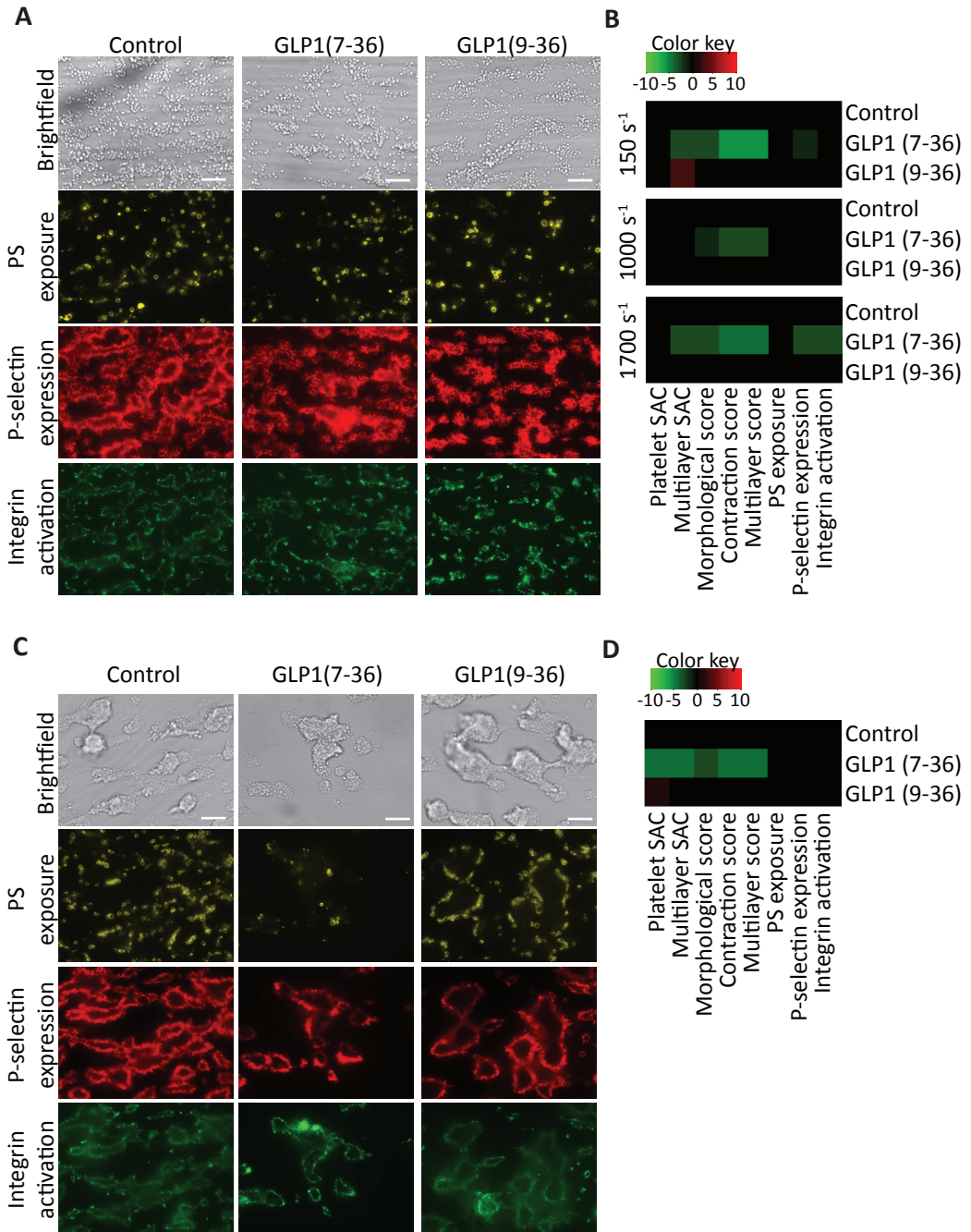


Figure 4. GLP1(7-36) suppresses human whole blood thrombus formation regardless of wall-shear rate. Human blood was pre-incubated with GLP1(7-36) (50 nM), GLP1(9-36) (50 nM) or vehicle control for 10 min. Sitagliptin (7 μ M) was present in all conditions. **A-B**, After recalcification, samples were perfused over collagen-I microspots at indicated wall-shear rates. Thrombi formed were post-stained for PS exposure, P-selectin expression and integrin activation, as for Figure 2. **A**, Representative brightfield and fluorescence

images at wall-shear rate of 1000 s^{-1} . **B**, Subtraction heatmap of scaled parameter values, compared to means of controls; filtering for differences with large effect size (Cohen's $d > 0.8$); $n=9$ for 1000 s^{-1} ; $n=4$ for 150 s^{-1} and 1700 s^{-1} . **C-D**, Additionally, after recalcification, blood samples were co-perfused with 2MeADP ($1\text{ }\mu\text{M}$) over collagen 1000 s^{-1} . **C**, Representative brightfield and fluorescence images ($n=4$). **D**, Subtraction heatmap of scaled values, compared to means of controls; filtering for large effect size as above. Scale bars = $20\text{ }\mu\text{m}$. Suppl. Figure 5 shows representative images for thrombus formation at shear rates 150 s^{-1} and 1700 s^{-1} .

($30.17 \pm 8.69\%$ (control) vs $25.25 \pm 14.38\%$ (GLP1(7-36))) as well as platelet aggregation triggered by the GLP1(7-36) peptide ($21.35 \pm 4.06\%$ (control) vs $8.76 \pm 3.54\%$ (GLP1(7-36))) (Figure 4C-D, Suppl. Figure 5C). In sharp contrast, equal concentrations of the DPP4-cleaved GLP1(9-36) were unable to reduce thrombus formation under flow, but instead triggered minor increases in adhesion-related parameters (multilayer SAC at 150 s^{-1} only) (Figure 4B).

Next, to assess the importance of shear flow in the GLP1-mediated effects, we examined aggregation of slowly stirred suspensions of washed human platelets or PRP using light transmission aggregometry. Strikingly, and in contrast to the clear GLP1-mediated effects on whole blood thrombus formation, neither GLP1(7-36) nor GLP1(9-36) did affect collagen-induced platelet aggregation responses in these stirred suspensions (fold change for GLP1(7-36): 1.13 ± 0.13 and 0.94 ± 0.04 in washed platelets and PRP, vs and PRP, vs 0.74 ± 0.03 in whole blood) (Figure 5). Along the same line, neither GLP1(7-36) nor GLP1(9-36) significantly altered the phosphorylation state of AKT or ERK1/2 in activated human platelets, if applied in combination with thrombin, ADP or CRP-XL (Suppl. Figure 6).

The two-dimensional microscopic images recorded from collagen-I surfaces suggested that GLP1(7-36) suppressed the three-dimensional buildup of thrombi under flow conditions. To confirm this, we quantified the thrombus volume by recording confocal z-stacks of thrombi consisting of DiOC₆-labeled platelets. Markedly, addition of GLP1(7-36) reduced thrombus volume and height (mean \pm SEM; Figure 6A-B), with an overall smaller thrombus area at each confocal plane (Figure 6C). In line with previous observations, the DPP4-cleaved GLP1(9-36) did not affect thrombus volume or height (Figure 6A-C).

Taken together, these results revealed a mechanism in which, *in vivo*, plasma-derived DPP4 activity promotes thrombus formation by cleaving active GLP1(7-36) to its inactive form. In the absence of DPP4 activity - either by genetic deficiency or by long-term inhibitory treatment - the bioactive form of GLP1 can accumulate in blood, suppressing the flow- and shear-dependent formation of thrombi by interacting with platelets, though without a major role for GLP1R under the investigated conditions.

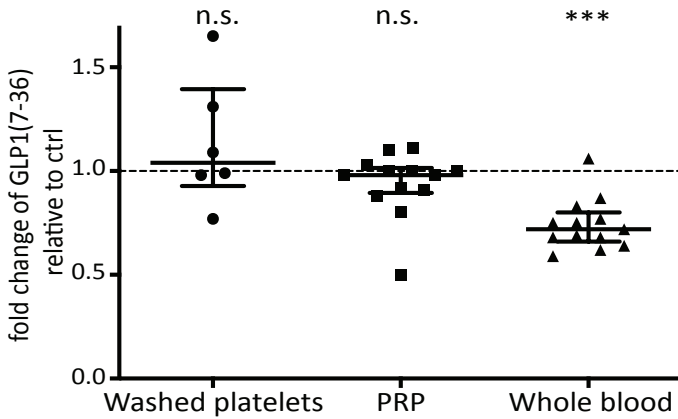


Figure 5. GLP1(7-36) impairs collagen-induced platelet aggregation only in flowed whole blood. Effect of GLP1(7-36) (50 nM) on collagen-induced aggregate formation of washed platelets, PRP, and platelets in flowed whole blood. Collagen-induced maximal aggregation of slowly stirred washed platelets (n=6) and PRP (n=14) was measured using a lumi-aggregometer. Collagen-dependent aggregate formation under flow at 1000 s^{-1} was measured from overall aggregation parameters (multilayers, morphological, contraction and multilayer scores) (n=13). Present was $7\text{ }\mu\text{M}$ sitagliptin in all conditions. Effects of GLP1(7-36) are expressed as fold changes relative to vehicle control, and are displayed as dot plots with indication of median \pm IQR. One-sample Wilcoxon signed rank test for comparison vs. control. *** $P < 0.001$; n.s. = not significant.

Discussion

In this paper, we provide novel clarification for the antithrombotic effect of DPP4 inhibition, acting through suppressed inactivation of the incretin hormone GLP1. Our findings demonstrate that inhibition or genetic deficiency of DPP4 in mice results in reduced thrombus formation under flow, in conditions of hyperlipidemia and hyperglycemia, as well as in non-lipid- or sugar-primed conditions. This effect could be confirmed in human whole blood samples by the bioactive peptide GLP1(7-36), *i.e.* a main substrate of DPP4. Here, elevation of GLP1(7-36) but not of GLP1(9-36) resulted in the formation of smaller and less contracted thrombi formed on collagen, at both venous and arterial flow conditions.

Several earlier studies have shown that DPP4 is expressed by different blood-related cells, including endothelial cells and T-lymphocytes,^{3,32} but platelet DPP4-like activity had not been studied in detail before. Here, we show that the DPP4-like activity, measurable in platelets, is primarily due to the DASH proteases DPP8/9 and not to DPP4. These results are in line with recent data reporting that megakaryocytes and platelets do not harbor detectable DPP4 enzyme activity,¹⁴ and do express DPP2, DPP3 and DPP9 but not DPP4 according to proteomics analyses.³³ Accordingly, a DPP4 activity detected in platelet releasate might have been derived from plasma remnants, *e.g.* present in the open canicular system of platelets. Further, we could confirm that plasma reveals high DPP4 activity, which by its proteolytic activity can indirectly affect platelet properties.

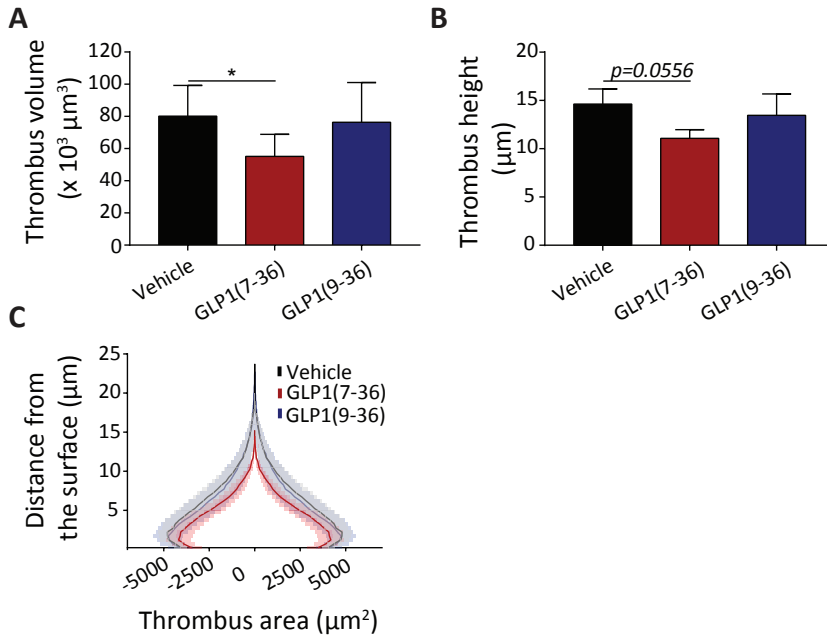


Figure 6. GLP1(7-36) reduces thrombus size under flow. Human blood was incubated for 10 min with vehicle, GLP1(7-36) (50 nM) or GLP1(9-36) (50 nM) in the presence of 7 μM sitagliptin. Platelets in the blood were pre-labeled with DiOC₆. After flow perfusion at 1000 s^{-1} , z-stacks were recorded of thrombi formed on collagen-I microspots. **A-B**, Microscopic images analyzed for overall thrombus volume (**A**) and thrombus height (**B**). Data are displayed as means \pm SEM, $n=4$. One-way ANOVA with Dunn's multiple comparisons test vs. vehicle; * $P<0.05$. **C**, Graphical representation of mean thrombus area (μm^2) with SEM (shaded area), for indicated distances from collagen surface.

When DPP4 activity was deficient in mice either by long-term *in vivo* administration of linagliptin in *ApoE*^{-/-} mice or by genetic deficiency of DPP4, we observed marked reductions in collagen-dependent platelet adhesion and aggregation under flow. Markedly, DPP4 inhibition by linagliptin in the hyperlipidemic mice led to a greater inhibition of thrombus formation, accompanied by distinctly decreased parameters of platelet activation, such as PS exposure and integrin activation. A likely explanation for the difference between the two models is a greater possibility for downregulation of platelet aggregation under hyperlipidemic and hyperglycemic conditions. In line with this, both hyperlipidemia and hyperglycemia are associated with platelet hyper-reactivity^{3,4,35}

Other authors have reported that a short-time (20 min) treatment of isolated human platelets with the DPP4 inhibitor sitagliptin (5-10 $\mu\text{g}/\text{mL}$, equivalent to 10-20 μM) reduced thrombin-induced Ca^{2+} rises and aggregate formation.¹² It was speculated that this is due to sitagliptin effects on platelets independent of DPP4,¹⁴ the latter being in line with our finding that DPP4-like activity in platelets is not derived from DPP4 itself, but instead from the related enzymes DPP8/9. We found that short-time treatment of

whole blood with 7 μ M sitagliptin almost completely abolished DPP4 activity, although this did not influence whole blood thrombus formation under flow. Taking into account the reduced thrombus formation after long-term *in vivo* inhibition of DPP4 with a DPP4 inhibitor or upon genetic DPP4 deficiency in mice, it seems that the thrombus formation under flow is modulated by an accumulation of non-cleaved over cleaved DPP4 substrates, rather than by an immediate effect of DPP4 enzymatic activity. These findings do also exclude off-target (non-DPP4 related) effects of sitagliptin in the present setting.

One of the best described DPP4 substrates is GLP1(7-36), which is cleaved by DPP4 to the inactive form GLP1(9-36).³ Physiologically, the half-life of GLP1(7-36) is short (1.5 – 5 min), because of the proteolytic cleavage in plasma.³⁶ Accordingly, the stable GLP1(7-36) analog liraglutide (97% amino acid sequence identity) and the peptide exenatide (a synthetic form of the GLP1R agonist exendin-4, with 50% sequence identity to GLP1(7-36)¹⁵) are of improved efficacy in the clinical therapy of hyperglycemia. Alternatively, DPP4 inhibitors are being used to rise the endogenous levels of uncleaved, bioactive GLP1.³⁷ In this context, and because previous studies analyzed the effects of exendin-4 and exenatide as GLP1R agonists on platelet responses,^{13,14} we specifically focused on the platelet effects of the physiological, bioactive vs. DPP4-cleaved GLP1 peptides. In accordance with the phenotypes of DPP4 deficiency and long-term linagliptin treatment, we could establish that increased levels of bioactive GLP1(7-36), but not of cleaved GLP1(9-36), reduce whole blood thrombus formation at a variety of flow ranges. In these experiments, we always added the DPP4 inhibitor sitagliptin to prevent inactivation of the GLP1(7-36).

DPP4 deficiency caused much lower inhibitory effects on platelet adhesion and aggregation than the established cAMP-elevating agent iloprost as prostacyclin analogue. Though increased intracellular cAMP levels and PKA activation were previously identified as one possible signaling pathway for the anti-aggregatory effects of GLP-1 and the GLP1R agonist exendin-4,^{13, 14} those studies also reported a 1.5-4x smaller effect on cAMP induction^{13, 14} and a 10-fold smaller effect on VASP-phosphorylation compared to prostacyclin,¹³ thus in line with our observation of a reduced aggregatory effect of DPP4 deficiency compared to prostacyclin. Furthermore, in this study, *Dpp4*^{-/-} mice did not show significant differences in platelet deposition and multilayer thrombus formation in the absence vs. presence of the GLP1R antagonist exendin-9, which binds to but does not activate GLP1R as truncated version of exendin 4.³⁸ Also, collagen-induced thrombus formation under flow was unaltered in *Glp1r*^{-/-} mice, which argues against an important role of GLP1R on mouse platelets in the investigated settings. In this context, expression of GLP1R on platelets has been a matter of debate: On the one hand, western blot and

flow cytometry experiments have demonstrated expression of GLP1R on human platelets as well as on mouse platelets.^{13,14,39} On the other hand, proteomic analyses could not detect GLP1R in human platelets³³ or with only 2% sequence coverage,⁴⁰ and also only low GLP1R mRNA levels were detected in the megakaryocyte platelet lineage.⁴¹ That GLP1 can modulate platelets independent of GLP1R was recently demonstrated by Barale *et al.*, who showed GLP1(7-36) to increase the inhibitory effects of the NO donor sodium nitroprusside on platelet aggregation via cGMP and independently of cAMP modulation and GLP1R.³⁹ Also, GLP1/GLP1R-independent effects of linagliptin were previously shown in relation to the survival of septic mice.¹³

Our findings with both human and mouse platelets jointly indicate that the largest and most consistent effects of GLP1(7-36) supplementation or DPP4 deficiency are observed under conditions of shear flow. Markedly, in flowed human blood, GLP1(7-36) significantly decreased thrombus volume and height. In contrast, this peptide was unable to reduce platelet aggregation in slowly stirred suspension of washed platelets or platelet-rich plasma. Together with the findings from Barale *et al.*³⁹ where GLP1(7-36) alone was also unable to reduce collagen-induced platelet aggregation, our data suggest that a shear stress as present in flow conditions is needed to achieve GLP1(7-36)-mediated platelet inhibition. As VWF-GPIb interactions are essential for shear mediated platelet adhesion,¹⁷ we also examined a role of GLP1(7-36) under conditions of low/venous shear rate (150 s^{-1}), where platelet adhesion and activation occurs independently of the VWF-GPIb axis. However, at all three flow shear rates examined ($150, 1000, 1700\text{ s}^{-1}$), we observed a similar reduction of platelet aggregation parameters, strongly indicating that the effect of GLP1(7-36) is independent of VWF. Since platelet aggregation under flow is a complex and dynamic process, we hypothesize that the bioactive GLP1 requires a combination of plasma factors and shear stress, perhaps including the marginalization of platelets by erythrocytes, in order to reduce the thrombotic process. Since the GLP1(7-36) analogue liraglutide ($10\text{-}100\text{ }\mu\text{M}$) did previously reduce ADP-induced platelet aggregation in stirred platelet-rich plasma,¹³ our data do not exclude that platelet aggregation is differentially affected by GLP1(7-36) depending on the platelet agonist as well as by higher concentrations of GLP1(7-36) (analogue).

Diabetic patients present with platelet hyperactivity and are at increased risk of development of cardiovascular disease. In accordance, antiplatelet therapy is clinically used to prevent atherothrombotic recurrences in these patients and also primary prevention with anti-platelet agents could reduce thrombotic complications in diabetes, although at the expense of an increased risk of bleeding.¹¹ A recent international consensus paper compared clinical trials on effects of DPP4 inhibitors and GLP1R agonists

on cardiovascular outcomes. Potential of cardiovascular protection was revealed mainly for liraglutide and semaglutide, being the peptides most similar to bioactive GLP1 (with 97% and 94% sequence identity, respectively), and this independent of glucose control. In contrast, the GLP1R agonists lixasenatide and exenatide, both sharing sequence similarity to exendin-4 instead, were not, respectively, only to a minor extent, associated with cardioprotection.⁴² In this context, our data provide a mechanistic explanation for such protection, in that bioactive GLP1 can antagonize the flow-dependent platelet response of thrombus formation. Especially in conditions of increased thrombosis, such as in our study of hyperlipidemia/-glycemia (Figure 2) or ADP co-infusion (Figure 4), effects of increased GLP1(7-36) over GLP1(9-36) ratios were strikingly beneficial. In this context, GLP1(7-36) could be regarded as a natural suppressor of platelet aggregation and thrombus growth under physiological flow conditions. As overall DPP4 inhibitors could not provide cardioprotection in clinical trials in contrast to analogs of GLP1(7-36),⁴² it can currently not be excluded that simultaneous stabilization of other DPP4 substrates (*e.g.*, substance P or fibrin^{43,44}) may interfere with GLP1(7-36) mediated anti-platelet effects of DPP4 inhibitors *in vivo*, thus requiring further investigation.

In conclusion, our data provide novel evidence that *i)* reduced DPP4 activity decreases thrombus formation under flow, both in conditions of hyperlipidemia and hyperglycemia, as well as in normolipidemic conditions; and *ii)* GLP1(7-36) but not GLP1(9-36) reduces whole blood thrombus formation at both venous and arterial flow shear rates, resulting in the formation of smaller and less contracted thrombi. Thus, these data advice on a closer investigation of thrombus formation under flow in diabetic patients treated with DPP4 inhibitors vs. liraglutide as GLP1 analog.

Highlights

- Inhibition of DPP4 enzyme activity *in vivo* or absence of DPP4 suppresses collagen-mediated thrombus formation under flow.
- Bioactive GLP1(7-36) but not DPP4-cleaved GLP1(9-36) reduces thrombus formation at both arterial and venous shear flow conditions.
- The presence of both flow and plasma is required for GLP1(7-36) mediated platelet inhibition.

Acknowledgements

We kindly thank Prof. D. Marguet and Prof. D. Reinhold for providing the *Dpp4*-deficient mice.

Sources of funding

This work was supported by the German Research Foundation (DFG SFB/TRR219-M05 to H.N. and N.M., SFB/TRR219-C04 to J.J. and SFB/TRR219-M03 to M.L. and N.M.); by a grant from the Interdisciplinary Centre for Clinical Research (IZKF) within the faculty of Medicine at the RWTH Aachen University [IZKF K7-1 to H.N. and IZKF 105/13 to W.T.]. M.N. and J.W.M.H. received funding from the Cardiovascular Centre (HVC) Maastricht and the Interreg V Euregio Meuse-Rhine program (Poly-Valve). C.B. was supported by the Alexander von Humboldt foundation.

Disclosures

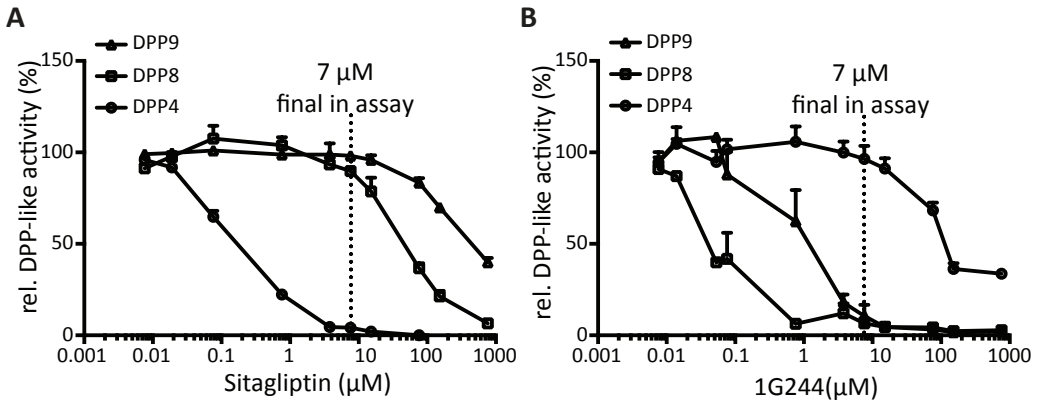
J.W.M.H. is a co-founder and shareholder of FlowChamber. The other authors declare no conflicts of interest exist.

References

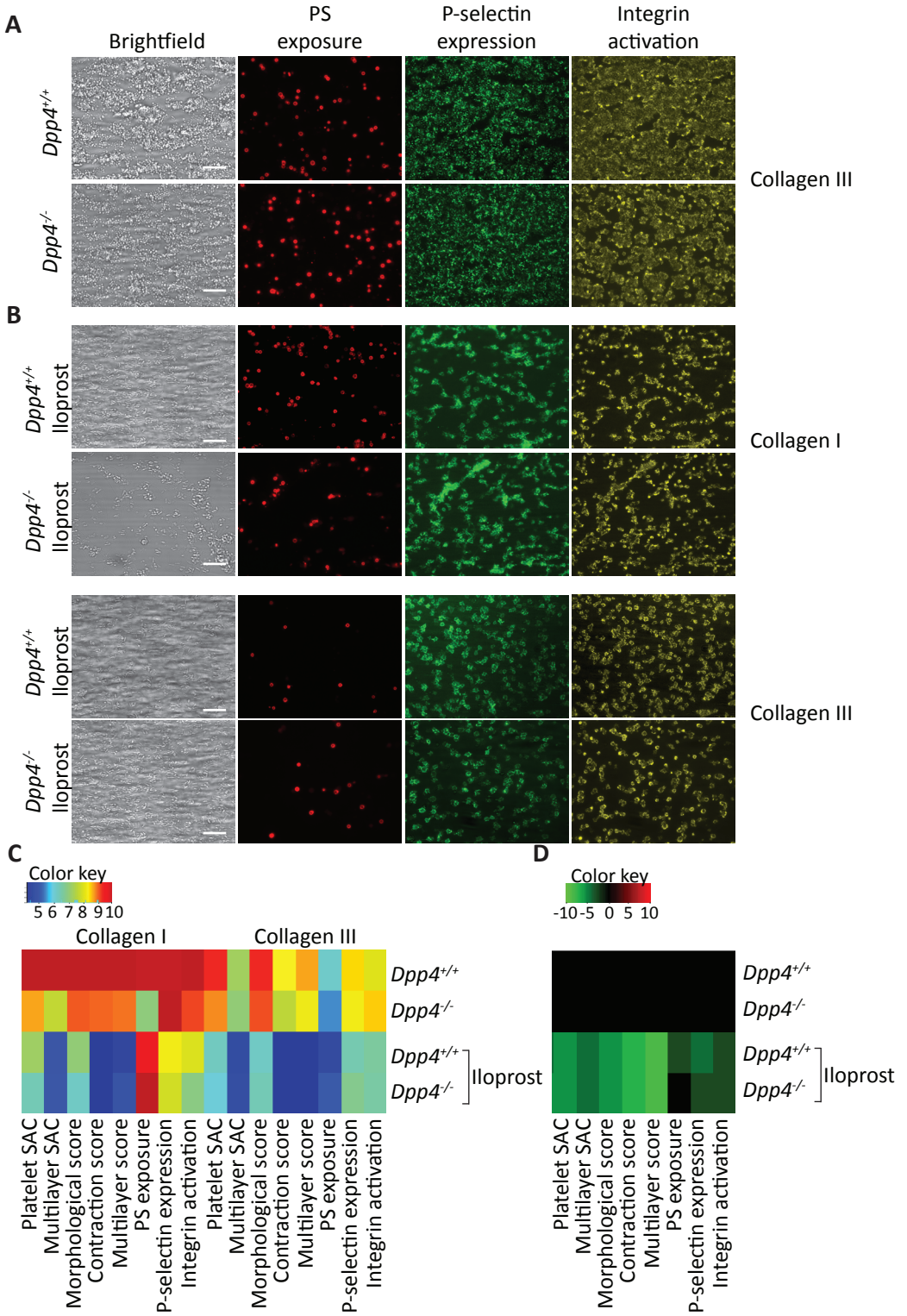
1. Rohrborn D, Wronkowitz N, Eckel J. DPP4 in Diabetes. *Front Immunol.* 2015; 6: 386.
2. Ussher JR, Drucker DJ. Cardiovascular actions of incretin-based therapies. *Circ Res.* 2014; 114: 1788-1803.
3. Zhong J, Maiseyeu A, Davis SN, Rajagopalan S. DPP4 in cardiometabolic disease: recent insights from the laboratory and clinical trials of DPP4 inhibition. *Circ Res.* 2015; 116: 1491-1504.
4. Beckman JA, Creager MA, Libby P. Diabetes and atherosclerosis: epidemiology, pathophysiology, and management. *JAMA.* 2002; 287: 2570-2581.
5. Ferroni P, Basili S, Falco A, Davi G. Platelet activation in type 2 diabetes mellitus. *J Thromb Haemost.* 2004; 2: 1282-1291.
6. Gawaz M. Role of platelets in coronary thrombosis and reperfusion of ischemic myocardium. *Cardiovasc Res.* 2004; 61: 498-511.
7. Weber C, Noels H. Atherosclerosis: current pathogenesis and therapeutic options. *Nat Med.* 2011; 17: 1410-1422.
8. Koenen RR, Weber C. Platelet-derived chemokines in vascular remodeling and atherosclerosis. *Semin Thromb Hemost.* 2010; 36: 163-169.
9. Dhindsa DS, Sandesara PB, Shapiro MD. The Intersection of Diabetes and Cardiovascular Disease-A Focus on New Therapies. *Front Cardiovasc Med.* 2018; 5: 160.
10. Rivas Rios JR, Franchi F, Rollini F, Angiolillo DJ. Diabetes and antiplatelet therapy: from bench to bedside. *Cardiovasc Diagn Ther.* 2018; 8: 594-609.
11. Group ASC, Bowman L, Mafham M, et al. Effects of Aspirin for Primary Prevention in Persons with Diabetes Mellitus. *N Engl J Med.* 2018; 379: 1529-1539.
12. Gupta AK, Verma AK, Kailashiya J, Singh SK, Kumar N. Sitagliptin: anti-platelet effect in diabetes and healthy volunteers. *Platelets.* 2012; 23: 565-570.
13. Steven S, Jurk K, Kopp M, et al. Glucagon-like peptide-1 receptor signalling reduces microvascular thrombosis, nitro-oxidative stress and platelet activation in endotoxaemic mice. *Br J Pharmacol.* 2017; 174: 1620-1632.
14. Cameron-Vendrig A, Reheman A, Siraj MA, et al. Glucagon-like peptide 1 receptor activation attenuates platelet aggregation and thrombosis. *Diabetes.* 2016; 65: 1714-1723.
15. Drucker DJ. The biology of incretin hormones. *Cell Metab.* 2006; 3: 153-165.
16. Baaten C, Meacham S, de Witt SM, et al. A synthesis approach of mouse studies to identify genes and proteins in arterial thrombosis and bleeding. *Blood.* 2018; 132: e35-e46.
17. de Witt SM, Swieringa F, Cavill R, et al. Identification of platelet function defects by multi-parameter assessment of thrombus formation. *Nat Commun.* 2014; 5: 4257.
18. Baaten C, Swieringa F, Misztal T, et al. Platelet heterogeneity in activation-induced glycoprotein shedding: functional effects. *Blood Adv.* 2018; 2: 2320-2331.

19. Marguet D, Baggio L, Kobayashi T, *et al.* Enhanced insulin secretion and improved glucose tolerance in mice lacking CD26. *Proc Natl Acad Sci U S A.* 2000; 97: 6874-6879.
20. Scrocchi LA, Brown TJ, McClusky N, *et al.* Glucose intolerance but normal satiety in mice with a null mutation in the glucagon-like peptide 1 receptor gene. *Nat Med.* 1996; 2: 1254-1258.
21. Piedrahita JA, Zhang SH, Hageman JR, Oliver PM, Maeda N. Generation of mice carrying a mutant apolipoprotein E gene inactivated by gene targeting in embryonic stem cells. *Proc Natl Acad Sci U S A.* 1992; 89: 4471-4475.
22. Dubois V, Van Ginneken C, De Cock H, *et al.* Enzyme activity and immunohistochemical localization of dipeptidyl peptidase 8 and 9 in male reproductive tissues. *J Histochem Cytochem.* 2009; 57: 531-541.
23. Matheeußen V, Waumans Y, Martinet W, *et al.* Dipeptidyl peptidases in atherosclerosis: expression and role in macrophage differentiation, activation and apoptosis. *Basic Res Cardiol.* 2013; 108: 350.
24. Kuijpers MJ, de Witt S, Nergiz-Unal R, *et al.* Supporting roles of platelet thrombospondin-1 and CD36 in thrombus formation on collagen. *Arterioscler Thromb Vasc Biol.* 2014; 34: 1187-1192.
25. Schindelin J, Arganda-Carreras I, Frise E, *et al.* Fiji: an open-source platform for biological-image analysis. *Nat Methods.* 2012; 9: 676-682.
26. Van Geffen JP, Brouns SLN, Batista J, *et al.* High-throughput elucidation of thrombus formation reveals sources of platelet function variability. *Haematologica.* 2019. *In press*
27. Team R Core. R: A language and environment for statistical computing. R Foundation for Statistical Computing, Vienna, Austria <https://www.R-project.org/>.
28. Lakens D. Calculating and reporting effect sizes to facilitate cumulative science: a practical primer for t-tests and ANOVAs. *Front Psychol.* 2013; 4: 863.
29. Sortino MA, Sinagra T, Canonico PL. Linagliptin: A thorough characterization beyond Its clinical efficacy. *Front Endocrinol (Lausanne).* 2013; 4: 16.
30. Kroller-Schon S, Knorr M, Hausding M, *et al.* Glucose-independent improvement of vascular dysfunction in experimental sepsis by dipeptidyl-peptidase 4 inhibition. *Cardiovasc Res.* 2012; 96: 140-149.
31. Van der Meijden PEJ, Heemskerk JWM. Platelet biology and functions: new concepts and clinical perspectives. *Nat Rev Cardiol.* 2019; 16: 166-179.
32. Waumans Y, Baerts L, Kehoe K, Lambeir AM, De Meester I. The dipeptidyl peptidase family, prolyl oligopeptidase, and prolyl carboxypeptidase in the immune system and inflammatory disease, including atherosclerosis. *Front Immunol.* 2015; 6: 387.
33. Burkhart JM, Vaudel M, Gambaryan S, *et al.* The first comprehensive and quantitative analysis of human platelet protein composition allows the comparative analysis of structural and functional pathways. *Blood.* 2012; 120: e73-82.
34. Greslele P, Guglielmini G, De Angelis M, *et al.* Acute, short-term hyperglycemia enhances shear stress-induced platelet activation in patients with type II diabetes mellitus. *J Am Coll Cardiol.* 2003; 41: 1013-1020.
35. Wang N, Tall AR. Cholesterol in platelet biogenesis and activation. *Blood.* 2016; 127: 1949-1953.
36. Hui H, Farilla L, Merkel P, Perfetti R. The short half-life of glucagon-like peptide-1 in plasma does not reflect its long-lasting beneficial effects. *Eur J Endocrinol.* 2002; 146: 863-869.
37. Brunton S. GLP-1 receptor agonists vs. DPP-4 inhibitors for type 2 diabetes: is one approach more successful or preferable than the other? *Int J Clin Pract.* 2014; 68: 557-567.
38. Raufman JP, Singh L, Eng J. Exendin-3, a novel peptide from *Heloderma horridum* venom, interacts with vasoactive intestinal peptide receptors and a newly described receptor on dispersed acini from guinea pig pancreas. Description of exendin-3(9-39) amide, a specific exendin receptor antagonist. *J Biol Chem.* 1991; 266: 2897-2902.
39. Barale C, Buracco S, Cavalot F, *et al.* Glucagon-like peptide 1-related peptides increase nitric oxide effects to reduce platelet activation. *Thromb Haemost.* 2017; 117: 1115-1128.
40. Schmidt T, Samaras P, Frejno M, *et al.* ProteomicsDB. *Nucleic Acids Res.* 2018; 46: D1271-D1281.
41. Blueprint Consortium. Blueprint Progenitors <https://blueprint.haem.cam.ac.uk/login>; 2019
42. Patti G, Cavallari I, Andreotti F, *et al.* Prevention of atherothrombotic events in patients with diabetes mellitus: from antithrombotic therapies to new-generation glucose-lowering drugs. *Nat Rev Cardiol.* 2019; 16: 113-130.
43. Mentlein R, Heymann E. Dipeptidyl peptidase IV inhibits the polymerization of fibrin monomers. *Arch Biochem Biophys.* 1982; 217: 748-750.
44. Graham GJ, Stevens JM, Page NM, *et al.* Tachykinins regulate the function of platelets. *Blood.* 2004; 104: 1058-1065.

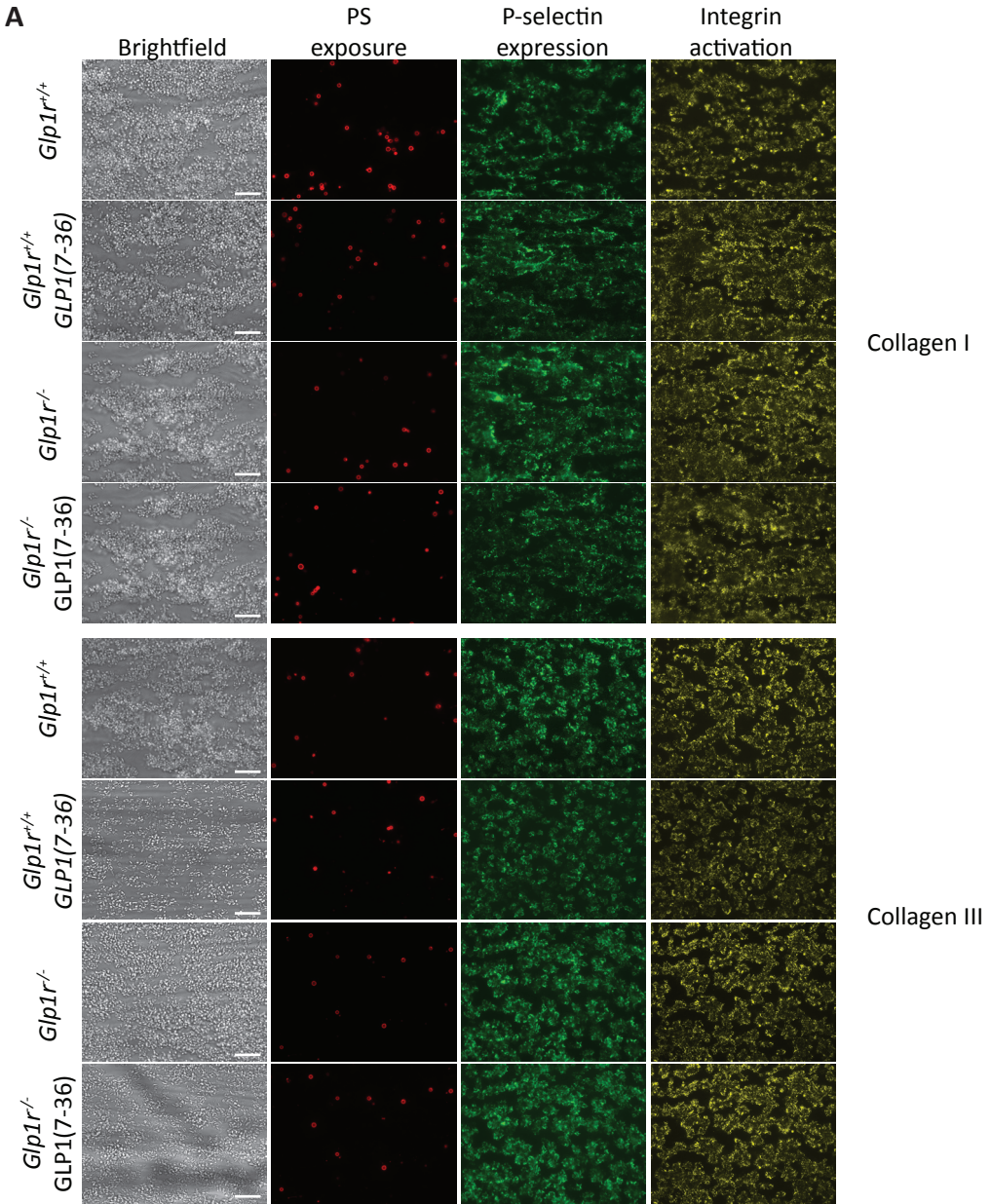
Supplemental material

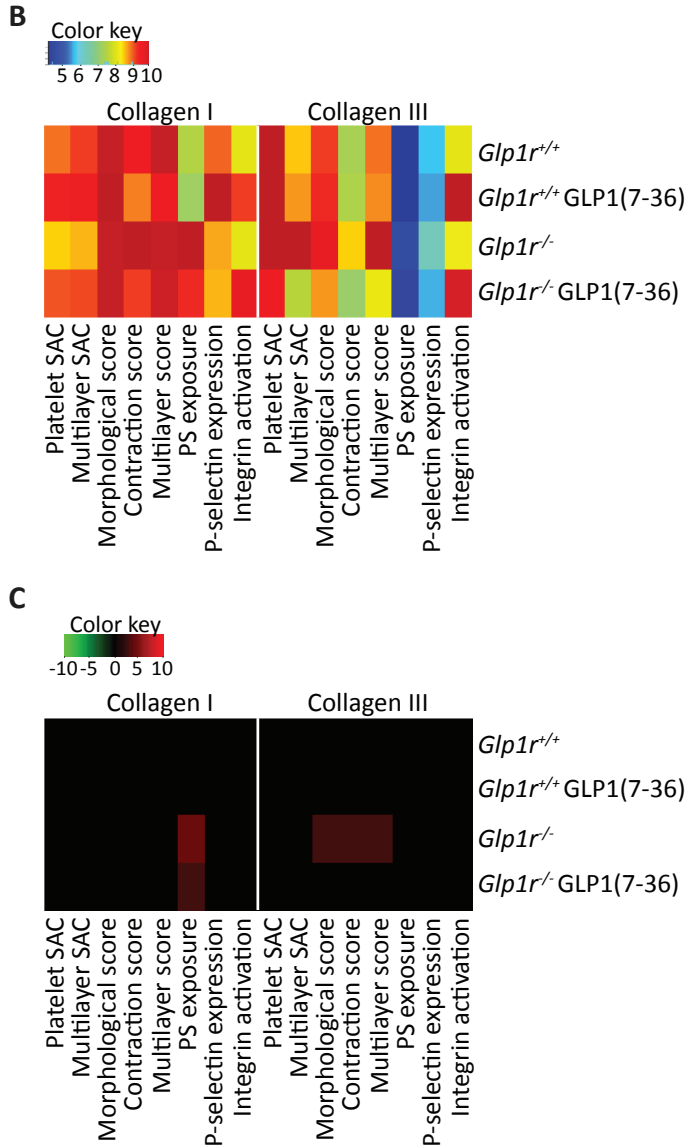


Suppl. Figure 1. Assessment of optimal concentrations of DPP inhibitors for selective inhibition of DPP4 or DPP8/9. **A**, Recombinant human DPP4 (0.04 ng/mL), DPP8 (0.05 ng/mL) or DPP9 (0.05 ng/mL) were incubated with increasing concentrations of sitagliptin, and total DPP activity was measured using the DPPIV-Glo protease assay. **B**, Recombinant human DPP4 (0.04 ng/mL), DPP8 (0.05 ng/mL) or DPP9 (0.05 ng/mL) were incubated with increasing concentrations of inhibitor 1G244, and DPP activity was measured using the DPPIV-Glo protease assay. **A-B**, Means \pm SEM, of 3-5 independent experiments. For subsequent experiments, the inhibitors were used at concentrations as indicated.

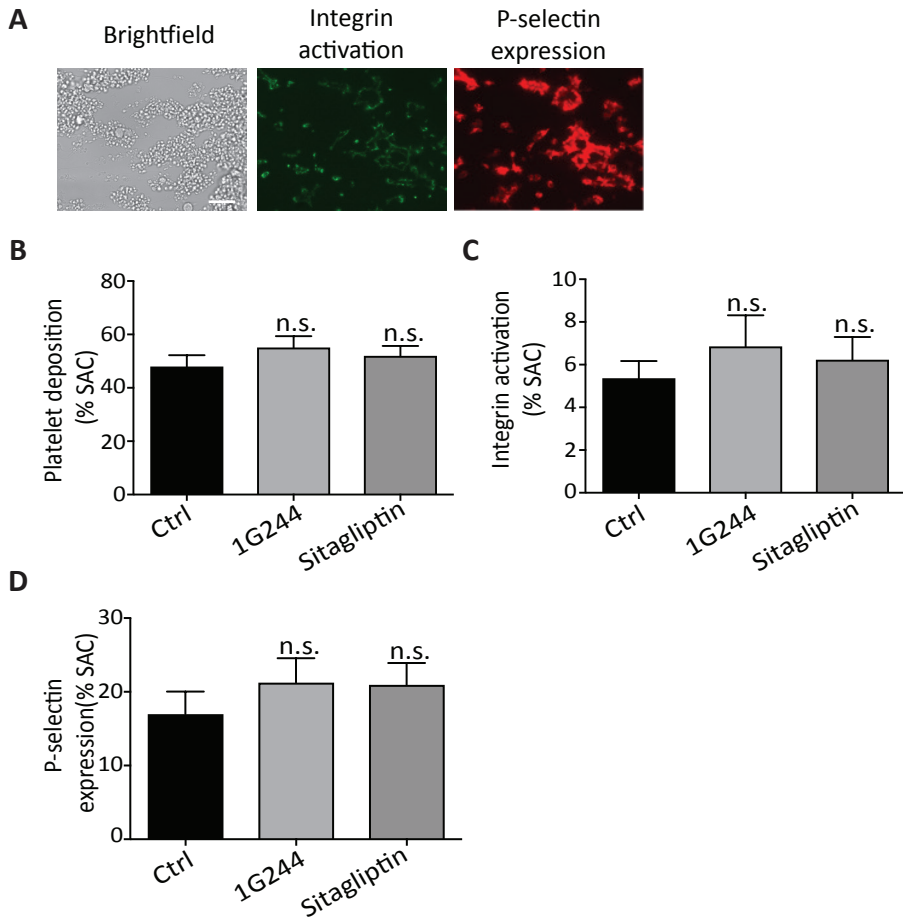


Suppl. Figure 2. DPP4 deficiency in mouse impairs whole blood thrombus formation. Whole blood from *Dpp4*^{-/-} or corresponding *Dpp4*^{+/+} mice was perfused over collagen-I and III microspots at 1000 s⁻¹ for 3.5 min. Where indicated, blood samples were pretreated with iloprost (0.55 μM) for 30 min. Thrombi were stained by post-perfusion with FITC-labeled anti-P-selectin mAb (platelet secretion), PE-labeled JON/A mAb (integrin activation) and AF647-annexin A5 (PS exposure). **A**, Representative brightfield and fluorescence images for collagen-III microspots. **B**, Representative brightfield and fluorescence images for collagen-I and collagen-III microspots (*Dpp4*^{+/+} and *Dpp4*^{-/-} in the presence of iloprost). Scale bars = 20 μm. **C**, Heatmap of univariate scaled values (0-10) for *Dpp4*^{+/+} and *Dpp4*^{-/-} mice with(out) iloprost. **D**, Subtraction heatmap of scaled values, compared to wildtype without treatment (collagen-III), filtered for differences with large effect size (Cohen's $d > 0.8$); n=10.

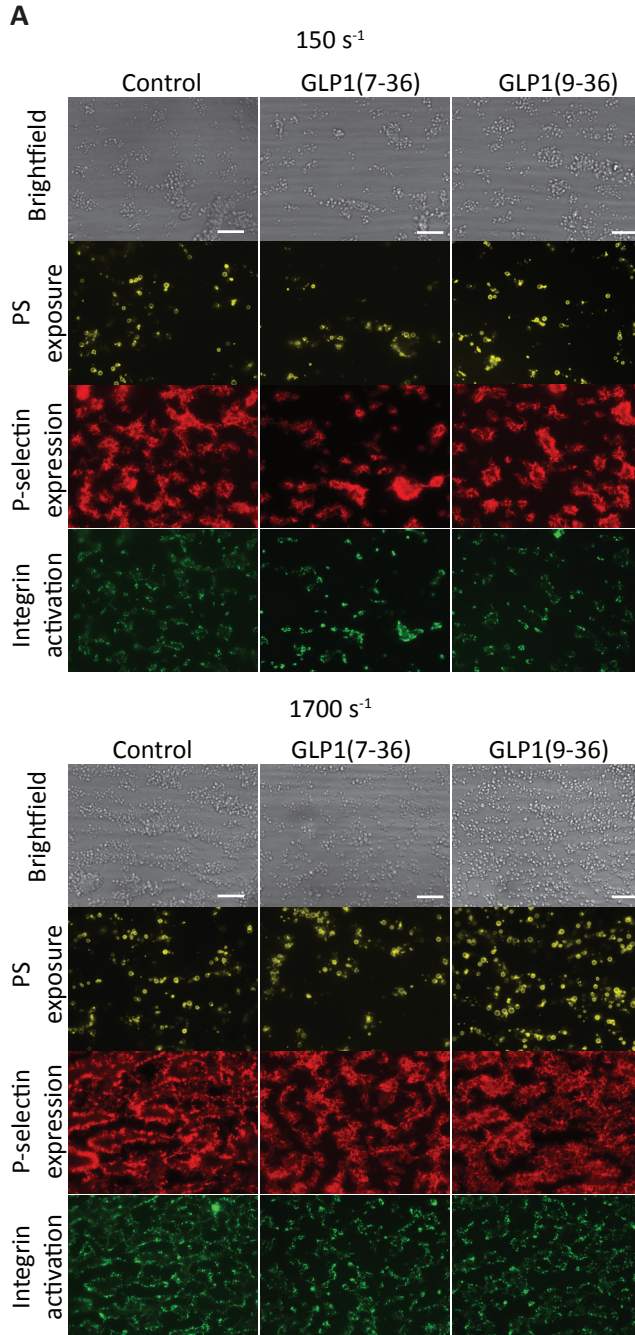


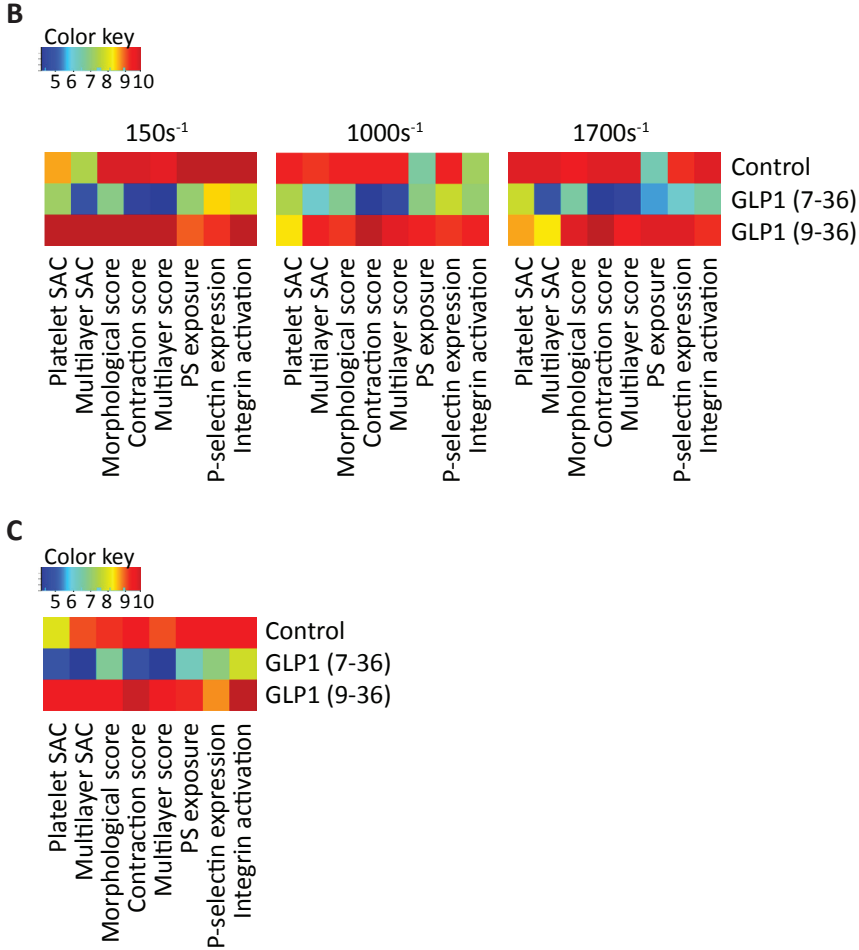


Suppl. Figure 3. Thrombus formation under flow is unaltered in *Glp1r^{-/-}* mice. Blood from *Glp1r^{-/-}* or corresponding wildtype mice (*Glp1r^{+/+}*) was perfused over collagen microspots, as indicated for Suppl. Figure 2. Blood samples were pretreated for 10 min with sitagliptin (7 μ M) in combination with GLP1(7-36) (50 nM) vs. vehicle for 10 min before perfusion. Thrombi formed were post-stained as in Suppl. Figure 2. **A**, Representative brightfield and fluorescence images. Scale bar = 20 μ m. **B**, Heatmap of scaled values (0-10) for *Glp1r^{+/+}* and *Glp1r^{-/-}* mice with(out) GLP1(7-36). **C**, Subtraction heatmap of scaled values, compared to wildtype without treatment, filtered for differences with large effect size (Cohen's $d > 0.8$); $n = 10$.

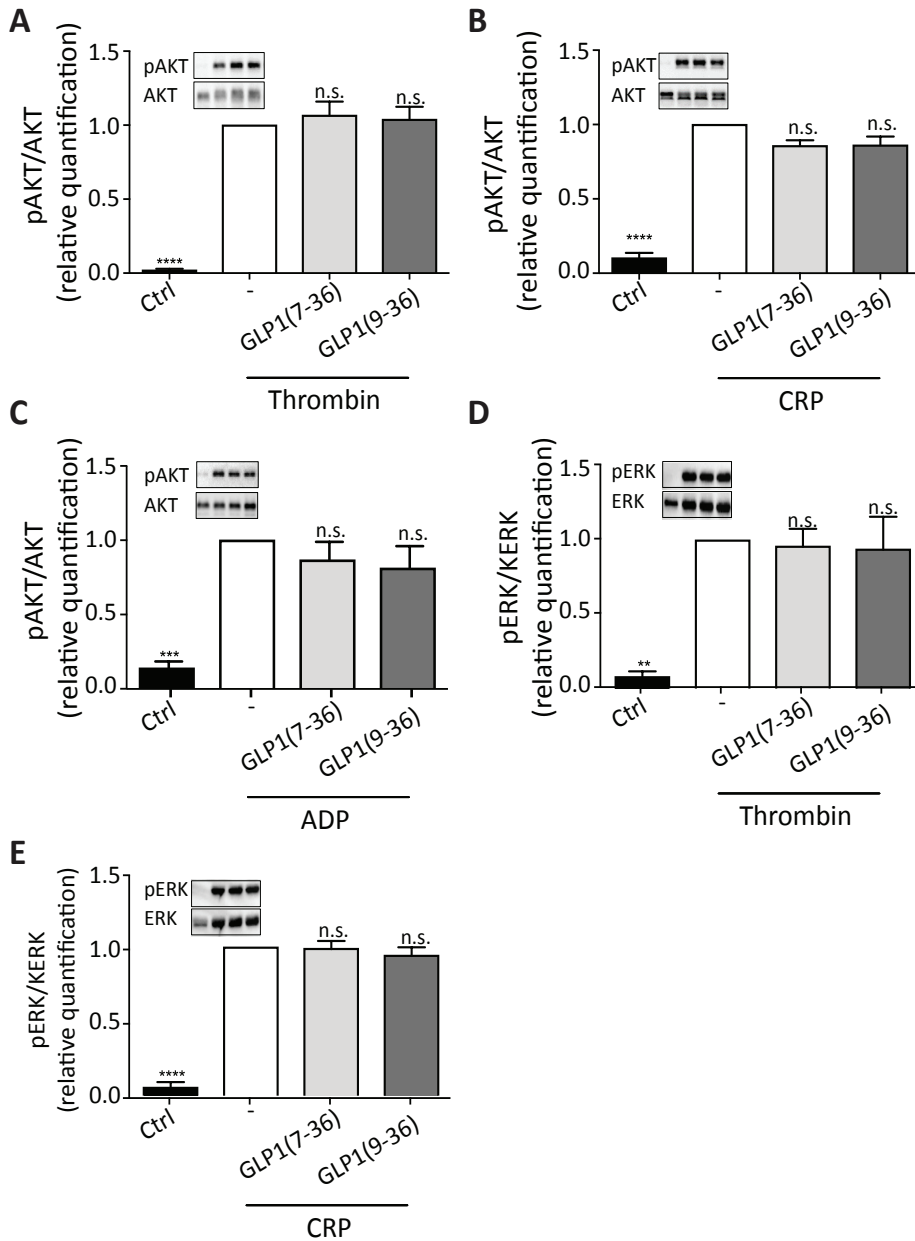


Suppl. Figure 4. Short-time inhibition of DPP4 or DPP8/9 *ex vivo* does not affect whole blood thrombus formation. Human blood was pre-incubated with inhibitor 1G244 (7 μM) or sitagliptin (7 μM) for 20 min at room temperature, and then recalcified in the presence of PPACK. Blood samples were perfused over collagen-I at 1000 s^{-1} for 3.5 min. Thrombi were poststained to measure P-selectin expression and integrin activation. **A**, Representative brightfield and fluorescence images. Scale bar = 20 μm . **B**, Platelet deposition, **C**, integrin activation and **D**, P-selectin expression, all expressed as % SAC. Means \pm SEM. $n=6$. One-way ANOVA with Bonferroni's multiple comparisons test vs. ctrl; n.s., not significant.





Suppl. Figure 5. GLP1(7-36) suppresses whole blood thrombus formation regardless of shear rate. Human blood was preincubated with sitagliptin (7 μM) plus GLP1(7-36) (50 nM), GLP1(9-36) (50 nM) or vehicle for 10 min at room temperature before re-calcification in the presence of PPACK. Blood samples were perfused over collagen-I at wall shear rates of 150 s^{-1} for 6 min, or at 1000 s^{-1} or 1700 s^{-1} for 3.5 min. Thrombi were labeled for PS exposure, P-selectin expression and integrin activation as in Suppl. Figure 2. **A**, Representative brightfield and fluorescence images. Scale bar = 20 μm . **B**, Heatmap of scaled (1-10) values for control and GLP1-treated blood. $n=9$ for 1000 s^{-1} ; $n=4$ for 150 s^{-1} and 1700 s^{-1} . **C**, Additionally, after recalcification, samples were co-perfused with 2MeADP (10 μM) and flowed over collagen-I at a shear rate of 1000 s^{-1} . Heatmap of univariate scaled values (0-10) for control and GLP1-treated blood; $n=4$.



Suppl. Figure 6. GLP1 does not affect stimulation-induced AKT or ERK phosphorylation in washed platelets. Washed human platelets were preincubated with vehicle, GLP1(7-36) or GLP1(9-36) (50 nM) in the presence of sitagliptin (7 μ M), and subsequently stimulated with thrombin (1 U/mL), CRP-XL (5 μ g/mL) or 2MeS-ADP (10 μ M) at 37 $^{\circ}$ C for 10 min, as indicated. As a negative control (ctrl), platelets were treated with prostacyclin (0.1 μ g/mL). After cell lysis, phosphorylation of AKT (pAKT) and ERK (pERK) was quantified, relatively to the total amounts of AKT and ERK, using western blot analysis. **A-C**, Ratio of pAKT/AKT, relative to stimulation with thrombin (**A**), CRP-XL (**B**) or ADP (**C**) or **D-E**, Ratio of pERK/ERK, relative to stimulation with thrombin (**D**) or CRP-XL (**E**). **A-E**, Means \pm SEM, n=3. One-way ANOVA with Dunn's multiple comparisons test for comparison vs. vehicle; *P<0.05, n.s. = not significant.

Chapter 10

General discussion

This thesis focuses on novel aspects of whole-blood thrombus formation in order to better understand in greater detail how blood platelets regulate this process in interaction with the blood plasma, leukocytes and vessel wall components. Below, I will discuss major findings of my work, which provide new insights into: (i) diverse platelet functions being assessed using microfluidics tests; (ii) the complex role of store-operated Ca^{2+} entry in platelet functions; (iii) the platelet-dependent neutrophil activation; (iv) new junctional interactions between connecting platelets, and (v) a *novel* platelet priming mechanism by plasma factors.

New insights into platelet functions in whole blood thrombus formation using microfluidics tests

A unifying methodology in this thesis is the use of the Maastricht flow chamber, which is a parallel-plate microfluidic device that allows for real-time examination of multiple platelet activation processes in small blood samples under controlled shear and (non-)coagulant conditions (Table 1).

This microfluidic device is successfully employed to assess platelet-dependent coagulation (*Chapter 2*) and to identify altered platelet functions in patients with genetically linked-immune deficiencies due to a mutation in *ORAI1*, *STIM1* or *FERMT3* (fermitin family member 3) (*Chapters 3-4*). By applying a multi-parameter analysis of the formed thrombi with patient blood, it became clear that the extent of alteration in platelet properties depended on the type of thrombogenic surface. This is in line with earlier studies using blood from healthy subjects in which the differences in thrombogenic activity of platelet-adhesive surfaces were investigated under flow conditions.^{1,2}

Table 1. Overview of applications of the microfluidic Maastricht flow chamber, resulting in novel pieces of information on the roles of platelets in thrombus formation. Also indicated is involvement of the platelet collagen receptor, glycoprotein VI (GPVI).

New insights into platelet function	Source of blood	GPVI involved	Chapter
Platelet dependent coagulation	human and mouse	yes	2
Role of Ca^{2+} entry (SOCE)	immune deficient patients	yes	3,4
Neutrophil activation	healthy subjects	yes	5
Role of GPVI	genetically modified mice	yes	6
Thrombus stability	healthy subjects	yes	7
Tight contacts	healthy subjects	yes	8
Priming via dipeptidyl protease	healthy subjects, genetically modified mice	yes	9

In *Chapter 6*, a novel multi-parameter analysis was applied to data from earlier microfluidic studies to compare the results from the flow measurements with blood from 38 genetically modified mouse strains and blood from corresponding wild types. These studies had been performed over the past decade with the same microfluidic device and essentially the same experimental protocol. Comparison of the flow runs for the sets of wild type mice showed limited variation in the six parameters of thrombus formation on collagen, hence indicating a consistent performance of the Maastricht flow chamber. This is a relevant finding, because earlier it was recognized that variety in the construction and use of microfluidic devices may impede the suitability of this technique for routine diagnostic testing of platelet functions.^{3,4} Our results prove good reproducibility for mouse blood analysis over years, provided that the same protocol and the same device is used. In order to evaluate this for human blood samples, the Standardization Committee of the ISTH has initiated a multi-center study to compare microfluidic devices between laboratories.⁵

Store-operated Ca²⁺ entry in platelets and immune blood cells

Controlled elevation of the cytosolic Ca²⁺ concentration, as a second messenger, is commonly regarded as essential for normal cell functions. In blood cells, including platelets, neutrophils and immune cells, the process of store-operated Ca²⁺ entry (SOCE) acts as a key regulatory mechanism of cytosolic Ca²⁺ homeostasis, thereby contributing to a proper function of these cells, such as reviewed in *Chapter 3*. In humans, genetic deficiencies are known of the Orai1 Ca²⁺ channel and of the regulatory protein STIM1, in each case associated with serious immune defects.⁶

Rare mutations in *ORAI1* or *STIM1* can result in either a loss-of-function or gain-of-function of platelet SOCE. Only incidental studies have reported on such (immune-compromised) patients with expected alterations in Ca²⁺ homeostasis and platelet properties. *Chapter 4* provides a first detailed study in these patient groups, comparing individuals either carrying a loss-of function mutation in *STIM1* or *ORAI1*, or a gain-of-function mutation in *ORAI1*. This study made an inventory of altered platelet activation, altered Ca²⁺ signaling and SOCE, changes in thrombus formation, and the relation with changes in platelet count. The overall reduced platelet reactivity in these patients is in agreement with earlier mice studies, investigating how the absence of STIM1 or Orai1 in the bone marrow affects platelet activation processes.^{7,8} A remarkable finding was that platelets from two patients with the same (loss-of-function) *ORAI1* mutation were differently compromised in SOCE and thrombus formation. In both patients, mild thrombocytopenia was observed, which together with the functional platelet defect could

explain the reduced thrombus formation. A full explanation of the differences between patients with same mutation will require omics analyses, as well as the examination of additional patients. However, for these two patients of *Chapter 4*, it can already be stated that there appears to be a different penetration of the mutated *ORAI1* allele into platelet functional changes.

Mouse platelets deficient in either protein presented impaired SOCE signals, which was accompanied by a reduced *in vitro* thrombus formation and a protection from *in vivo* arterial thrombosis.^{7,9} Markedly, a full knock-out of either gene in mice led to perinatal lethality,¹⁰ meaning that only bone marrow chimeras with STIM1 or Orai1 deficiency could be investigated.

Inhibition of SOCE in platelets and leukocytes has been proposed as a possible therapeutic target for treatment of thrombo-inflammatory diseases, thus stimulating the search for new pharmacological agents (*Chapter 3*). Several of these drugs, including 2-aminoethoxydiphenyl borate (2-ABP), have extensively been studied for effects on platelet activation, and were found to alter mouse platelet functionality in a similar way as genetic deletion of *Orai1*.¹¹ Given the reported negative association between platelet expression levels of STIM1 and Orai1 and clinical outcome of patients with an experienced stroke,¹² one can consider that such drugs may be beneficial for such patient groups. However, the fact that Orai1 is also expressed in immune cells and that *ORAI1* mutations are linked to the immune deficiency point a potential side effects of targeting Orai1. Hence, investigations are required to assess the balance of antithrombotic effects and (immune) disadvantageous effects of these inhibitors.

Regarding STIM1, a recent genome wide association study (GWAS) has revealed several single nucleotide polymorphisms (SNPs) in *STIM1* that are associated with an increased platelet volume and platelet distribution width.¹³ Considering the suggestion of different activation profiles of small and large platelets,¹⁴ carriers of these SNPs may differ in platelet functionality. This association may also point to STIM1-dependent priming effects on platelet count and function, that require further investigation.

How do platelets in a thrombus activate neutrophils?

In textbooks, platelets are considered to regulate leukocyte functions in the context of thrombo-inflammation, but precisely how this is achieved is still unclear (*Chapter 1*). Indications for a regulated cross-talk between platelets and leukocytes also come from recent observations that appreciable numbers of leukocytes accumulate in platelet-containing arterial and venous thrombi, which are retrieved from thrombotic patients by surgery.¹⁵ This may point to a role of the white blood cells also after thrombus formation.

Chapter 5 examines under which conditions and by which mechanisms platelet activation processes during thrombus formation influence neutrophil responses. This chapter untangles a multifactorial process wherein: (i) platelet activation supports initial neutrophil attachment; (ii) continuous platelet secretion ensures neutrophil chemotaxis; and (iii) platelet-secretory agents induce ongoing neutrophil activation. Herein, multiple platelet secretion products appear to act together in causing neutrophil Ca^{2+} rises. Markedly, irrespective of the extent of platelet activation in a thrombus or the numbers of neutrophils accumulated, hardly any of the adhered cells developed neutrophil extracellular traps (NETs).

These findings are in line with *in vivo* and *in vitro* studies recognizing multiple receptor-ligand interactions in platelet-neutrophil interaction.¹⁶ The finding that continuous platelet activation stimulates neutrophil trafficking is in agreement with the observation that neutrophils can follow a chemotactic gradient to traffic within a thrombus *in vivo*.^{17,18}

The neutrophils trapped in a thrombus appeared to contribute to the degradation of collagen below the thrombus, and even to endocytose the proteolyzed collagen. Thus, the present findings point to a coordinated mechanism of collagen degradation by neutrophils and activated platelets¹⁹, with as a consequence a facilitated efflux of neutrophils and influx of vascular cells at the thrombotic site.

Regarding the platelet secretion products, CXCL7 had a consistent role in the neutrophil-activating Ca^{2+} fluxes, whereas other chemokines such as CCL5 and CXCL4 contributed to a lesser extent. All these chemokines have been identified in the human platelet proteome.²⁰ In support of our findings, CXCL4, CCL5 and CXCL7 are all considered to play a role in the recruitment and migration of neutrophils.^{17,21,22} For CXCL7, it is known that this chemokine attracts migrating neutrophils to sites of vascular injury.¹⁷

Interesting is the activity of other bioactive lipoyxygenase products in platelet-neutrophil interaction, in particular 12-hydroxyeicosatetraenoic acid (12-HETE).²³ The data in *Chapter 5* indicate that blockage of platelet cyclooxygenase with indomethacin did not cause a notable effect on neutrophil activation. In contrast, blockage of lipoyxygenase-12 in platelets, thereby inhibiting the release of 12-HETE, dampened the neutrophil Ca^{2+} rises. In line with this finding, is that purified 12-HETE activates neutrophils in terms of a rise in cytosolic Ca^{2+} .²⁴

Another novel finding is the discovered inhibitory role of platelet integrin $\alpha_{\text{IIb}}\beta_3$ in platelet-neutrophil interactions. Using blood from Glanzmann's thrombasthenia patient lacking $\alpha_{\text{IIb}}\beta_3$ or by *in vitro* inhibition of this integrin, we found a >10 fold increase in

neutrophil attachment under flow conditions. However, neutrophil activation measured as increased cytosolic Ca^{2+} appeared to be decreased in these conditions. Interestingly, in control blood samples obtained from healthy volunteers, we found that several of the neutrophils interacted with procoagulant, phosphatidylserine-exposed platelets. This has also been observed by another laboratory.²⁵ A potential explanation for the finding is that the selective closing of integrin $\alpha_{\text{IIb}}\beta_3$ in phosphatidylserine-exposing platelets, described earlier in our group,²⁶ enforces platelet-dependent neutrophil interaction and activation.

Given the roles of platelets and neutrophils in thrombo-inflammation,²⁷ the blockage of platelet secretion might be beneficial to decrease neutrophil attraction and activation under such circumstances.

New insights into the role of glycoprotein VI and platelet-platelet interactions

Microfluidic devices can be used to elucidate the glycoprotein (GP)VI-dependent signaling pathway in collagen-dependent thrombus formation, such as indicated in *Chapter 6*. In earlier analyses, only platelet deposition (measured as surface area coverage) was used to evaluate the platelet phenotype. In *Chapter 6*, more in-depth information could be gained by also assessing other thrombus parameters, including platelet aggregation, thrombus morphology and thrombus contraction. We find that this multi-parameter analysis results in a more precise determination of the severity of platelet abnormalities, for instance to distinguish between altered platelet adhesion or aggregation, and to relate the defect to specific signaling pathways. A similar assessment of thrombus signatures, based on multi-parameter analyses, has also been described by our group for human blood samples.² For mouse it appeared that the summed changes in thrombus parameters *in vitro* reflected well the changes in arterial thrombosis *in vivo* quite well (*Chapter 6*). These data thereby extend the earlier found correlation between flow-dependent platelet adhesion determined by microfluidic devices and models of experimental arterial thrombosis *in vivo* in mouse.²⁸ The present multiparameter analysis of thrombus formation may help with the translation of *in vitro* to *in vivo* in mouse, and lead to a further reduction and refinement of animal use.

Considering a central role of GPVI in collagen-induced thrombus formation, in *Chapter 7* studied the inhibitory effect of two small molecules, honokiol and losartan, with supposed selective inhibitory effects on GPVI was studied. Both compounds indeed accomplished a decreased thrombus formation on a collagen surface, manifested as thrombi formed with a reduced height and loose structure. However, either compound

appeared not to be selective for GPVI inhibition, as they also impaired CLEC-2 mediated platelet activation. Furthermore, in comparison to specific anti-GPVI blocking antibodies,²⁹⁻³¹ these small molecules showed less potency in inhibiting GPVI-induced signaling. Considering that GPVI can also ligand fibrin(ogen),³² we can not rule out that the loose thrombus structure caused by honokiol and losartan is still GPVI-dependent.

Thrombus stability relies, among others, on persistent interactions between the platelets in an aggregate. *Chapter 8* proposes a new type of contact between connecting platelets, *i.e.* via junctional connections. For the first time, we report that the tight junction scaffold protein, *zona occludens-2* (ZO-2) is accumulated at the sites of platelet-platelet and platelet-endothelial cell contacts, in a way pointing to junctional formation such as present in endothelia and epithelia. Furthermore, electron microscopy images demonstrated the merging of platelet plasma membrane at the sites of platelet-platelet connection. So far, platelets are not known to form tight junctions, albeit gap junctional proteins have been reported to regulate platelet function. On the other hand, the junctional molecule-A (JAM-A) has been recognized as a negative regulator of integrin $\alpha_{IIb}\beta_3$ activation,^{33,34} and the related endothelial cell specific adhesion molecule (ESAM) is known to play a role in platelet-dependent clot retraction.³⁵

Given the established role of all these junctional proteins in epithelial barrier function, including an association of JAM-A with ZO-2,³⁶ we presumed that also in platelets ZO-2 may act in establishing cell-cell interactions. Considering the known function of tight junctions in tissue-forming cells, ZO-2 may help to form tight inter-platelet contacts within a thrombus core containing tightly packed platelets.³⁷ However, further investigation is required to unravel the mechanism of tight junction formation between adjacent platelets, and to establish how these structures contribute to thrombus formation.

Platelet priming by a new plasma factor

Platelet can be primed by a variety of mediators in a negative (*i.e.* lower activation tendency) or positive (higher activation tendency) way, leading to hypoactive or hyperactive platelets. Whereas negative priming is mainly regulated by endothelial mediators (prostacyclin, nitric oxide), positive priming can also come from plasma-derived mediators (epinephrine, thrombopoietin).³⁸⁻⁴⁰ Positive priming effects of platelets have been associated with several diseases, including diabetes, cancer and renal failure.

Patients with type II diabetes mellitus are reported to have hyperactive platelets, *i.e.* positively primed platelets associated with an increased risk of cardiovascular disease. Treatment of these patients with inhibitors of dipeptidyl peptidase-4 (DPP4) appeared to

improve their cardiovascular state.^{41,42} Chapter 9 examined how DPP4 inhibition affected platelet reactivity in whole-blood thrombus formation. Our results clarified that DPP4 activity is primarily originated in the blood plasma, thus indicating that direct effects of DPP4 inhibitors on platelets are unlikely.

Investigations then continued on the most described substrate of DPP4, *i.e.* the incretin hormone glucagon-like peptide-1 (GLP1), which is enzymatically cleaved by DPP4 into an inactive form.⁴³ In pancreatic cells, the active GLP1 binds to the receptor GLP1R, thus stimulating insulin secretion. Therefore it is also targeted as a novel antidiabetic agent and clinical studies revealed similar beneficial effect on cardiovascular state when using DPP4 inhibitors or GLP1R agonists on diabetic patients.⁴² In Chapter 9, we found that under conditions where the active GLP1 form is high, *i.e.* in blood from mice deficient in DPP4 (*Dpp4*^{-/-}) or in human blood supplemented with the active GLP1 active, whole-blood thrombus formation was mitigated. Previously, GLP1 was considered to inhibit platelets by elevating cyclic AMP via a the GLP1R receptor.⁴⁴ However, we were unable to reproduce the *Dpp4*^{-/-} phenotype in blood from *Glp1r*^{-/-} mice. A published transcriptome analysis of human megakaryocytes and platelets indicates no more than marginal expression of the *GLP1R* gene. Furthermore, GLP1 has also been reported to enhance nitric oxide effects and then inhibiting platelet activity via cyclic GMP.⁴⁵ Accordingly, the pathway by which the DPP4-GLP1 axis alters platelet activation properties remains still unknown.

Yet, our results point to a negative priming effect of the GLP1 active isoform on platelets. Remarkably, this suppressive effect was most clearly seen in whole blood when flow was present, thus pointing to a novel, flow-dependent mechanism of platelet inhibition. The latter finding can be relevant for establishing the effectiveness of (other) medications that cause negative platelet priming. There is clearly a balance, since positive priming mediators were found to reduce the inhibitory effect of aspirin.³⁹ Together, our results may have partly unraveled why drugs targeting DPP4 can reduce the cardiovascular risk in diabetic patients.

Concluding remark

This thesis provided several new insights into pathways of collagen-dependent thrombus formation (Figure 1). The progress made includes: (i) consistent and elaborate use of the Maastricht flow chamber for the identification of altered platelet function in immune deficient patients and genetically modified mice; (ii) identification of new regulatory mechanism in platelet-dependent neutrophil activation by unraveling the roles of platelet-derived chemokines, lipoxygenases and integrins; (iii) development

and application of standardized multiparameter analysis of thrombus formation to rate the antithrombotic profile of genetically modified mice in relation to GPVI activity; (iv) applications to mechanically study the effect of possible GPVI inhibitors on platelet signaling mechanism and thrombus formation; (v) identification of a new junctional structure implicated in platelet-platelet interactions; and (vi) application of the flow chamber to unravel negative priming effect of a plasma protein on platelet function.

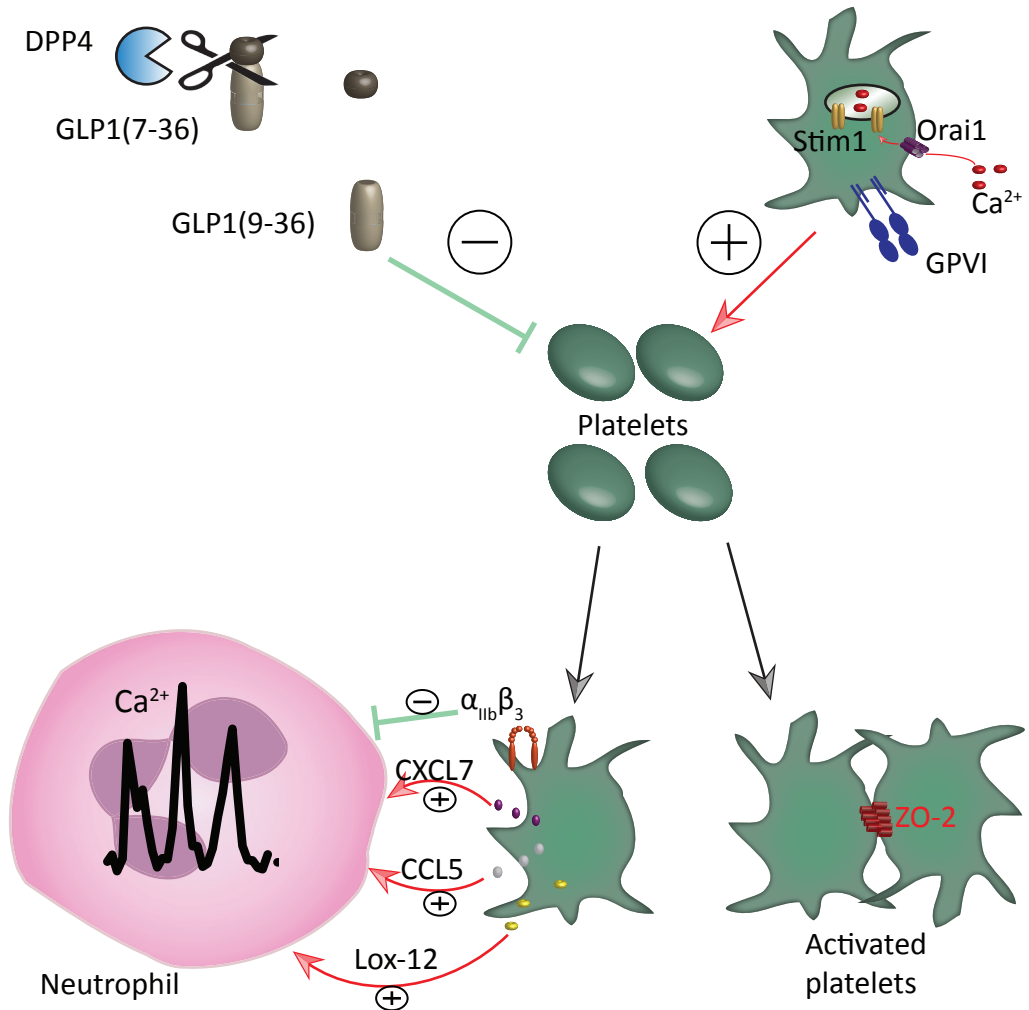


Figure 1. Schematic presentation of the main findings of this thesis. For explanation, see text.

References:

1. De Witt SM, Swieringa F, Cavill R, *et al.* Identification of platelet function defects by multi-parameter assessment of thrombus formation. *Nat Commun.* 2014; 5: 4257.
2. Van Geffen JP, Brouns SLN, Batista J, *et al.* High-throughput elucidation of thrombus formation reveals sources of platelet function variability. *Haematologica.* 2018. *In print.*
3. Zwaginga JJ, Nash G, King MR, *et al.* Flow-based assays for global assessment of hemostasis. Part 1: Biorheologic considerations. *J Thromb Haemost.* 2006; 4: 2486-2487.
4. Roest M, Reininger A, Zwaginga JJ, King MR, Heemskerk JW. Flow chamber-based assays to measure thrombus formation in vitro: requirements for standardization. *J Thromb Haemost.* 2011; 9: 2322-2324.
5. Scientific and Standardization Committee (SSC) of ISTH. SSC Subcommittee on Biorheology. Multi-center study on flow assay protocols and designs. <https://www.isth.org/page/SSC>; 2019
6. Lacruz RS, Feske S. Diseases caused by mutations in ORAI1 and STIM1. *Ann N Y Acad Sci.* 2015; 1356: 45-79.
7. Braun A, Varga-Szabo D, Kleinschnitz C, *et al.* Orai1 (CRACM1) is the platelet SOC channel and essential for pathological thrombus formation. *Blood.* 2009; 113: 2056-2063.
8. Gilio K, van Kruchten R, Braun A, *et al.* Roles of platelet STIM1 and Orai1 in glycoprotein VI- and thrombin-dependent procoagulant activity and thrombus formation. *J Biol Chem.* 2010; 285: 23629-23638.
9. Varga-Szabo D, Braun A, Kleinschnitz C, *et al.* The calcium sensor STIM1 is an essential mediator of arterial thrombosis and ischemic brain infarction. *J Exp Med.* 2008; 205: 1583-1591.
10. Collins HE, Zhu-Mauldin X, Marchase RB, Chatham JC. STIM1/Orai1-mediated SOCE: current perspectives and potential roles in cardiac function and pathology. *Am J Physiol Heart Circ Physiol.* 2013; 305: H446-458.
11. Van Kruchten R, Braun A, Feijge MA, *et al.* Antithrombotic potential of blockers of store-operated calcium channels in platelets. *Arterioscler Thromb Vasc Biol.* 2012; 32: 1717-1723.
12. Dong M, Zheng N, Ren LJ, Zhou H, Liu J. Increased expression of STIM1/Orai1 in platelets of stroke patients predictive of poor outcomes. *Eur J Neurol.* 2017; 24: 912-919.
13. Buniello A, MacArthur JAL, Cerezo M, *et al.* The NHGRI-EBI GWAS Catalog of published genome-wide association studies, targeted arrays and summary statistics 2019. *Nucleic Acids Res. search.* 2019; 47: D1005-1012.
14. Handtke S, Steil L, Palankar R, *et al.* Role of platelet size revisited-function and protein composition of large and small platelets. *Thromb Haemost.* 2019; 119: 407-420.
15. Riegger J, Byrne RA, Joner M, *et al.* Histopathological evaluation of thrombus in patients presenting with stent thrombosis. A multicenter European study: a report of the prevention of late stent thrombosis by an interdisciplinary global European effort consortium. *Eur Heart J.* 2016; 37: 1538-1549.
16. Li J, Kim K, Barazia A, Tseng A, Cho J. Platelet-neutrophil interactions under thromboinflammatory conditions. *Cell Mol Life Sci.* 2015; 72: 2627-2643.
17. Ghasemzadeh M, Kaplan ZS, Alwis I, *et al.* The CXCR1/2 ligand NAP-2 promotes directed intravascular leukocyte migration through platelet thrombi. *Blood.* 2013; 121: 4555-4566.
18. Darbousset R, Mezouar S, Dignat-George F, Panicot-Dubois L, Dubois C. Involvement of neutrophils in thrombus formation in living mice. *Pathol Biol (Paris).* 2014; 62: 1-9.
19. Mastenbroek TG, Feijge MA, Kremers RM, *et al.* Platelet-associated matrix metalloproteinases regulate thrombus formation and exert local collagenolytic activity. *Arterioscler Thromb Vasc Biol.* 2015; 35: 2554-2561.
20. Burkhart JM, Vaudel M, Gambaryan S, *et al.* The first comprehensive and quantitative analysis of human platelet protein composition allows the comparative analysis of structural and functional pathways. *Blood.* 2012; 120: e73-82.
21. Kasper B, Brandt E, Bulfone-Paus S, Petersen F. Platelet factor 4 (PF-4)-induced neutrophil adhesion is controlled by src-kinases, whereas PF-4-mediated exocytosis requires the additional activation of p38 MAP kinase and phosphatidylinositol 3-kinase. *Blood.* 2004; 103: 1602-1610.
22. Yu C, Zhang S, Wang Y, *et al.* Platelet-Derived CCL5 Regulates CXC chemokine formation and neutrophil recruitment in acute experimental colitis. *J Cell Physiol.* 2016; 231: 370-376.
23. Pasqualini ME, Mohn CE, Petit JP, Manzo P, Eynard AR. COX and LOX eicosanoids modulate platelet activation and procoagulation induced by two murine cancer cells. *Prostaglandins Leukot Essent Fatty Acids.* 2000; 63: 377-383.
24. Reynaud D, Pace-Asciak CR. 12-HETE and 12-HPETE potently stimulate intracellular release of cal-

- cium in intact human neutrophils. *Prostaglandins Leukot Essent Fatty Acids*. 1997; 56: 9-12.
25. Kulkarni S, Woollard KJ, Thomas S, Oxley D, Jackson SP. Conversion of platelets from a proaggregatory to a proinflammatory adhesive phenotype: role of PAF in spatially regulating neutrophil adhesion and spreading. *Blood*. 2007; 110: 1879-1886.
 26. Mattheij NJ, Gilio K, van Kruchten R, *et al*. Dual mechanism of integrin $\alpha_{IIb}\beta_3$ closure in procoagulant platelets. *J Biol Chem*. 2013; 288: 13325-13336.
 27. Soehnlein O. Decision shaping neutrophil-platelet interplay in inflammation: From physiology to intervention. *Eur J Clin Invest*. 2018; 48.
 28. Baaten C, Meacham S, de Witt SM, *et al*. A synthesis approach of mouse studies to identify genes and proteins in arterial thrombosis and bleeding. *Blood*. 2018; 132: e35-e46.
 29. Lecut C, Feeney LA, Kingsbury G, *et al*. Human platelet glycoprotein VI function is antagonized by monoclonal antibody-derived Fab fragments. *J Thromb Haemost*. 2003; 1: 2653-2662.
 30. Massberg S, Konrad I, Bultmann A, *et al*. Soluble glycoprotein VI dimer inhibits platelet adhesion and aggregation to the injured vessel wall in vivo. *Faseb J*. 2004; 18: 397-399.
 31. Ohlmann P, Hechler B, Ravanat C, *et al*. Ex vivo inhibition of thrombus formation by an anti-glycoprotein VI Fab fragment in non-human primates without modification of glycoprotein VI expression. *J Thromb Haemost*. 2008; 6: 1003-1011.
 32. Mangin PH, Onselae MB, Receveur N, *et al*. Immobilized fibrinogen activates human platelets through glycoprotein VI. *Haematologica*. 2018; 103: 898-907.
 33. Naik MU, Stalker TJ, Brass LF, Naik UP. JAM-A protects from thrombosis by suppressing integrin $\alpha_{IIb}\beta_3$ -dependent outside-in signaling in platelets. *Blood*. 2012; 119: 3352-3360.
 34. Karshovska E, Zhao Z, Blanchet X, *et al*. Hyperreactivity of junctional adhesion molecule A-deficient platelets accelerates atherosclerosis in hyperlipidemic mice. *Circ Res*. 2015; 116: 587-599.
 35. Stalker TJ, Wu J, Morgans A, *et al*. Endothelial cell specific adhesion molecule (ESAM) localizes to platelet-platelet contacts and regulates thrombus formation in vivo. *J Thromb Haemost*. 2009; 7: 1886-1896.
 36. Monteiro AC, Sumagin R, Rankin CR, *et al*. JAM-A associates with ZO-2, afadin, and PDZ-GEF1 to activate Rap2c and regulate epithelial barrier function. *Mol Biol Cell*. 2013; 24: 2849-2860.
 37. Stalker TJ, Welsh JD, Tomaiuolo M, *et al*. A systems approach to hemostasis: 3. Thrombus consolidation regulates intrathrombus solute transport and local thrombin activity. *Blood*. 2014; 124: 1824-1831.
 38. Baaten C, Ten Cate H, van der Meijden PEJ, Heemskerk JWM. Platelet populations and priming in hematological diseases. *Blood Rev*. 2017; 31: 389-399.
 39. Blair TA, Moore SF, Hers I. Circulating primers enhance platelet function and induce resistance to antiplatelet therapy. *J Thromb Haemost*. 2015; 13: 1479-1493.
 40. Blair TA, Moore SF, Walsh TG, *et al*. Phosphoinositide 3-kinase p110 α negatively regulates thrombopoietin-mediated platelet activation and thrombus formation. *Cell Signal*. 2018; 50: 111-120.
 41. Alvarez CA, Lingvay I, Vuylsteke V, Koffarnus RL, McGuire DK. Cardiovascular Risk in Diabetes Mellitus: Complication of the Disease or of Antihyperglycemic Medications. *Clin Pharmacol Ther*. 2015; 98: 145-161.
 42. Patti G, Cavallari I, Andreotti F, *et al*. Prevention of atherothrombotic events in patients with diabetes mellitus: from antithrombotic therapies to new-generation glucose-lowering drugs. *Nat Rev Cardiol*. 2019; 16: 113-130.
 43. Zhong J, Rao X, Rajagopalan S. An emerging role of dipeptidyl peptidase 4 (DPP4) beyond glucose control: potential implications in cardiovascular disease. *Atherosclerosis*. 2013; 226: 305-314.
 44. Steven S, Jurk K, Kopp M, *et al*. Glucagon-like peptide-1 receptor signalling reduces microvascular thrombosis, nitro-oxidative stress and platelet activation in endotoxaemic mice. *Br J Pharmacol*. 2017; 174: 1620-1632.
 45. Barale C, Buracco S, Cavalot F, *et al*. Glucagon-like peptide 1-related peptides increase nitric oxide effects to reduce platelet activation. *Thromb Haemost*. 2017; 117: 1115-1128.

Chapter 11

Summary

Samenvatting

Valorization

Curriculum Vitae

Publications

Acknowledgment

Summary

Chapter 1 provides background information on mechanisms of blood platelet activation, collagen-induced thrombus formation and platelet-platelet interactions. Highlighted are the central roles of the collagen receptor glycoprotein VI (GPVI) and the signaling via cytosolic Ca^{2+} rises in these processes. Regarding thrombus formation on atherosclerotic plaques, an introduction is given of the known interactions of platelets with leukocyte subsets. This chapter also introduces the use of microfluidic devices for investigating the processes of thrombosis and hemostasis. Besides the Maastricht flow chamber employed in this thesis, also other custom-made and commercially devices are presented. **Chapter 2** gives an overview of the use of such devices for the study of platelet activation and coagulation in flowed whole blood. Included is a guidance on technical aspects that need to be taken care of, when platelet and coagulation activities are simultaneously assessed in microfluidic devices. Choices encompass variables in the actual flow method, in the way of microscopic image capture, and in the kind of image analysis. Furthermore, the chapter provides an inventory of the current approaches for unraveling the mechanisms underlying platelet-dependent coagulation. Based on the described proof-of-principle studies with mouse and patient blood samples, the review also lists some limitations for the use of microfluidics assays in the clinical practice.

Given the importance of Ca^{2+} homeostasis for proper functioning of platelets and immune cells, **Chapter 3** focuses on the regulation of cytosolic Ca^{2+} in these blood cells. Within the context of thrombosis and thrombo-inflammation, this chapter in particular focuses on the process of store-operated Ca^{2+} entry (SOCE). In blood cells, SOCE is the main mechanism by which extracellular Ca^{2+} enters especially via the Ca^{2+} channel *ORAI1* and the intracellular Ca^{2+} sensor *STIM1*. How these two proteins interact and how they regulate the activities of platelets and immune cells is extensively described. The consequences are discussed of dysfunctional SOCE for pathophysiological processes such as atherothrombosis and ischemic stroke. Evidence for a role of *ORAI1* and *STIM1* in these processes comes from genetic mouse models and specific patients. Consistently, deficiency in *ORAI1* or *STIM1* leads to decreased thrombotic reactions without major bleeding complications, both in human and mouse. Given the limited role of platelet SOCE in normal hemostasis, inhibition of Ca^{2+} entry has been proposed as a new potential way to target thrombo-inflammatory diseases. However, pharmacological inhibitors tested so far have undesired side effects, in particular by influencing other cell types and tissues.

Genetic dysfunction of the SOCE-regulating proteins has been associated with development of immunodeficiency as well as with aberrant platelet functioning. In **Chapter 4**, the consequences of specific mutations in the *ORAI1* or *STIM1* genes are investigated for platelet activation and thrombus formation. While previous reports

on platelets only examined individual patients, we were able to study a larger group of patients with a confirmed mutation in *ORAI1* or *STIM1*. The platelets from most of these patients displayed altered Ca^{2+} signaling, when compared to control platelets. A loss-of-function mutation of *ORAI1* led to a reduced SOCE, whereas a gain-of-function mutation in the channel tended to increase the SOCE signal. Interestingly, platelets from two patients with the same gain-of-function mutation in *ORAI1* showed differences in the extent of SOCE. Blood samples from all patients were also evaluated using a multiparameter assay of thrombus formation, which provided detailed information on platelet adhesion, aggregation and activation on an array of thrombogenic surfaces. With blood from 4 out of 6 patients, parameters of thrombus formation on collagen were impaired, partly due to a lower platelet count. However, on other thrombogenic surfaces, the detected impairments in thrombus formation were independent of the platelet count, but were clearly associated with the SOCE abnormality. The dissimilar platelet responses seen in patients with the same *ORAI1* mutation might be explained by a different penetration of the mutated *ORAI1* allele in the bone marrow. Two young patients with a homozygous loss-of function mutation received a bone marrow transplantation, after which the flow test detected a clear improvement in platelet functioning. Overall, our study highlighted the ability of multi-parameter microfluidic testing to detect combined effects of quantitative and qualitative platelet abnormalities.

Earlier studies revealed that platelets and neutrophils interact during thrombosis and inflammation. In **Chapter 5**, we investigated how the platelets in a thrombus affected neutrophils. We found that the activation state of the platelets controlled the adhesion as well as the micro-location of neutrophils in a flow-dependent way. A stable thrombus consisting of thrombin-activated and procoagulant platelets was most effective in attracting neutrophils, which remained there for up to 16 hours. Adhesive receptors on activated platelets (CD62P, CD40L) mediated the interaction of neutrophils, whereas platelet secretion products steered neutrophil movements and activation processes. Strikingly, highly activated, secreting platelets induced patterns of repetitive intracellular Ca^{2+} rises in the attracted neutrophils. Silencing of platelets or blockage of platelet-derived chemokines (CCL5, CXCL7) caused an overall reduction of the Ca^{2+} rises, thus pointing to lower neutrophil activation stages. Heterogeneities in the thrombus structure influenced the movement patterns of neutrophils. Furthermore, using blood from Glanzmann patients, lacking the platelet integrin $\alpha_{\text{IIb}}\beta_3$, we detected a negative role of this integrin in neutrophil attraction. Taken together, these results pointed to a multi-step process of platelet-neutrophil interactions, wherein glycoprotein receptors regulate neutrophil adhesion and platelet secretion products define the activation state of neutrophils in a thrombus.

Genetic mouse models are frequently employed in cardiovascular research to study particular proteins or signaling pathways in platelets. Microfluidics chambers are extensively used for assessing altered platelet functions, but comparisons of studies have not been performed so far. In **Chapter 6**, a re-analysis is presented of microfluidic thrombus formation of whole blood from 38 different strains of genetically modified mice, such as in comparison with blood from the corresponding wild type mice. The monogenetic knockout mice lacked a range of platelet receptors, protein kinases or other signaling proteins. In all cases, the studies were performed with the Maastricht flow chamber, the same experimental set up, and recording brightfield microscopic images. In this chapter, the images obtained from those experiments were uniformly re-analyzed to specifically assess alterations in platelet adhesion, aggregation and activation properties, according to a newly developed multiparameter approach. This re-analysis resolved high homogeneity of the results obtained with the various wild type mice, which then allowed us to also compare the modified mouse strains. Based on this multiparameter comparison, a network was constructed, unraveling the relative impact of the genes on thrombus formation and identifying clusters of genes implicated in GPVI-induced signaling. The unraveled phenotypic changes *in vitro* reflected well the alterations due to genetic knockout on arterial thrombosis tendency and tail bleeding *in vivo*. The multiparameter analysis allowed to judge on the severity of platelet defects regarding sub-processes of thrombus formation (platelet adhesion, aggregation and activation). Furthermore, for a subset of genes, also a comparison could be made of platelet-adhesive and signaling pathways induced by GPVI and other relevant adhesive receptors, such as C-type lectin like receptor 2 (CLEC2) and integrin $\alpha_6\beta_1$. Considering that thrombus formation *in vivo* is mediated not only by collagen, but also by other extracellular matrix proteins, we reasoned that the combination of multiple platelet-adhesive surfaces provides more complete insight into the consequences of platelet defects for arterial thrombosis.

Given the central role for GPVI in platelet activation and thrombus formation and its restricted expression in platelets with blood, GPVI is becoming a promising new target for antiplatelet therapy. In **Chapter 7**, we compared two small molecules, losartan and honokiol, with reported inhibitory effects on collagen-induced, GPVI-dependent platelet aggregation. While confirming this inhibition with GPVI ligands, we also noted inhibition when platelets were stimulated with a CLEC2 ligand. Furthermore, both compounds did not appear to affect platelet spreading nor GPVI clustering on the platelet membrane. However, losartan and honokiol suppressed platelet thrombus formation on a collagen surface. Jointly, these data indicated that these compounds are not acting as specific GPVI antagonists. Further studies are required to unravel the exact inhibitory mechanisms.

In vivo mouse studies have revealed that arterial thrombi consist of separate inner core and outer shell regions, wherein the core region is crucial for stabilization of the thrombi. This stabilization is considered to rely on tight platelet-platelet contacts, which are mediated by integrins and gap junctional proteins. In **Chapter 8**, we investigated another possible way of inter-platelet contacts via the formation of tight junctions. Here, we focused on the localization of the tight junction protein, *zona occludens 2* (ZO-2), which is abundantly expressed in platelets. Upon spreading, interacting platelets showed a redistribution of ZO-2 from the cytosol to the cell periphery. Ultimately, clusters of ZO-2 were seen at platelet-platelet contact sites, as demonstrated by high resolution confocal and super-resolution microscopy. Similar staining patterns for ZO-2 were also seen at sites of platelet-endothelial cell interactions, in a way resembling the structures between confluent endothelial cells. These first observations suggest that tight junctions of ZO-2 are formed between activated, interacting platelets, supporting their stable contacts.

Platelet reactivity can be increased in various diseases, such as obesity and diabetes mellitus. Since this hyperreactivity is associated with an increased risk of cardiovascular events, it is important to know the overall platelet functions in these patient groups. **Chapter 9** investigates how a treatment with dipeptidyl peptidase 4 (DPP4) inhibitors - *i.e.* drugs regularly prescribed to diabetic patients - can influence platelet activity. Using various genetically modified mice, we found that abrogation of DPP4 by either pharmacological blockage or genetic deletion resulted in impaired thrombus formation. It is known that DPP4 inhibition leads to an increase in plasma of the bioactive form of glucagon-like peptide-1 (GLP1). We thus monitored how *in vitro* addition of bioactive GLP1 altered platelets. When added to human blood, GLP1 also resulted in a reduced thrombus volume. By contrast, the inactive form of GLP1 (*i.e.* the DPP4-cleaved GLP1) was without effect here. Interestingly, the GLP1 effect was only measurable in the presence of plasma or blood, suggesting that the presence of a plasma factor and perhaps flow is required for the inhibitory effect. We propose that in plasma the active GLP1 causes a negative priming effect on platelets, which results in a lower platelet activation capacity. These results provide new mechanistic insight into the cardioprotective effect of DPP4 inhibition in diabetic patients.

The final **Chapter 10** discusses key findings of this thesis in view of the recent literature. It is reasoned that elaborate measurements of the thrombus-forming process using microfluidics techniques can disclose even small, relevant differences in the functions of human and murine platelets.

Samenvatting

Hoofdstuk 1 biedt relevante achtergrondinformatie over de mechanismen van plaatjesactivering, collageen-afhankelijke trombus-vorming en plaatjes-plaatjes interacties. Aandacht is besteed aan de centrale rol van de collageenreceptor glycoproteïne VI (GPVI) en de signalering door verhoging van het cytosolisch Ca^{2+} in deze processen. Beschreven is verder op welke wijzen bloedplaatjes een interactie kunnen aangaan met verschillende typen leukocyten bij de trombusvorming op atherosclerotische plaques. Dit hoofdstuk geeft voorts aan hoe *microfluidic* kamers gebruikt kunnen worden bij de bestudering van trombose- en hemostaseprocessen. Naast de Maastricht flow-kamer gebruikt in dit proefschrift, worden ook andere al dan niet commercieel verkrijgbare kamers gepresenteerd. **Hoofdstuk 2** geeft een overzicht van het gebruik van dergelijke kamers voor bepalingen van de plaatjesactivering en de stolling in stromend bloed. Richtlijnen zijn gegeven voor de technische procedures die gevolgd kunnen worden om degelijke metingen succesvol te kunnen verrichten. Keuzes moeten gemaakt worden wat betreft de flow-methode, de wijze van microscopie en beeldvorming, en de procedure van beeldanalyse. Dit hoofdstuk beschrijft verder de mogelijke experimentele benaderingen voor het ophelderen van de mechanismen van plaatjes-afhankelijke bloedstolling. Op basis van enige *proof-of-principle* studies met bloed van muizen of patiënten wordt ook ingegaan op de beperkingen van het gebruik van *microfluidic* testen in de klinische praktijk.

Een goede Ca^{2+} homeostase is van essentieel belang voor het adequaat functioneren van plaatjes en immuuncellen. **Hoofdstuk 3** geeft een overzicht van de regulatie van de cytosolische Ca^{2+} -concentratie in dergelijke bloedcellen. Met als aandachtspunten trombose en ontsteking gaat dit hoofdstuk uitgebreid in op het proces van *store-operated Ca^{2+} entry* (SOCE). In bloedcellen is SOCE het belangrijkste mechanisme waardoor Ca^{2+} van buiten de cel binnenkomt via het Ca^{2+} -kanaal ORAI1 en de intracellulaire Ca^{2+} -sensor STIM1. Beschreven is hoe deze twee eiwitten een interactie met elkaar aangaan, en hoe zij tezamen de activeringspatronen van plaatjes en immuuncellen bepalen. Ook is aangegeven welke de gevolgen zijn van een verstoorde SOCE bij de pathofysiologie van atherotrombose en een ischemisch herseninfarct. De aanwijzingen voor een rol van ORAI1 en STIM1 bij deze processen komen uit studies met genetische gemodificeerde muizen en met specifieke patiëntengroepen. Een defecte werking van ORAI1 of STIM1 resulteert in een verminderde tromboseneiging, echter zonder grote bloedingscomplicaties zowel bij mens als muis. Gezien de beperkte rol van SOCE bij de normale hemostase is er verondersteld dat remming van de Ca^{2+} -instroom een manier kan zijn

om te interveniëren bij trombotische aandoeningen. Evenwel blijken de farmacologische remmers die tot dusver zijn getest, ongewenste bijeffecten te hebben als gevolg van beïnvloeding van andere cellen en weefsels.

Mutaties in de eiwitten die SOCE reguleren kunnen gepaard gaan met immuundefecten dan wel met functieverlies van bloedplaatjes. In **Hoofdstuk 4** zijn de gevolgen onderzocht van mutaties in de *ORAI1* of *STIM1* genen voor de plaatjesactivering en trombusvorming. In tegenstelling tot eerder werk, waarin alleen enkele patiënten gerapporteerd zijn, konden wij hier een grotere groep patiënten bestuderen, allen met dysfunctionele mutaties in *ORAI1* of *STIM1*. De plaatjes van de meesten van deze patiënten vertoonden een abnormaal Ca^{2+} -signaal in vergelijking tot controleplaatjes. Een *loss-of-function* mutatie in *ORAI1* resulteerde in een verminderde SOCE, terwijl een *gain-of-function* mutatie in dit kanaal soms een verhoogd SOCE-signaal liet zien. Een markante bevinding was dat de plaatjes van twee patiënten met dezelfde *gain-of-function* mutatie in *ORAI1* verschilden in de mate van SOCE-activiteit. Het bloed van al deze patiënten werd ook gebruikt voor bepaling van de trombusvorming. Hiervoor werd een multiparameter-test gebruikt, die detail informatie geeft over de adhesie, aggregatie en activering van plaatjes op verschillende trombogene oppervlakken. Bij bloed van 4 van de 6 patiënten bleek de trombusvorming op een collageenoppervlak verminderd te zijn, ten dele als gevolg van een matig verlaagde plaatjesconcentratie. Anderzijds was de verminderde trombusvorming op andere oppervlakken onafhankelijk van de lagere plaatjesconcentratie, en was deze duidelijker gelinkt aan het SOCE-defect. De waargenomen verschillen in plaatjesreactiviteit tussen patiënten met eenzelfde *ORAI1* mutatie kan verklaard worden door een ongelijke penetratie van het gemuteerde *ORAI1* allel in het beenmerg. Twee jonge patiënten (kinderen) met een homozygote *loss-of function* mutatie ondergingen een beenmergtransplantatie, waarna dezelfde flowtest een duidelijke verbetering toonde van het plaatjesfunctieprofiel. Samengevat demonstreert deze studie de mogelijkheden van multiparameter testen met behulp van flow-kamers bij het opsporen van gecombineerde effecten van kwantitatieve en kwalitatieve plaatjesafwijkingen.

Eerder werk heeft laten zien dat plaatjes en granulaire leukocyten (neutrofielen) met elkaar interacties kunnen aangaan bij tromboses en ontstekingen. In **Hoofdstuk 5** hebben we onderzocht op welke wijze de plaatjes in een trombus invloed kunnen uitoefenen op naburige neutrofielen. Het bleek dat de activeringsstatus van de plaatjes bepalend was voor de aanhechting en de micro-locatie van neutrofielen uit bloed op een flow-afhankelijke manier. Een stabiele trombus opgebouwd uit trombine-geactiveerde en procoagulante plaatjes was meest effectief in het aantrekken van neutrofielen, die vervolgens tot 16

uur ter plekke bleven. Adhesieve receptoren op geactiveerde plaatjes (CD62P, CD40L) bewerkstelligden de hechting van neutrofielen, terwijl secretieproducten van plaatjes een sturende werking hadden op de bewegingspatronen en activeringsprocessen van de neutrofielen. Met name sterk geactiveerde, secreterende plaatjes zorgden voor een patroon van herhaalde Ca^{2+} -verhogingen in naburige neutrofielen. Wanneer de plaatjes tot rust gebracht werden of wanneer chemokines afkomstig uit de plaatjes geblokkeerd werden (CCL5, CXCL7), gaf dit een vermindering van de Ca^{2+} -responsen, en als gevolg daarvan een verlaagde activeringsstatus van de neutrofielen. Onregelmatigheden in trombusstructuur waren van invloed op de bewegingspatronen van de witte bloedcellen. Verder vonden we, gebruik makend van het bloed van Glanzmann patiënten - bij wie integrine $\alpha_{\text{IIb}}\beta_3$ op plaatjes ontbreekt -, dat dit integrine een negatieve rol had bij het aantrekken van neutrofielen. Samengevat wijzen de resultaten in dit hoofdstuk op een multi-stap proces van neutrofiel-plaatjes interacties, waarin glycoproteïne-receptoren bepalend zijn voor de neutrofiel-adhesie en plaatjes-secretieproducten zorg dragen voor een verhoogde activeringsstatus van de neutrofielen in een trombus.

In het cardiovasculaire onderzoek worden genetische gemodificeerde muizen veelvuldig gebruikt om specifieke eiwitten of signaleringspaden in plaatjes te bestuderen. Flow-kamers worden daarbij regelmatig toegepast om veranderingen vast te stellen in de plaatjeseigenschappen. Echter een goede vergelijking van dergelijke studies ontbreekt nog. **Hoofdstuk 6** bestaat uit een hernieuwde analyse van eerder werk, waarin de trombusvorming middels flow-kamers bepaald was met bloed van 38 verschillende stammen van genetisch gemodificeerde muizen, die steeds onderzocht waren in vergelijking met bloed van bijbehorende wildtype-muizen. De betreffende *knockout*-muizen hadden alle een mono-genetische deficiëntie in plaatjes-receptoren, proteïne-kinasen of andere signaleringseiwitten. In alle gevallen waren de oorspronkelijke studies uitgevoerd met dezelfde Maastricht flow-kamer, gebruik makend van dezelfde experimentele opzet, en van camera-opnames van microscopische helderveld-beelden. Beschreven is hoe de microscopie-beelden opnieuw zijn geanalyseerd om een beter inzicht te krijgen in de veranderingen in plaatjesadhesie, -aggregatie en -activering, daarbij gebruik makend van nieuwe multiparameter analysemethoden. Wij vonden sterk gelijkende resultaten voor de verschillende wildtype-muizen, waarmee het mogelijk werd om ook de genetisch gemodificeerde muizen onderling te vergelijken. Middels vergelijking van de diverse parameters konden we een netwerk van genen construeren, waarmee enerzijds beter inzicht verkregen werd in het relatieve belang van betreffende genen voor de trombusvorming, en anderzijds genenclusters naar voren kwamen, betrokken bij

de GPVI-afhankelijke signalering. De aldus bepaalde fenotypische veranderingen bleken goed overeen te komen met de effecten van genetische modificatie *in vivo* op de arteriële tromboseneiging en op staartbloedingstijden. Daarmee is deze multiparameter-analyse in staat een uitspraak te doen over de mate van plaatjesdysfunctie voor wat betreft sub-processen van trombusvorming (plaatjesadhesie, -aggregatie en -activering). Voorts kon voor een aantal genen ook een vergelijking gemaakt worden tussen signaleringsroutes, die gemedieerd worden door GPVI, *C-type lectin like receptor 2* (CLEC2) of integrine $\alpha_6\beta_1$. Aangezien trombusvorming *in vivo* niet uitsluitend door collageen maar ook door andere extracellulaire matrixeiwitten gemedieerd wordt, stipuleren wij dat de combinatie van plaatjes-adhesieve oppervlakken een meer compleet inzicht geeft in de gevolgen van plaatjesdefecten voor de arteriële trombose.

Uitgaande van een centrale rol van GPVI bij de plaatjesactivering en trombusvorming - een eiwit dat in bloed alleen in plaatjes tot expressie komt -, is het duidelijk dat GPVI wordt beschouwd als een veelbelovende nieuwe target voor antiplaatjestherapie. In **Hoofdstuk 7** hebben wij twee moleculen vergeleken, losartan en honokiol, waarvan een remmend effect beschreven is van de collageen-geïnduceerde en GPVI-afhankelijke plaatjesaggregatie. Deze waarnemingen konden wij bevestigen. Echter daarnaast maten we een inhibitie na stimulering van de plaatjes met CLEC2-ligand. Beide moleculen hadden geen effect op de spreiding van plaatjes of op de clustering van GPVI op het plaatjesmembraan. Echter zowel losartan als honokiol onderdrukten de trombusvorming op collageen. Tezamen geven deze bevindingen aan dat de betreffende moleculen niet werkzaam zijn als specifieke GPVI-antagonisten. Verder onderzoek is nodig om de precieze remmingsmechanismen te bepalen.

Experimenten met muizen *in vivo* hebben aangetoond dat arteriële trombi opgebouwd zijn uit een binnenste compacte structuur en daarbuiten een schil van los geaggregeerde plaatjes. Hierbij blijkt de binnen laag cruciaal te zijn voor de trombusstabilisatie. Deze stabilisatie wordt bewerkstelligd door vaste plaatjes-plaatjes contacten onder meer middels integrines en *gap-junction* eiwitten. In **Hoofdstuk 8** exploreerden we een aanvullend mechanisme van contactvorming tussen plaatjes, namelijk via de vorming van *tight-junctions*. Het onderzoek was vooral gericht op de sub-cellulaire lokalisatie van het *tight-junction* eiwit *zona occludens 2* (ZO-2), welke in hoge mate tot expressie komt in plaatjes. Plaatjes die spreidden en daarmee met elkaar in contact kwamen, lieten een herverdeling zien van het ZO-2 van het cytosol naar de celperiferie. Hoge resolutie confocale microscopie en super-resolutie microscopie onthulden de vorming van ZO-2 clusters in de contactplaatsen. Een soortgelijk kleuringspatroon

voor ZO-2 was ook aanwezig op contactplaatsen plaatjes met endotheelcellen, analoog aan de structuren tussen confluente endotheelcellen. Deze bevindingen suggereren dat er tussen geactiveerde, contact-makende plaatjes *tight-junctions* van ZO-2 gevormd worden, die van belang zijn voor stabiele plaatjes-plaatjes interacties.

De activiteit van plaatjes is vaak verhoogd bij aandoeningen als obesitas en diabetes mellitus. Aangezien een dergelijke hyperreactiviteit associeert met een verhoogd risico op hart- en vaatziekten, is het van belang om de plaatjesfuncties in deze patiëntengroepen goed te kennen. **Hoofdstuk 9** beschrijft hoe behandeling met remmers van *dipeptidyl peptidase 4* (DPP4) - medicatie die regelmatig wordt voorgeschreven aan diabetici - van invloed is op de plaatjesactiviteit. Gebruik makend van genetisch gemodificeerde muizen konden wij vaststellen, dat een defect in DPP4 middels een farmacologische remmer of genetische modificatie, resulteerde in verminderde trombusvorming. Bekend was dat de remming van DPP4 leidt tot een toename in plasma van de bioactieve vorm van *glucagon-like peptide-1* (GLP1). Daarom onderzochten wij het effect van toevoeging van bioactief GLP1 op plaatjes *in vitro*. In humaan bloed zorgde GLP1 voor een kleiner trombusvolume. Daarentegen was de inactieve vorm van GLP1 (d.w.z. het DPP4-geknipt GLP1) zonder effect. Een verdere interessante bevinding was dat het bioactieve GLP1 alleen werkzaam was in de aanwezigheid van plasma of bloed, hetgeen suggereert dat er een plasmafactor (of ook flow) nodig is voor het remmende effect. Daarmee konden we postuleren, dat in de aanwezigheid van plasma het actieve GLP1 voor een negatief *priming* effect op plaatjes zorgt, waardoor de plaatjesactivering verlaagt. Deze resultaten bieden daarmee een mechanistisch inzicht in de manier waarop DPP4-remming beschermend kan zijn voor cardiovasculaire aandoeningen in patiënten met diabetes.

Het laatste **Hoofdstuk 10** bediscussieert de belangrijkste bevindingen van deze dissertatie, gezien de recente literatuur. Beargumenteerd is dat uitgebreide analyse van het proces van trombusvorming met behulp van *microfluidic* technieken zelfs kleine, relevante verschillen kan detecteren in de functies van humane en muizenplaatjes.



Valorization

In recent years, an increasing pressure has been put on researchers to provide not only scientific impact, but also social or economic impact of their scientific findings.¹ Given the different nature of science, it is not equally straightforward to have a clear sight of the beneficial outcome of scientific research for society. Whereas in applied research one focuses on pragmatic questions and aspires to develop applications that can be implemented directly in current practice, in basic research emphasis lies more in expanding and exploring the underlying mechanism(s) of processes of interest without primarily aiming to develop specific applications. However, these two types of research should ideally complement each other in order to span the entire trajectory from bedside to bench and vice versa.²

Platelets have an essential role in hemostatic system. Upon vascular damage, platelets are in the frontline and rapidly form a platelet plug in order to cessate bleeding. However, aberrant platelet function can cause imbalance of the hemostatic process, potentially leading to thrombosis or bleeding, and hence cardiovascular events.³ Commonly, anti-platelet drugs are chosen to prevent cardiovascular events of the arteries, in conjunction with lipid-lowering medication and anti-hypertensive agents. Bleeding is the main negative side effect of anti-platelet drugs. Unfortunately, current platelet function tests in general lack sensitivity for predicting bleeding or thrombosis risks. Studies evaluating methods for monitoring platelet function upon anti-platelet treatment revealed that results from light transmission aggregometry (LTA), PFA-100, VerifyNow do not correlate well.^{4,5} Furthermore, clinical studies have also shown that the correction of anti-platelet treatment based on results from platelet function analysis did not improve the clinical outcome in patients.⁶ So far, it is unknown whether monitoring is actually useful for clinical practice.

In my thesis, I focused on unraveling the consequences of the effect of changes in platelet function, either due to genetic deficiency or pharmacological modulation, on platelet function and thrombus formation. Throughout the thesis, an *in vitro* microfluidic device was employed to study platelet function under shear conditions. The capability of this test to monitor platelet function has been shown before,⁷ however it has not been extensively used with patient blood. In Chapter 4, this microfluidic device has been employed to characterize platelet function in platelets from immunodeficient patients. For the first time, we could confirm that the genetic alteration causing immunodeficiency affected platelet function, which could explain the increased bleeding risk. Improvement of platelet function could also be recognized by this method as in samples from the same patients after bone marrow transplantation an improved platelet function was detected

Besides studying the effect of genetic alterations on platelet thrombus formation, this microfluidic device can be also used for testing the effect of pharmacological agents, such as drug candidates with direct effect on platelets or with regards to monitoring the indirect effect of other medication on platelet function, as is described in Chapter 7 and 9. Chapter 9 aimed to explain the reduction in cardiovascular events upon Dipeptidyl peptidase-4 antagonist treatment by linagliptin and sitagliptin. By using this microfluidic device, we unraveled a negative priming effect on platelets as an indirect effect of this treatment. The latter illustrates the diverse range of applicability of *in vitro* microfluidic devices.

Furthermore, microfluidic devices are ideal to investigate the interplay between platelets and other cell types, for instance endothelial cells⁸ or immune cells. In Chapter 5, the interaction between platelets and leukocytes have been extensively studied thereby focusing on the consequences of platelet inhibition on leukocyte activation and responses. Here, the inhibition of platelet secretion is appeared to reduce the leukocyte activation *in vitro*. Given the increasing interest in thrombo-inflammation, it is important aspect to be able to monitor such interactions between platelets and inflammatory/inflamed cells.

A recent paper highlighted that *in vitro* thrombus formation measurements are good reflection of results obtained in experimental mouse models for collagen-dependent arterial thrombosis,⁹ supporting the relevance of such an *in vitro* device and suggesting their possible involvement into the 3R approaches by reducing, refining and replacing animal experiments. In Chapter 6, we have compared the *in vitro* thrombus formation results assayed with blood from 33 different genetically modified mouse strains using a standardized image analysis protocol. The original microfluid experiments were performed over the last decade using the same protocol and device but in different laboratories. These comparisons unraveled that despite of the difference in time, the results are comparable. This is an important finding for future application and for developing a possible point-of-care device.

In this thesis, only one type of microfluidic device has been employed, but there are many commercial and costume-made microfluidic devices available for studying platelet functions under physiological and pathological conditions.¹⁰ Currently, no uniform guidelines exist on how to employ microfluidic devices and how to report the obtained results. In theory, laboratories using the same devices, could perform the experiment differently, thereby hampering comparison of results. To overcome this problem, the Biorheology Subcommittee of the Scientific and Standardization Committee of the

ISTH initiated a multi-center study on flow assay protocols and designs in which the results of one common microfluidic device and one custom microfluidic device will be compared across several centers/laboratories. One of the goals of this multicenter study is to formulate a general guideline regarding the most crucial aspects of performing microfluidic experiments.¹¹ As already been demonstrated in Chapter 6, using the same protocol and device can provide highly comparable results regardless of the executor.

Given the broad applicability of the microfluidic devices, its usage as a point-of-care (POC) test to assess platelet function has been postulated for already a number of years and several devices have been tested.¹² For instance, the total thrombus formation analysis system (T-TAS) has appeared to be suitable for recognizing the effect of antiplatelet and anticoagulant treatment in patients with coronary artery disease, acute coronary syndrome or ischemic stroke.¹² However, there are issues that have to be solved regarding preanalytical variables and on how to perform the test in a standardized manner, but also on how to interpret the outcome of the test.¹³ At present no uniform cut off values have been set for microfluidic assays with regard to platelet function. Given the natural variability in platelet function within the normal population, cut off values have to be set carefully. In addition, in order to improve and understand the results from patients with different disease states.¹³

Taken together, the results obtained from different patients, healthy volunteers and mice give a good overview of the usefulness of microfluidic devices in unravelling defective platelet function. Depending on the construction, it is possible to monitor both loss- and gain-of-function of the platelets leading to hemorrhage or thrombosis as it was proven for the Maastricht flow chamber in Chapter 6.

References

1. De Jonge B, Louwaars N. Valorizing science: whose values? Science & society series on convergence research. *EMBO Rep.* 2009; 10: 535-539.
2. James CR. Science unshackled: how obscure, abstract, seemingly useless scientific research turned out to be the basis for modern life? (2014).
3. Gregg D, Goldschmidt-Clermont PJ. Cardiology patient page. Platelets and cardiovascular disease. *Circulation.* 2003; 108: e88-90.
4. Lordkipanidze M, Pharand C, Schampaert E, *et al.* A comparison of six major platelet function tests to determine the prevalence of aspirin resistance in patients with stable coronary artery disease. *Eur Heart J.* 2007; 28: 1702-1708.
5. Moenen F, Vries MJA, Nelemans PJ, *et al.* Screening for platelet function disorders with Multiplate and platelet function analyzer. *Platelets.* 2019; 30: 81-87.
6. Deharo P, Cuisset T. Monitoring platelet function: what have we learned from randomized clinical trials? *Cardiovasc Diagn Ther.* 2018; 8: 621-629.
7. de Witt SM, Swieringa F, Cavill R, *et al.* Identification of platelet function defects by multi-parameter assessment of thrombus formation. *Nat Commun.* 2014; 5: 4257.

8. Coenen DM, Mastenbroek TG, Cosemans J. Platelet interaction with activated endothelium: mechanistic insights from microfluidics. *Blood*. 2017; 130: 2819-2828.
9. Baaten C, Meacham S, de Witt SM, *et al*. A synthesis approach of mouse studies to identify genes and proteins in arterial thrombosis and bleeding. *Blood*. 2018; 132: e35-e46.
10. Nagy M, Heemskerk JWM, Swieringa F. Use of microfluidics to assess the platelet-based control of coagulation. *Platelets*. 2017; 28: 441-448.
11. ISTH SSCot. Biorheology. <https://www.isth.org/members/group.aspx?id=100344>;
12. Lee H, Na W, Lee BK, Lim CS, Shin S. Recent advances in microfluidic platelet function assays: Moving microfluidics into clinical applications. *Clin Hemorheol Microcirc*. 2019; 71: 249-266.
13. Branchford BR, Ng CJ, Neeves KB, Di Paola J. Microfluidic technology as an emerging clinical tool to evaluate thrombosis and hemostasis. *Thromb Res*. 2015; 136: 13-19.

Curriculum Vitae

Curriculum Vitae

Magdolna Nagy was born on December 3rd 1988 in Cegléd, Hungary. In 1999, she went to secondary school at the Kossuth Lajos Gymnasium in Cegléd, where she obtained her gymnasium degree in 2007. In 2008, she started the bachelor study of Medical Laboratorial Diagnostic Imaging Analysis, dedicated to medical research laboratory analysis at the University of Debrecen. With the bachelor's degree, she continued education by following a master in Clinical Laboratory Sciences at the same university. During these studies, she joined the rheology laboratory of Dr. J. Hársfalvi to investigate blood platelet functions using different assays. She also received an ERASMUS scholarship to perform research in the laboratory of Prof. J.W.M. Heemskerk at Maastricht University. In 2014, she obtained her master's degree with honor, and in September of that year she started as a PhD student at the Department of Biochemistry in the Cardiovascular Research Institute Maastricht (CARIM) of Maastricht University. Under the supervision of Prof. J.W.M. Heemskerk, Prof. S.P. Watson and Dr. J.M.E.M. Cosemans, she performed research in the field of thrombosis and hemostasis, as described in this thesis. During the PhD period, she also visited the laboratories of Prof. W. Ouwehand (Cambridge, United Kingdom), Prof. B. Nieswandt (Würzburg, Germany), Prof. S. Watson (Birmingham, United Kingdom), Dr. H. Noels (Aachen, Germany), Prof. D. Mezzano (Santiago, Chile), Prof. V. O'Donnell (Cardiff, Wales, United Kingdom) and Dr. K. Jurk (Mainz, Germany). She presented this research at international conferences in Bad Homburg (Germany), Basel (Switzerland), Berlin (Germany), Bath (United Kingdom) and Bruges (Belgium), and also received an International Society of Thrombosis and Haemostasis (ISTH) Young Investigators Award. Currently, she works as post-doctoral researcher in the group of Prof. H. ten Cate and Dr. H.M.H. Spronk at the Department of Biochemistry at Maastricht University.

Curriculum Vitae

Magdolna Nagy werd geboren op 3 december 1988 te Cegléd, Hongarije. In 1999 begon ze de middelbare schoolopleiding aan het Kossuth Lajos Gymnasium te Cegléd, waar ze haar gymnasiumdiploma behaalde in 2007. Vervolgens startte ze een bacheloropleiding Medisch-laboratorium Beeldanalyse in de Diagnostiek met als specialisatie onderzoeklaboratoriumanalyse aan de Universiteit van Debrecen. Na het behalen van het bachelorsdiploma, volgde ze aan dezelfde universiteit een masteropleiding Klinische Laboratoriumwetenschappen. Tijdens deze studies werkte ze in reologisch laboratorium van Dr. J. Hársfalvi als studentonderzoeker. Het betreffende project was gericht op metingen van bloedplaatjesfuncties. Hiervoor ontving ze ook een ERASMUS-studiebeurs, waarmee ze onderzoek kon uitvoeren in het laboratorium van Prof. J.W.M. Heemskerk aan de Universiteit Maastricht. In 2014 ontving ze haar masterdiploma met aantekening cum laude. Op 1 september van dat jaar startte ze als PhD-student aan het Cardiovascular Research Institute Maastricht (CARIM) van de Universiteit Maastricht, binnen de Vakgroep Biochemie. Onder begeleiding van Prof. J.W.M. Heemskerk, Prof. S.P. Watson en Dr. J.M.E.M. Cosemans voerde ze onderzoek uit op het gebied van trombose en hemostase, zoals beschreven in dit proefschrift. Tijdens deze periode bezocht ze ook de laboratoria van Prof. W. Ouwehand (Cambridge, Verenigd Koninkrijk), Prof. B. Nieswandt (Würzburg, Duitsland), Prof. S. Watson (Birmingham, Verenigd Koninkrijk), Dr. H. Noels (Aken, Duitsland), Prof. D. Mezzano (Santiago, Chili), Prof. V. O'Donnell (Cardiff, Wales, Verenigd Koninkrijk) en Dr. K. Jurk (Mainz, Duitsland). Haar promotieonderzoek presenteerde ze op internationale congressen in Bad Homburg (Duitsland), Basel (Zwitserland), Berlijn (Duitsland), Bath (Verenigd Koninkrijk) en Brugge (België); hiervoor kreeg ze ook een International Society of Thrombosis and Haemostasis (ISTH) Young Investigators Award. Momenteel is zij werkzaam bij de vakgroep Biochemie aan de Universiteit Maastricht als post-doctoral onderzoeker in de groep van prof. H. ten Cate en Dr. H.M.H. Spronk.

Önéletrajz

Nagy Magdolna 1988. december 3-án született Cegléden. 1999-ben a gimnáziumi tanulmányait a ceglédi Kossuth Lajos Gimnáziumban kezdte meg, amelyet 2007-ben sikeres érettségi vizsga letételével zárt. 2008-ban a felsőfokú tanulmányait a Debreceni Egyetem laboratóriumi és képalkotó diagnosztikai analitikus alapképzésén kezdte meg. A kutatólaboratóriumi analitikus alapképzés megszerzését követően, tanulmányait a Debreceni Egyetem klinikai laboratóriumi kutató mesterképzésén folytatta. Az egyetemi tanulmányai alatt Dr. Hársfalvi Jolán reológia laboratóriumához csatlakozott, ahol különböző technikákat alkalmazva a trombociták működését tanulmányozta. Ezen időszak alatt ERASMUS ösztöndíjban részesült, amely segítségével kutatását a Maastricht Egyetemen prof. J.W.M. Heemskerk laboratóriumában folytathatta. A kiváló minősítésű mesterdiploma átvétele után, 2014 szeptemberében megkezdte a doktori (PhD) képzését a Maastricht Egyetem Biokémia Intézetében Prof. J.W.M. Heemskerk, Prof. S.P. Watson és Dr. J.M.E.M. Cosemans témavezetése alatt. A trombózis és hemosztázis területén végzett kutatásának eredményei ebben a disszertációban kerültek leírásra. A doktori képzés ideje alatt többek között prof. W. Ouwenhand (Cambridge, Egyesült Királyság), prof. B. Nieswandt (Würzburg, Németország), prof. S. Watson (Birmingham, Egyesült Királyság), Dr. H. Noels (Aachen, Németország), prof. D. Mezzano (Santiago, Chile), prof. V. O'Donnell (Cardiff, Wales, Egyesült Királyság) és Dr. K. Jurk (Mainz, Németország) laboratóriumában tett látogatást. Kutatási eredményeiről különböző nemzetközi konferenciákon számolt be Bad Homburgban (Németország), Bázelen (Svájc), Berlinben (Németország), Bathban (Egyesült Királyság) és Brugge-ben (Belgium) és a Nemzetközi Thrombosis és Haemostasis Társaság (ISTH) Fiatal Kutatók Díjában részesítette. Jelenleg posztdoktorális kutatóként dolgozik Prof. H. ten Cate és Dr. H.M.H. Spronk témavezetése alatt a Maastricht Egyetem Biokémia Intézetében.



Publications

Full papers

1. **Nagy M**, Heemskerk JWM, Swieringa F. Use of microfluidics to assess the platelet-based control of coagulation; *Platelets* 2017; 28(5):441-448.
2. Petersen R, Lambourne JJ, Javierre BM, Grassi L, Kreuzhuber R, Ruklisa D, Rosa IM, Tomé AR, Elding H, van Geffen JP, Jiang T, Farrow S, Cairns J, Al-Subaie AM, Ashford S, Attwood A, Batista J, Bouman H, Burden F, Choudry FA, Clarke L, Flicek P, Garner SF, Haimel M, Kempster C, Ladopoulos V, Lenaerts AS, Materek PM, McKinney H, Meacham S, Mead D, **Nagy M**, Penkett CJ, Rendon A, Seyres D, Sun B, Tuna S, van der Weide ME, Wingett SW, Martens JH, Stegle O, Richardson S, Vallier L, Roberts DJ, Freson K, Wernisch L, Stunnenberg HG, Danesh J, Fraser P, Soranzo N, Butterworth AS, Heemskerk JW, Turro E, Spivakov M, Ouwehand WH, Astle WJ, Downes K, Kostadima M, Frontini M. Platelet function is modified by common sequence variation in megakaryocyte super enhancers. *Nat Commun* 2017; 8:16058.
3. Spronk HMH, Padro T, Siland JE, Prochaska J, Winters J, van der Wal A, Posthuma JJ, Lowe G, d'Alessandro E, Wenzel P, Coenen D, Reitsma PH, Ruf W, van Gorp R, Koenen R, Vajen T, Alshaiikh N, Wolberg AS, Macrae F, Asquith N, Heemskerk J, Heinzmann A, Moorlag M, Mackman N, van der Meijden PE, Meijers JC, Heestermans M, Renné T, Dolleman S, Chayoua W, Ariens RA, Baaten C, **Nagy M**, Kuliopulos M, Posma J, Harrison P, Vries M, Crijs HJ, Dudink EA, Büller HR, Henskens Y, Sjalander A, Zwaveling S, Erkuner O., Eikelboom J, Gulpen A, Peeters FE, Douxfils J, Olie R, Baglin T, Leader A, Schotten U, Scaf B, van Beusekom HM, Mosnier L, van der Vorm L, Declerck P, Visser M, Dippel DW, Strijbis V, Pertiwi K, ten Cate-Hoek AJ, ten Cate H, Atherothrombosis and Thromboembolism; position paper from the 2nd Maastricht Consensus Conference on Thrombosis. *Thromb Haemost* 2018; 118(2):229-250.
4. **Nagy M**, Mastenbroek TG*, Mattheij NJA*, de Witt S, Clemetson KJ, Kirschner J, Schulz AS, Vraetz T, Speckmann C, Braun A, Cosemans JMEM, Zieger B*, Heemskerk JWM*. Variable impairment of platelet functions in patients with severe, genetically-linked immune deficiencies. *Haematologica* 2018; 103(3):540-549. (*equal contribution)
5. Vajen T, Heinzmann ACA, Dickhout A, Zhao Z, **Nagy M**, Heemskerk JWM, Koenen RR. Laminar flow-based assays to investigate leukocyte recruitment on cultured vascular cells and adherent platelets. *J Vis Exp* 2018; e134.
6. Tullemans BME, **Nagy M**, Sabrkhany S, Griffioen AW, oude Egbrink MGA, Aarts MJ, Heemskerk JWM, Kuijpers MJE. Tyrosine kinase inhibitor pazopanib inhibits platelet procoagulant activity in vitro and in renal cell carcinoma patients. *Front Cardiovasc Med* 2018; 5: e142.

7. Mammadova-Bach E, **Nagy M**, Heemskerk JWM, Nieswandt B, Braun A: Multiple roles of store-operated calcium entry in thrombo-inflammation. *Cell Calcium* 2019; 77:39-48.
8. Van Geffen JP, Brouns SLN, Batista J, McKinney H, Kempster C, **Nagy M**, Sivapalaratnam S, Baaten CC, Boury N, Frontini M, Swieringa F, Turro E, Verdoold R, Cavill R, Kuijpers MJE, Ouwehand WH, Downes K, Heemskerk JWM. High-throughput microfluidics of thrombus formation to elucidate platelet function variability. *Haematologica* 2019, 104:1256-1267.
9. Onselaer MB, **Nagy M**, Pallini C, Pike JA, Perrella G, Garcia Quintanilla L, Eble AJ Poulter NS, Heemskerk JWM, Watson SP Comparison of the GPVI inhibitors losartan and honokiol in platelet activation. *Platelets* 2019, 8:1-11.
10. Gotru SK,* van Geffen JP*, **Nagy M**, Eilenberger J, Manukjan G, Shulze H, Eber S, Schambeck C, Deppermann C, Mammadova-Bach E, Heinze K, Nurden P, Greinacher A, Sachs U, Nieswandt B, Hermanns HM, Heemskerk JWM, Braun A. Defective Zn²⁺ homeostasis of human and mouse platelets in storage pool disorders. Scientific Report 2019, 9:8333. (*equal contribution)
11. Kiouptsi K, Jackel S, Grill A, Kuijpers MJE, van der Vorst E, Sommer F, **Nagy M**, Neideck C, Ascher S, Formes H, Karwot C, Jansen Y, Subramaniam S, Rosenstiel P, Walter U, Jurk K, Heemskerk JWM, Weber C, Döring Y, Reinhardt C. The microbiota promotes thrombogenicity but does not affect late atherosclerotic lesion size of atherosclerotic Ldlr^{-/-} mice. *mBio*, *In print*.
12. **Nagy M**, van Geffen JP, Stegner D, Adams DJ, Braun A, de Witt SM, Elvers M, Geer MJ, Kuijper MJE, Kunzelmann K, Mori J, Oury C, Pircher J, Pleines I, Poole AW, Senis YA, Verdoold R, Weber C, Nieswandt B, Heemskerk JWM, Baaten CCFMJ. Comparative analysis of microfluidics thrombus formation in multiple genetically modified mice: link to thrombosis and hemostasis. *Front Cardiovasc Med* 2019, 6:99.
13. Sternkopf M*, **Nagy M***, Baaten CC, Theelen W, Wirth J, Mastenbroek TG, Lehrke M, Winnerling B, Baerts L, Cosemans JMEM, De Meester I, Daiber A, Jankowski J, Heemskerk JWM, Noels H. 13. Bioactive glucagon-like peptide 1 suppresses thrombus growth under flow: beneficial antithrombotic effect of dipeptidyl peptidase 4 inhibition. *Under revision*. (*equal contribution)
14. **Nagy M**, Bender M, Sickmann A, Brouns SLN, Koenen RR, Poulter N, Heemskerk JWM, Baaten CCFMJ. Tight Junction structures of zona occludens 2 in platelet-platelet interaction. *Submitted*

15. **Nagy M***, Perrella G*, Garcia Quintanilla L, Gardiner E, Heemsker JWM, Mezzano D, Watson SP. Glycoprotein VI is essential for the phosphatidylserine on collagen and non-collagenous surfaces. *Submitted. (*equal contribution)*
16. Mastebroek TG*, Karel MFA*, **Nagy M**, Coenen DM, Debets J, Chayouâ W, Brouns AE, Leenders PJA, van Essen H, van Oerle R, Heemsker JWM, Heitmeier S, Spronk HM, Kuijpers MJE, Cosemans JMEM. Injury-induced vascular changes and thrombus activity after aspirin or rivaroxaban treatment in mice. *To be submitted. (*equal contribution)*
17. **Nagy M**, Brouns SLN, Montague SJ, Burston J, Cosemans JMEM, Kerstin J, Koenen RR, Ni Ainle F, O'Donnell V, Soehnlein O, Watson SP, Heemsker JWM. Thrombus-induced micro-localisation and activation of neutrophils: roles of platelet-derived chemokines. *To be submitted.*

Abstracts

1. Mastebroek TG, Kuijpers MJE, **Nagy M**, Leenders PJA, Sluimer JC, Gijbels ML, Heemsker JWM, Cosemans JMEM. Platelet-thrombi induce an unstable plaques phenotype and arterial stiffening locally at the site of vascular injury. Proceedings of the 1st European Congress on thrombosis and Haemostasis, The Hague, The Netherlands, 2016.
2. **Nagy M**, Mastebroek TG, Mattheij NJA, de Witt S, Clemetson KJ, Kirschner J, Schulz AS, Cosemans JMEM, Zieger B, Heemsker JWM. Variable linkage with platelet functions of genetic mutations in ORAI1, STIM1 or FERMT3 in patients with severe immune deficiencies. Proceedings of the 3rd European Platelet Conference, Bad Homburg vor der Höhe, Germany, 2016.
3. Mastebroek TG, Kuijpers MJE, **Nagy M**, Leenders PJA, Sluimer JC, Gijbels ML, Heemsker JWM, Cosemans JMEM. Platelet-thrombi induce an unstable plaques phenotype and arterial stiffening locally at the site of vascular injury. Proceedings of the 3rd European Platelet Conference, Bad Homburg vor der Höhe, Germany, 2016.
4. Mastebroek TG, Kuijpers MJE, **Nagy M**, Leenders PJA, Sluimer JC, Gijbels ML, Cleutjens JPM, Heemsker JWM, Cosemans JMEM. Platelets promote MMP-dependent plaque destabilization locally at the site of vascular injury. *J Thromb Haemost.* 2016;14:Suppl 1.
5. **Nagy M**, Mastebroek TG, Mattheij NJA, de Witt S, Clemetson KJ, Kirschner J, Schulz AS, Cosemans JMEM, Zieger B, Heemsker JWM. Variable linkage with platelet functions of genetic mutations in ORAI1, STIM1 or FERMT3 in patients with severe im-

mune deficiencies. Proceedings of the 61st Annual Meeting of the Society of Thrombosis and Hemostasis Research, Basel, Switzerland, 2017.

6. **Nagy M**, Montague S, Brouns SLN, Feijge MAH, Mastenbroek TG, Egan K, Ní Áinle F, Koenen RR, Watson SP, Cosemans JMEM, Heemskerk JWM. Platelet-dependent leukocyte adhesion and fate in whole-blood thrombus formation: mechanism of platelet-induced neutrophils activation after whole-blood thrombus formation. Proceedings of the 1st Italian-UK platelet meeting, Bath, United Kingdom, 2017.
7. Tullemans BME, **Nagy M**, Sabrkhany S, Griffioen AW, oude Egbrink MGA, Aarts MJ, Heemskerk JWM, Kuijpers MJE. Platelet procoagulant activity is inhibited by tyrosine kinase inhibitor pazopanib in vitro and in renal cell carcinoma patients. *Platelets*. 2017;28(8):755.
8. **Nagy M**, Montague S, Feijge MAH, Mastenbroek TG, Egan K, Ní Áinle F, Koenen RR, Watson SP, Cosemans JMEM, Heemskerk JWM. Platelet-dependent leukocyte adhesion and fate in whole-blood thrombus formation. *Research and Practice in Thrombosis and Haemostasis*. 2017;1:Suppl S1.
9. **Nagy M**, Mastenbroek TG, Mattheij NJA, de Witt S, Clemetson KJ, Kirschner J, Schulz AS, Cosemans JMEM, Zieger B, Heemskerk JWM. Variable impairment of platelet function in patients with severe, genetically linked immune deficiencies. *Research and Practice in Thrombosis and Haemostasis*. 2017;1:Suppl S1.
10. Mastenbroek TG, Kuijpers MJE, **Nagy M**, Chayouâ W, Brouns AE, Leenders PJA, van Essen H, Heitmeier S, van Oerle R, Spronk HM, Heemskerk JWM, Cosemans JMEM. Effects of aspirin and rivaroxaban on murine arterial vessel wall remodeling after vascular injury. *Research and Practice in Thrombosis and Haemostasis*. 2017;1:Suppl S1.
11. Tullemans BME, **Nagy M**, Sabrkhany S, Aarts M, Heemskerk JWM, Kuijpers MJE. Tyrosine kinase inhibitor pazopanib inhibits platelets procoagulant activity in vitro and in cancer patients. *Research and Practice in Thrombosis and Haemostasis*. 2017;1: Suppl S1.
12. **Nagy M**, Brouns SLN, Montague S, Feijge MAH, Mastenbroek TG, Egan K, Ni Áinle F, Koenen RR, Watson SP, Cosemans JMEM, Heemskerk JWM. Platelet induced intracellular Ca²⁺ rises in neutrophils. Proceedings of the 4th European Platelet Network Conference (EUPLAN), Bruges, Belgium, 2018.
13. Tullemans BME, **Nagy M**, Sabrkhany S, Griffioen AW, oude Egbrink MGA, Aarts MJ, Heemskerk JWM, Kuijpers MJE. Anti-platelet effects of tyrosine kinase inhibitors used for cancer treatment: pazopanib as a proof of principle. Proceedings of the 4th European Platelet Network Conference (EUPLAN), Bruges, Belgium, 2018.

14. Karel MFA, Mastenbroek TG, **Nagy M**, Chayouâ W, Brouns AE, Leenders PJA, van Essen H, Heitmeier S, van Oerle R, Spronk HM, Heemskerk JWM, Kuijpers MJE, Cosemans JMEM. Effects of aspirin and rivaroxaban treatment on murine arterial vessel wall remodeling and thrombus activity. *Research and Practice in Thrombosis and Haemostasis*. 2018;2:Suppl 1:2.
15. Van den Kerkhof DL, **Nagy M**, Ippel JH, Heemskerk JWM, Hackeng TM, Dijkgraaf I. Disagregin: a possible new $\alpha_{IIb}\beta_3$ integrin inhibitor to prevent arterial thrombosis. Symposium of Netherlands Society on Thrombosis and Haemostasis (NVTH), Koudkerke, The Netherlands, 2019.
16. Karel MFA, Mastenbroek TG, **Nagy M**, Coenen DM, Chaoyua W, Bouns AE, Debets J, Leenders JA, Van Esse H, Van Oerle R, Heitmeier S, Spronk HM, Heemskerk JWM, Kuijpers JEM, Cosemans JMEM: Injury-induced vascular changes and thrombus activity after aspirin or rivaroxaban treatment in mice. 3rd ESM-EVBO Conference, Maastricht, The Netherlands, 2019.

Oral and poster presentations

1. **Nagy M**. Platelet induced calcium responses in neutrophils, 4th European Platelet Conference, Bruges, Belgium, September 2018 (oral).
2. **Nagy M**. Mechanism of platelet-induced neutrophil activation after whole blood thrombus formation, 1st Italian-UK Platelet Meeting, Bath, United Kingdom, September 2017 (oral).
3. **Nagy M**. Variable impairment of platelet function in patients with severe, genetically linked immune deficiencies; XXVIth Congress of the International Society on Thrombosis and Haemostasis, Berlin, Germany, July 2017 (poster).
4. **Nagy M**. Platelet-dependent leukocyte adhesion and fate in whole blood thrombus formation; XXVIth Congress of the International Society on Thrombosis and Haemostasis, Berlin, Germany, July 2017 (oral).
5. **Nagy M**. Variable linkage with platelet functions of genetic mutations in ORAI1, STIM1 or FERMT3 in patients with severe immune deficiencies, 61st Annual Meeting on the Society of Thrombosis and Hemostasis Research, Basel, Switzerland, February 2016 (poster).
6. **Nagy M**. Variable linkage with platelet functions of genetic mutations in ORAI1, STIM1 or FERMT3 in patients with severe immune deficiencies. 3rd European Platelet Conference, Bad Homburg, Germany, September 2016 (oral).

Awards

1. 2017- Young Investigator Award – XXVIth Congress of the International Society on Thrombosis and Haemostasis, Berlin, Germany.
2. 2017- Top Rated Abstract Award - XXVIth Congress of the International Society on Thrombosis and Haemostasis, Berlin, Germany.
3. 2017- Top 20 Best Poster-61st Annual Meeting of the Society of Thrombosis and Hemostasis Research, Basel, Switzerland

Acknowledgement

On the way to achieve this thesis many people helped and supported me who I would like to express my gratitude to.

First of all, I would like to thank to my supervisory team. My promotors, Prof. Johan Heemskerk, Prof. Steve Watson and my co-promotor, Dr. Judith Cosemans. Johan, thank you for giving me the opportunity of joining the platelet group. Your door was always open for me whenever I needed help and support and you gave me numerous opportunities for self-growth. Steve, thank you for your support and the opportunity for being involved in a unique study. I really enjoyed our discussions, trips to Chile and I learned a lot from you about research and life. Judith, thank you for your support, help and open discussions. Your valuable input and advices helped me a lot along the way.

I would like to thank the members of the reading committee, Prof. Chris Reutelingsperger, Prof. Marc van Zandvoort, Dr. Martine Jandrot-Perrus, Prof. Ingeborg Hers and Dr. Erik Beckers for reviewing my thesis.

Super Platelet Team, a great team that I was really happy to be part of during my PhD. The group members had a big role during my PhD trajectory and I would like to thank them.

My paranymphs, Constance and Sanne, thank you for your support and friendship. Constance, you have been there for me since my first day and I learned a lot from you. It has been a pleasure to work with you regardless of the location (that we always managed to find eventually). Sanne, my lab partner in crime and making mess during experiments. Spending time with you in the lab was always fun as we ended up with the craziest nonsense ideas but I also knew that I could count on you.

Susanne, you were always on my side and I could come to you for advice or just for fun. I am really grateful for being able to call you my friend and still playing part of each other's life. Tom, you were my junior supervisor during my internship and made me feel welcome in the group and for that I cannot thank you enough. Thank you for your continuous support, help and friendship. Frauke, one of the biggest fans of Budapest who I know. Your flow expertise is indisputable, and you are always there for helping and creating a fun environment. Thank you for everything. Marijke, thank you for sharing your expertise and for the fun trips abroad. Paola, thank you for your input during the lab meetings. We have not worked together during my PhD, but that has changed, and

I am looking forward to working with you. Marion, Nadine, Remco and Siamack, thank you for your help and advices. Ankie, thank you for the nice trips abroad and for showing that hard work pays off. Daniëlle, the PhD student with the most memorable moments in her first year, thank you for the nice discussions. As the next one in the row within the platelet group, good luck with the last year and writing your thesis! Bibian, thank you for your help in the lab and with analysis and for the coffee breaks. Mieke, thank you for the nice chats and fun experiments behind the Zeiss. Alicia, your action in order to save us from that scary bug in Mainz makes me always smile. Thank you for the good discussions and do not forget to practice “egészségedre”. Isabella, Natalie, Delia and Ilaria, our TAPAS girls, you brought changes and new flow in the platelet group that inspired everyone. Natalie, thank you for the random facts about Germany. Gina, thank you for the fun time in Chile and in the lab. After all your stories, Naples got onto my list of cities to visit.

I would like to thank to my new group, the CTH group, as well for making me feel welcome in the group. Henri and Hugo, thank you for the opportunity to join your group as a postdoctoral researcher. Simone, thank you for your support and help that started during my PhD and keeps up until today. Arina, Yvonne, Jens, Renske, Bram, Aaron, Renè, Elisa, Billy, Patricia, Stefanie, Diane, Marieke and Marcel, thank you for your help and discussions. I look forward to the upcoming time in the group.

I would like to thank to the other employees of the Biochemistry Department for the nice atmosphere and nice chats. Daniëlle, we have started at almost the same time and collected quite some nice stories over the years. Thank you for the nice dinners, drinks and discussions. Danique, thank you for the fun discussions, experiments and for the pepernoten of course. Tanja, Annamiek and Alexandra, thank you for your help. Trees and Lidewij, thank you for all your help with arranging all paperwork related to the PhD and for the nice chats.

Furthermore, I would like to thank all my collaborators who I was lucky to visit and work with.

Hársfalvi Tanárnő, Ön indított el a kutató pályán és irányított Maastrichtba, amiért mindig hálás maradok. Az évek során beigazolódott, hogy a reológia laborban kapott tudás nagyon jó alapot biztosított a PhD-s évek alatt. Köszönöm, hogy nem csupán kutatóként, de mint ember is egy nagyon jó példával járt előttem.

Bea, még mindig emlékszem amikor azt terveztük, hogy majd egy albérletbe költözünk Szegeden az egyetemi évek alatt. Ugyan ez nem jött össze, de nagyon hálás vagyok, hogy a barátságunk még mindig megmaradt. Nóri, megannyi gimis emlék köt össze minket, amik száma azóta is növekedett szerencsére. Köszönöm a barátságod és a vendégszeretet akármikor otthon vagyok. Angi, nem gondoltuk volna az egyetemi évek alatt, hogy itt leszünk az életünk ezen szakaszában. Köszönöm, hogy mindig mellettem állsz és sokszor jobban hiszel bennem, mint én magamban. Valamint hálás vagyok, hogy végig kísérhettem és részese lehettem életed legfontosabb pillanatainak. Timi, köszönöm a barátságod és a jó emlékeket. Várom a jövő évi nagy napod! Mary, a mesterképzés óta megszínesítjük egymás életét és ugyan csak ritkán tudunk találkozni, de mindig olyan mintha csak tegnap beszéltünk volna. Köszönöm a támogatásod és belém vetett hited.

Els en Jo, bedankt voor het warme welkom dat jullie me gegeven hebben in de familie.

Anya és Apa, nem tudom kifejezni a hálát, amit érzek. Köszönöm a folyamatos támogatásokat, bizalmatokat és belém vetett hiteteket, amelyek nélkül nem tarthatnék most itt. Továbbá köszönöm, hogy egy biztos háttérrel biztosítotok, ahova bármikor hazatérhetek. Nálatok jobb szülőket nem is kívánhatnék magamnak. Köszönöm! Karcsi és Marika, köszönöm, hogy mindig támogattatok és jó példával jártatok előttem. Kati, Marcsi, Lilla, Öcsi, Reni, Fanni és Hugi, köszönöm, hogy mindig étellel telivé teszitek az otthonléteimet.

Raoul, you have been my rock ever since we met. Your patience, positive thinking and endless support help me more than you can imagine. Thank you for being on my side even during the most stressful situations. I am looking forward to our future together.

Hálás köszönettel mindenért,
Magdi

